

Supporting Information

Comparison of Two Zinc Hydride Precatalysts for Selective Dehydrogenative Borylation of Terminal Alkynes: A Detailed Mechanistic Study

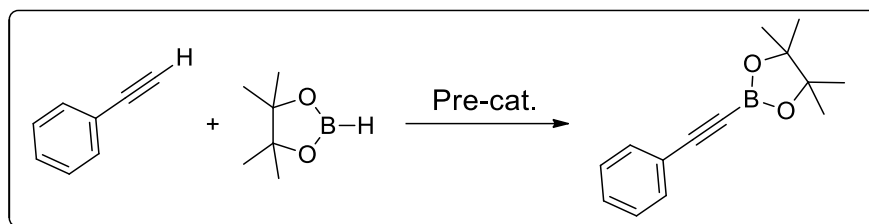
Rajata Kumar Sahoo, Arukela Ganesh Patro, Nabin Sarkar, and Sharanappa Nembenna*

School of Chemical Sciences, National Institute of Science Education and Research (NISER), Homi

Bhabha National Institute (HBNI), Bhubaneswar, 752 050, India

Contents

- Optimization of Zinc Catalyzed Dehydroborylation of Phenylacetylene.....S2
- Synthesis, Analytical Data, and NMR spectra (^1H , $^{13}\text{C}\{^1\text{H}\}$, ^{11}B NMR) of Stoichiometric ExperimentsS3–S38
- ^1H , $^{13}\text{C}\{^1\text{H}\}$ NMR spectra of **[L²ZnI]₂**, and **III**.....S13–S15
- ^1H , $^{13}\text{C}\{^1\text{H}\}$ and ^{11}B NMR Spectra of Dehydrogenative Borylation of Alkynes.....S39–S84
- ^1H , $^{13}\text{C}\{^1\text{H}\}$ and ^{11}B NMR Spectra of Intermolecular Chemoselective Reaction.....S85–S89
- X-ray Crystallographic Data of **II** and **IV**.....S90–S92
- References.....S93

Table S1: Optimization of Zinc Catalyzed Dehydroborylation of Phenylacetylene.

Entry	precatalyst	mol %	HBpin (eq.)	Solvent	Temp (° C)	Time (h)	Conv. (%)
1	---	---	1.05	neat	rt	6	0
2	I	10	1.05	neat	60	6	99
3	I	5	1.05	neat	rt	6	99
4	I	3	1.05	neat	rt	6	99
5	I	1.5	1.05	neat	rt	6	99
6	I	1.5	1.05	neat	rt	1	99
7	I	1	1.05	neat	rt	1	98
8	I	0.5	1.05	neat	rt	1	75
9	I	1.5	1.05	benzene	rt	6	99
10	I	1.5	1.05	toluene	rt	6	99
11	I	1.5	1.05	THF	rt	6	99
12	III	1.5	1.05	neat	rt	6	97
13	Cat. II	1.5	1.05	neat	rt	6	99
14	Cat. IV	1.5	1.05	neat	rt	6	97

Synthesis, Analytical Data, and NMR spectra (^1H , $^{13}\text{C}\{^1\text{H}\}$, ^{11}B NMR) of Stoichiometric Experiments.

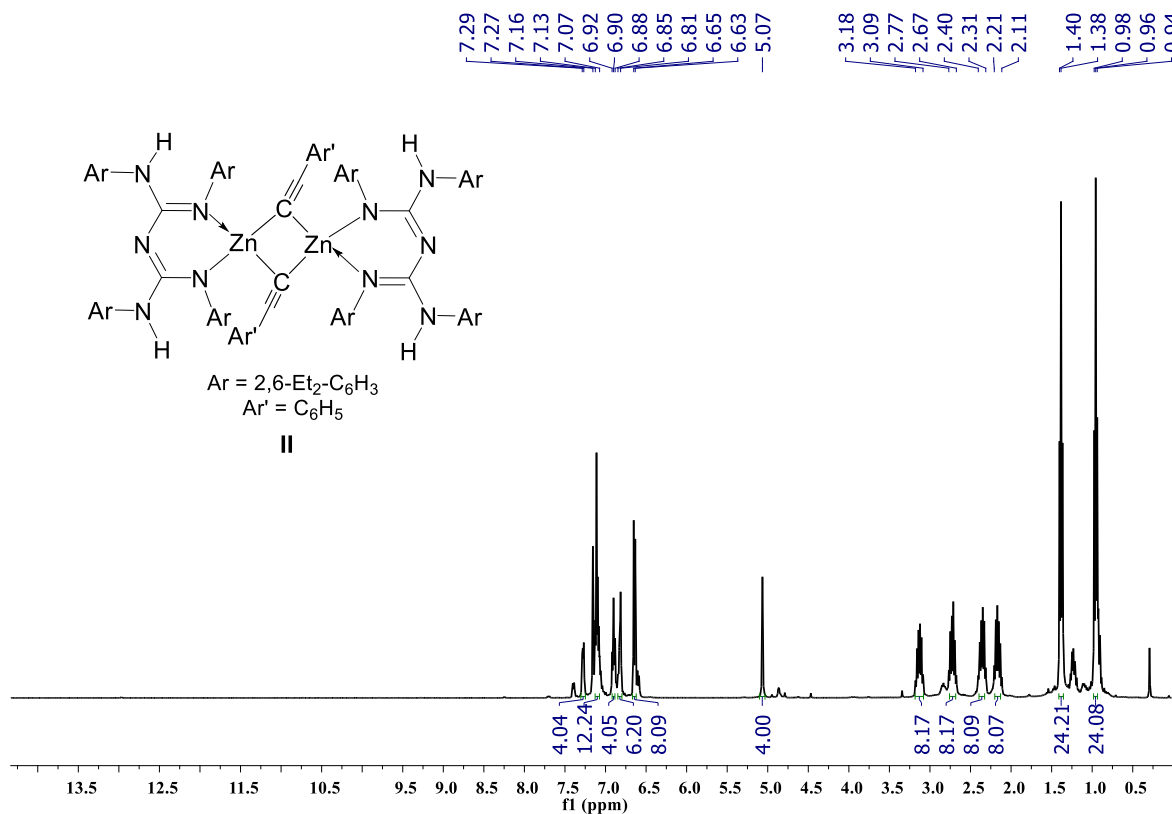


Figure S1: ^1H NMR (400 MHz, 25 °C, C_6D_6) spectrum of compound II.

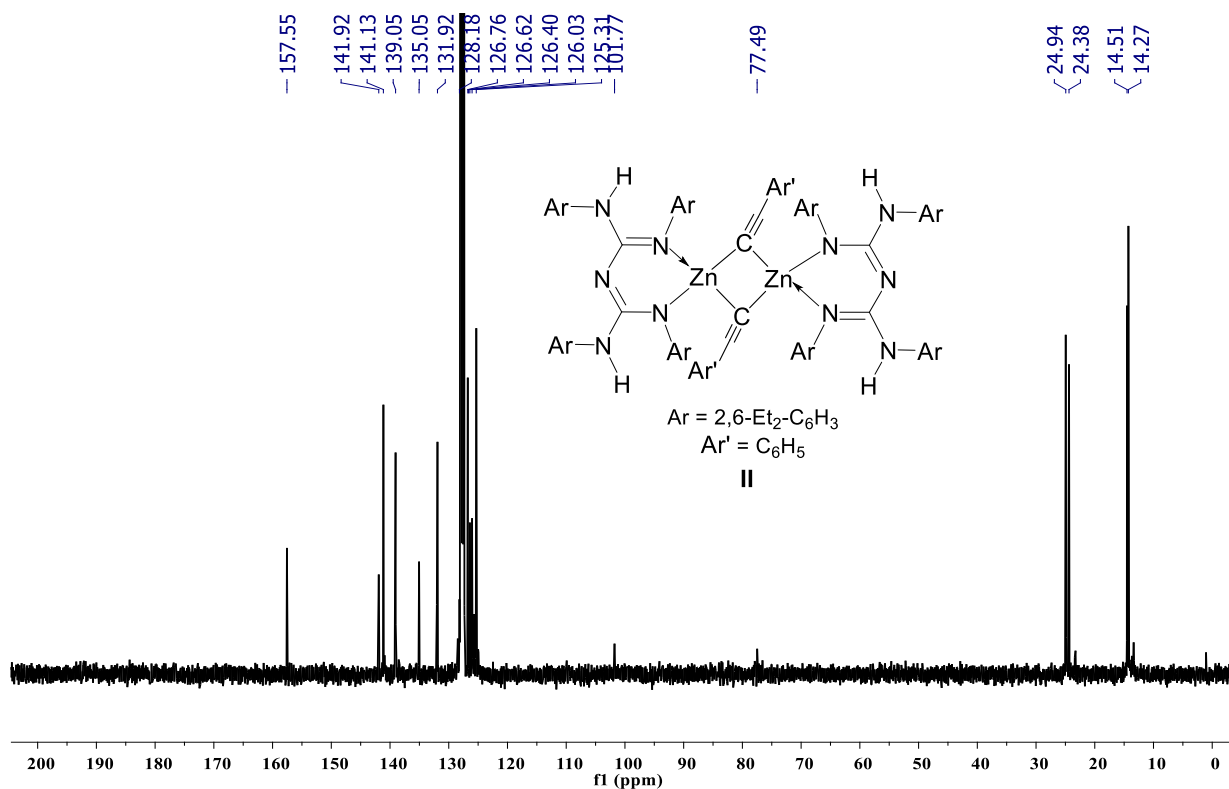


Figure S2: $^{13}\text{C}\{^1\text{H}\}$ NMR (100 MHz, 25 °C, C_6D_6) spectrum of compound II.

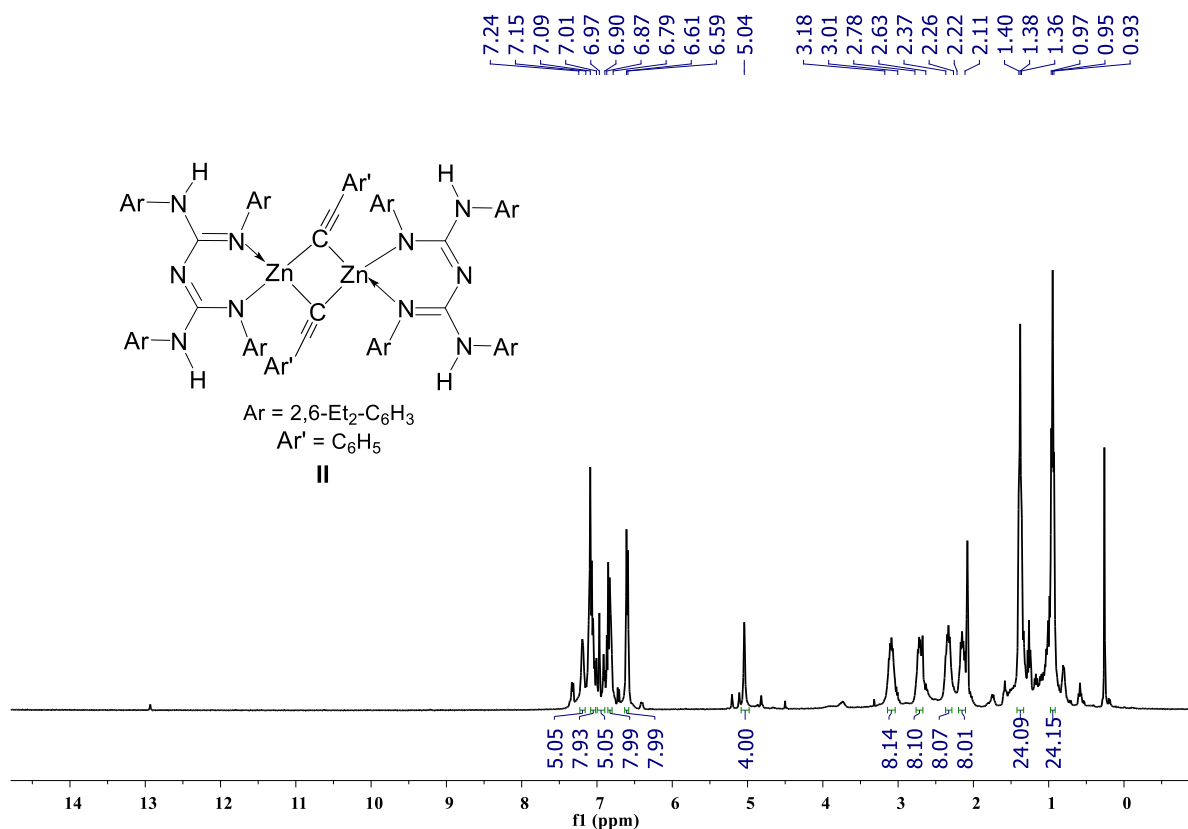


Figure S3: $^1\text{H NMR}$ (400 MHz, 25 °C, d_8 -toluene) spectrum of compound II.

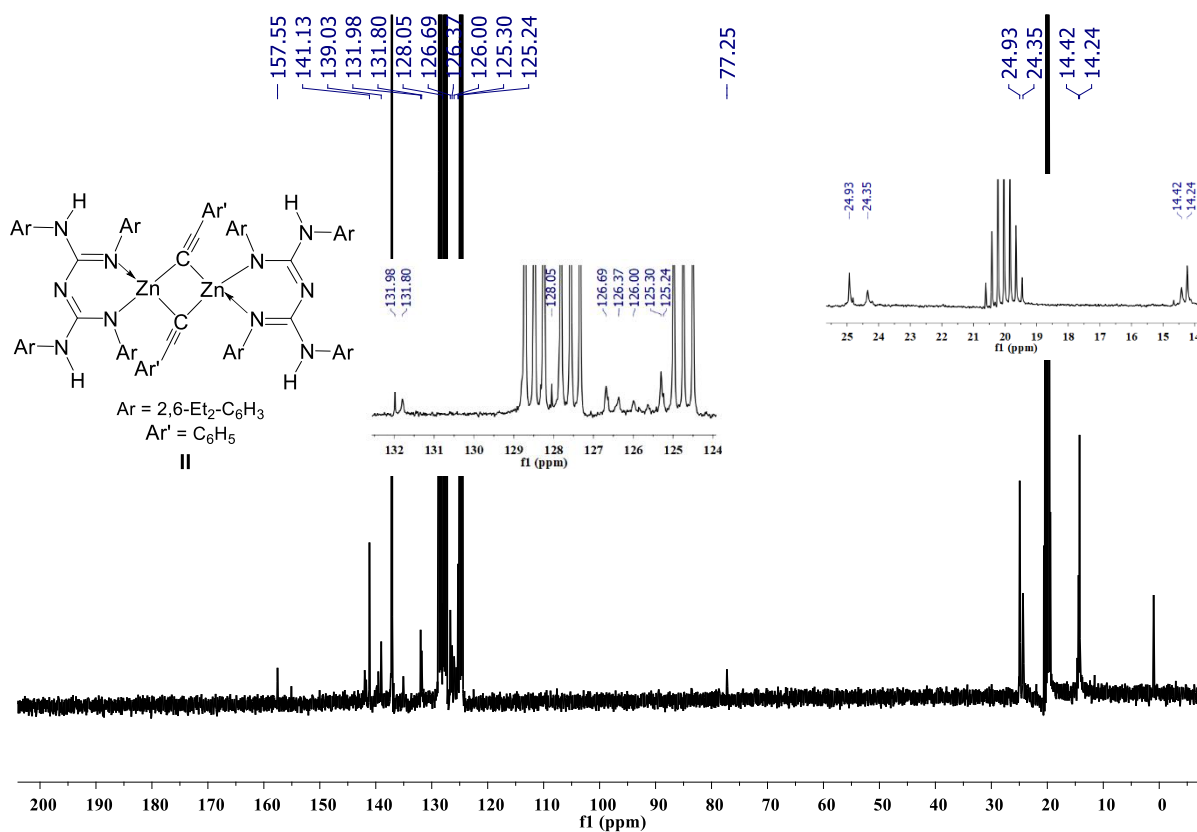


Figure S4: $^{13}\text{C}\{^1\text{H}\}$ NMR (100 MHz, 25 °C, d_8 -toluene) spectrum of compound II.

The reaction between zinc alkynyl **II and HBpin {NMR-Scale}: The addition of HBpin (4.06 μ L, 0.028 mmol) to a J. Young valve NMR tube containing a solution of compound **II** (0.014 mmol) in d_8 -toluene at room temperature after 30 minutes resulted in the formation of compounds **I** and **2a** with a 30% yield was observed by multinuclear NMR spectroscopy. ^1H and ^{11}B NMR spectroscopy revealed that the reaction had reached an equilibrium, best evidenced by the integration of resonance for Bpin moieties of **2a** and HBpin. Extended heating up to 24 h at 80 $^\circ\text{C}$ showed no change in the relative ratio of **2a** and **II**, suggesting that the equilibrium position had already been reached before heating. NMR Yield: (30%).**

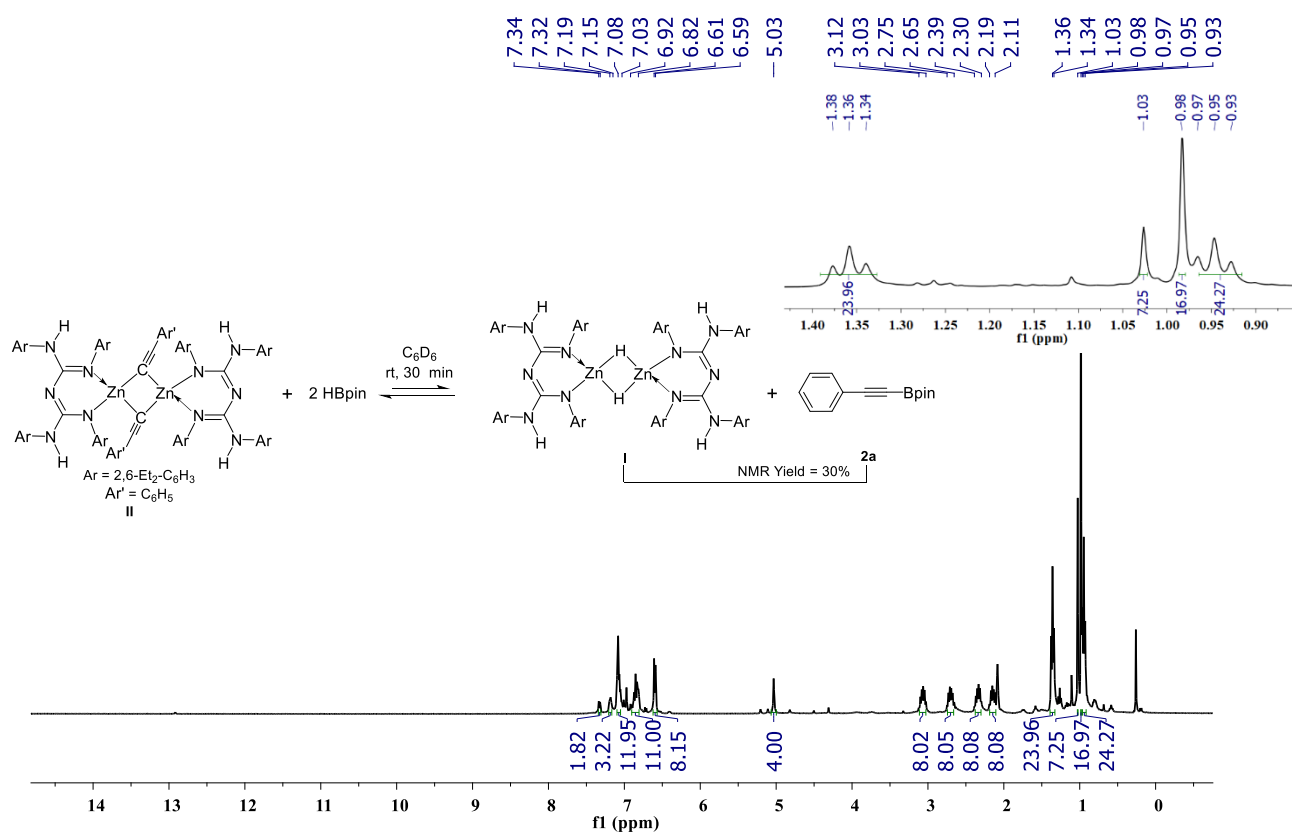


Figure S5: ^1H NMR (400 MHz, 25 $^\circ\text{C}$, d_8 -toluene) spectrum of compounds $[\text{L}^1\text{ZnH}]_2$ & **2a**.

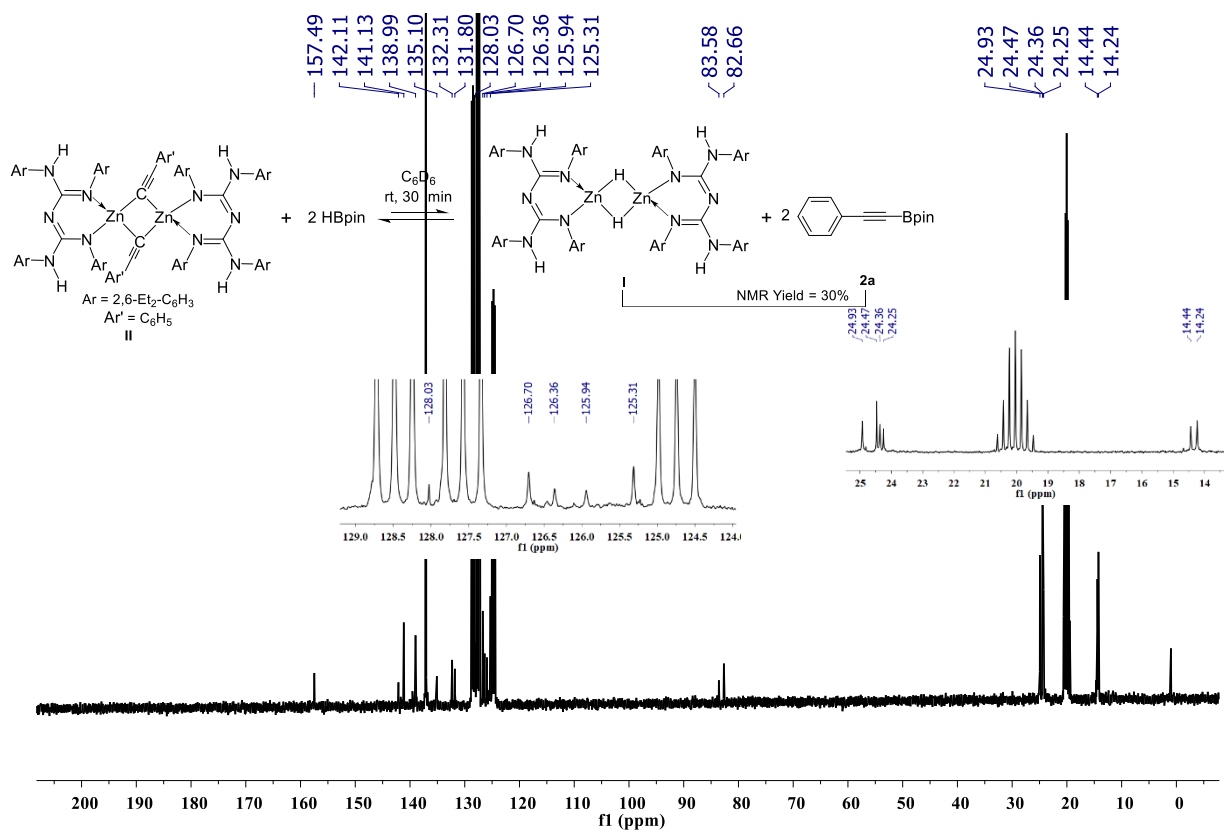


Figure S6: $^{13}\text{C}\{^1\text{H}\}$ NMR (100 MHz, 25 °C, d_8 -toluene) spectrum of compounds $[\text{L}^1\text{ZnH}]_2$ & **2a**.

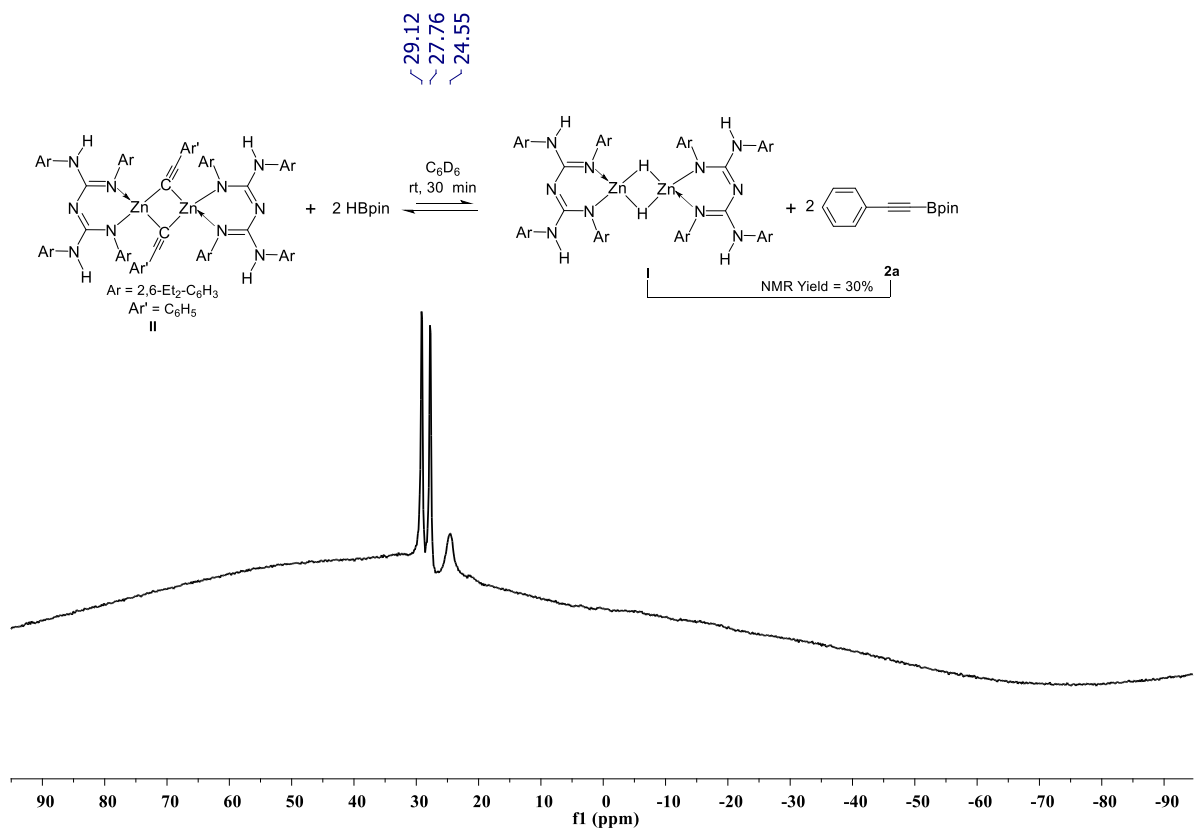


Figure S7: ^{11}B NMR (128 MHz, 25 °C, d_8 -toluene) spectrum of compounds $[\text{L}^1\text{ZnH}]_2$ & **2a**. A doublet peak at δ 27.76 – 29.12 ppm arises from free HBpin.

The reaction between zinc hydride I and 2a {NMR-Scale}: The addition of 2a (6.5 mg, 0.028 mmol) to a solution of complex I (0.020 g, 25 °C, 0.014 mmol) in *d*₈-toluene in a J. Young valve NMR tube after 1 h at 60 °C resulted in the formation of compound II, and HBpin with 70% yield was observed by ¹H and ¹¹B NMR spectroscopy. After 24 h at room temperature, no change was observed in the reaction mixture. ¹H and ¹¹B NMR spectroscopy revealed that the reaction reached an equilibrium, best evidenced by the integration of resonance for Bpin moieties of 2a and compound II. Extended heating up to 24 h at 80 °C showed no change in the relative ratio of 2a and II, suggesting that the equilibrium position had already been reached before heating. NMR Yield: (70%).

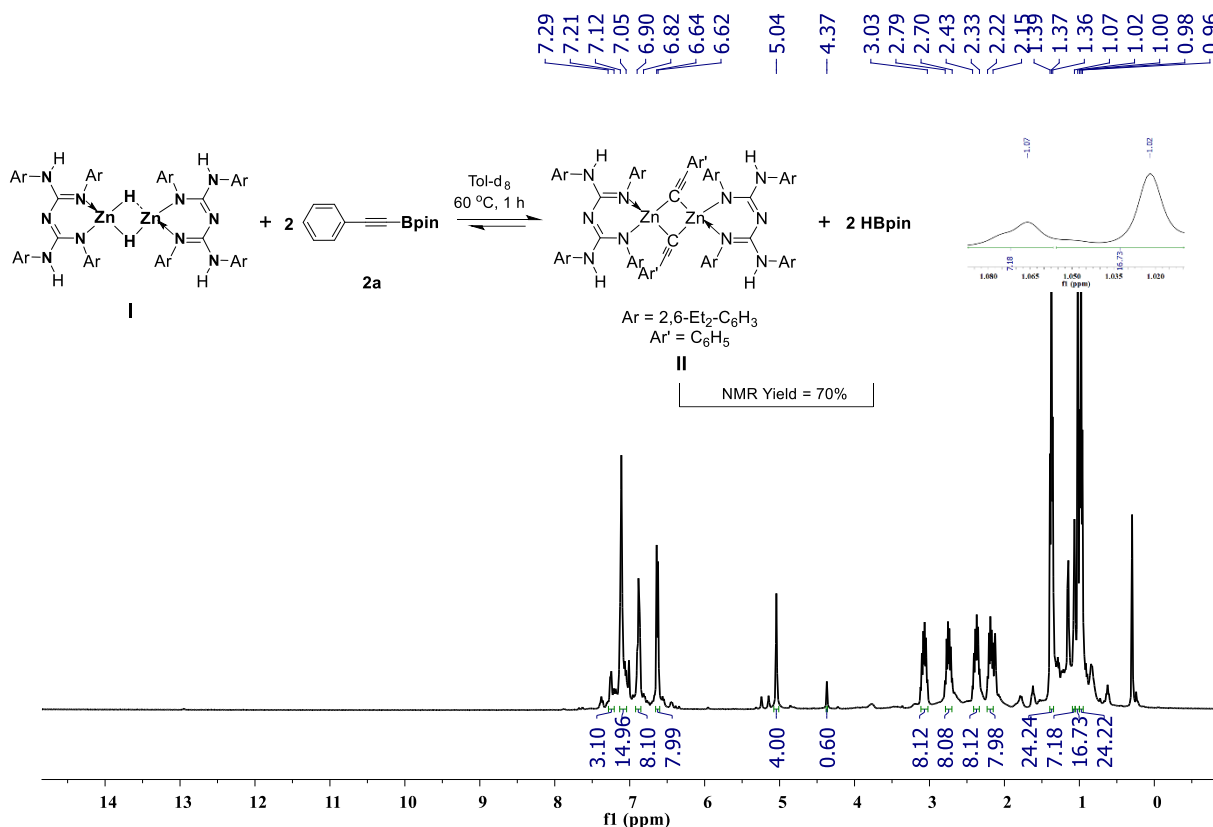


Figure S8: ¹H NMR (400 MHz, 25 °C, *d*₈-toluene) spectrum of compounds **II** & 2HBpin.

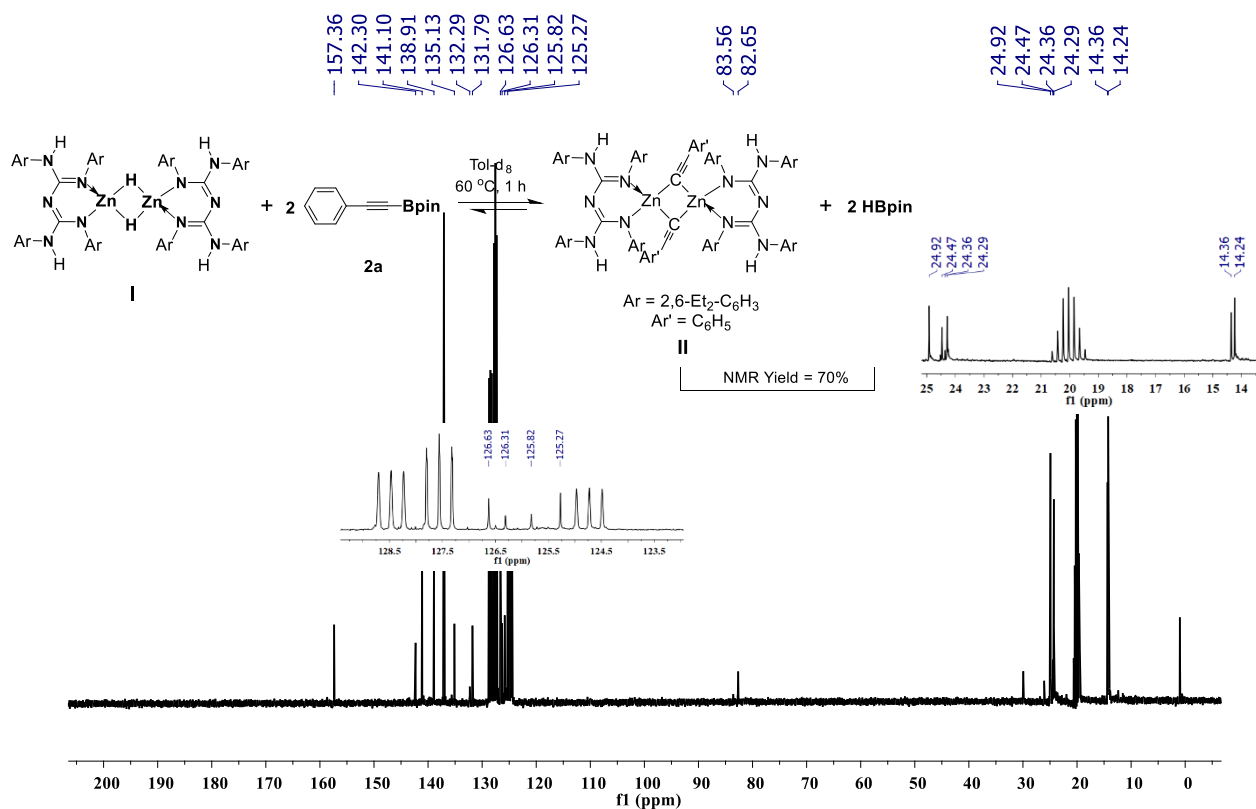


Figure S9: $^{13}\text{C}\{^1\text{H}\}$ NMR (100 MHz, 25 °C, d_8 -toluene) spectrum of compounds **II** & 2HBpin.

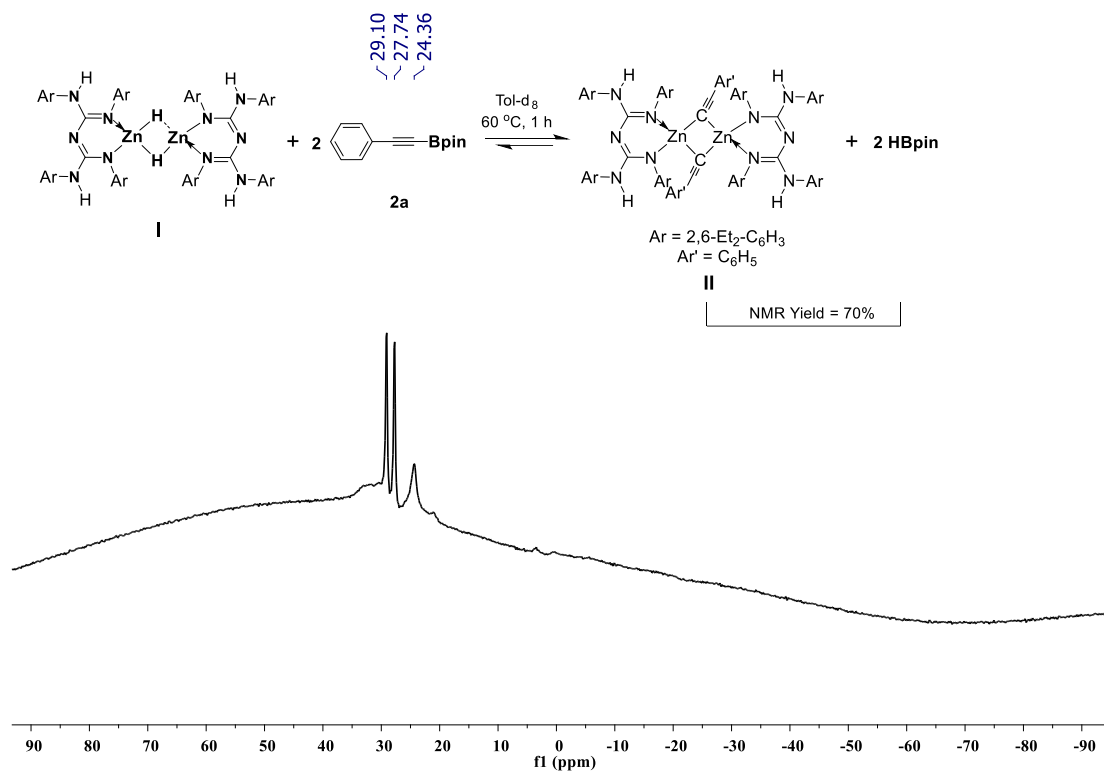


Figure S10: ^{11}B NMR (128 MHz, 25 °C, d_8 -toluene) spectrum of compounds **II** & 2HBpin. A doublet peak at δ 27.74 – 29.10 ppm arises from free HBpin.

Synthesis of compound II and 2a {NMR-Scale}: The addition of phenylacetylene (3.07 μ L, 0.028 mmol) to a J. Young valve NMR tube containing a solution of compound I and 2a (30%) in d_8 -toluene at room temperature after 15 minutes resulted in the complete formation of compound II and 2a was observed by ^1H and ^{11}B NMR spectroscopy. The above study indicates that once 30% compound 2a and I was formed, it immediately reacted with one additional equivalent of phenylacetylene to form a quantitative amount of product 2a and compound II. It stops the equilibrium reaction between compounds II and 2a. NMR Yield: (>99%). ^1H NMR (400 MHz, d_8 -toluene) δ 7.34 – 7.32 (m, 4H), 7.19 – 7.18 (m, 3H), 7.10 – 7.03 (m, 14H), 6.92 – 6.81 (m, 15H), 6.61 – 6.59 (d, $^3J_{\text{HH}} = 9.6$ Hz, 8H), 5.05 (s, 4H), 3.14 – 3.05 (m, 8H), 2.76 – 2.65 (m, 8H), 2.39 – 2.29 (m, 8H), 2.19 – 2.11 (m, 8H), 1.38 (t, $^3J_{\text{HH}} = 7.4$ Hz, 24H), 1.03 (s, 24H), 0.95 (t, $^3J_{\text{HH}} = 7.6$ Hz, 24H). $^{13}\text{C}\{^1\text{H}\}$ NMR (101 MHz, d_8 -toluene) δ 157.5, 141.1, 139.0, 135.0, 132.3, 131.9, 131.8, 128.7, 128.3, 128.0, 128.0, 126.6, 126.4, 126.3, 125.9, 125.3, 83.5, 77.2, 24.9, 24.3, 24.2, 14.4, 14.2. ^{11}B NMR (128 MHz, d_8 -toluene) δ 24.71.

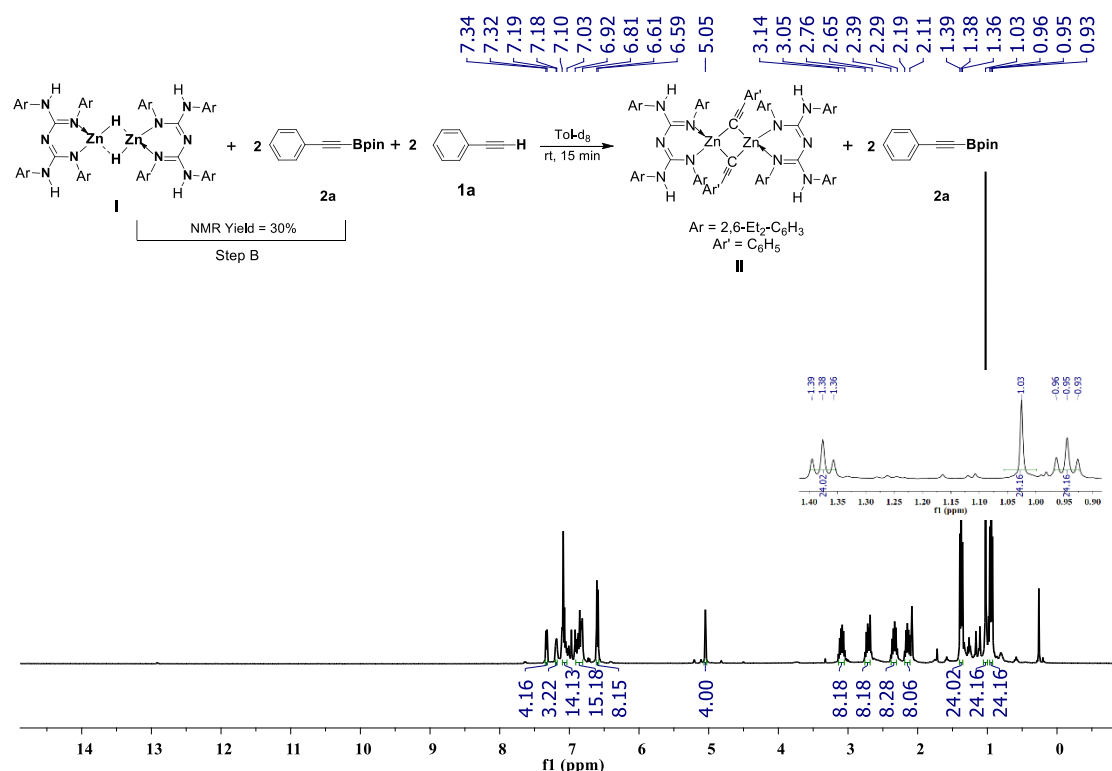


Figure S11: ^1H NMR (400 MHz, 25 °C, d_8 -toluene) spectrum of compounds II & 2a.

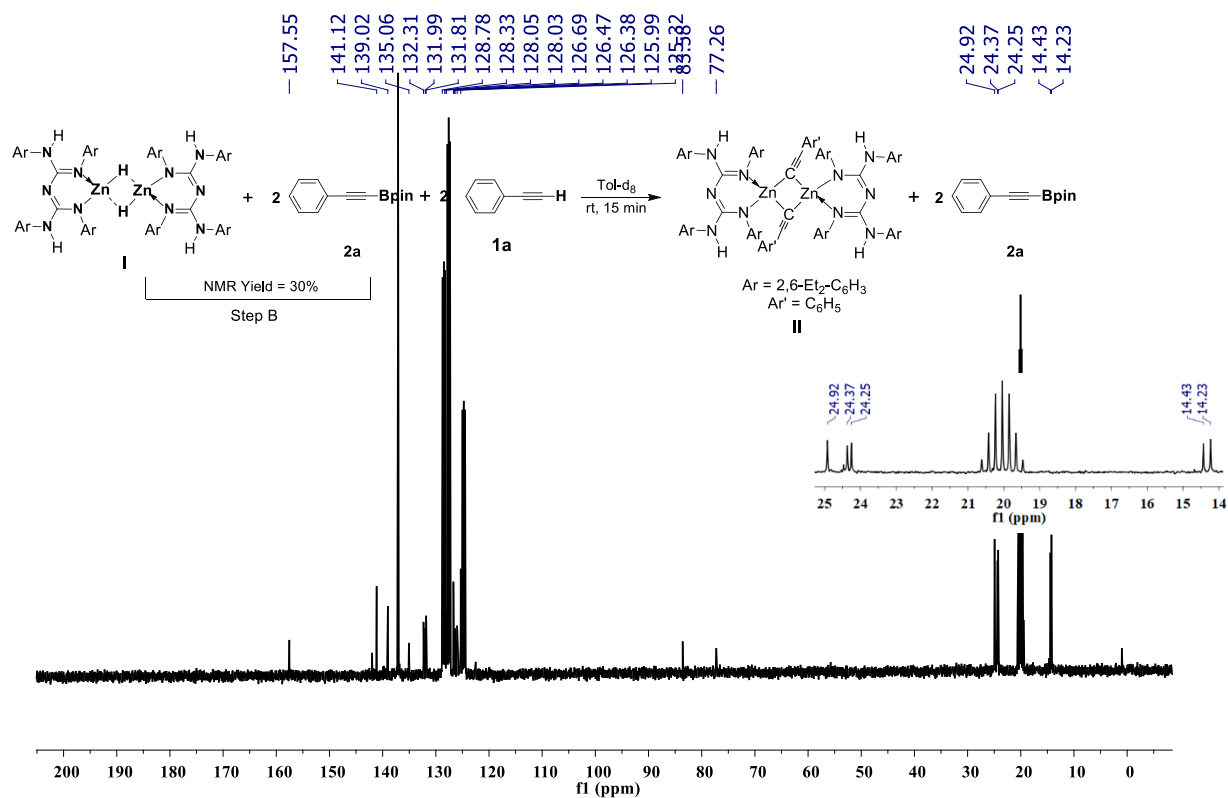


Figure S12: ¹³C{¹H} NMR (100 MHz, 25 °C, d₈-toluene) spectrum of compounds II & 2a.

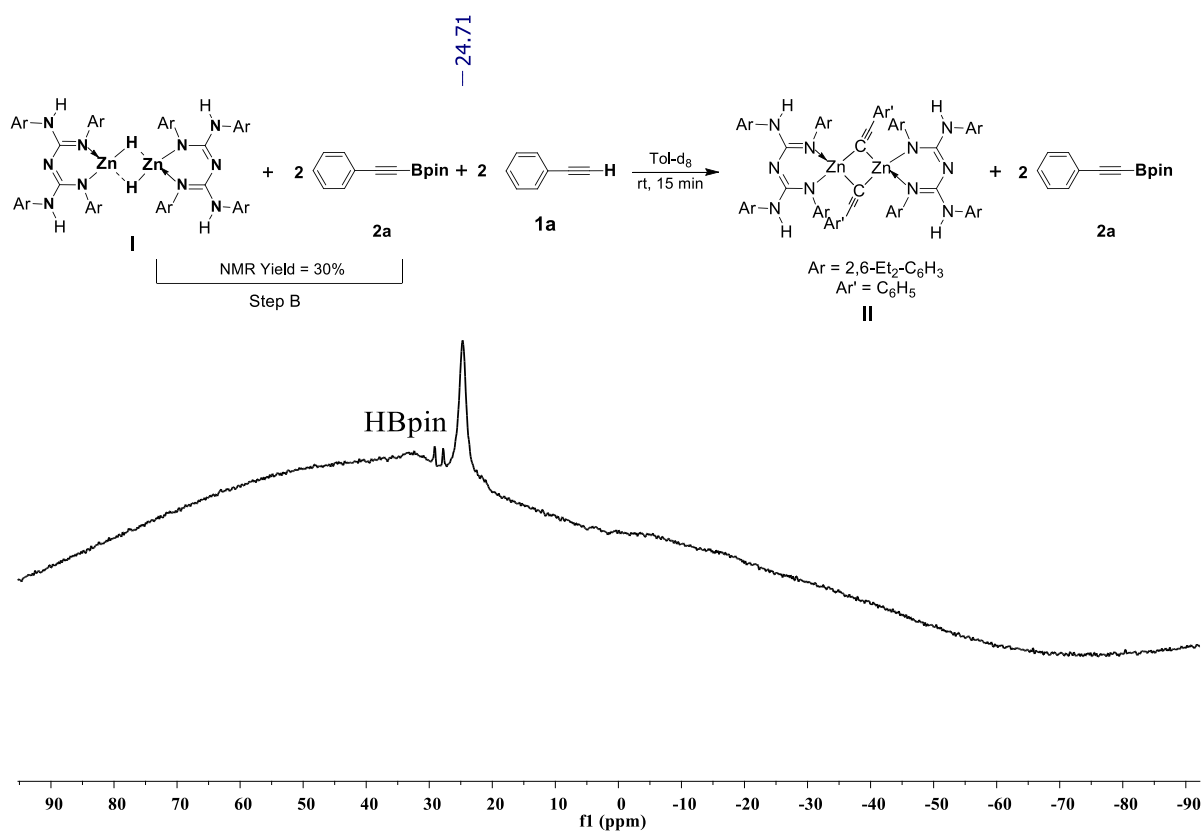


Figure S13: ¹¹B NMR (128 MHz, 25 °C, d₈-toluene) spectrum of compounds II & 2a.

The reaction between zinc hydride I, phenylacetylene, and compound 2a {NMR-Scale}:

In a J. Young valve NMR tube (0.020 g, 25 °C, 0.014 mmol) complex **I**, (6.5 mg, 0.028 mmol) of **2a**, and (3.07 μ L, 0.028 mmol) of phenylacetylene were added successively in d_8 -toluene. Reaction progress was monitored by ^1H NMR analyses, which confirmed that at room temperature after 20 minutes, the complete formation of compound **II** with the liberation of H_2 gas and unreacted compound **2a** was observed by ^1H and ^{11}B NMR spectroscopy. The above study indicates the exclusive formation of compound **II** with a quantitative yield, and compound **2a** was untouched. It again revealed that the presence of phenylacetylene stopped the equilibrium reaction between compounds **I** and **2a**. NMR Yield: (>99%). ^1H NMR (400 MHz, d_8 -toluene) δ 7.34 – 7.32 (m, 4H), 7.22 – 7.15 (m, 3H), 7.10 – 7.02 (m, 14H), 6.92 – 6.81 (m, 15H), 6.61 – 6.59 (d, $^3J_{\text{HH}} = 9.5$ Hz, 8H), 5.05 (s, 4H), 3.14 – 3.05 (m, 8H), 2.75 – 2.66 (m, 8H), 2.39 – 2.29 (m, 8H), 2.19 – 2.11 (m, 8H), 1.38 (t, $^3J_{\text{HH}} = 7.5$ Hz, 24H), 1.03 (s, 24H), 0.95 (t, $^3J_{\text{HH}} = 7.5$ Hz, 24H). $^{13}\text{C}\{^1\text{H}\}$ NMR (101 MHz, d_8 -toluene) δ 157.5, 141.1, 139.0, 135.0, 132.3, 131.9, 131.8, 128.7, 128.3, 128.0, 128.0, 126.7, 126.3, 126.0, 125.3, 101.6, 83.5, 77.2, 24.9, 24.3, 24.2, 14.4, 14.2. ^{11}B NMR (128 MHz, d_8 -toluene) δ 24.69.

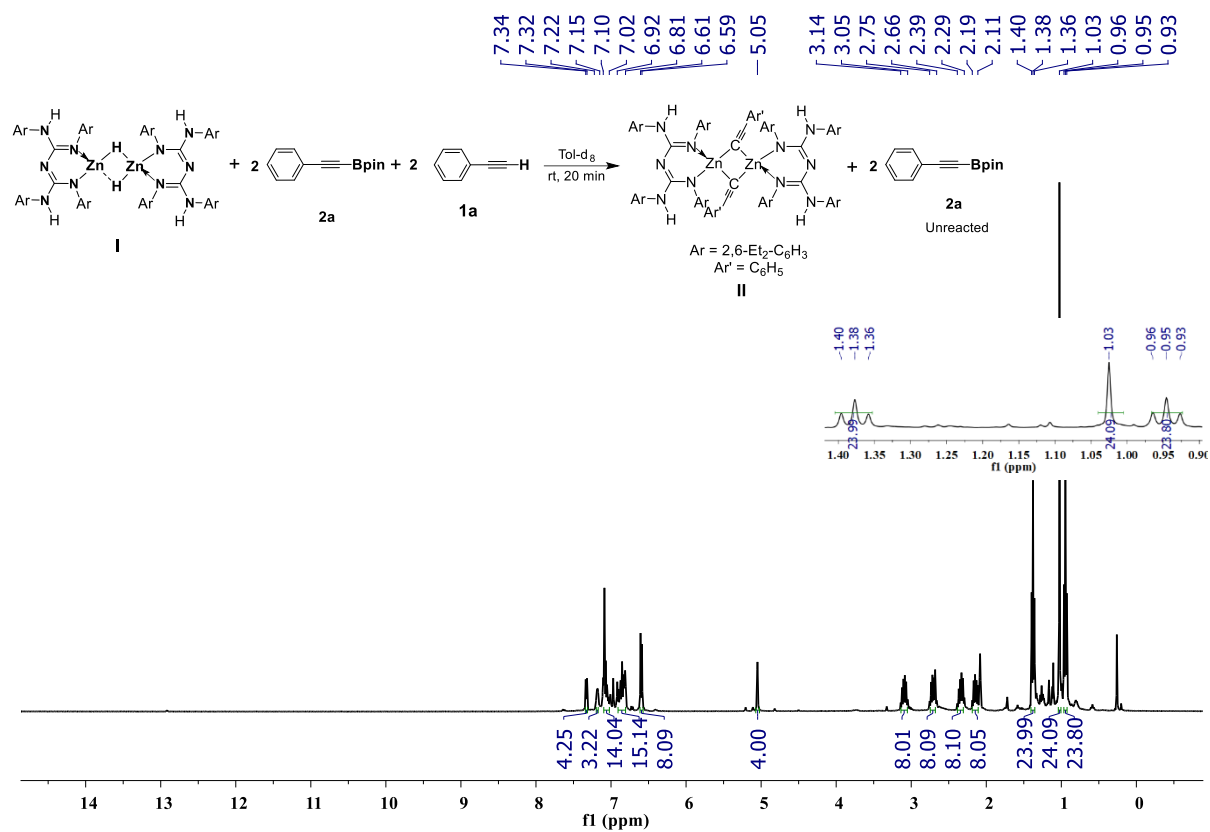


Figure S14: ¹H NMR (400 MHz, 25 °C, d₈-toluene) spectrum of compounds **II** & **2a**.

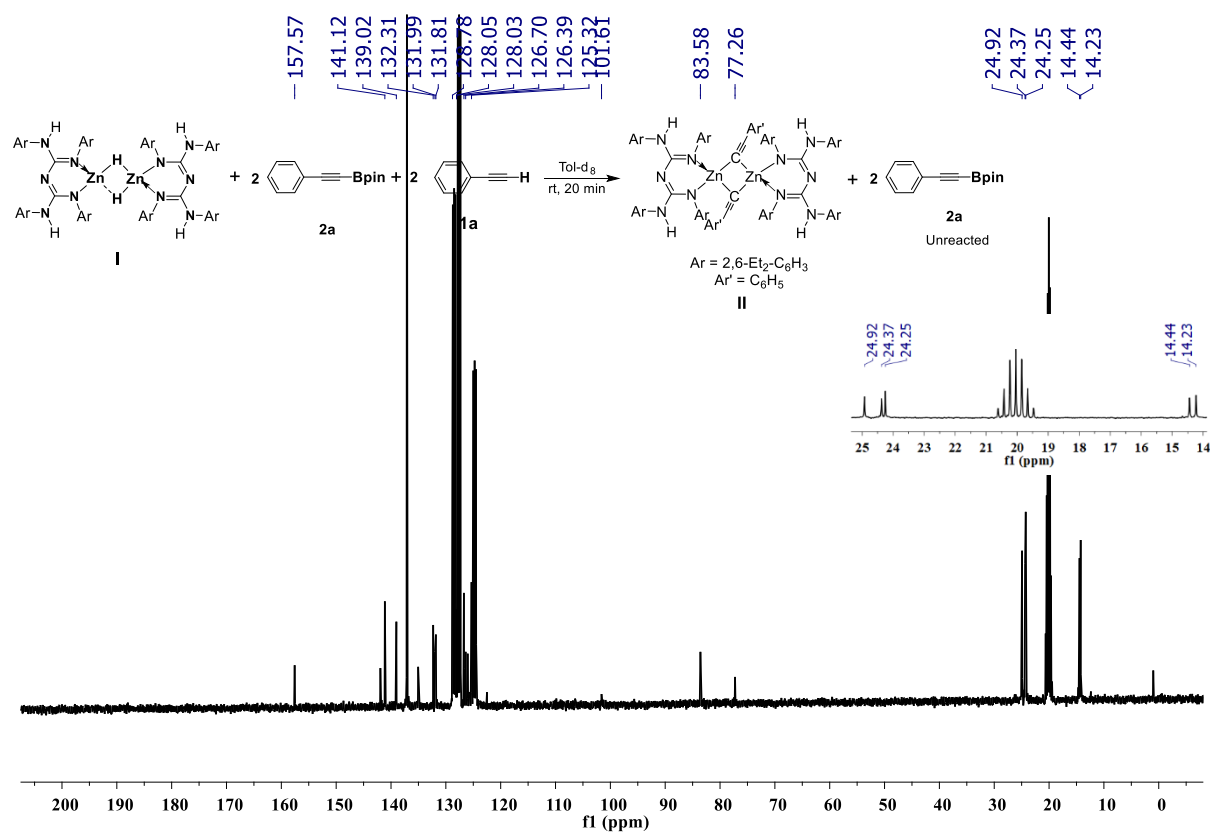


Figure S15: ¹³C{¹H} NMR (100 MHz, 25 °C, d₈-toluene) spectrum of compounds **II** & **2a**.

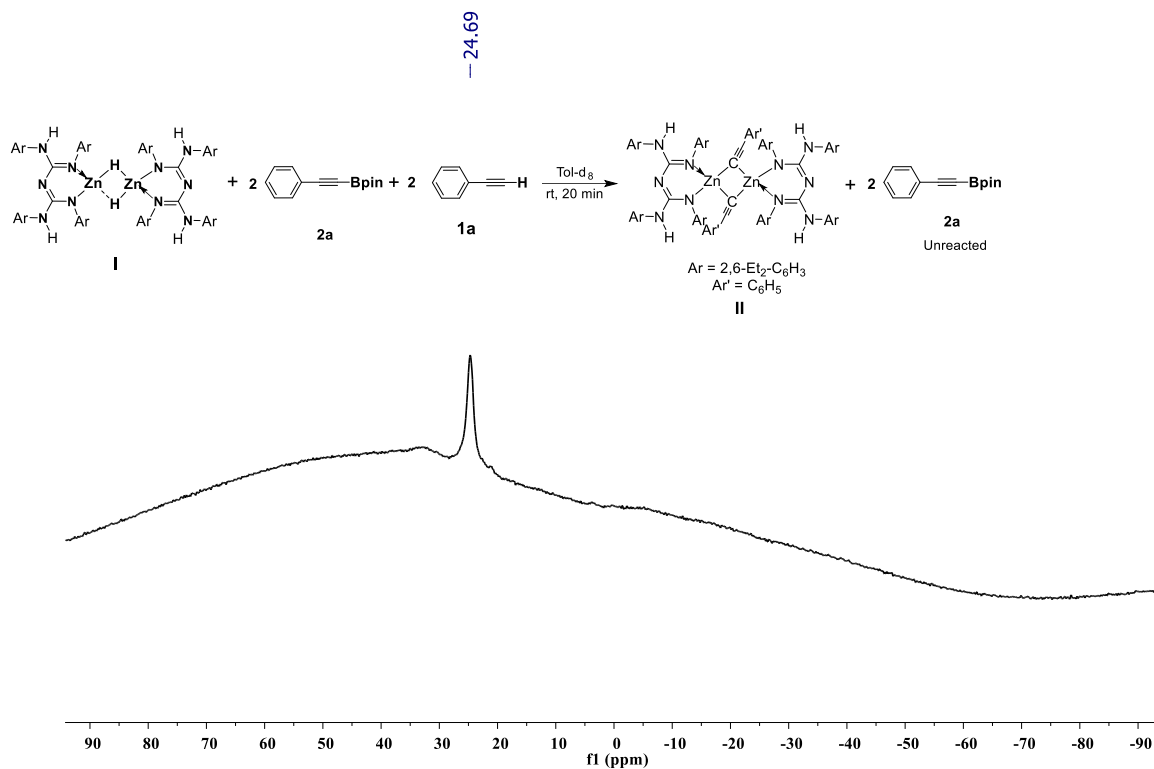


Figure S16: ¹¹B NMR (128 MHz, 25 °C, *d*₈-toluene) spectrum of compounds **II** & **2a**.

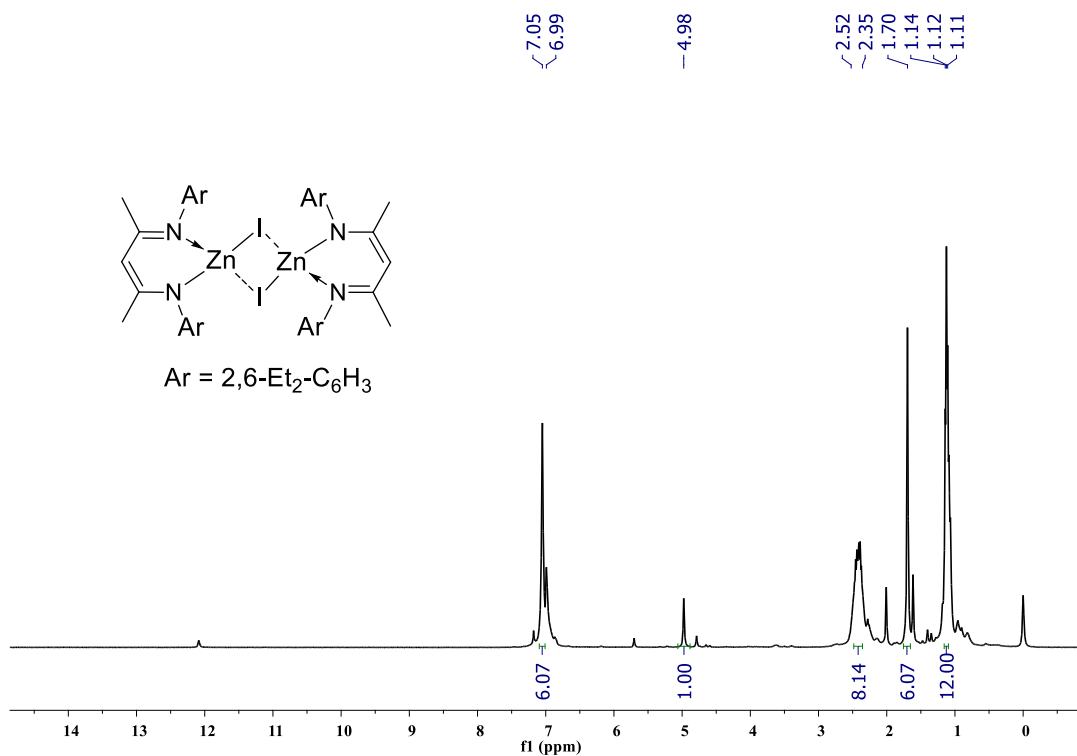


Figure S17: ¹H NMR (400 MHz, 25 °C, CDCl₃) spectrum of compound [L²ZnI]₂.

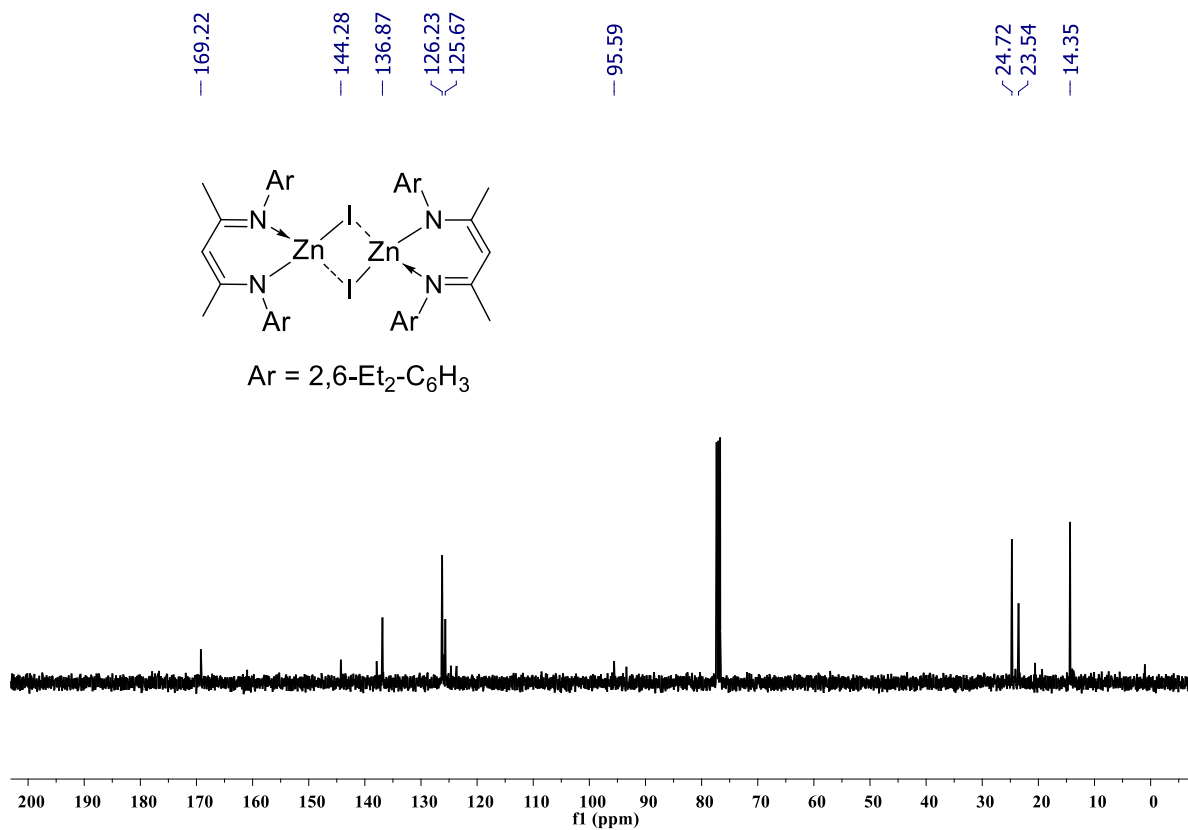


Figure S18: $^{13}\text{C}\{^1\text{H}\}$ NMR (100 MHz, 25 °C, CDCl_3) spectrum of compound **I**.

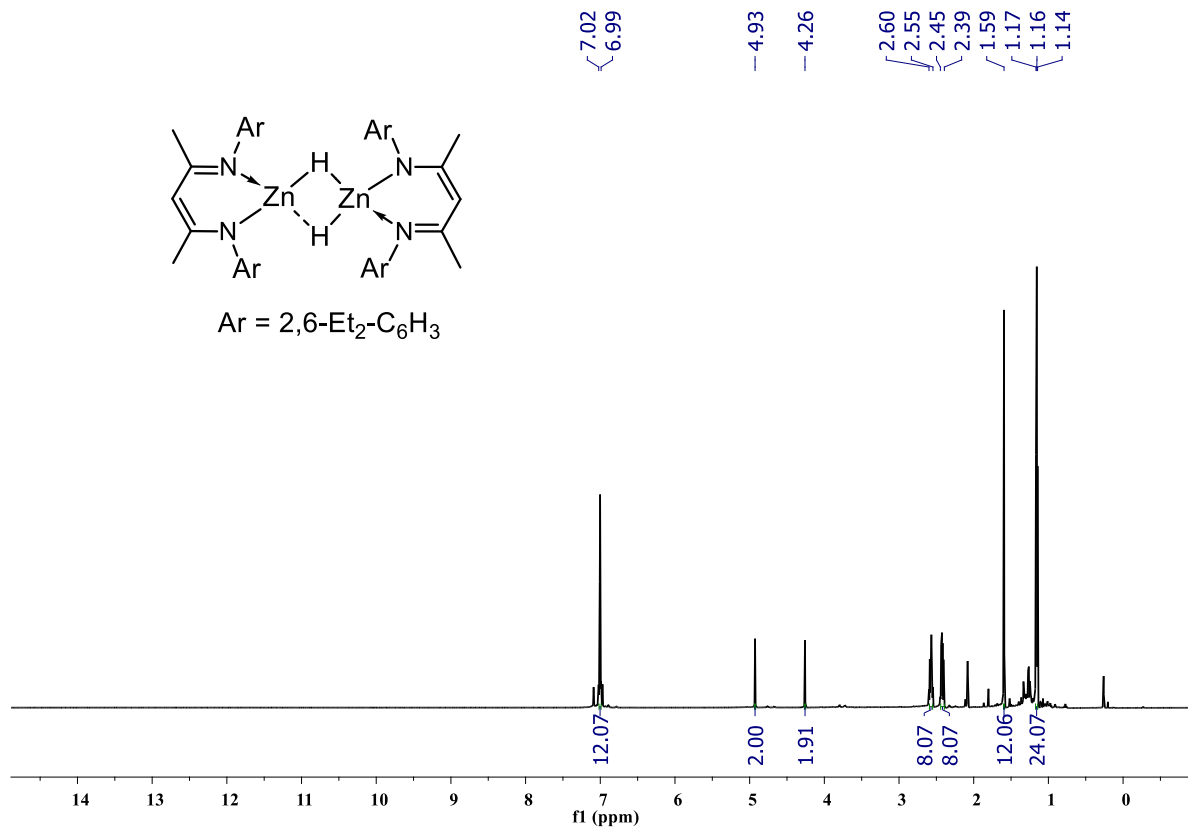


Figure S19: ^1H NMR (700 MHz, 25 °C, d_8 -toluene) spectrum of compound **III**.

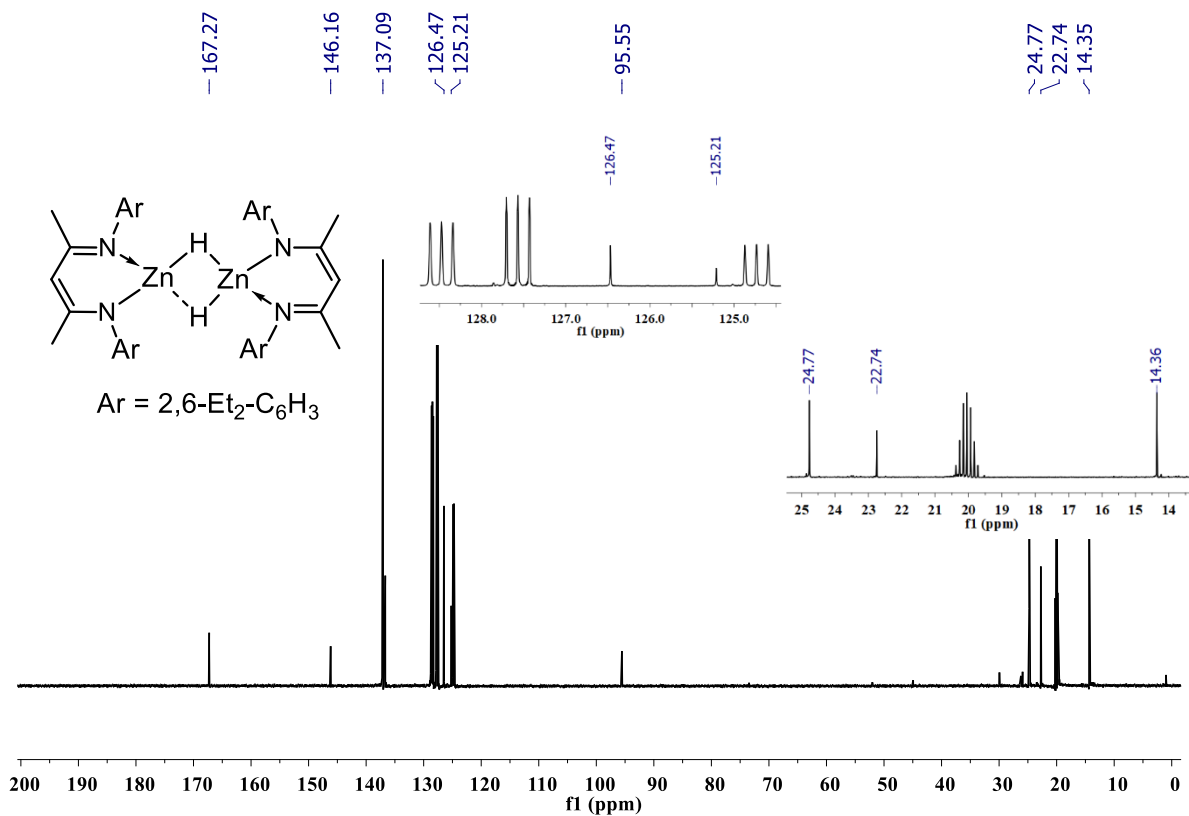


Figure S20: ¹³C{¹H} NMR (176 MHz, 25 °C, *d*₈-toluene) spectrum of compound III.

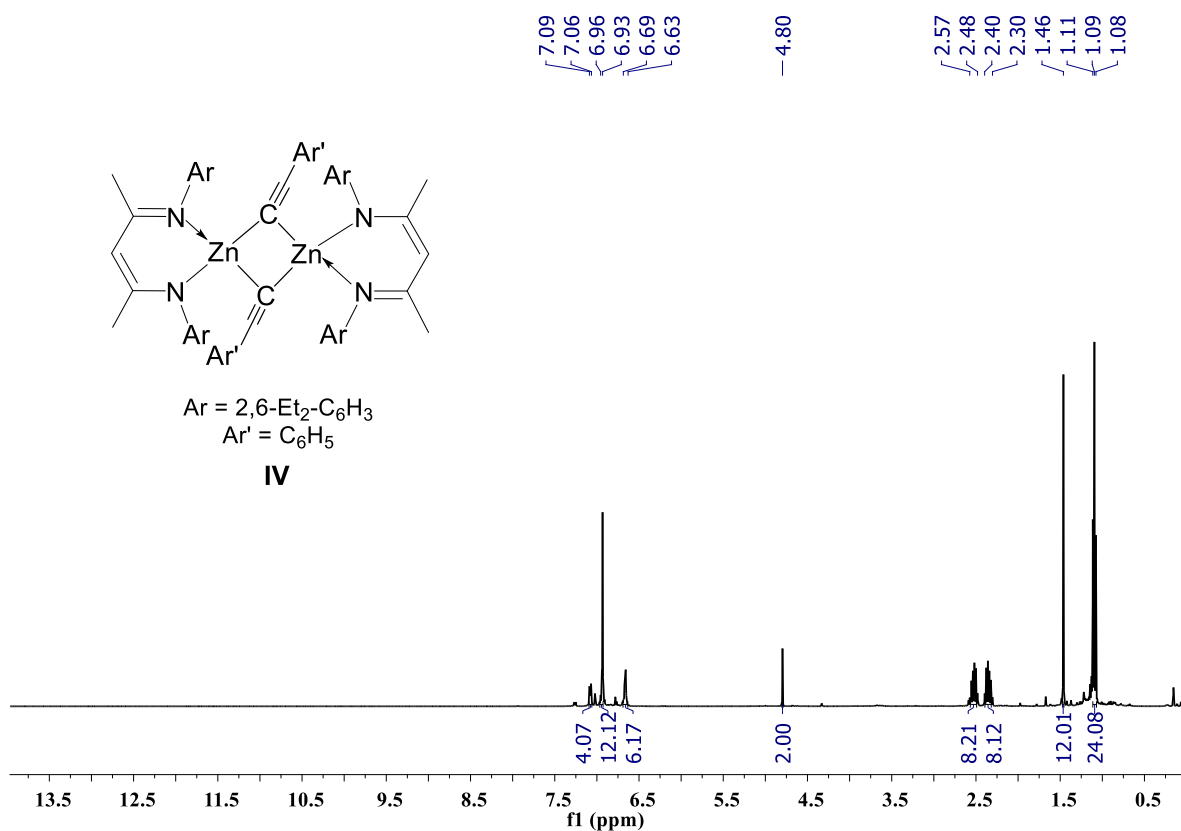


Figure S21: ¹H NMR (400 MHz, 25 °C, C₆D₆) spectrum of compound IV.

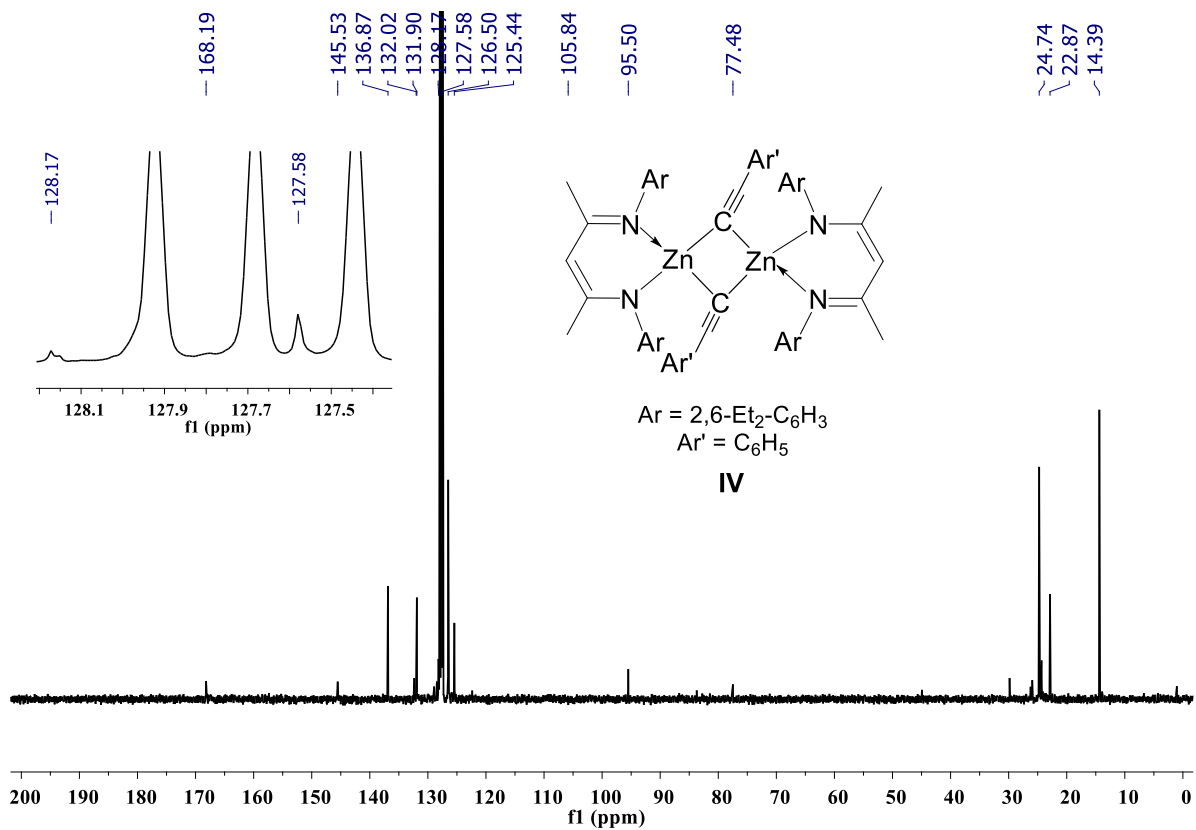


Figure S22: $^{13}\text{C}\{^1\text{H}\}$ NMR (100 MHz, 25 °C, C_6D_6) spectrum of compound IV.

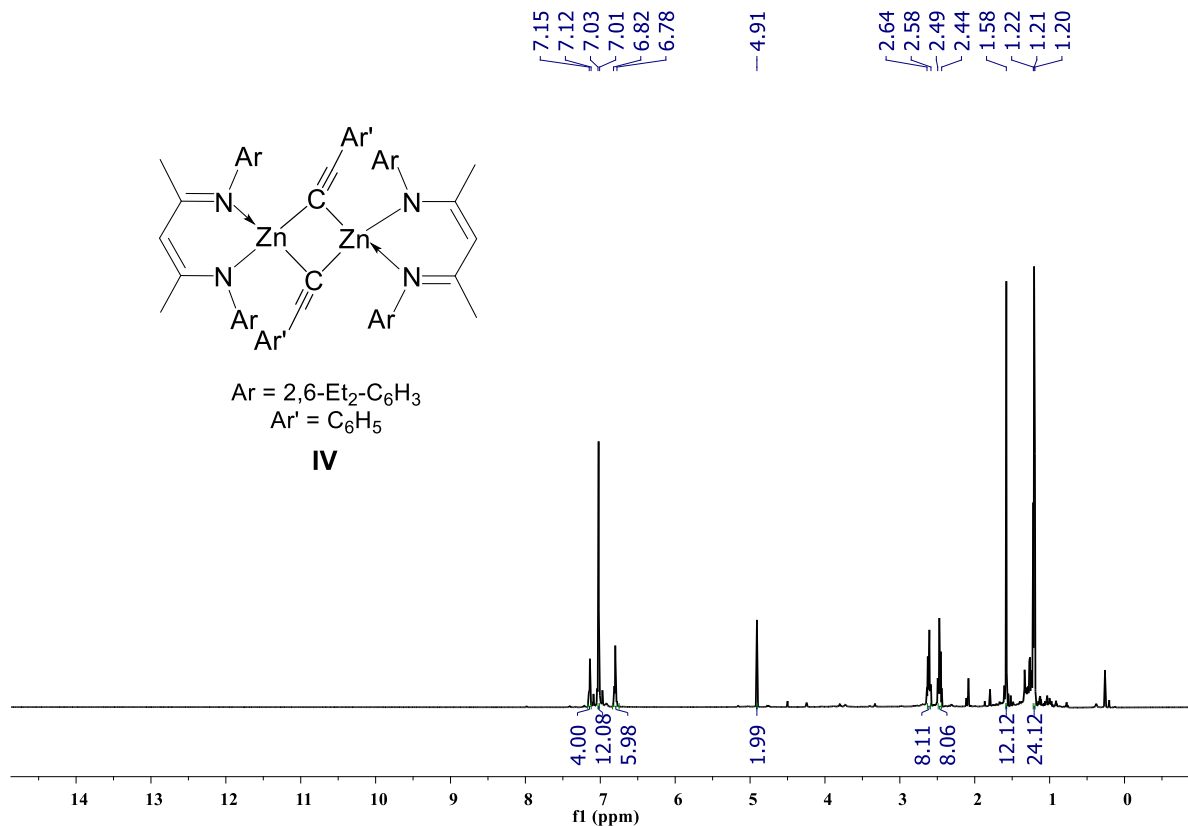


Figure S23: ^1H NMR (700 MHz, 25 °C, d_8 -toluene) spectrum of compound IV.

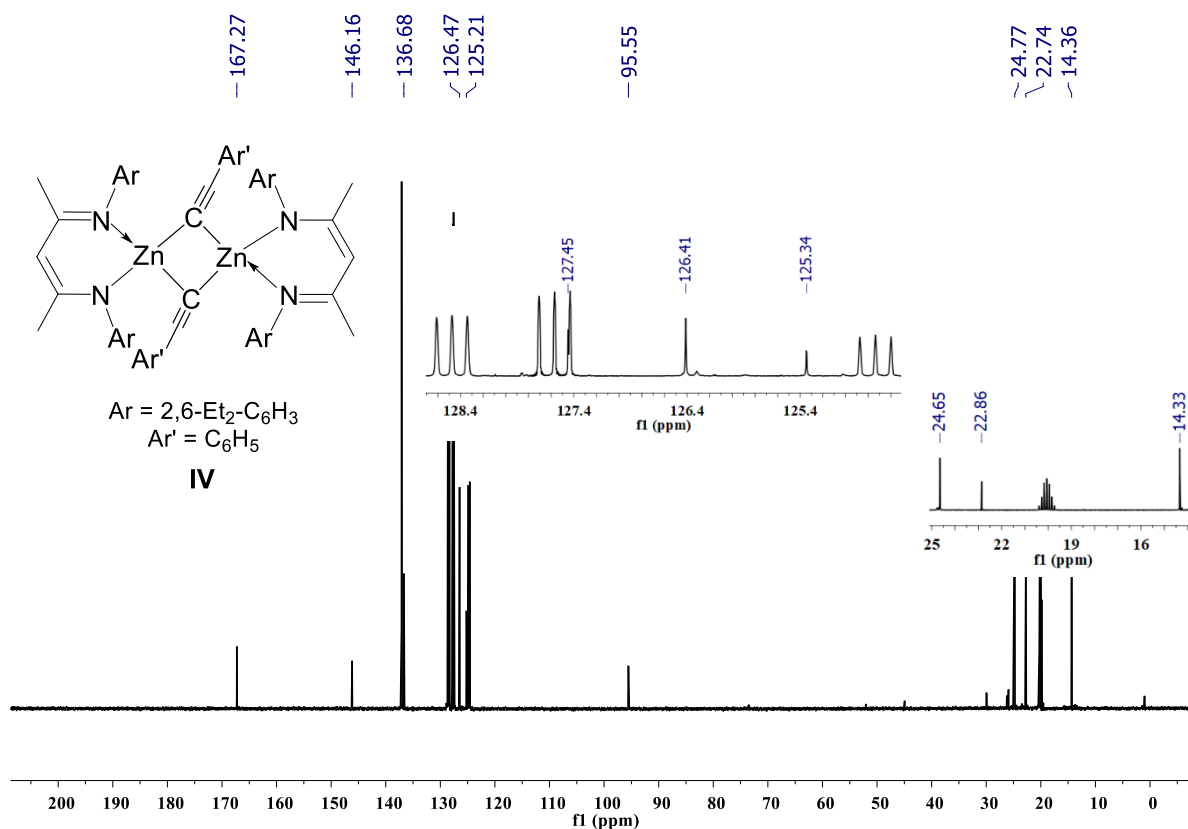


Figure S24: ¹³C{¹H} NMR (176 MHz, 25 °C, *d*₈-toluene) spectrum of compound **IV**.

The reaction between zinc alkynyl **IV and HBpin {NMR-Scale}:** The addition of HBpin (6.81 μL, 0.047 mmol) to a J. Young valve NMR tube containing a solution of compound **IV** (0.023 mmol) in *d*₈-toluene at room temperature after 30 min. resulted in the formation of compounds **III** and **2a**, with a 25% yield observed by multinuclear NMR spectroscopy. ¹H and ¹¹B NMR spectroscopy revealed that the reaction has reached an equilibrium best evident by the integration of resonance for Bpin moieties of **2a** and HBpin. Extended heating up to 24 h at 80 °C showed no change in the relative ratio of **2a** and **IV**, suggesting that the equilibrium position had already been reached before heating. NMR Yield: (25%).

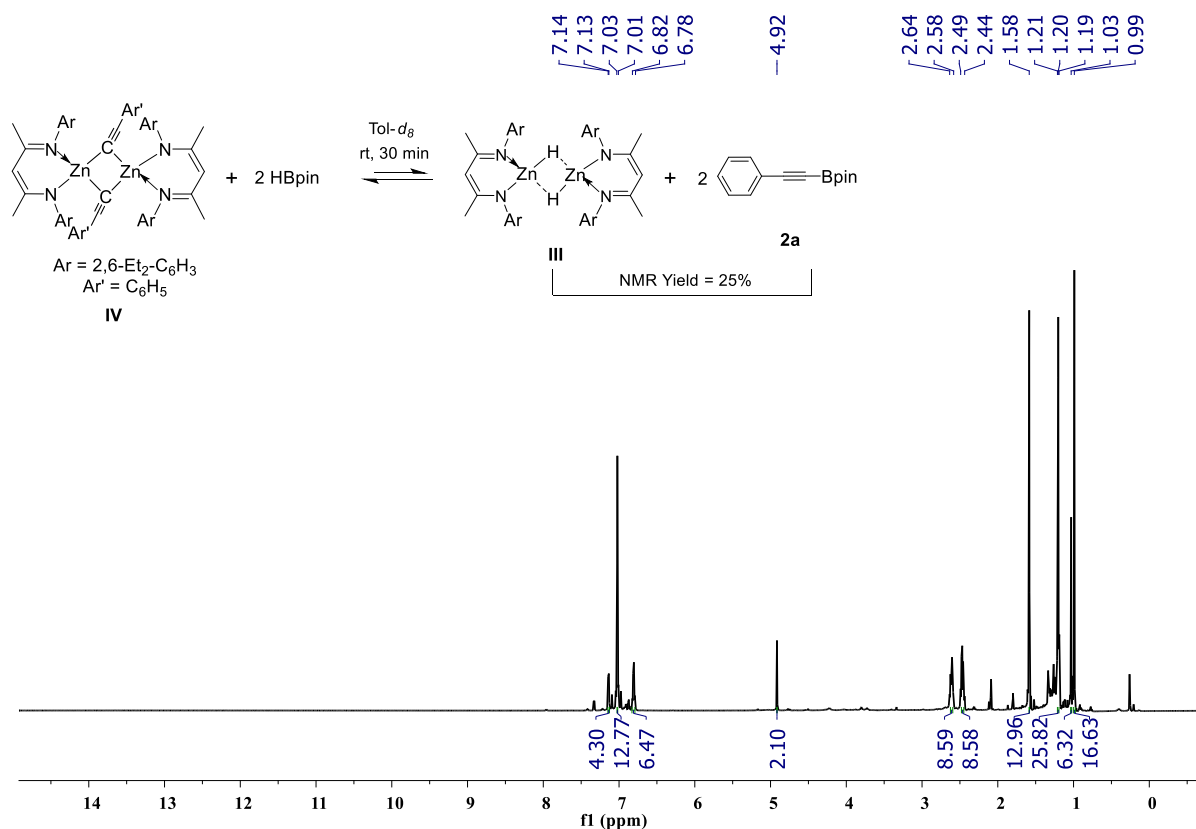


Figure S25: ¹H NMR (700 MHz, 25 °C, *d*₈-toluene) spectrum of compounds [L²ZnH]₂ & **2a**.

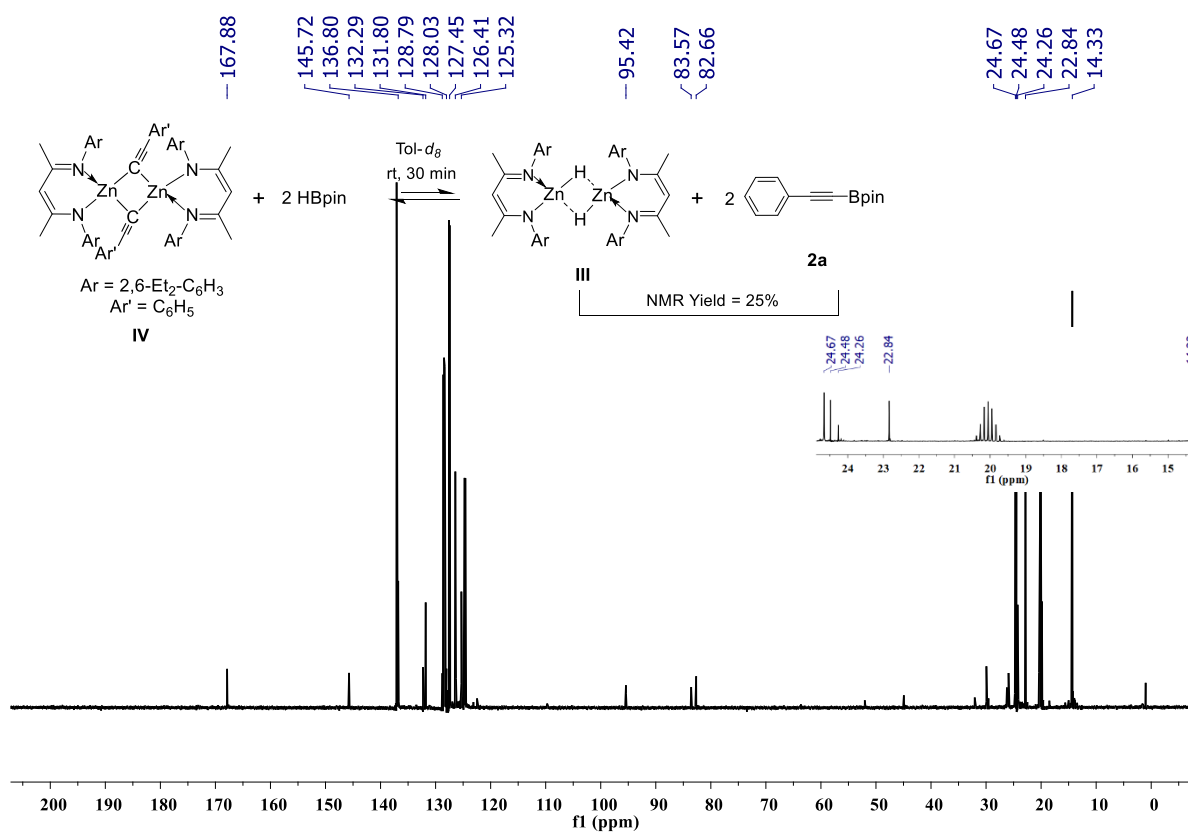


Figure S26: ¹³C{¹H} NMR (176 MHz, 25 °C, *d*₈-toluene) spectrum of compounds [L²ZnH]₂ & **2a**.

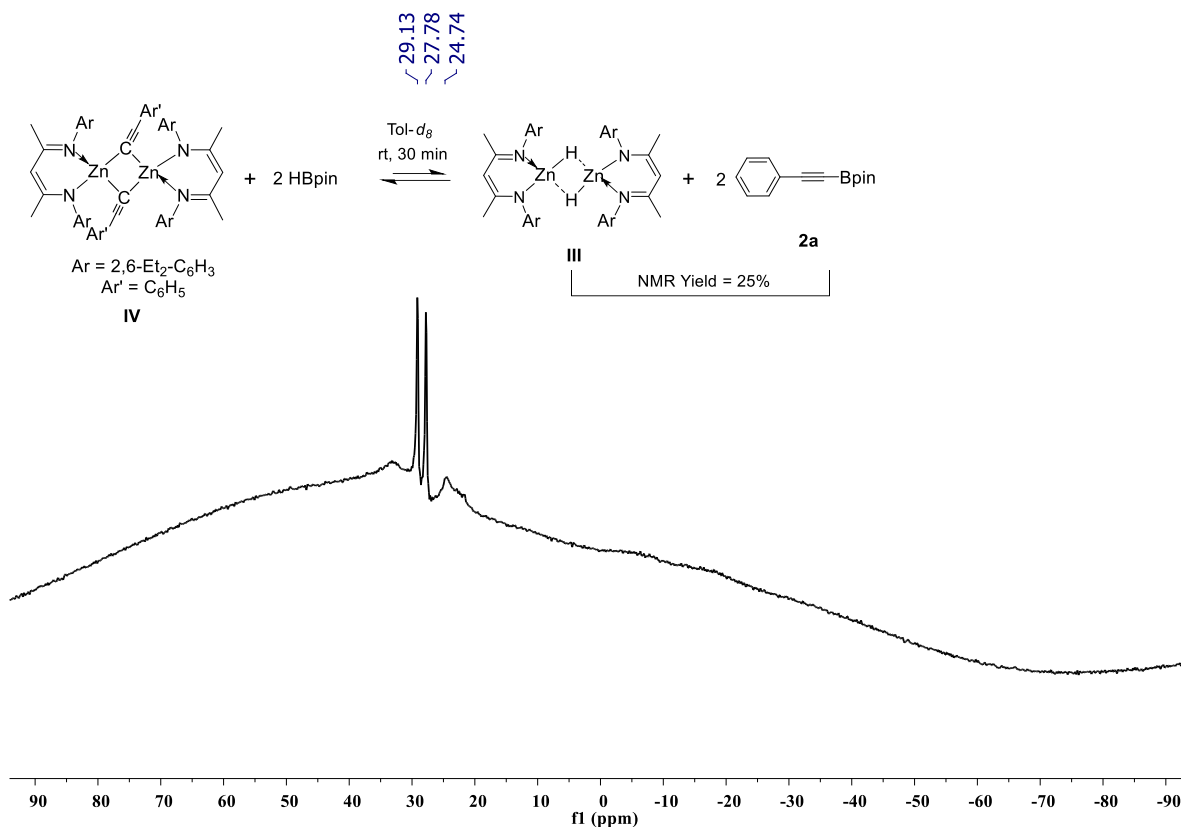


Figure S27: ^{11}B NMR (128 MHz, 25 °C, d_8 -toluene) spectrum of compounds $[\text{L}^2\text{ZnH}]_2$ & **2a**. A doublet peak at δ 27.78 – 29.13 ppm arises from free HBpin.

The reaction between zinc hydride III and 2a {NMR-Scale}: The addition of **2a** (10.71 mg, 0.047 mmol) to a solution of complex **III** (0.020 g, 25 °C, 0.023 mmol) in d_8 -toluene in a J. Young valve NMR tube after 1h at 60 °C resulted in the formation of compound **IV** and HBpin with 75% yield observed by multinuclear NMR spectroscopy. ^1H and ^{11}B NMR spectroscopy revealed that the reaction has reached an equilibrium best evident by the integration of resonance for Bpin moieties of **2a** and **IV**. Extended heating up to 24 h at 80 °C showed no change in the relative ratio of **2a** and **IV**, suggesting that the equilibrium position had already been reached before heating. NMR Yield: (75%).

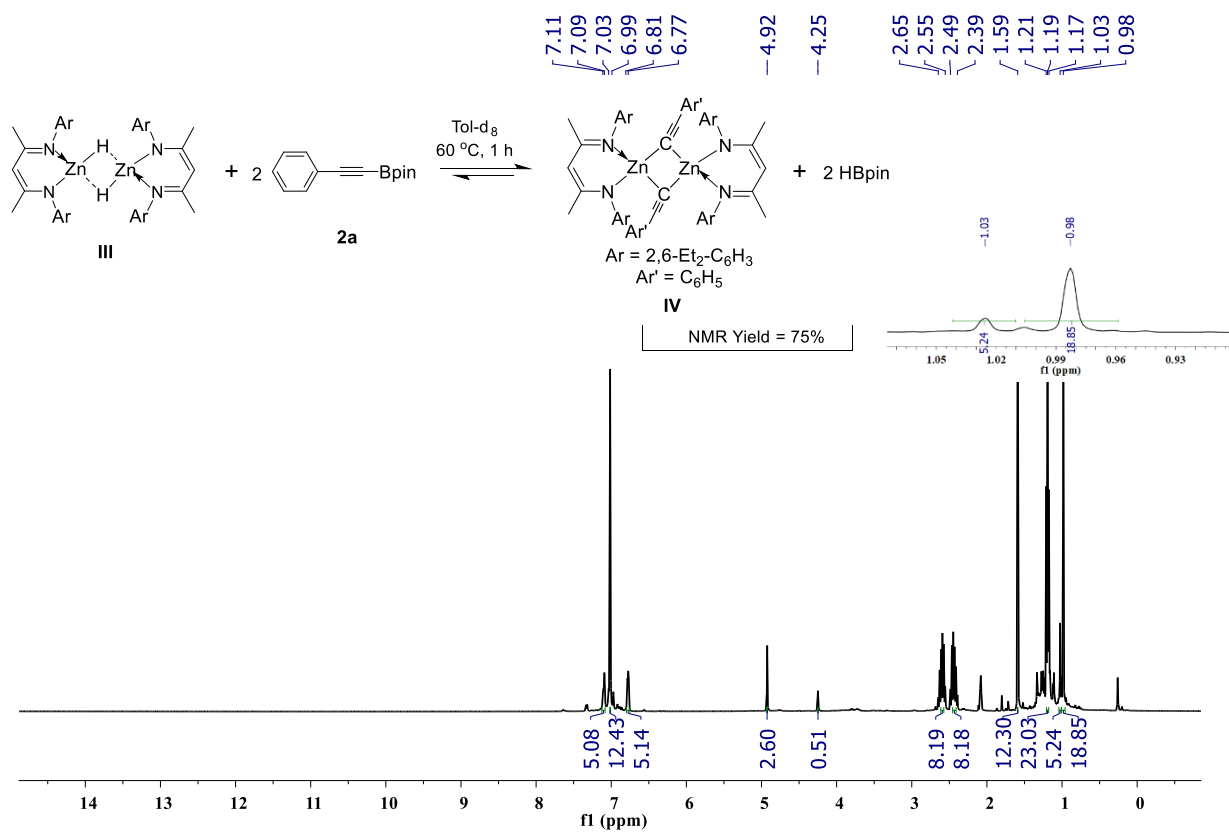


Figure S28: ^1H NMR (400 MHz, 25°C , d_8 -toluene) spectrum of compounds IV & 2HBpin.

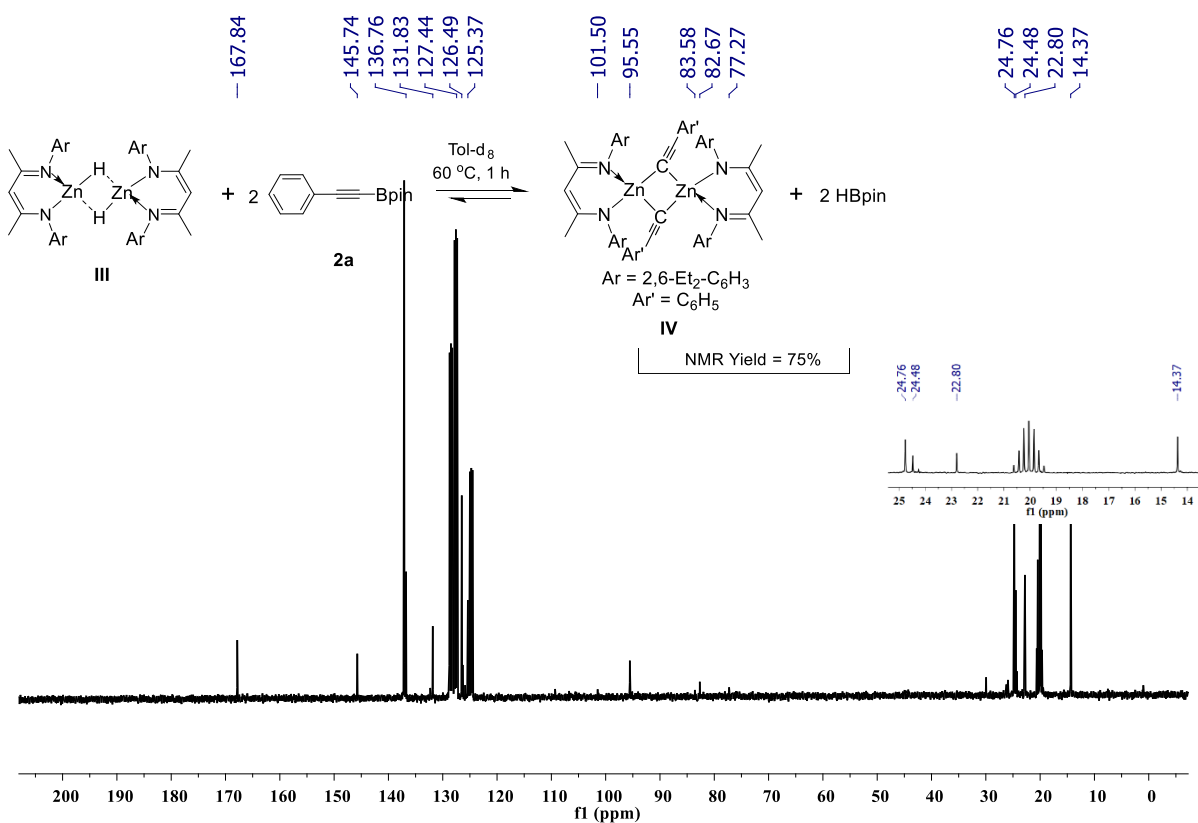


Figure S29: $^{13}\text{C}\{^1\text{H}\}$ NMR (100 MHz, 25°C , d_8 -toluene) spectrum of compounds IV & 2HBpin.

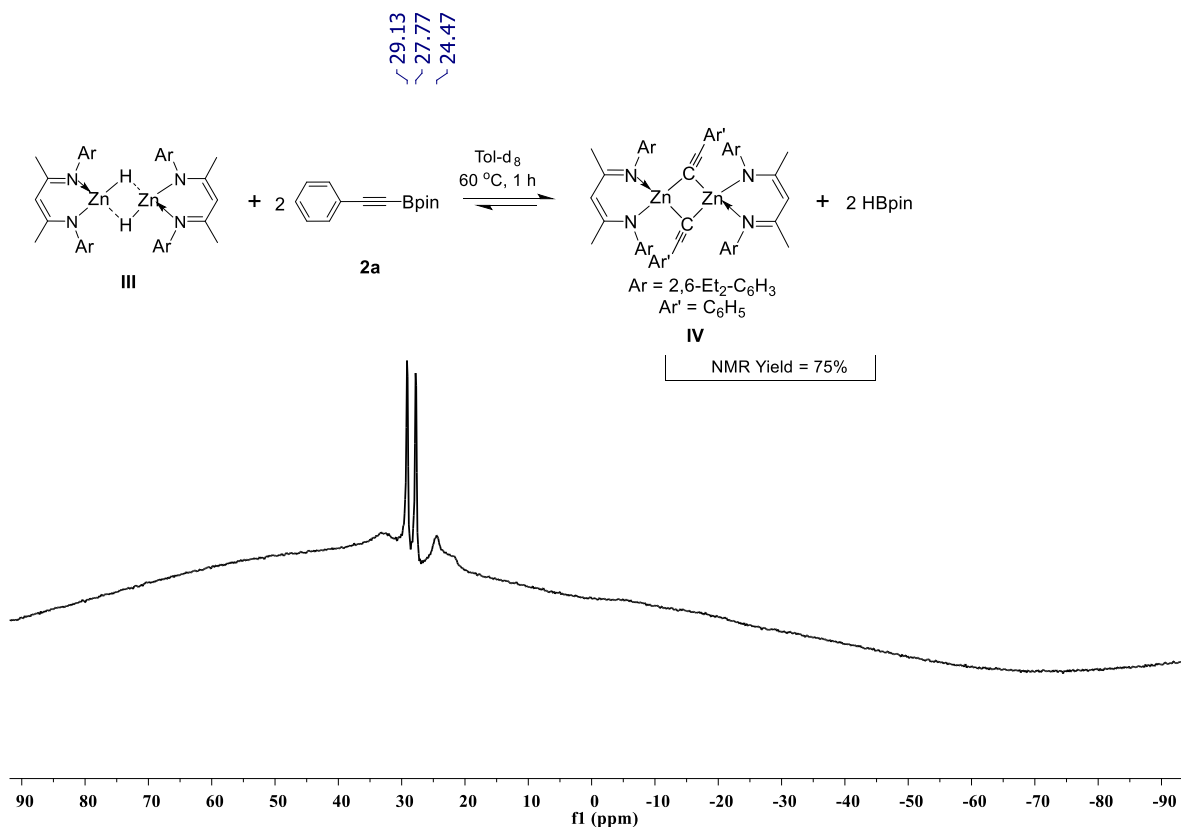


Figure S30: ^{11}B NMR (128 MHz, 25 °C, d_8 -toluene) spectrum of compounds **IV** & 2HBpin. A doublet peak at δ 27.77 – 29.13 ppm arises from free HBpin.

Synthesis of compound IV and 2a {NMR-Scale}: The addition of phenylacetylene (5.15 μL , 0.047 mmol) to a J. Young valve NMR tube containing a solution of compound **III** and **2a** (25%) in d_8 -toluene at room temperature after 20 min. resulted in the complete formation of compounds **IV** and **2a** was observed by ^1H and ^{11}B NMR spectroscopy. The above study indicates that once 25% of compound **III** and **2a** were formed, it immediately reacted with one additional equivalent of phenylacetylene to form a quantitative amount of product **2a** and compound **IV**. It stops the equilibrium reaction between compounds **IV** and **2a**. NMR Yield: (>99%). ^1H NMR (700 MHz, d_8 -toluene) δ 7.34 – 7.33 (m, 4H), 7.14 – 7.13 (m, 4H), 7.05 – 7.02 (m, 12H), 6.92 (t, $^3J_{\text{HH}} = 7.1$ Hz, 3H), 6.88 (t, $^3J_{\text{HH}} = 7.1$ Hz, 3H), 6.81 – 6.79 (m, 6H), 4.92 (s, 2H), 2.63 – 2.57 (m, 8H), 2.49 – 2.44 (m, 8H), 1.58 (s, 12 H), 1.21 (t, $^3J_{\text{HH}} = 7.3$ Hz, 24H), 1.04 (s, 24H). $^{13}\text{C}\{^1\text{H}\}$ NMR (176 MHz, d_8 -toluene) δ 168.1, 145.5, 136.8, 132.2, 131.9,

131.8, 128.8, 128.0, 128.0, 126.4, 125.3, 122.4, 95.4, 83.5, 77.3, 29.9, 24.2, 22.8, 14.3. ^{11}B
 NMR (128 MHz, C_6D_6) δ 24.38.

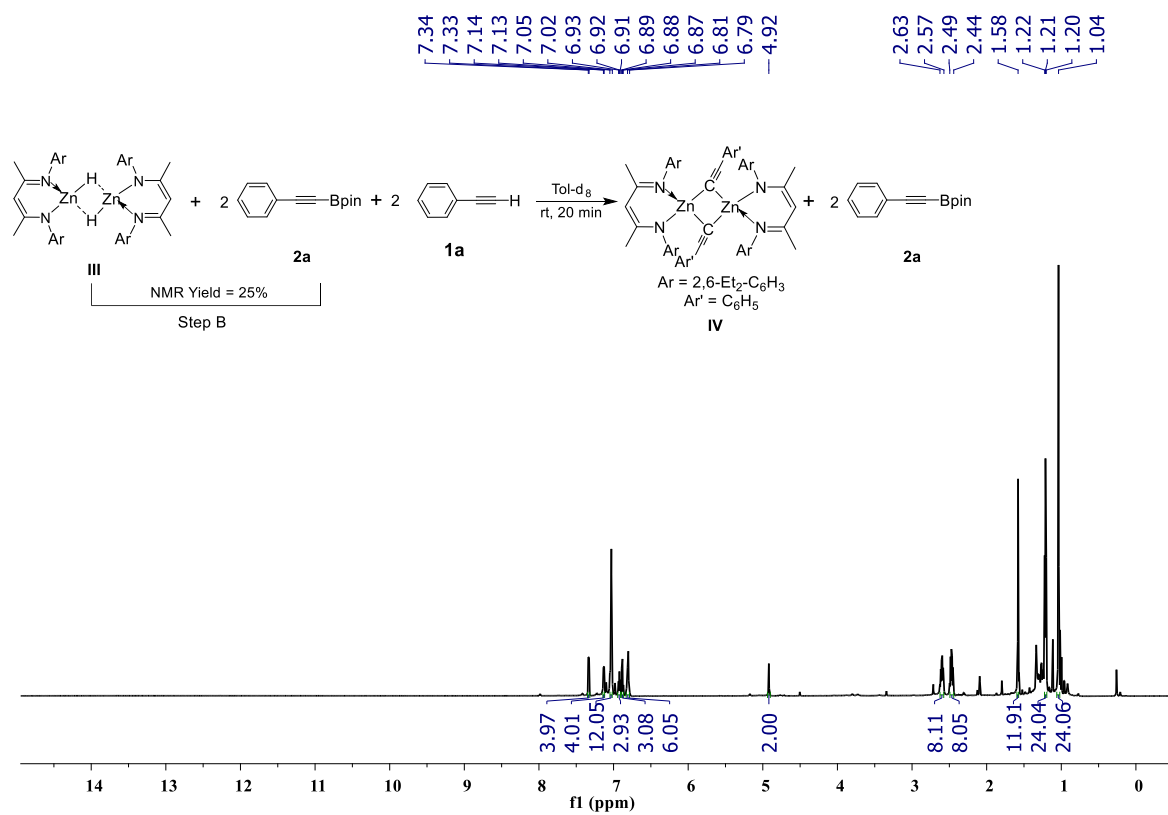


Figure S31: ^1H NMR (700 MHz, 25 °C, d_8 -toluene) spectrum of compounds IV & 2a.

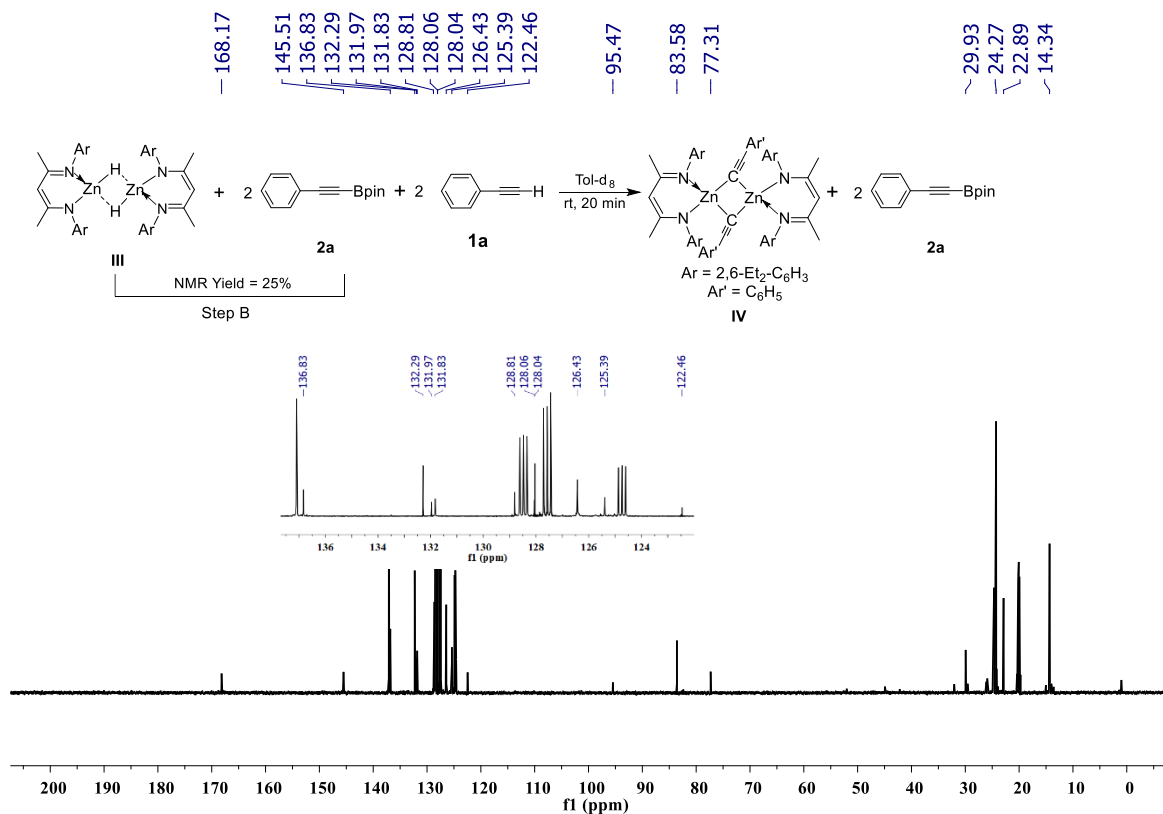


Figure S32: $^{13}\text{C}\{^1\text{H}\}$ NMR (176 MHz, 25 °C, d_8 -toluene) spectrum of compounds IV & 2a.

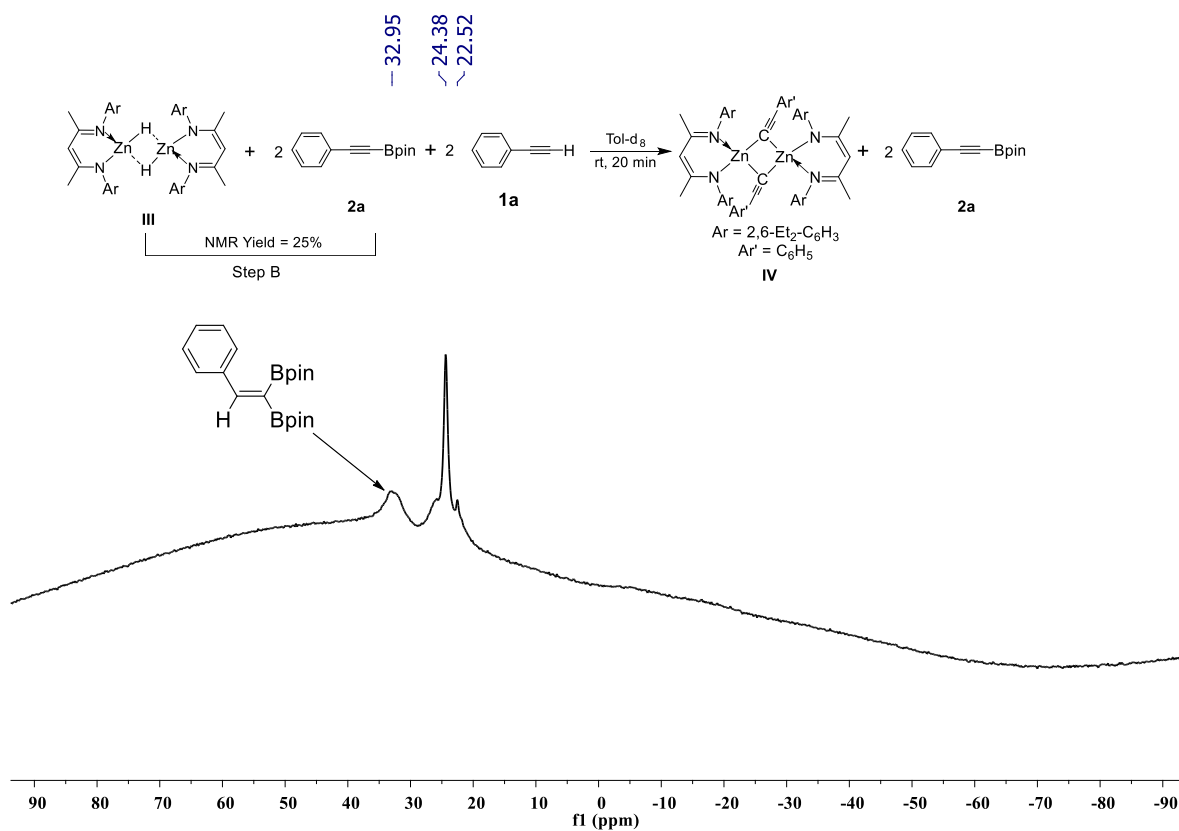


Figure S33: ^{11}B NMR (128 MHz, 25 °C, C_6D_6) spectrum of compounds IV & 2a.

The reaction between zinc hydride **III, phenylacetylene, and compound **2a** {NMR-Scale}:**

In a J. Young valve NMR tube (0.020 g, 25 °C, 0.023 mmol) complex **I**, (10.71 mg, 0.047 mmol) of **2a**, and (5.15 μ L, 0.047 mmol) of phenylacetylene were added successively in *d*₈-toluene. Reaction progress was monitored by ¹H NMR analyses, which confirmed at room temperature after 25 min complete formation of compound **IV** with the liberation of H₂ gas, and unreacted compound **2a** was observed by ¹H and ¹¹B NMR spectroscopy. The above study indicates that the exclusive formation of compound **IV** with a quantitative yield and compound **2a** was untouched. It again revealed that phenylacetylene's presence stops the equilibrium reaction between compounds **III** and **2a**. NMR Yield: (>99%). ¹H NMR (700 MHz, *d*₈-toluene) δ 7.34 – 7.33 (m, 4H), 7.14 – 7.13 (m, 4H), 7.05 – 7.02 (m, 12H), 6.92 (t, ³J_{HH} = 7.0 Hz, 3H), 6.88 (t, ³J_{HH} = 7.2 Hz, 3H), 6.81 – 6.78 (m, 6H), 4.92 (s, 2H), 2.63 – 2.57 (m, 8H), 2.49 – 2.44 (m, 8H), 1.58 (s, 12 H), 1.21 (t, ³J_{HH} = 7.3 Hz, 24H), 1.04 (s, 24H). ¹³C{¹H} NMR (176 MHz, *d*₈-toluene) δ 168.1, 145.5, 136.8, 132.3, 131.9, 131.8, 128.8, 128.0, 128.0, 126.4, 125.4, 122.4, 95.4, 83.5, 77.3, 24.6, 24.2, 22.8, 14.3. ¹¹B NMR (128 MHz, *d*₈-toluene) δ 24.70.

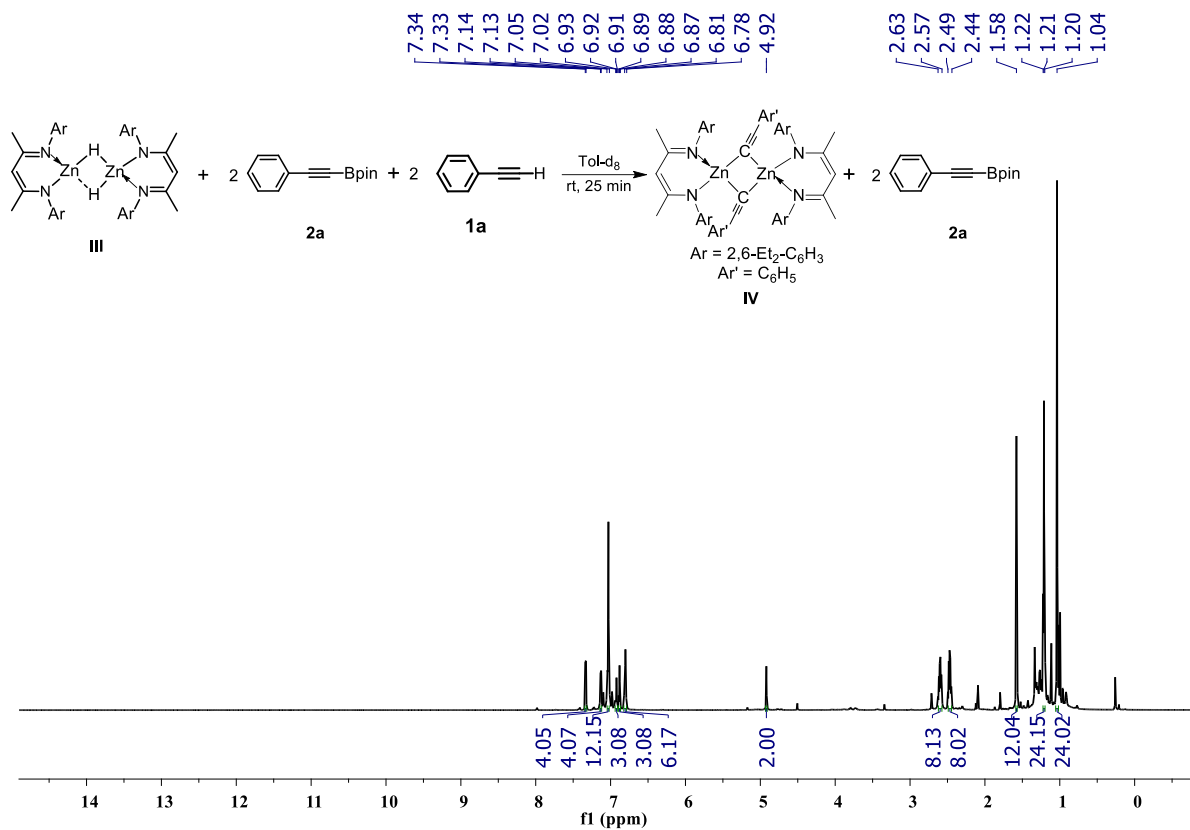


Figure S34: ¹H NMR (700 MHz, 25 °C, d₈-toluene) spectrum of compounds IV & 2a.

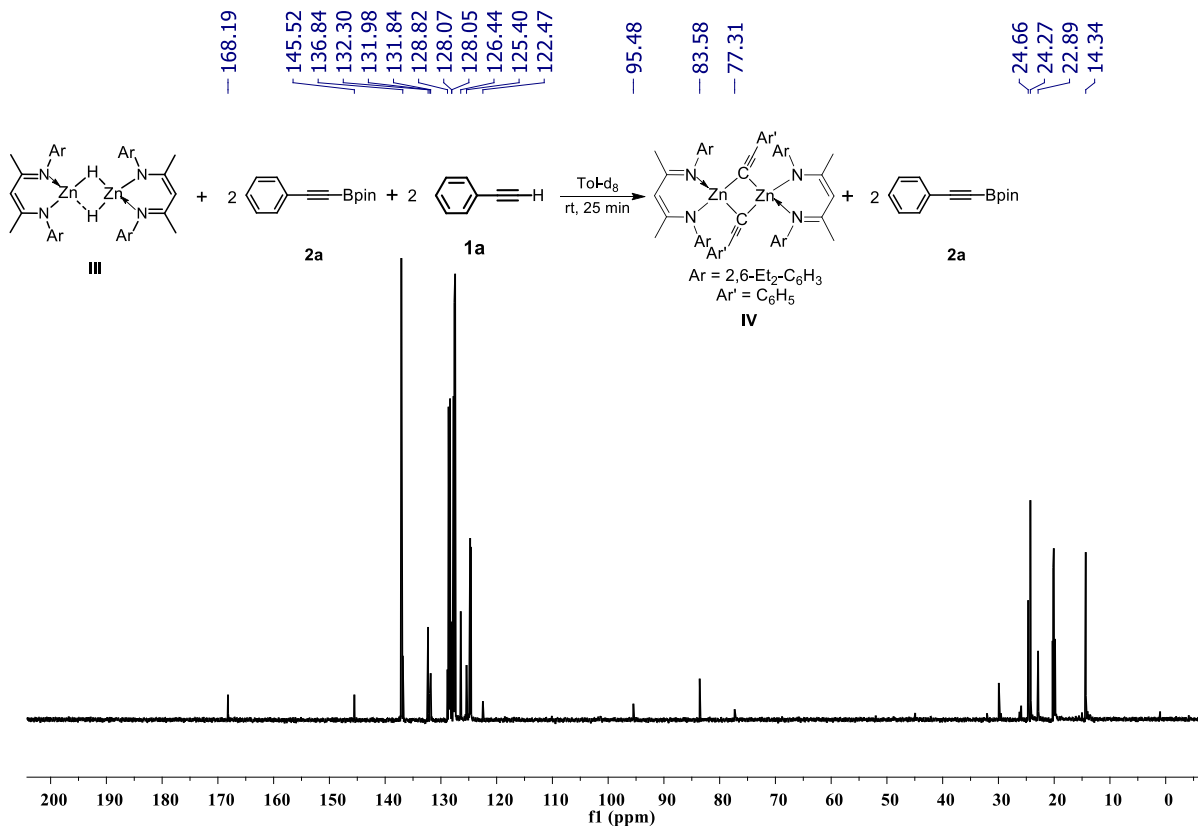


Figure S35: ¹³C{¹H} NMR (176 MHz, 25 °C, d₈-toluene) spectrum of compounds IV & 2a.

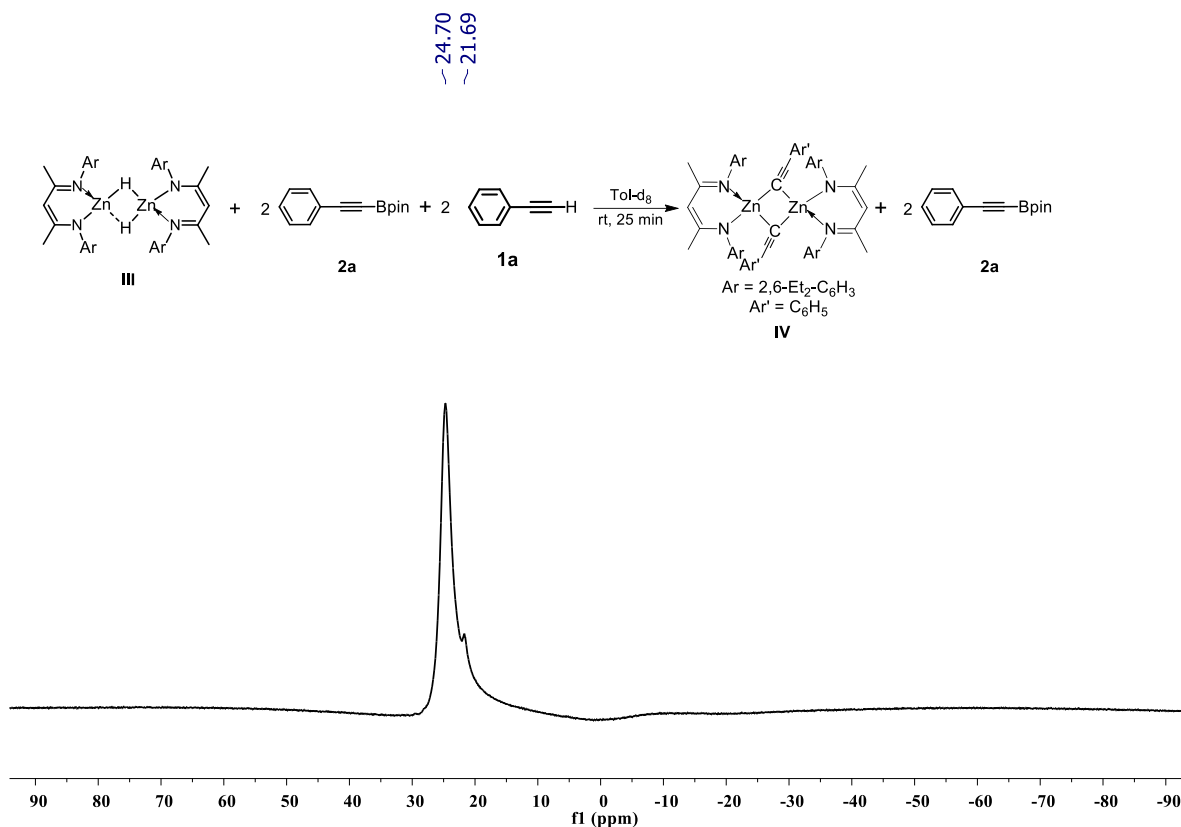
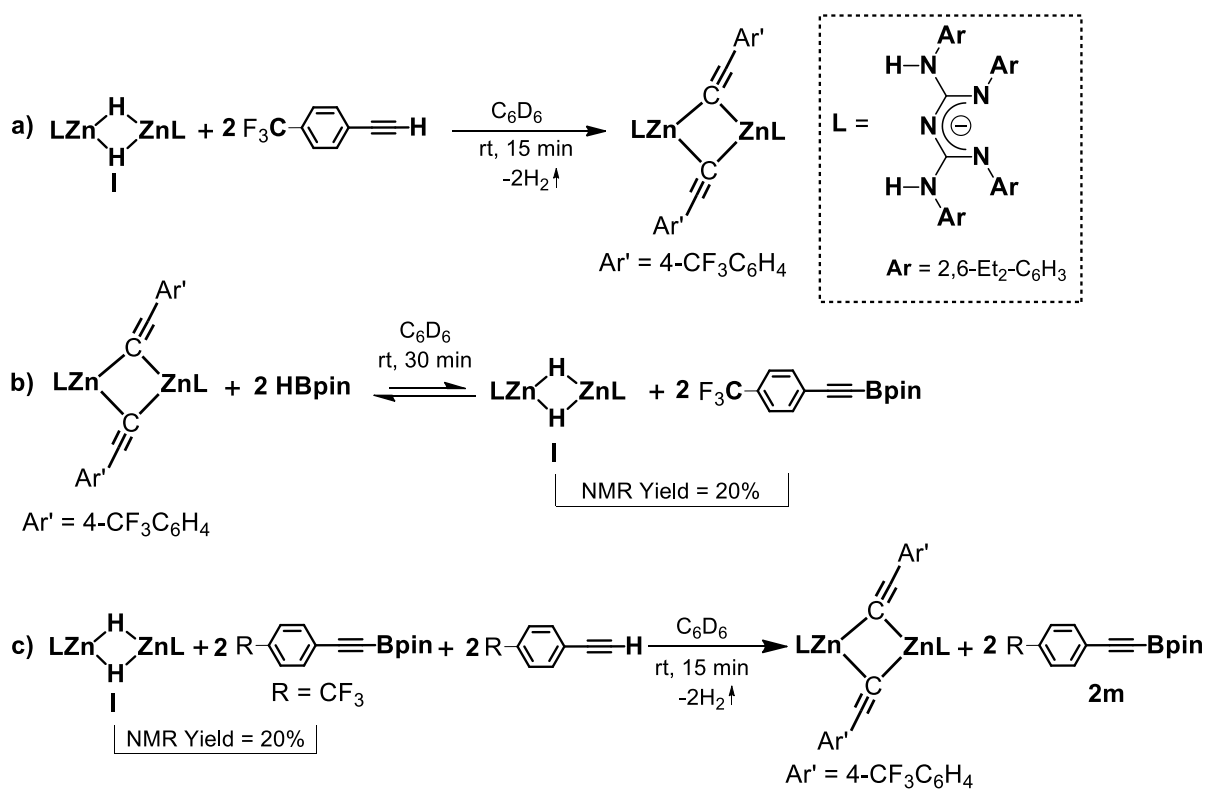


Figure S36: ^{11}B NMR (128 MHz, 25 °C, d_8 -toluene) spectrum of compounds **IV** & **2a**.

Scheme S1. Stoichiometric Experiments for Dehydroborylation of Terminal Alkynes



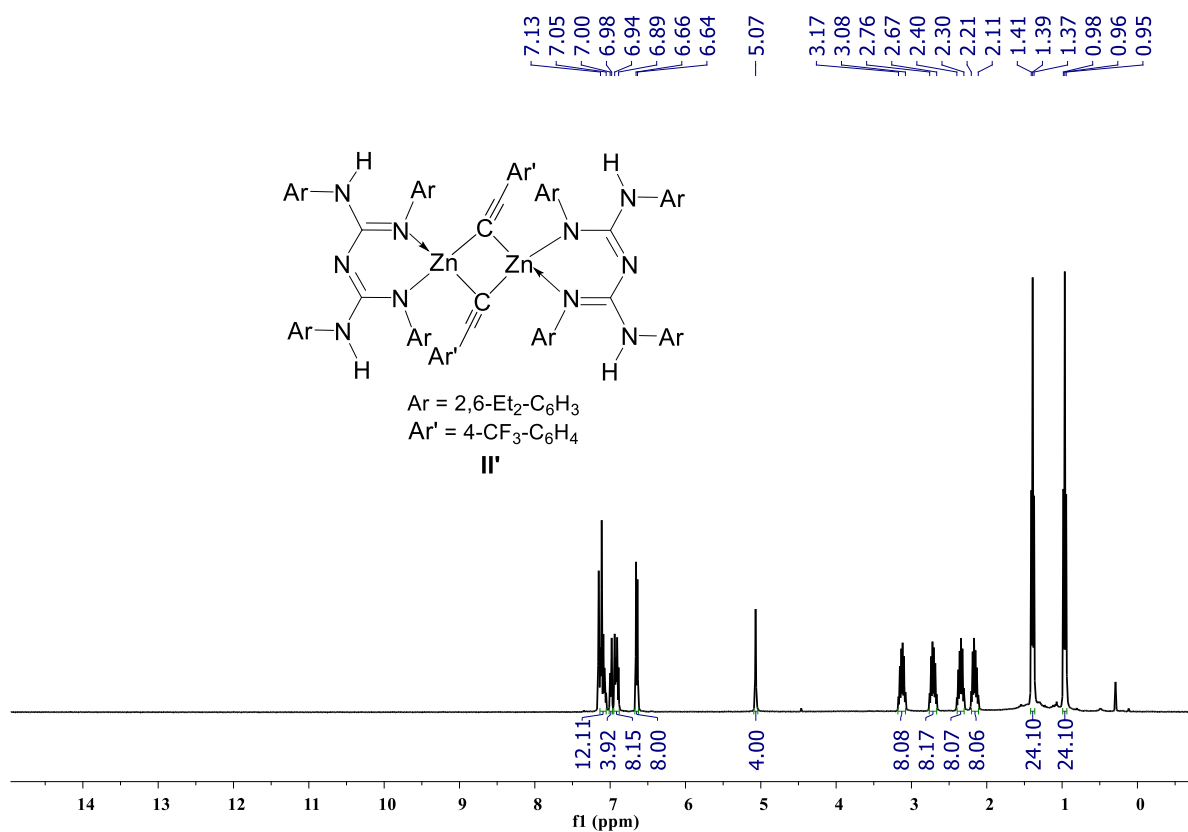


Figure S37: ¹H NMR (400 MHz, 25 °C, C₆D₆) spectrum of compound II'.

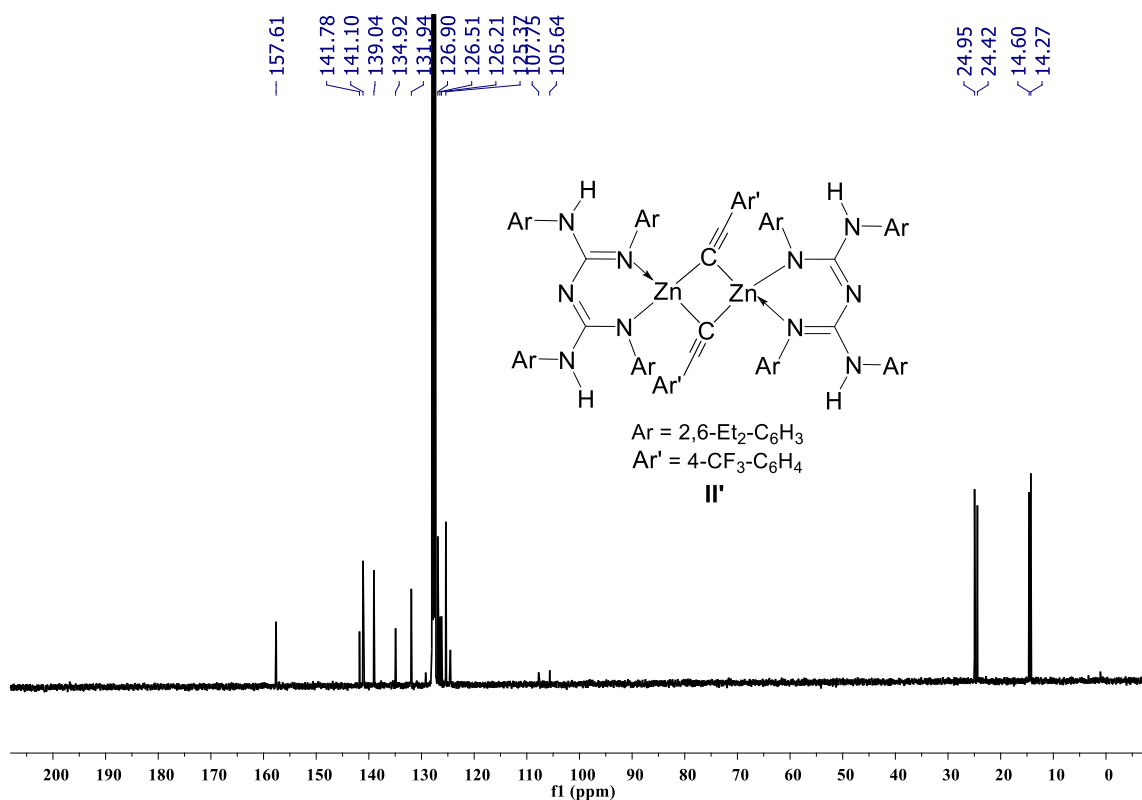


Figure S38: ¹³C{¹H} NMR (100 MHz, 25 °C, C₆D₆) spectrum of compound II'.

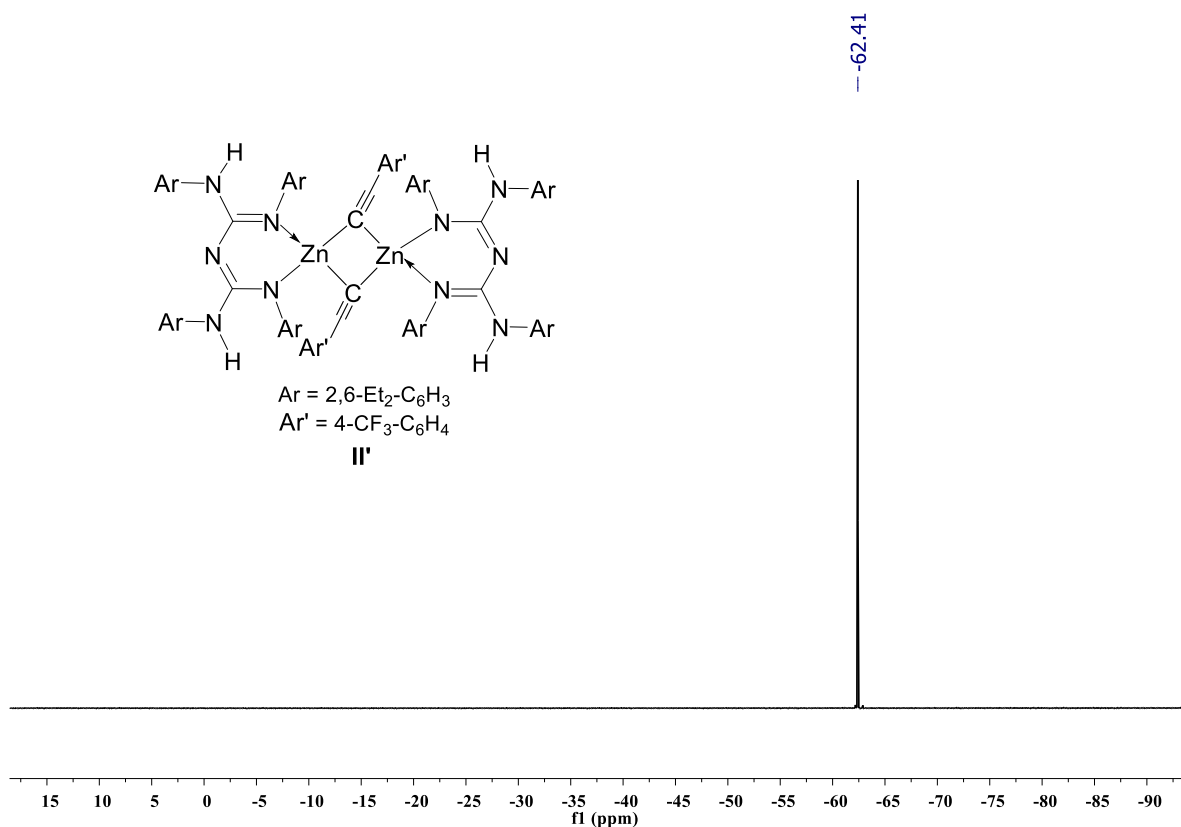


Figure S39: $^{19}\text{F}\{^1\text{H}\}$ NMR (377 MHz, 25 °C, C_6D_6) spectrum of compound **II'**.

The reaction between zinc alkynyl **II' and HBpin {NMR-Scale}:** The addition of HBpin (4.06 μL , 0.028 mmol) to a J. Young valve NMR tube containing a solution of compound **II'** (0.014 mmol) in d_8 -toluene at room temperature after 30 minutes resulted in the formation of compounds **I** and **2m** with a 20% yield were observed by multinuclear NMR spectroscopy. ^1H and ^{11}B NMR spectroscopy revealed that the reaction had reached an equilibrium, best evidenced by the integration of resonance for Bpin moieties of **2m** and HBpin. Extended heating up to 24 h at 80 °C showed no change in the relative ratio of **2m** and **II'**, suggesting that the equilibrium position had already been reached before heating. NMR Yield: (20%).

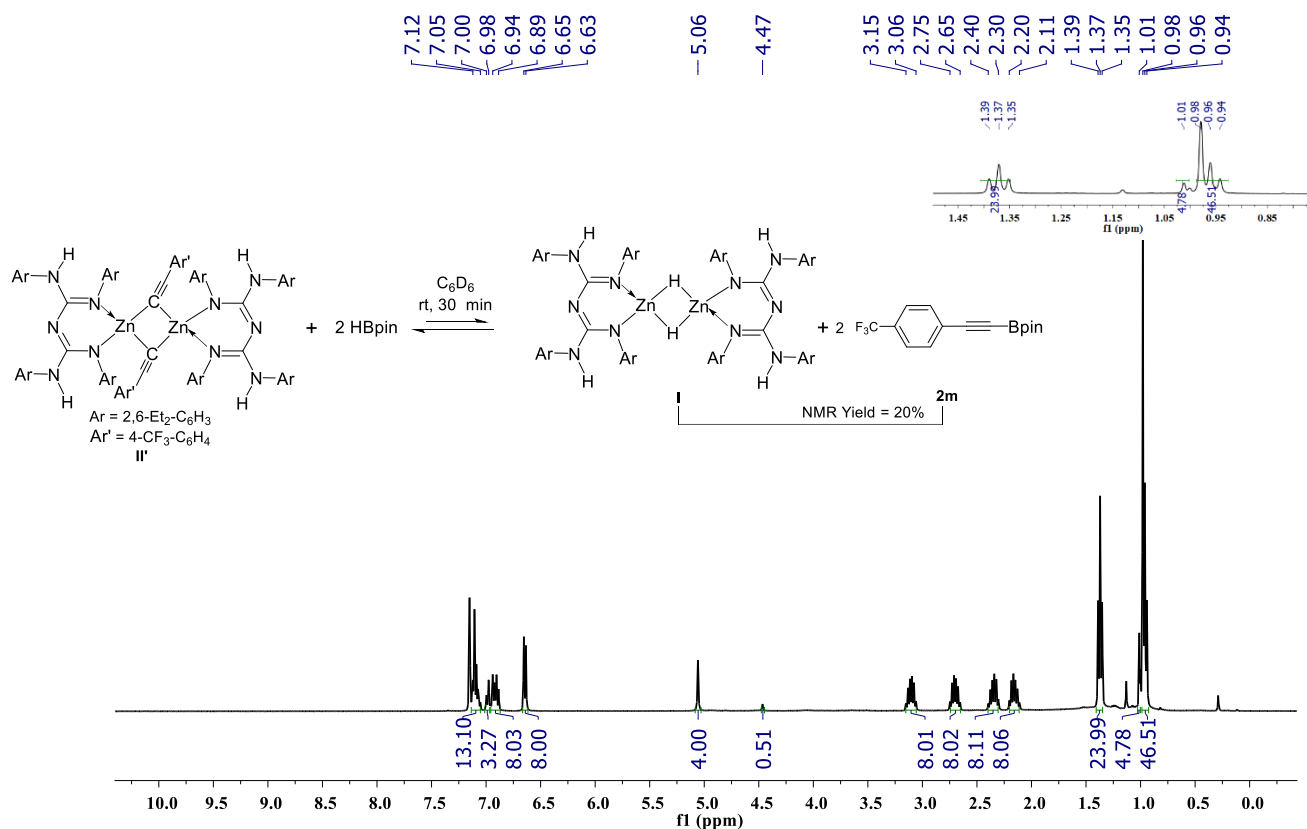


Figure 40: ^1H NMR (400 MHz, 25 °C, C_6D_6) spectrum of compounds $[\text{L}^1\text{ZnH}]_2$ & 2m .

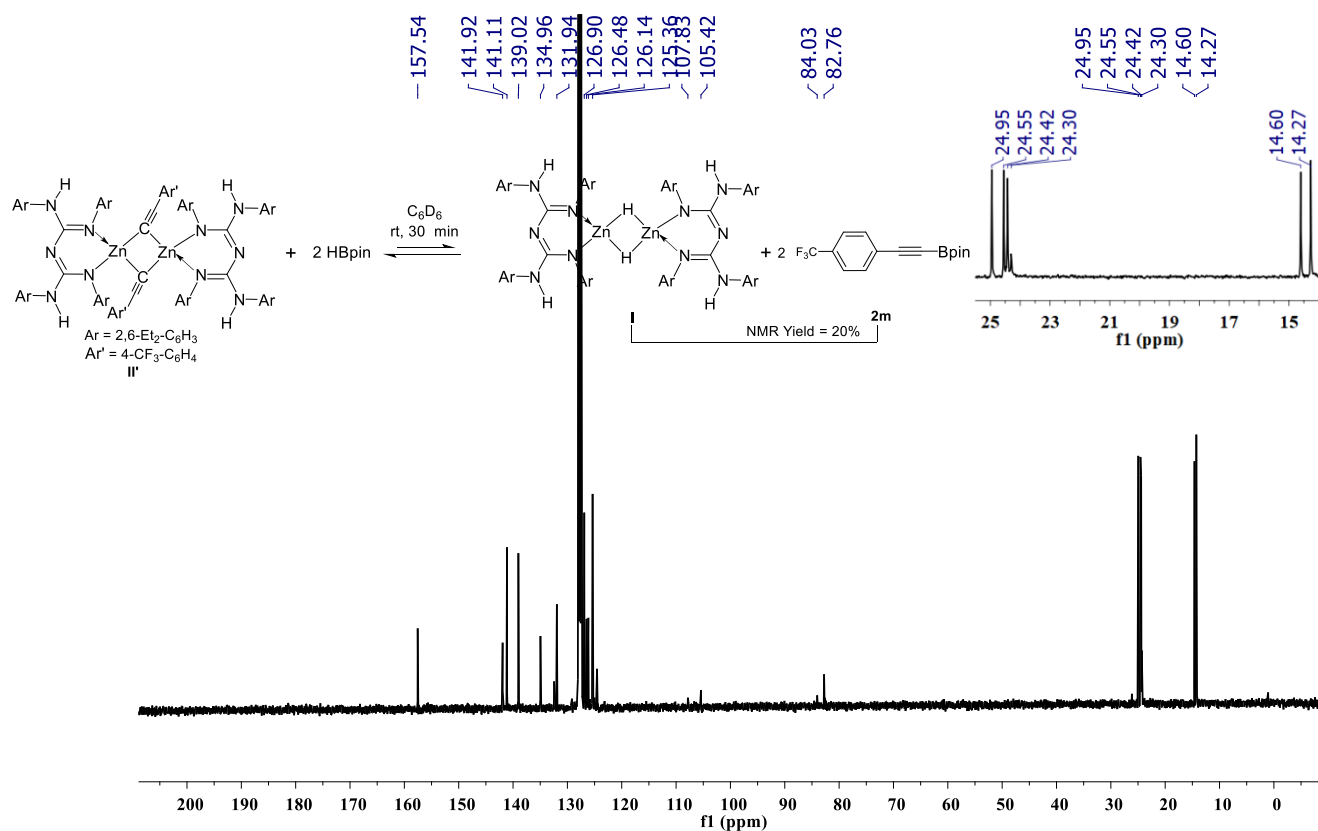


Figure S41: $^{13}\text{C}\{^1\text{H}\}$ NMR (100 MHz, 25 °C, C_6D_6) spectrum of compounds $[\text{L}^1\text{ZnH}]_2$ & 2m .

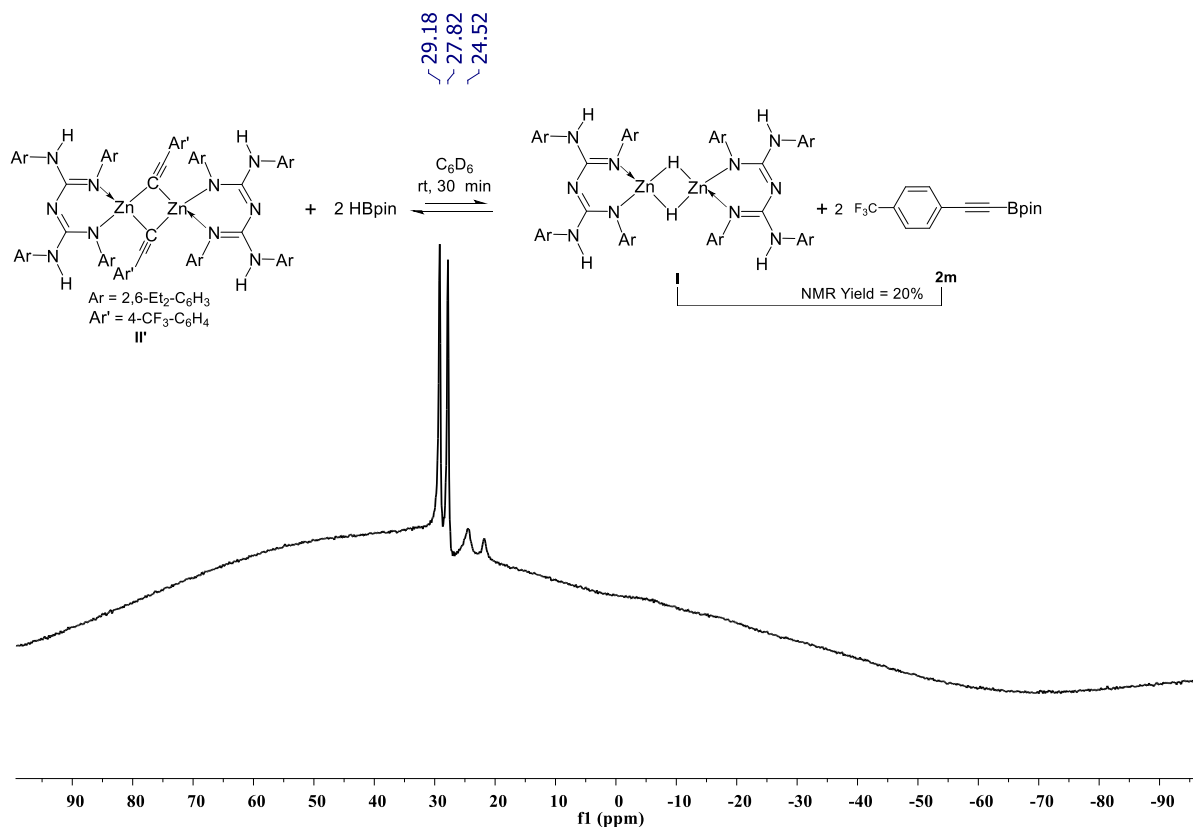


Figure S42: ^{11}B NMR (128 MHz, 25 °C, C_6D_6) spectrum of compounds $[\text{L}^1\text{ZnH}]_2$ & **2m**. A doublet peak at δ 27.82 – 29.18 ppm arises from free HBpin.

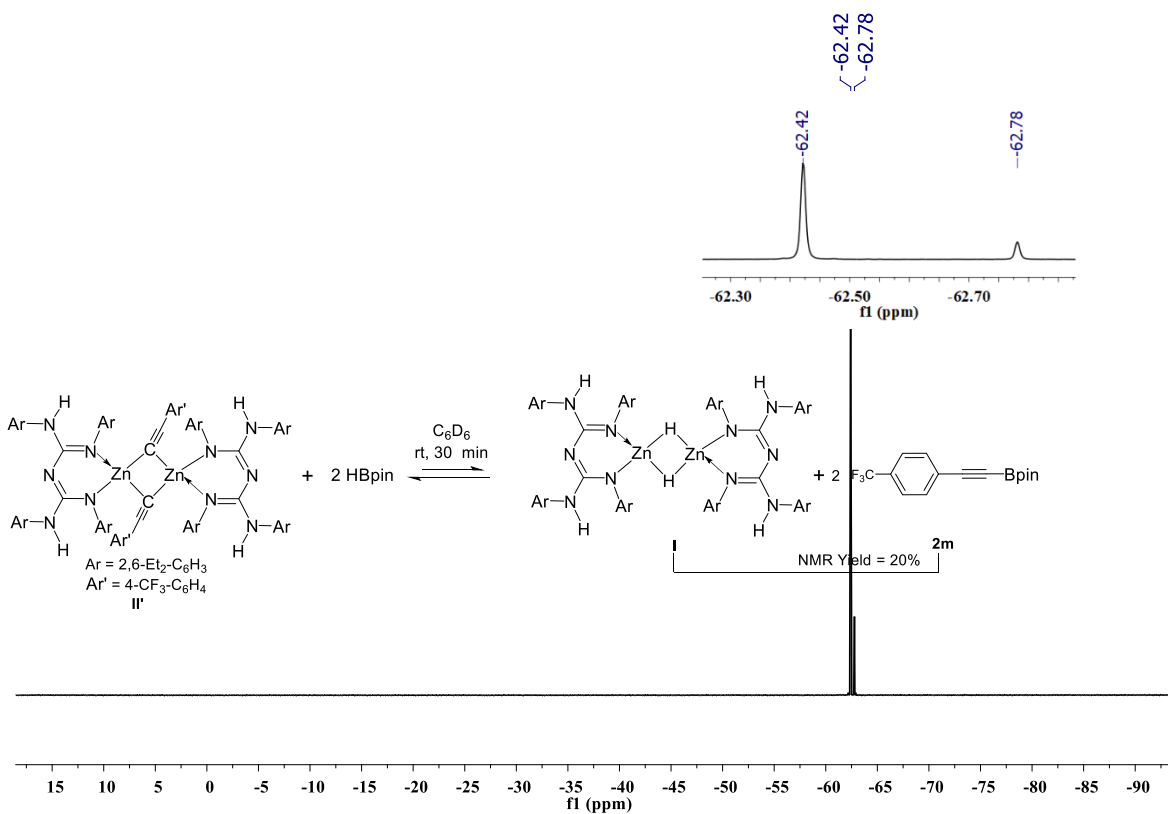


Figure S43: $^{19}\text{F}\{^1\text{H}\}$ NMR (377 MHz, 25 °C, C_6D_6) spectrum of compounds $[\text{L}^1\text{ZnH}]_2$ & **2m**.

Synthesis of compound II' and 2m {NMR-Scale}: The addition of 4-(trifluoromethyl)phenylacetylene (1m) (4.5 μ L, 0.028 mmol) to a J. Young valve NMR tube containing a solution of compound I and 2m (20%) in d_8 -toluene at room temperature after 15 minutes resulted in the complete formation of compound II' and 2m was observed by ^1H and ^{11}B NMR spectroscopy. The above study indicates that once 20% compound 2m and I was formed, it immediately reacted with one additional equivalent of 4-(trifluoromethyl)phenylacetylene to form a quantitative amount of product 2m and compound II'. It stops the equilibrium reaction between compounds or II' and 2m. NMR Yield: (>99%).

^1H NMR (400 MHz, C_6D_6) δ 7.12 – 7.07 (m, 16H), 6.99 – 6.89 (m, 16H), 6.65 – 6.63 (d, $^3J_{\text{HH}} = 9.6$ Hz, 8H), 5.07 (s, 4H), 3.16 – 3.07 (m, 8H), 2.75 – 2.66 (m, 8H), 2.39 – 2.30 (m, 8H), 2.20 – 2.11 (m, 8H), 1.39 (t, $^3J_{\text{HH}} = 7.4$ Hz, 24H), 1.01 (s, 24H), 0.96 (t, $^3J_{\text{HH}} = 7.6$ Hz, 24H).

$^{13}\text{C}\{^1\text{H}\}$ NMR (101 MHz, C_6D_6) δ 157.6, 141.7, 141.0, 139.0, 134.9, 132.4, 131.9, 126.9, 126.5, 126.3, 126.2, 125.0, 125.0, 125.0, 124.9, 124.5, 124.5, 124.5, 124.4, 107.7, 105.4, 84.0, 24.9, 24.4, 24.3, 14.6, 14.2. ^{11}B NMR (128 MHz, C_6D_6) δ 24.60. $^{19}\text{F}\{^1\text{H}\}$ NMR (377 MHz, C_6D_6) δ -62.42, -62.78.

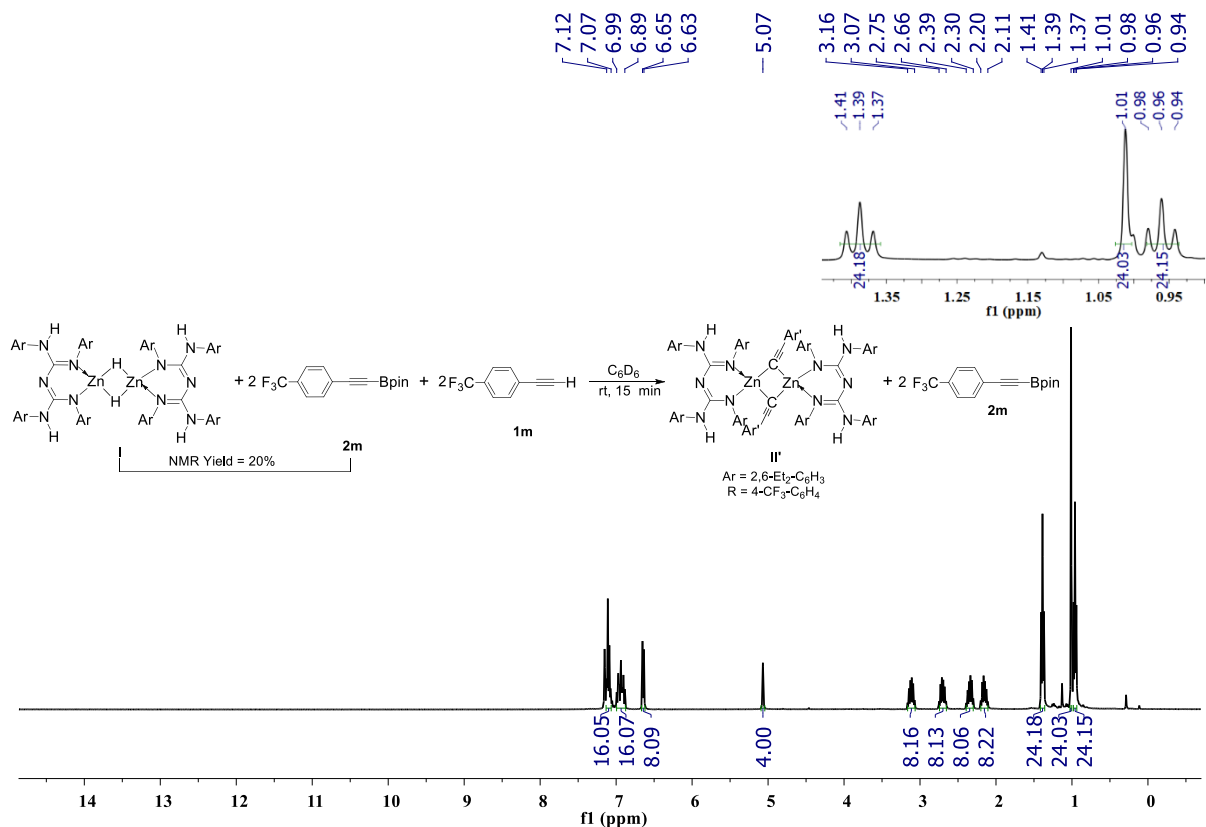


Figure S44: ^1H NMR (400 MHz, 25 °C, C_6D_6) spectrum of compounds II' & 2m.

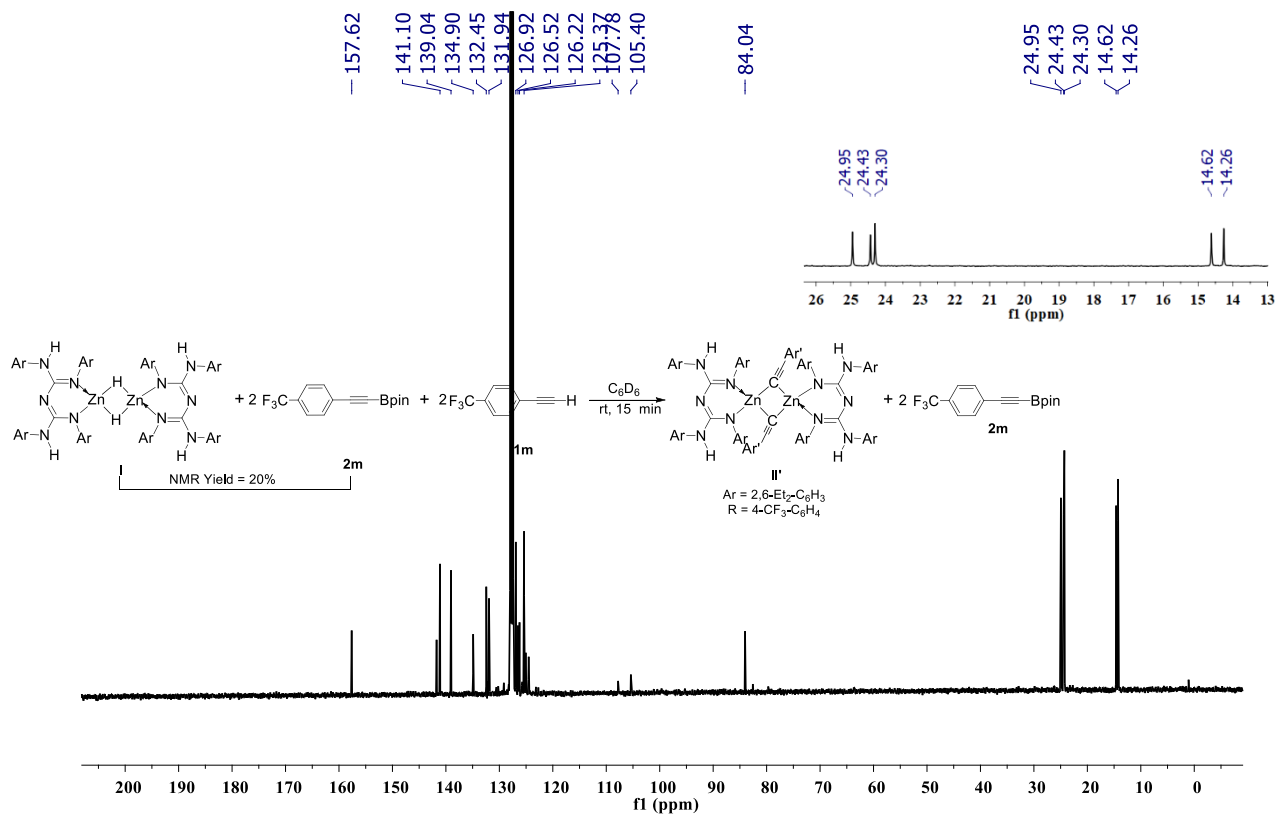


Figure S45: $^{13}\text{C}\{^1\text{H}\}$ NMR (100 MHz, 25 °C, C_6D_6) spectrum of compounds II' & 2m.

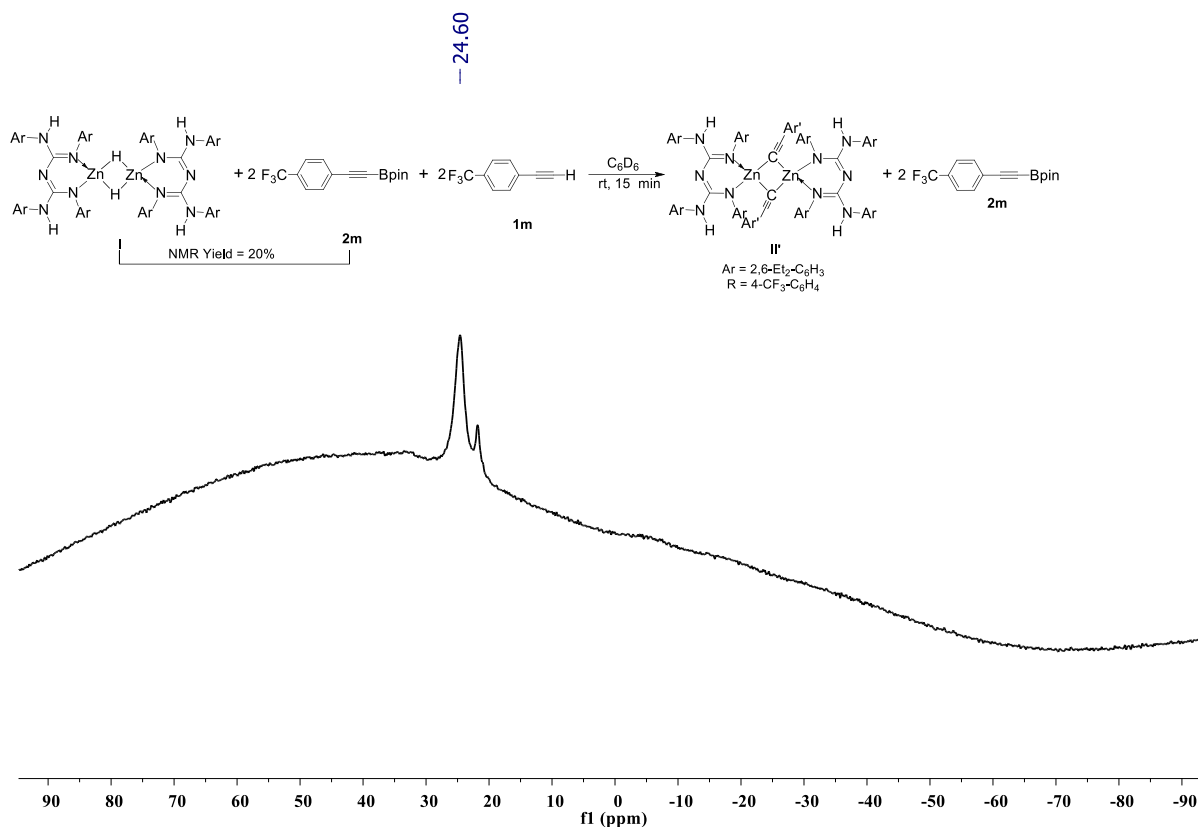


Figure S46: ¹¹B NMR (128 MHz, 25 °C, C₆D₆) spectrum of compounds II' & 2m.

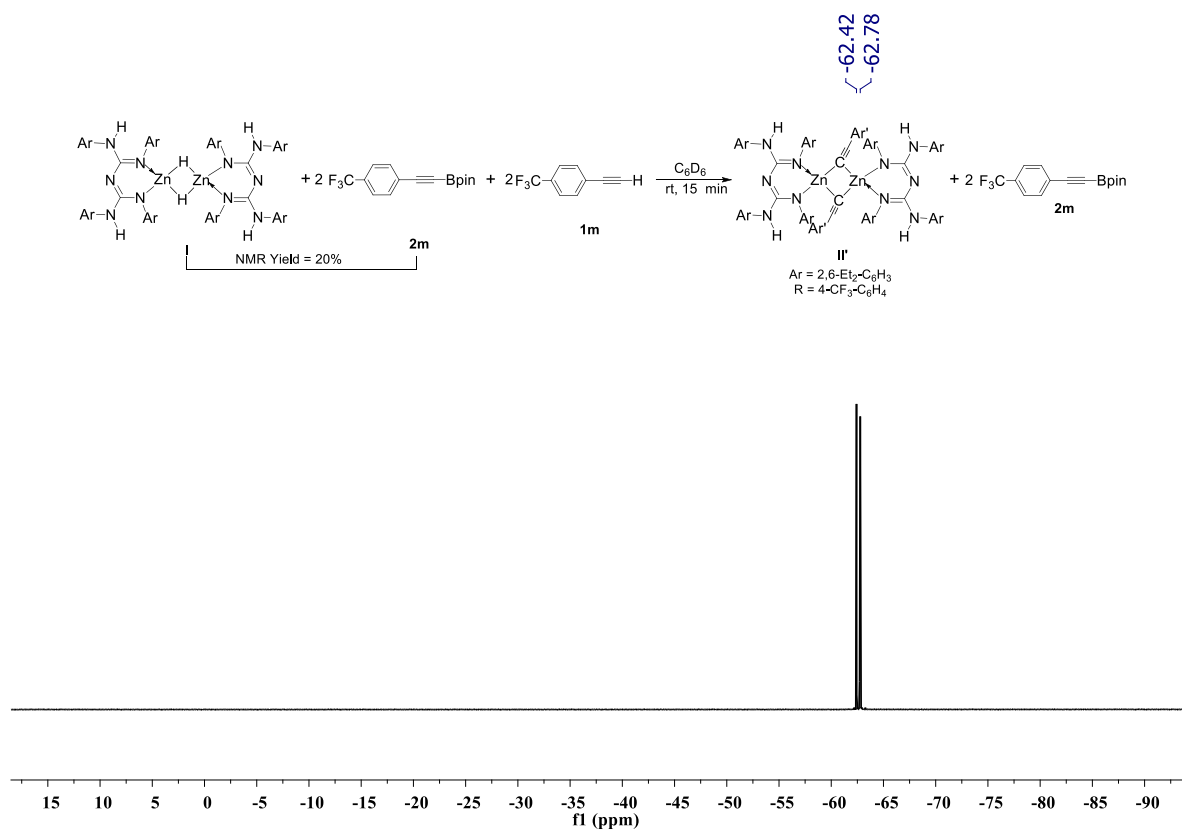


Figure S47: ¹⁹F{¹H} NMR (377 MHz, 25 °C, C₆D₆) spectrum of compounds II' & 2m.

Scheme S2. Stoichiometric Experiments for Dehydroborylation of Terminal Alkynes

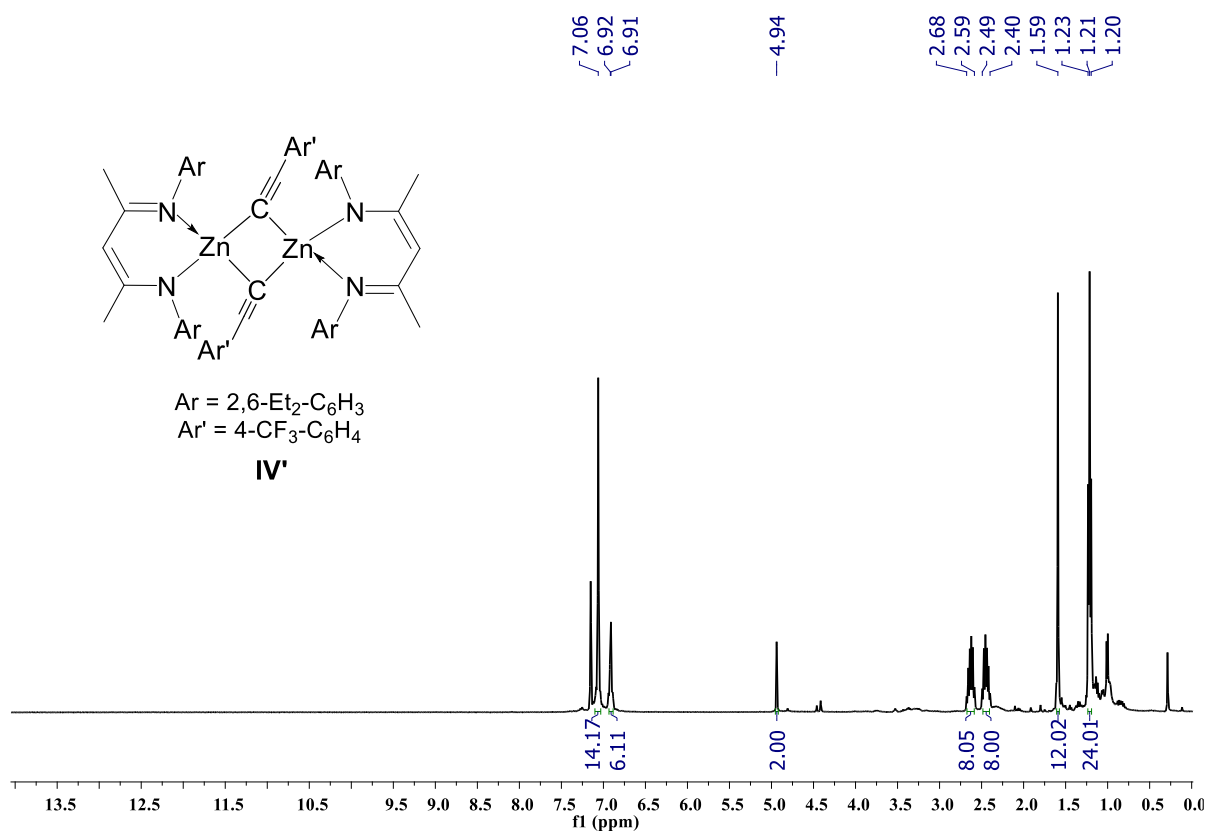
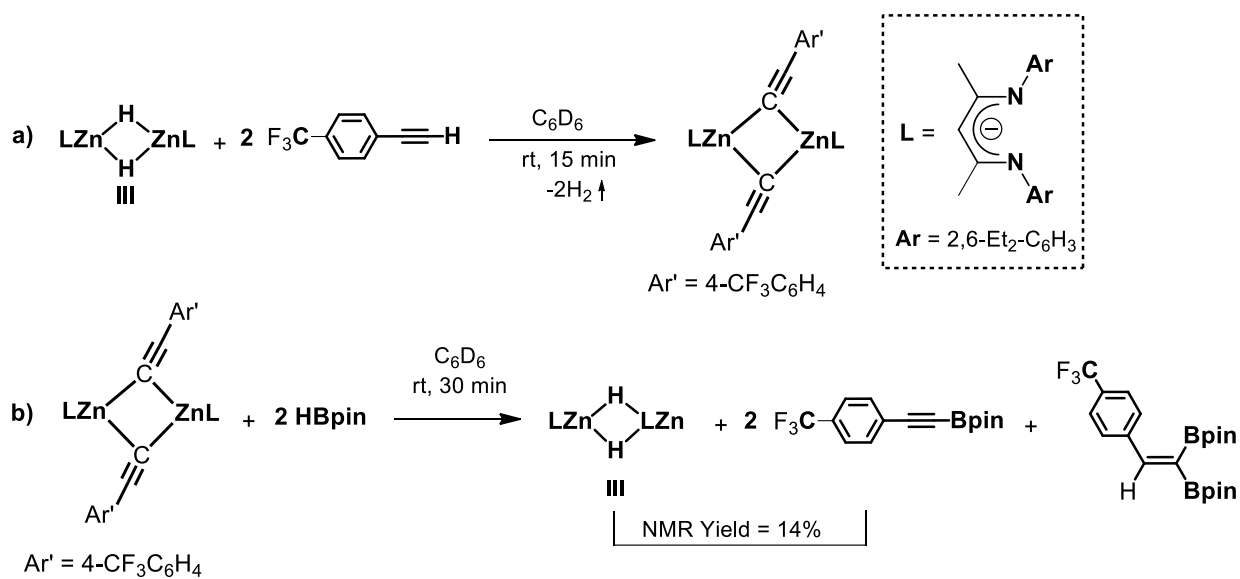


Figure S48: ^1H NMR (400 MHz, 25 °C, C_6D_6) spectrum of compound IV'.

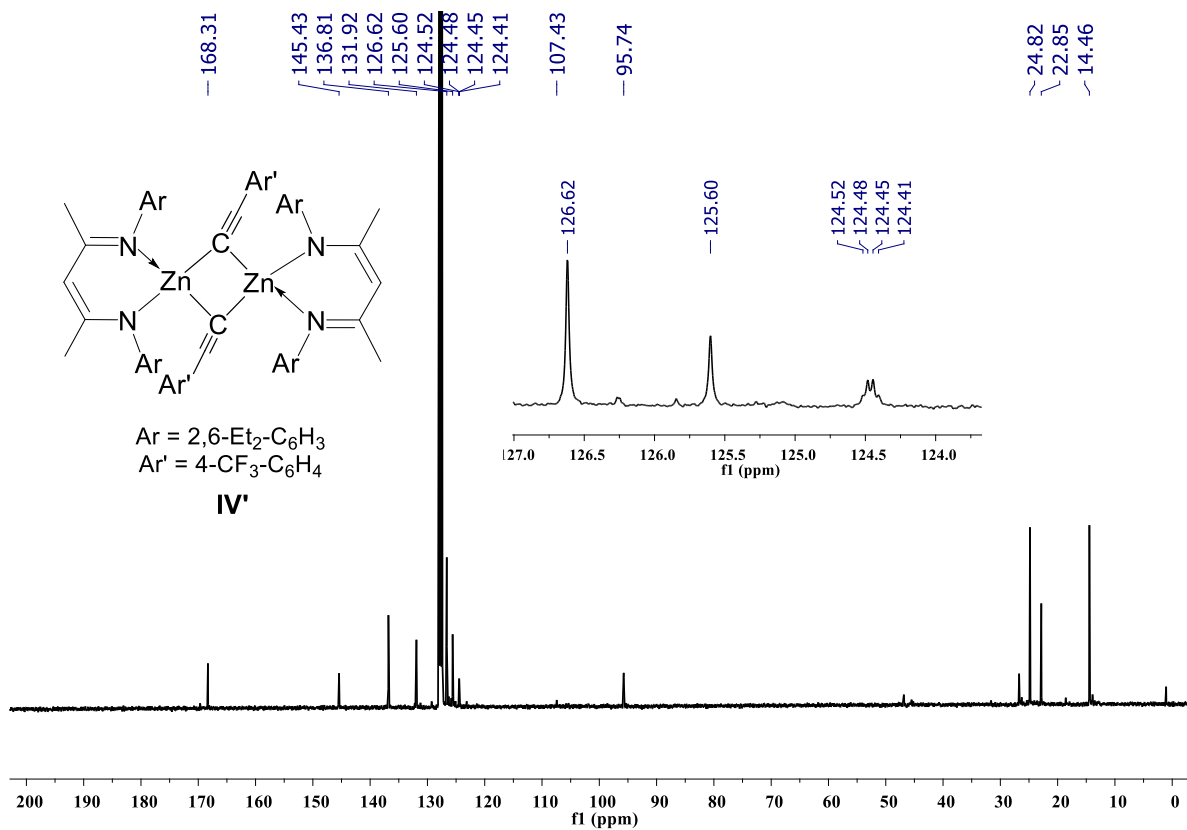


Figure S49: ¹³C{¹H} NMR (400 MHz, 25 °C, C₆D₆) spectrum of compound IV'.

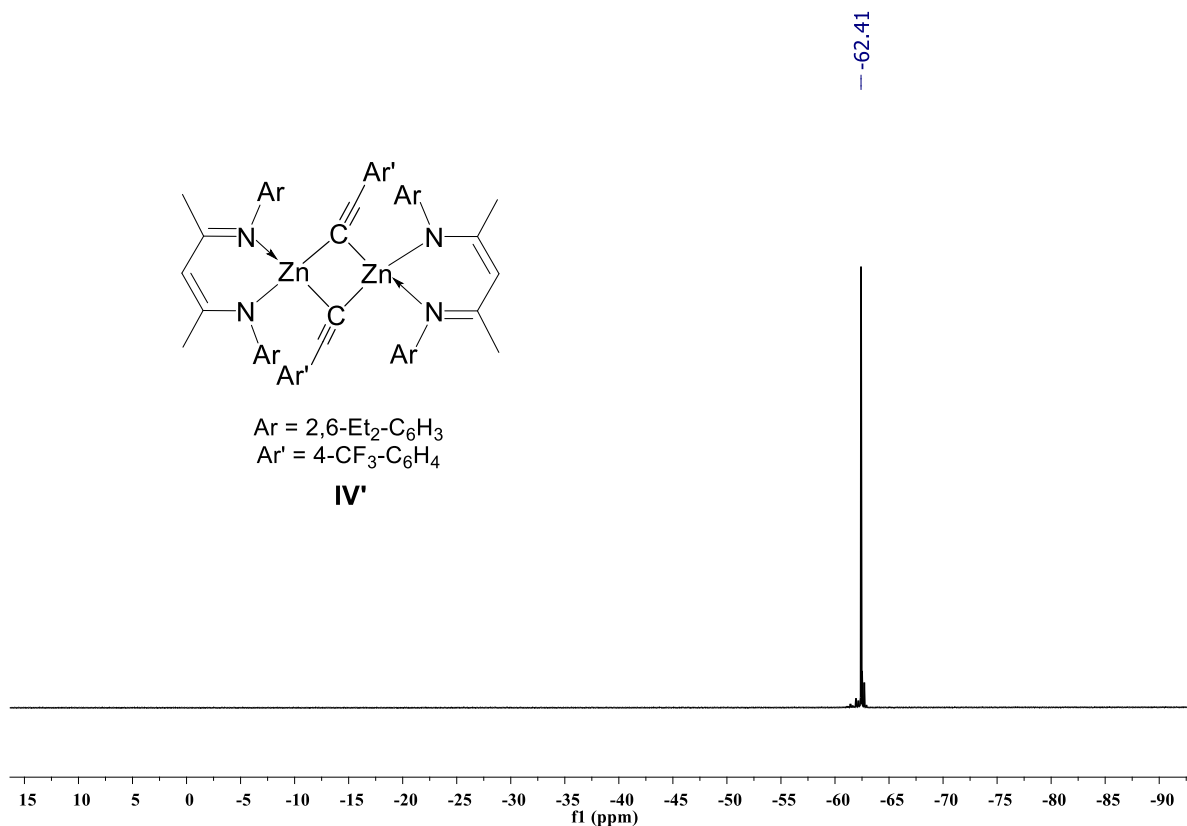


Figure S50: ¹⁹F{¹H} NMR (377 MHz, 25 °C, C₆D₆) spectrum of compound IV'.

The reaction between zinc alkynyl IV' and HBpin {NMR-Scale}: The addition of HBpin (6.81 μ L, 0.047 mmol) to a J. Young valve NMR tube containing a solution of compound IV' (0.023 mmol) in C_6D_6 at room temperature after 30 minutes resulted in the formation of compounds **III and **2m** with a 14% yield along with 1,1-diborylated alkenes product are confirmed by multinuclear NMR (1H , $^{13}C\{^1H\}$, ^{11}B , $^{19}F\{^1H\}$). When prolonged the heating, the alkynylborates convert to the 1,1-diborylated alkenes are observed by ^{11}B NMR.**

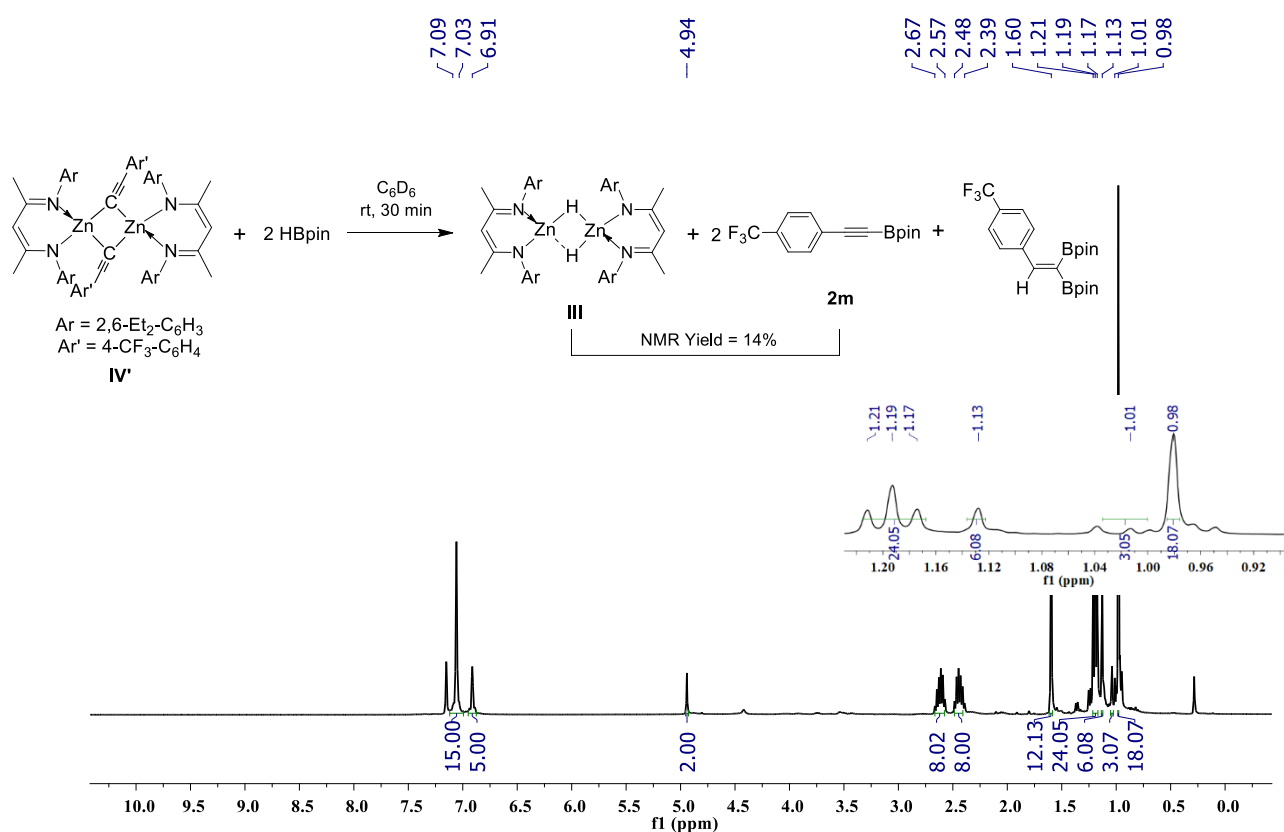


Figure S51: 1H NMR (400 MHz, 25 °C, C_6D_6) spectrum of compounds $[L^2ZnH]_2$ & **2m**.

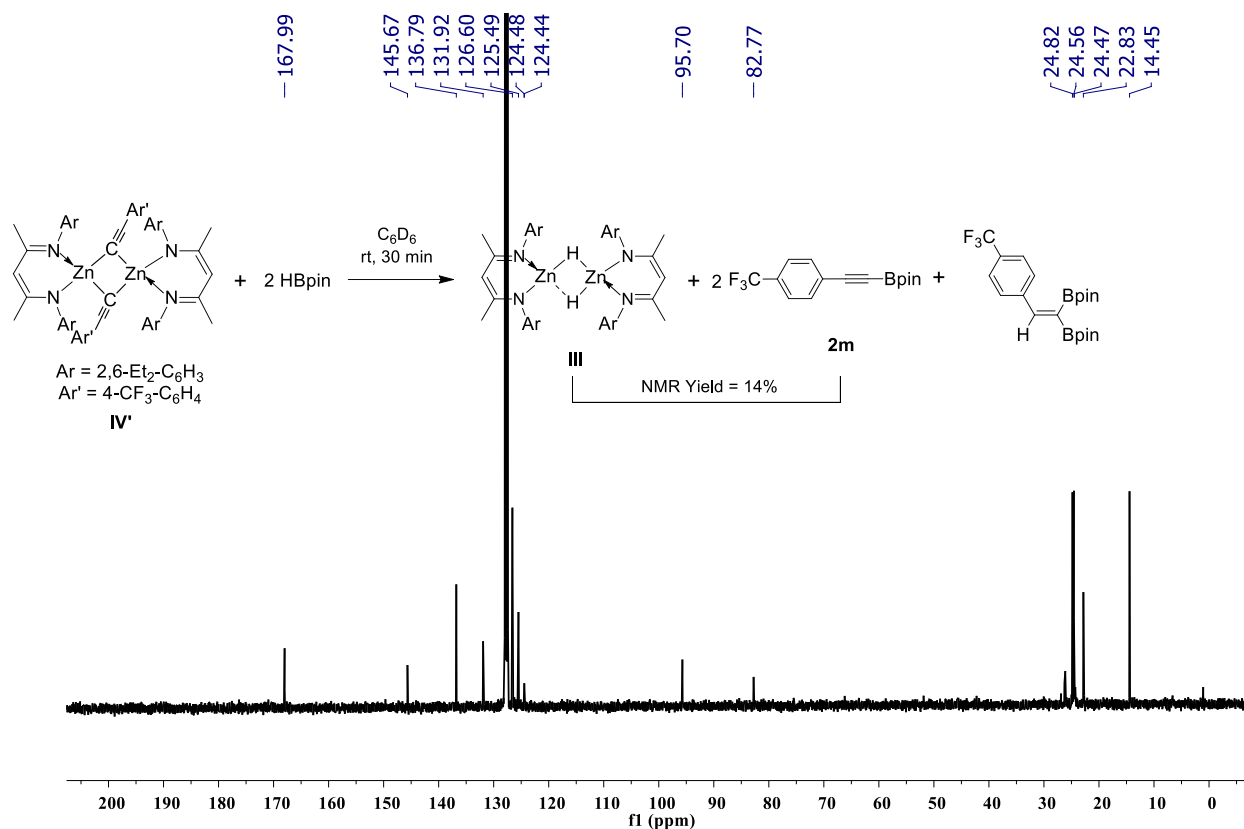


Figure S52: ¹³C{¹H} NMR (100 MHz, 25 °C, C₆D₆) spectrum of compounds [L²ZnH]₂ & 2m.

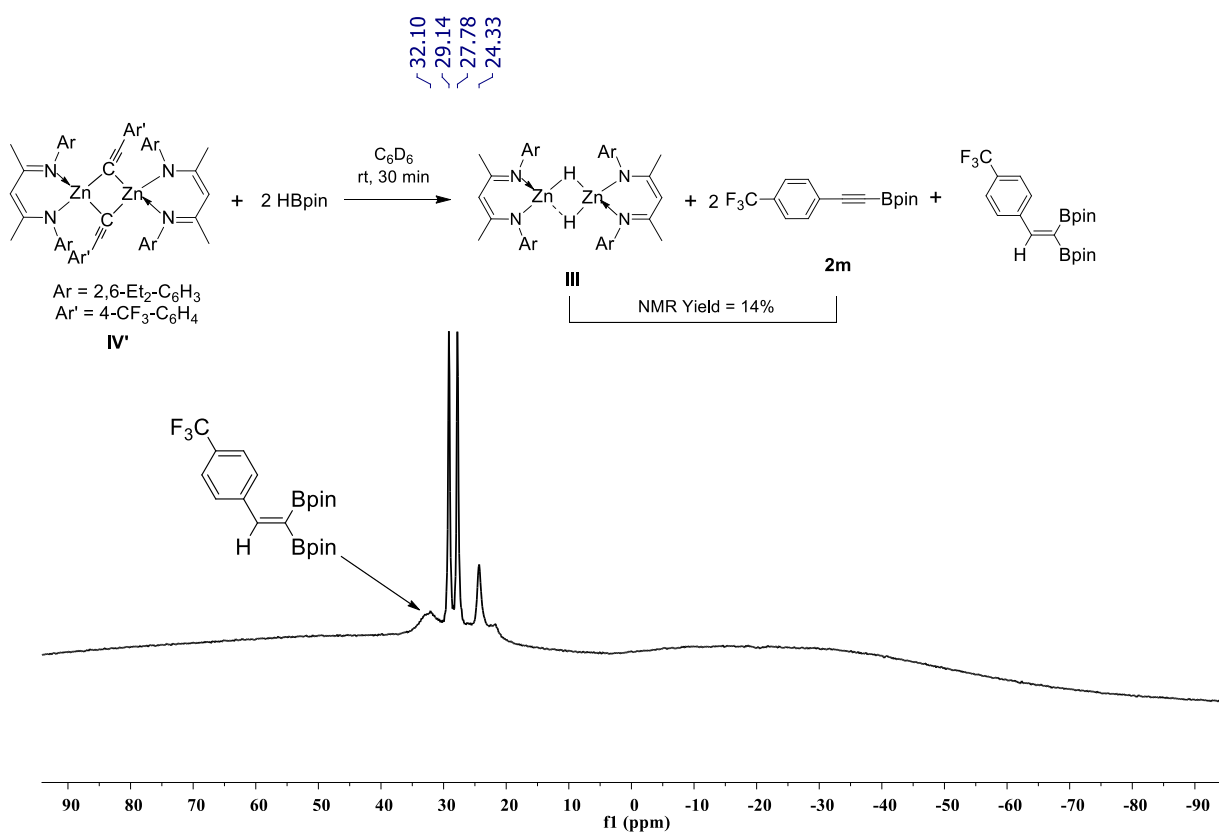


Figure S53: ¹¹B NMR (128 MHz, 25 °C, C₆D₆) spectrum of compounds [L²ZnH]₂ & 2m. A doublet peak at δ 27.78 – 29.14 ppm arises from free HBpin.

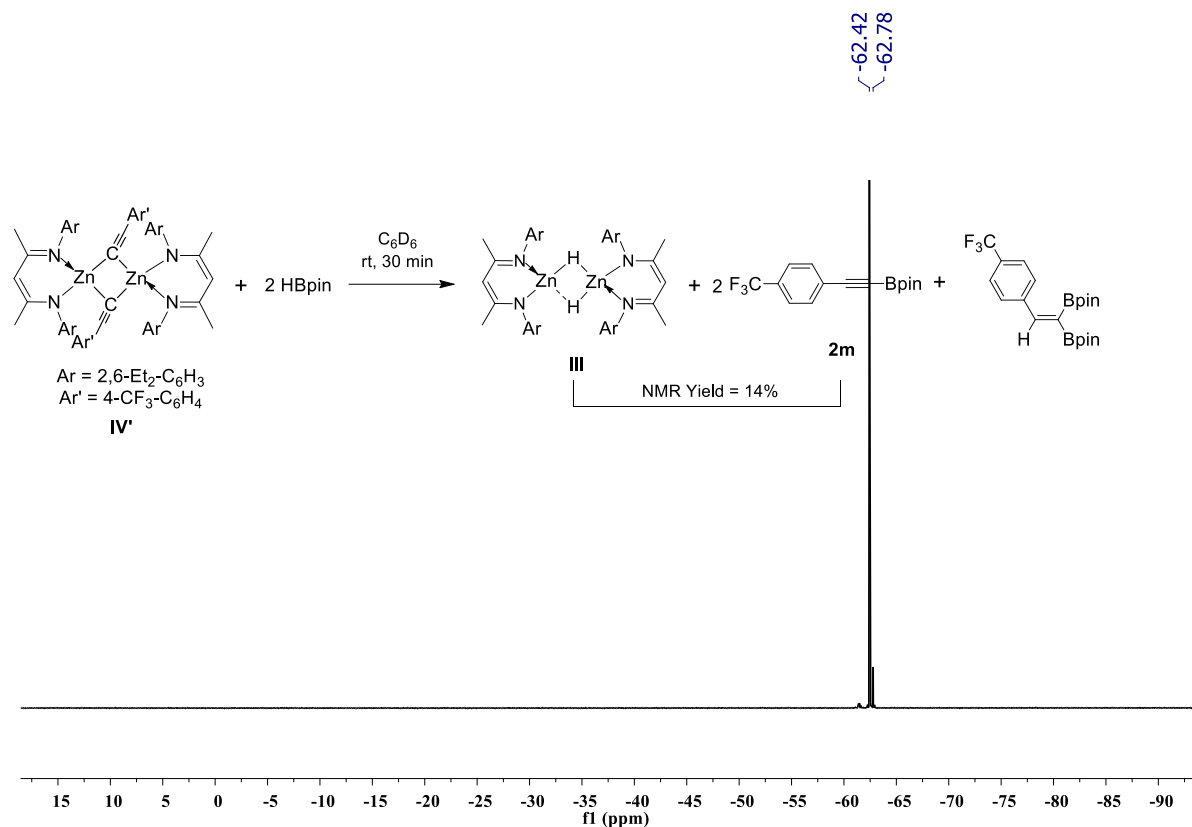


Figure S54: $^{19}\text{F}\{^1\text{H}\}$ NMR (377 MHz, 25 °C, C_6D_6) spectrum of compounds $[\text{L}^2\text{ZnH}]_2$ & **2m**.

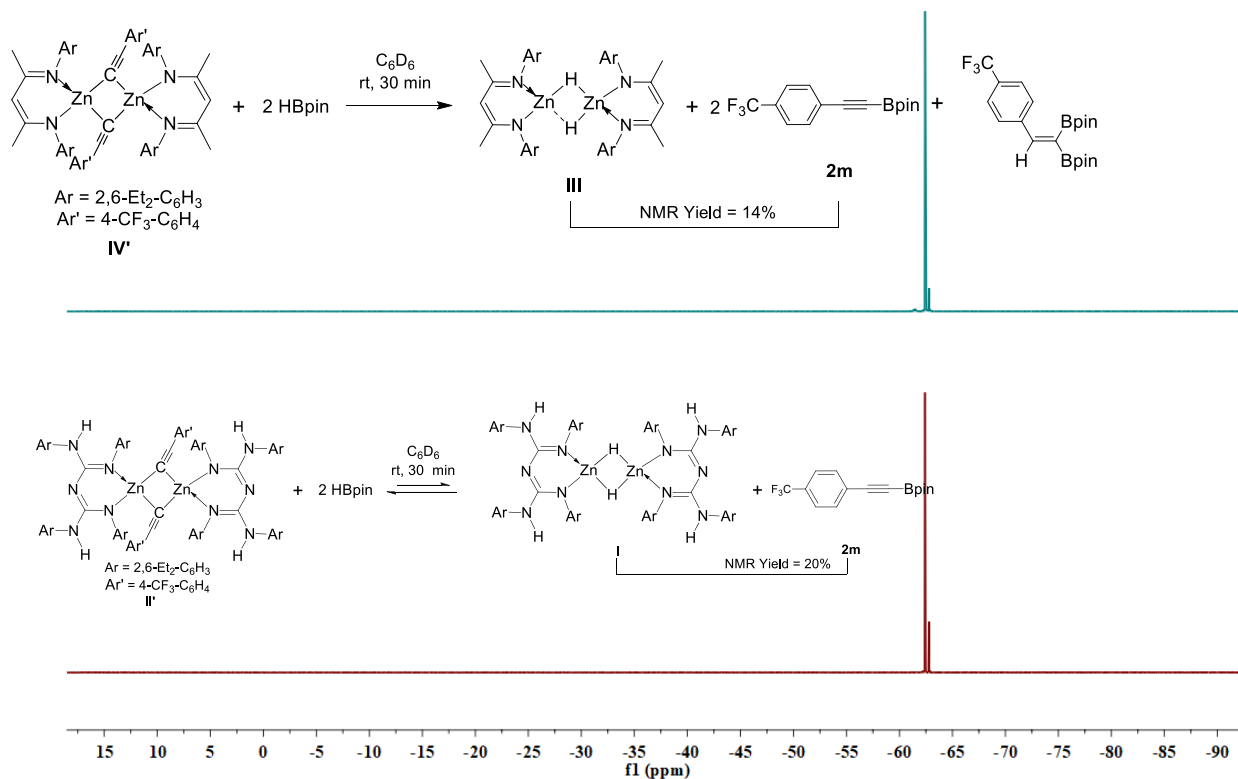


Figure S55: $^{19}\text{F}\{^1\text{H}\}$ NMR (377 MHz, 25 °C, C_6D_6) spectrum of $[\text{L}^1\text{ZnH}]_2$ & **2m** Vs. $[\text{L}^2\text{ZnH}]_2$ & **2m**.

^1H , $^{13}\text{C}\{^1\text{H}\}$ and ^{11}B NMR Spectra of Dehydrogenative Borylation of Alkynes

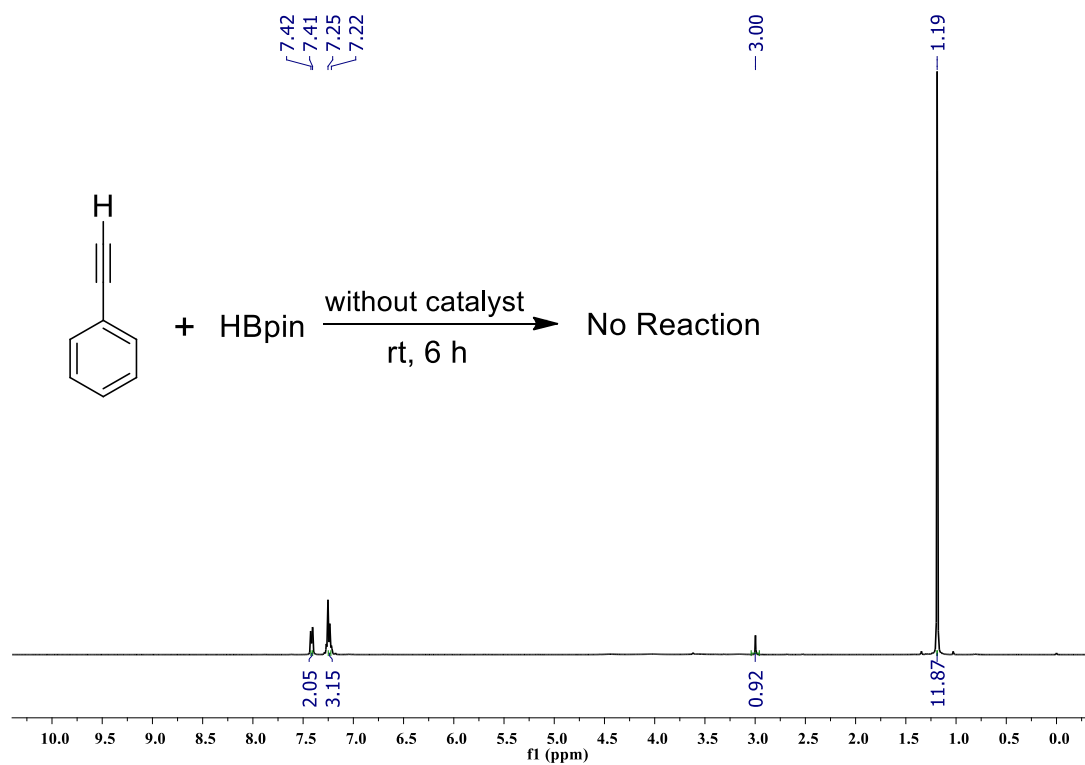


Figure S56: ^1H NMR spectrum of compound **2a** (400 MHz, CDCl_3).

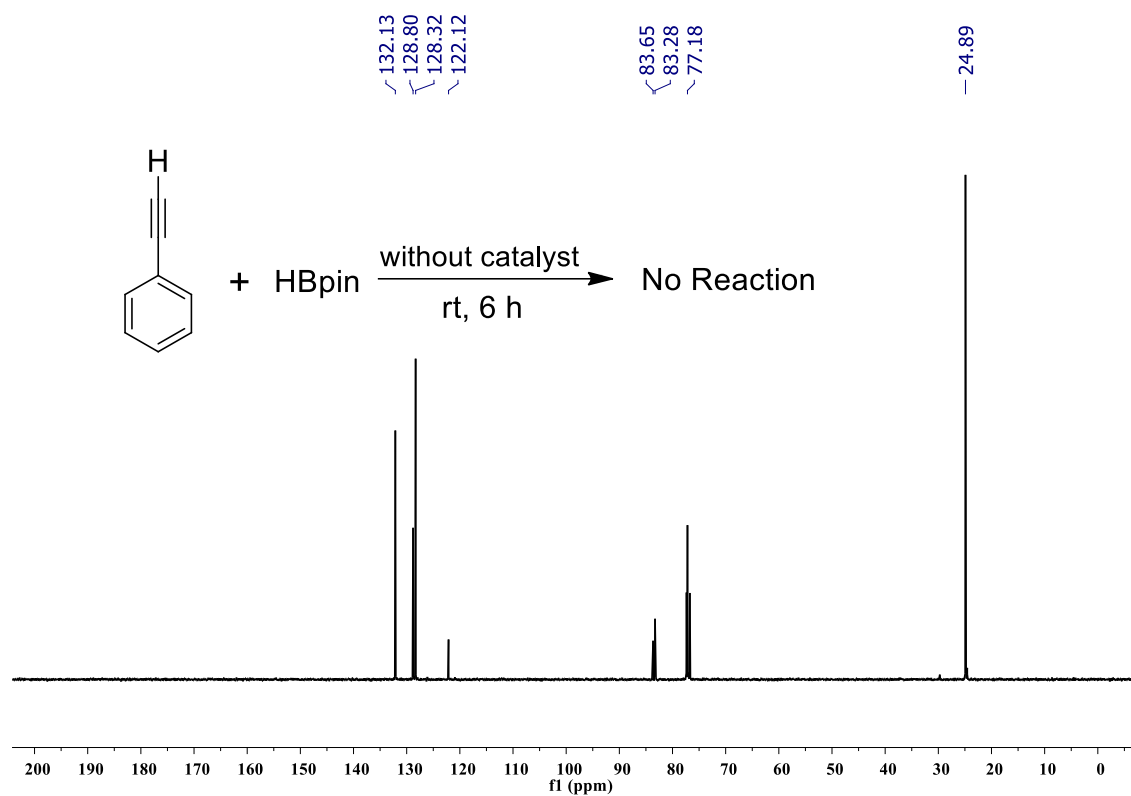


Figure S57: $^{13}\text{C}\{^1\text{H}\}$ NMR spectrum of compound **2a** (100 MHz, CDCl_3).

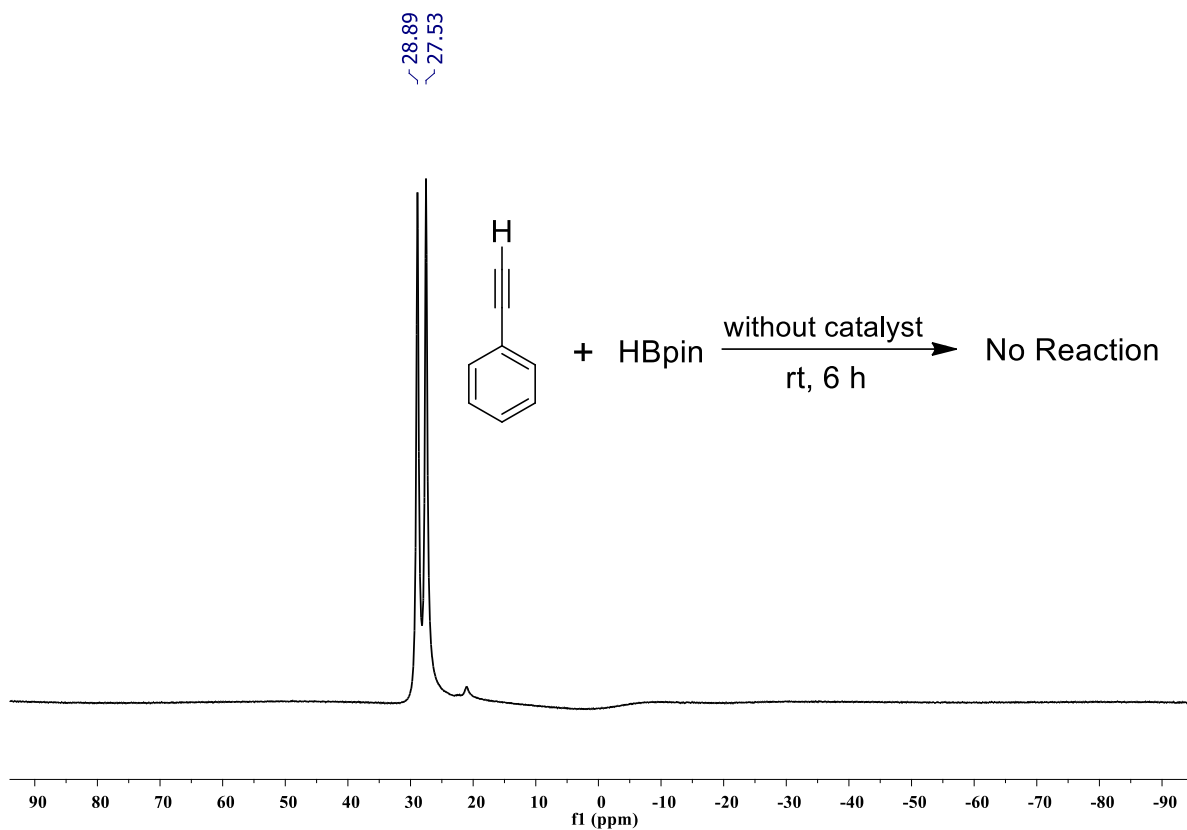


Figure S58: ^{11}B NMR spectrum of compound **2a** (128 MHz, CDCl_3).

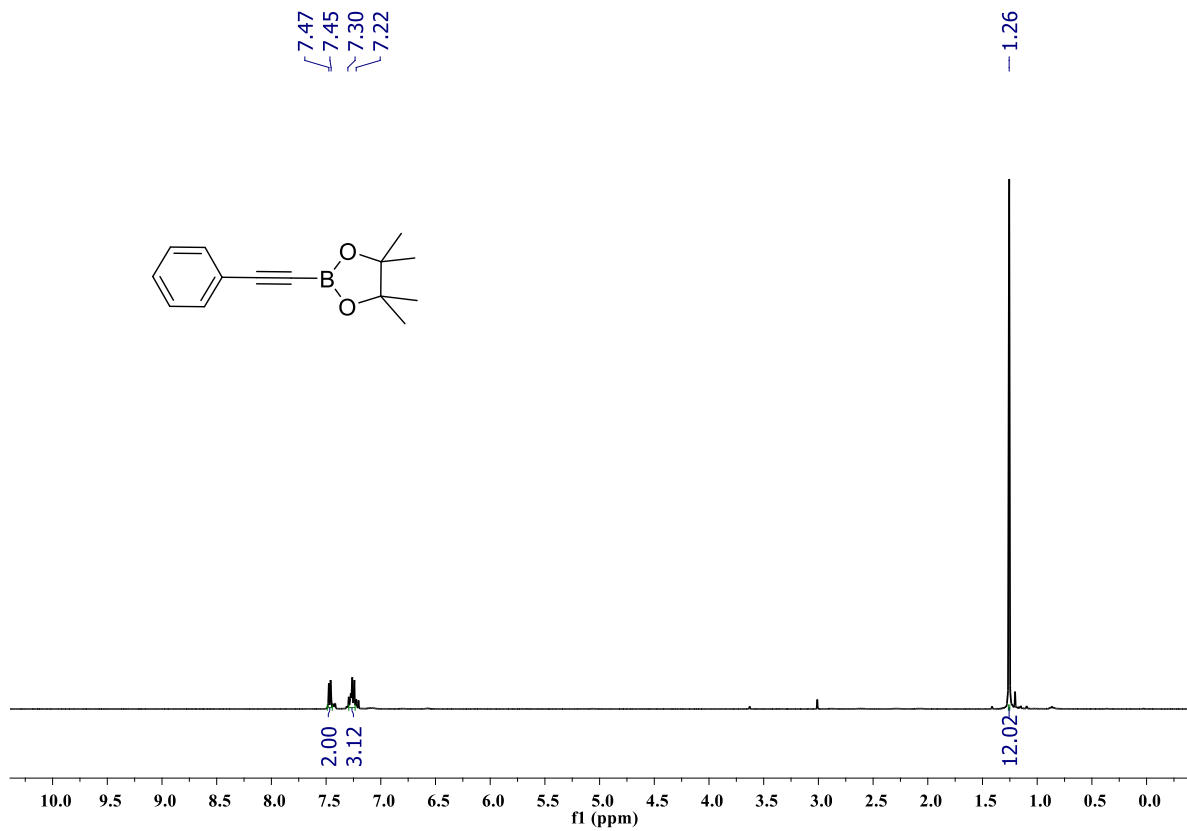


Figure S59: ^1H NMR spectrum of compound **2a** (400 MHz, CDCl_3).

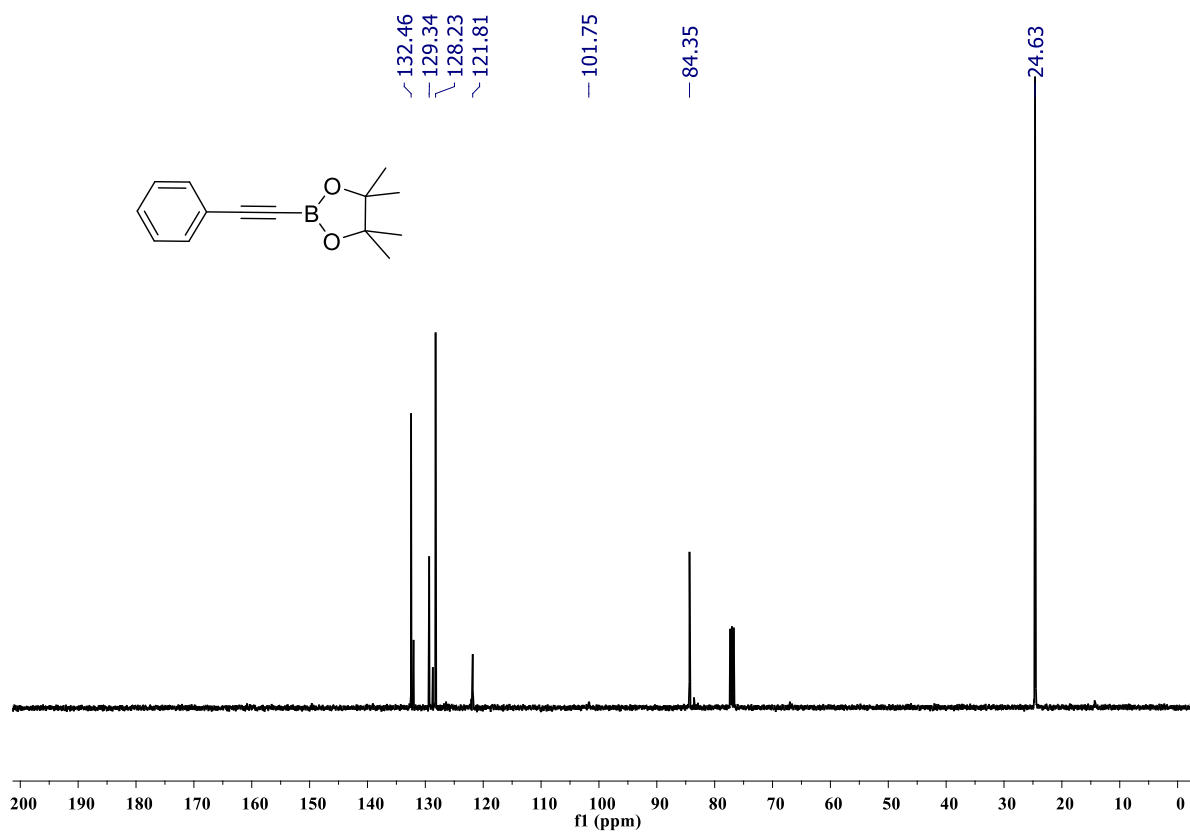


Figure S60: $^{13}\text{C}\{^1\text{H}\}$ NMR spectrum of compound **2a** (100 MHz, CDCl_3).

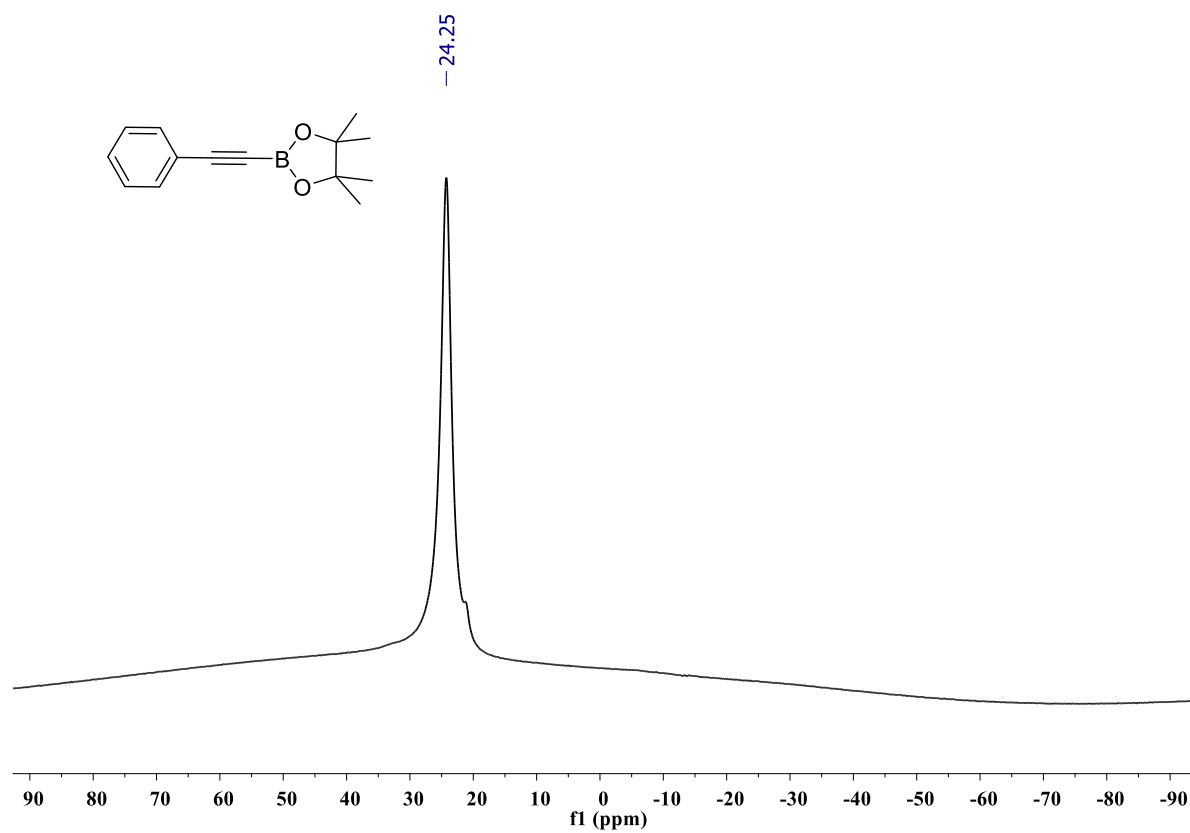


Figure S61: ^{11}B NMR spectrum of compound **2a** (128 MHz, CDCl_3).

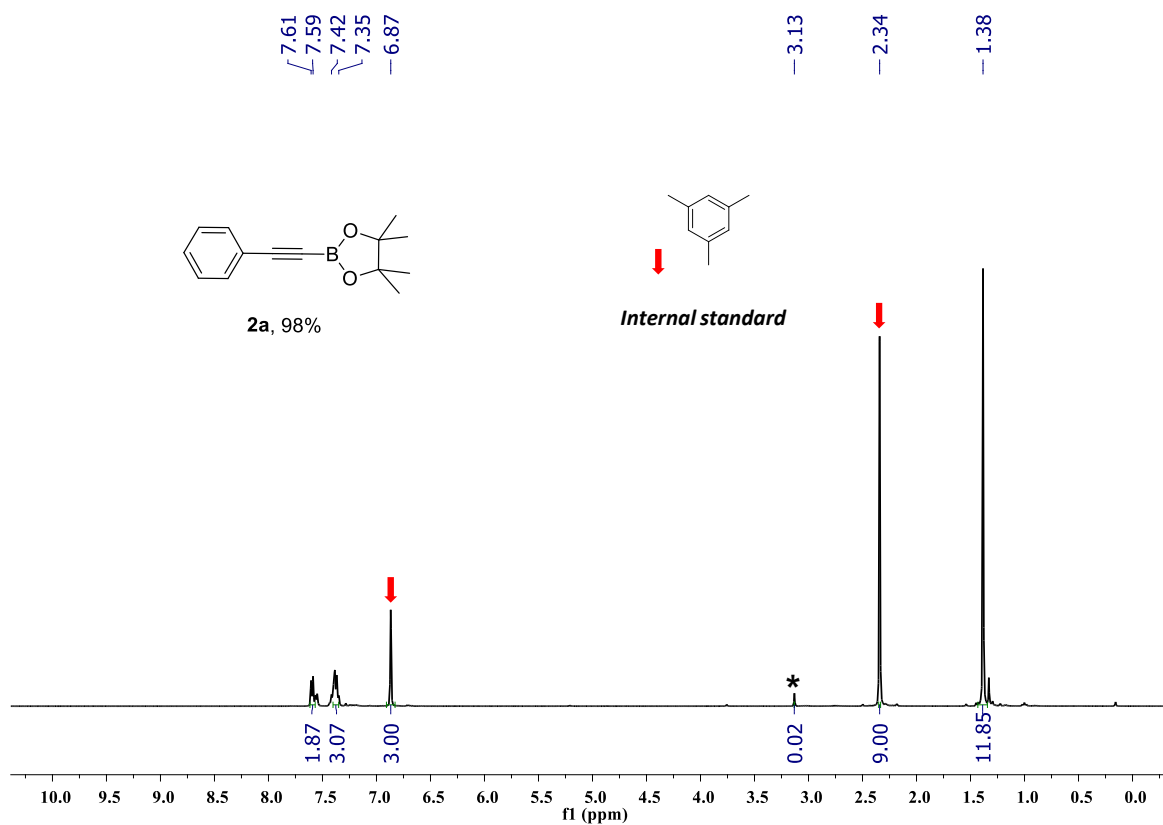


Figure S62: ¹H NMR spectrum of compound **2a** (400 MHz, CDCl₃). Mesitylene was used as an internal standard. * = unreacted compound **1a**.

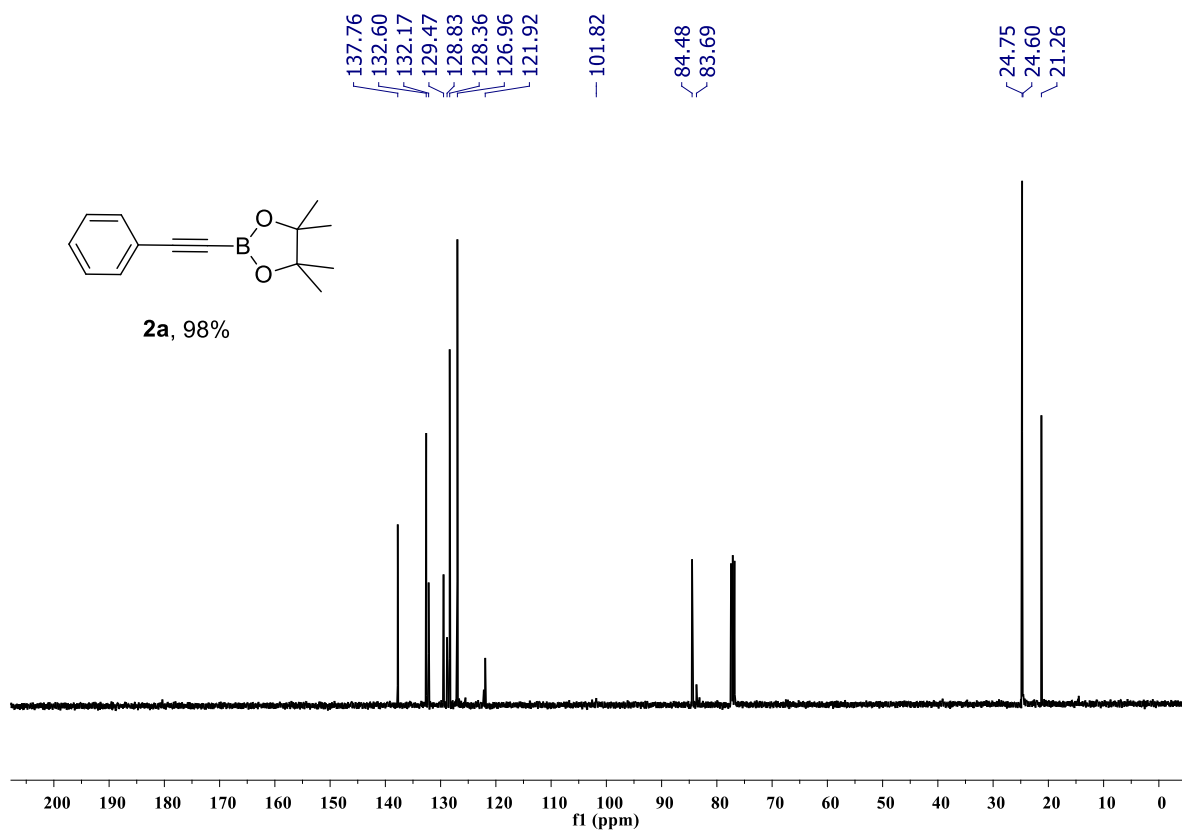


Figure S63: ¹³C{¹H} NMR spectrum of compound **2a** (100 MHz, CDCl₃). Mesitylene was used as an internal standard.

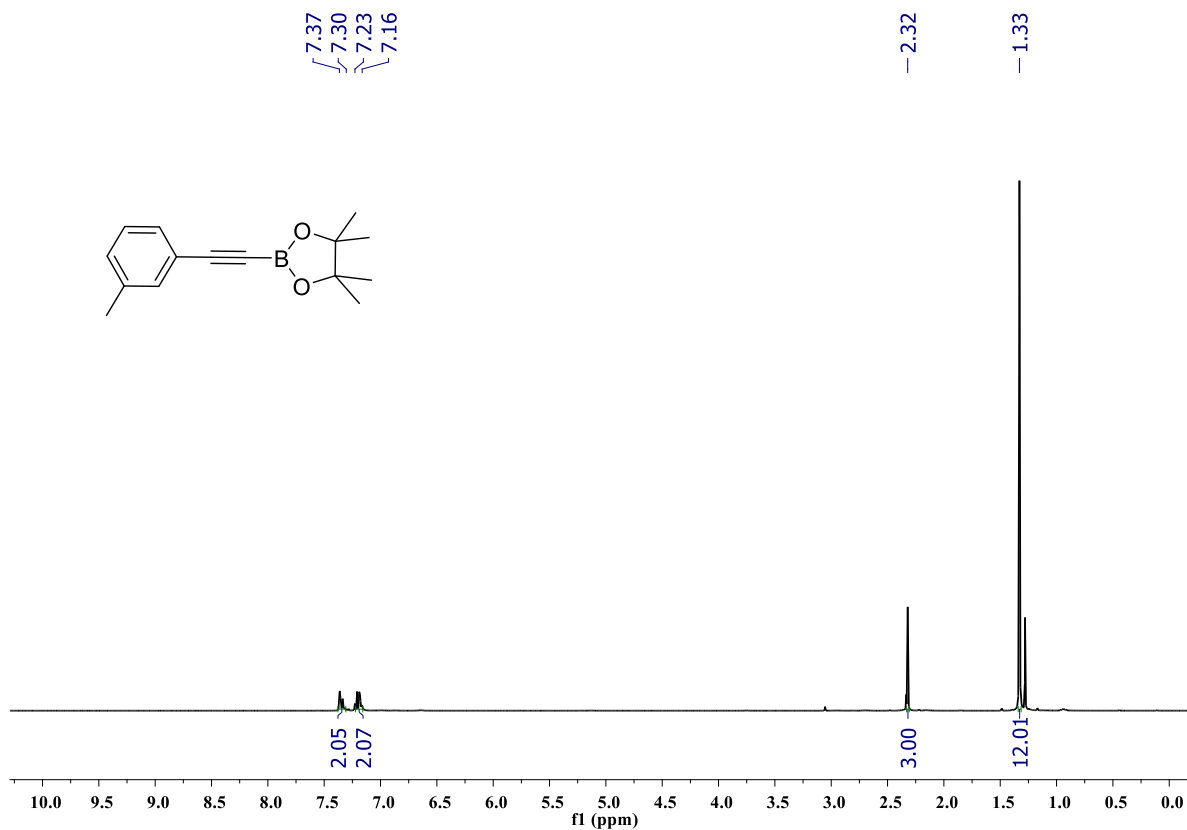


Figure S64: ^1H NMR spectrum of compound **2b** (400 MHz, CDCl_3).

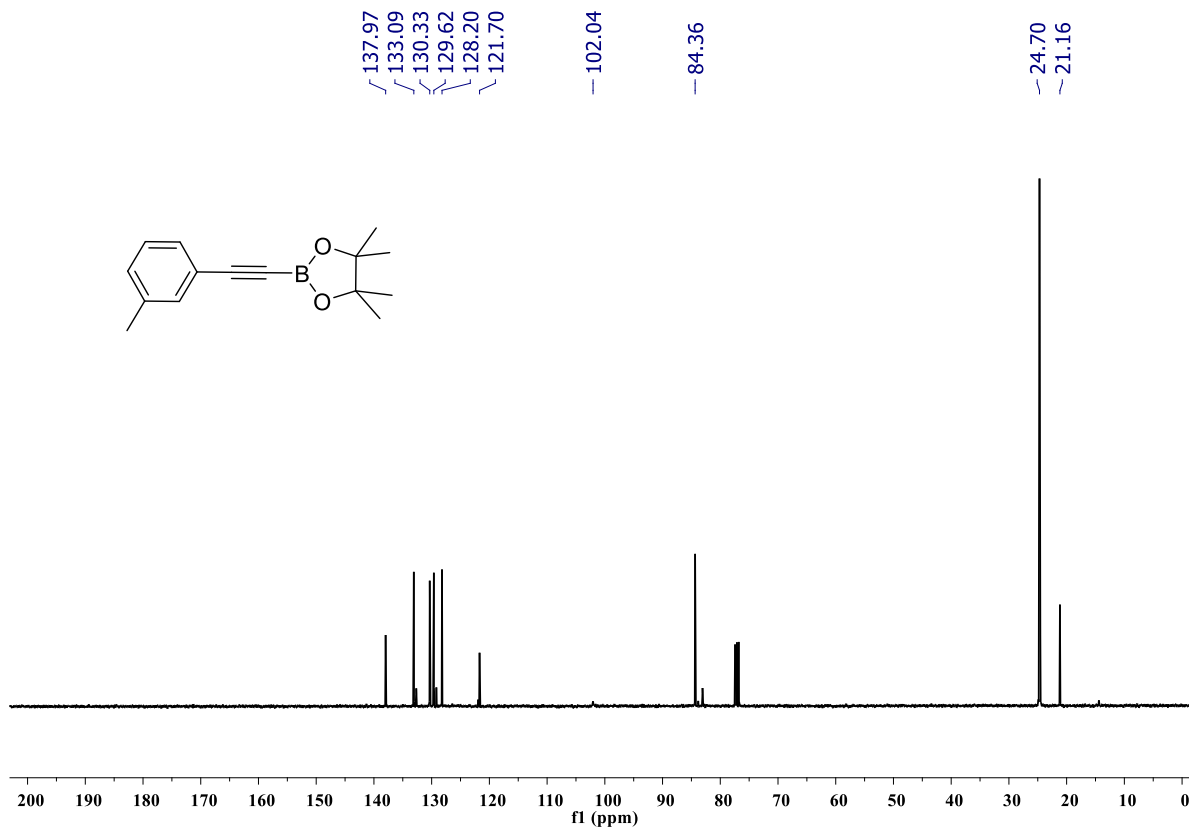


Figure S65: $^{13}\text{C}\{^1\text{H}\}$ NMR spectrum of compound **2b** (100 MHz, CDCl_3).

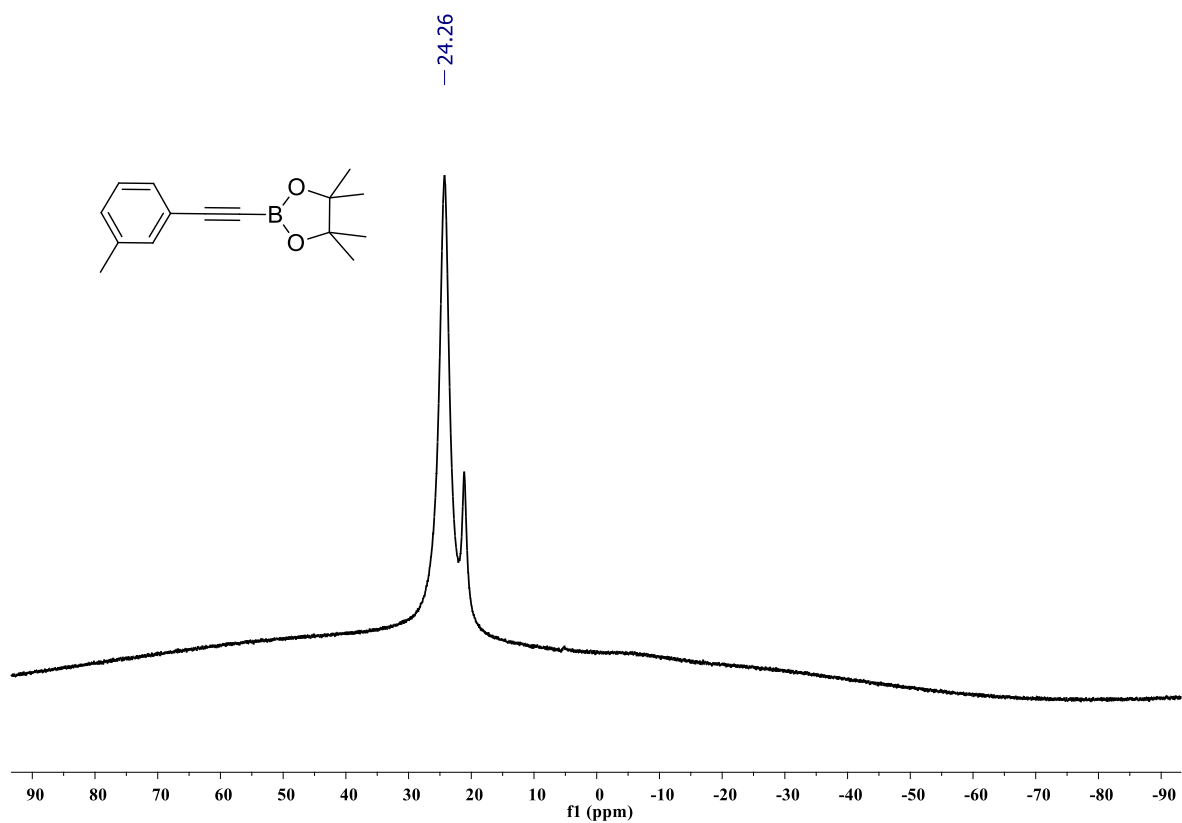


Figure S66: ^{11}B NMR spectrum of compound **2b** (128 MHz, CDCl_3).

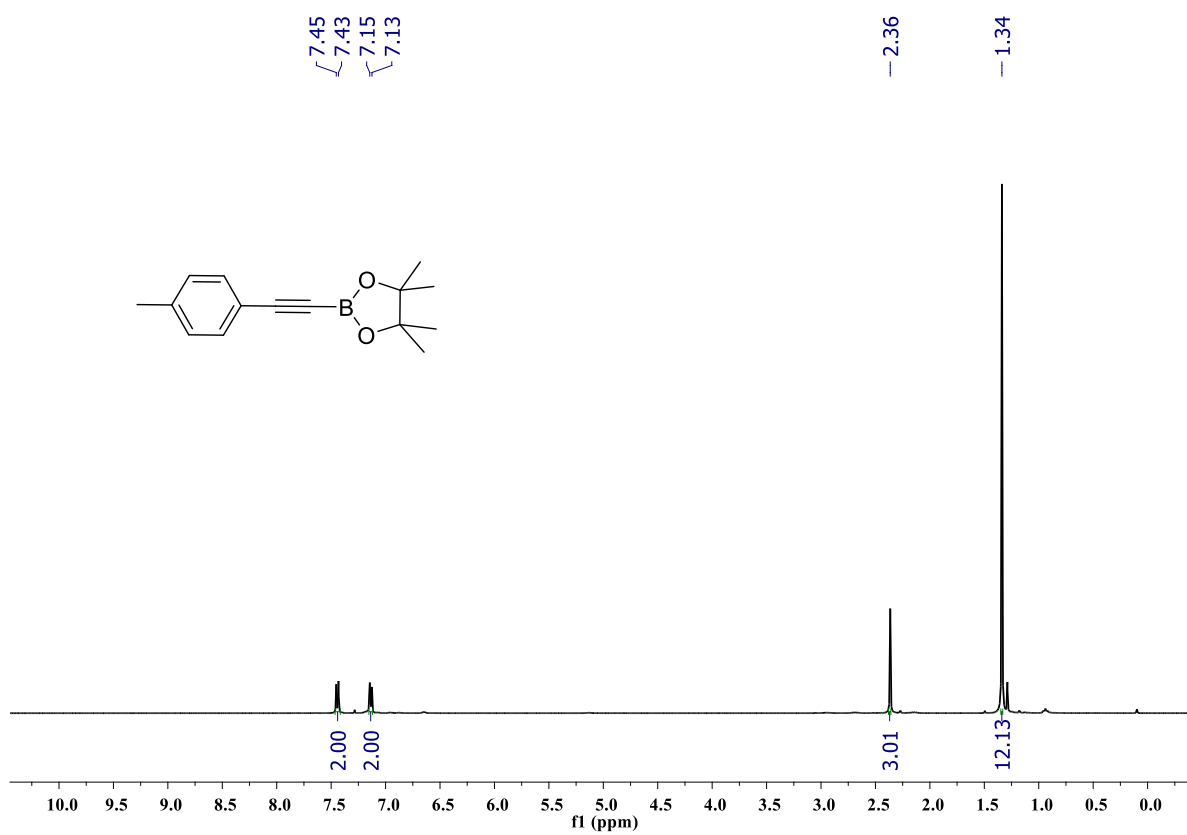


Figure S67: ^1H NMR spectrum of compound **2c** (400 MHz, CDCl_3).

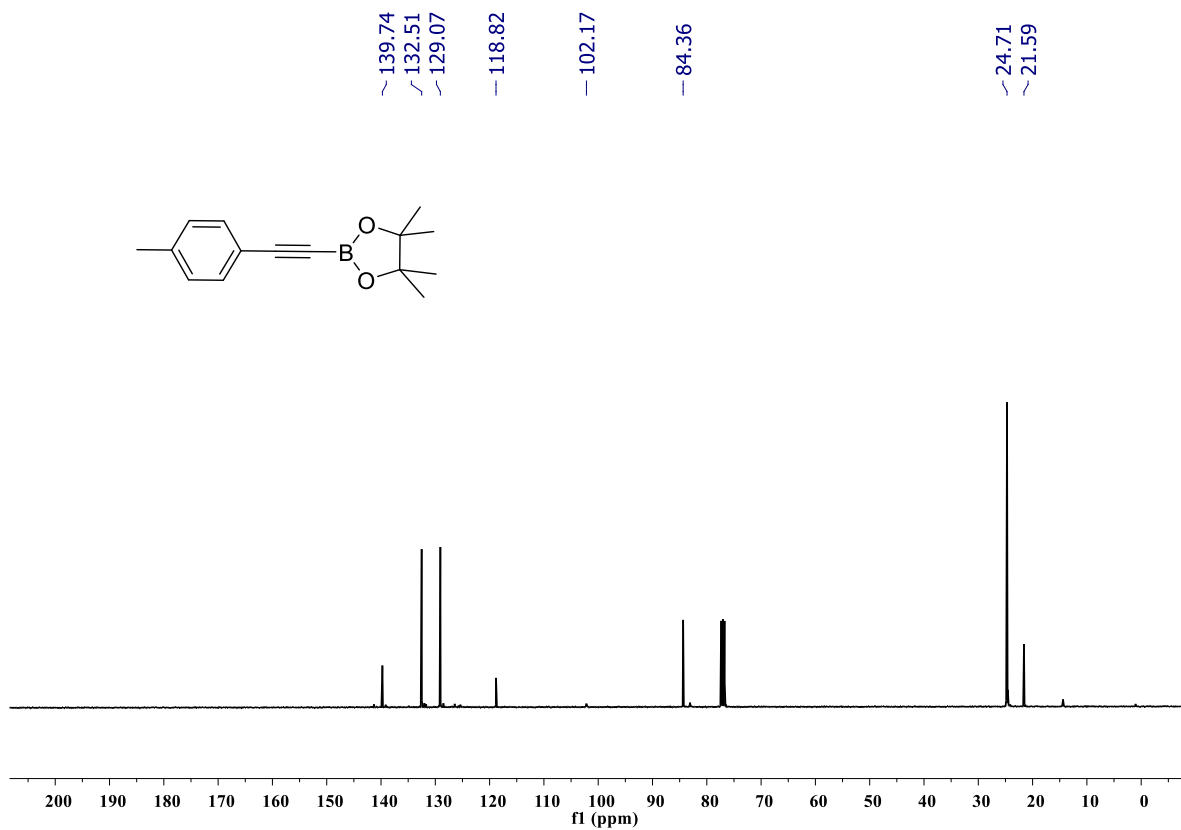


Figure S68: $^{13}\text{C}\{^1\text{H}\}$ NMR spectrum of compound **2c** (100 MHz, CDCl_3).

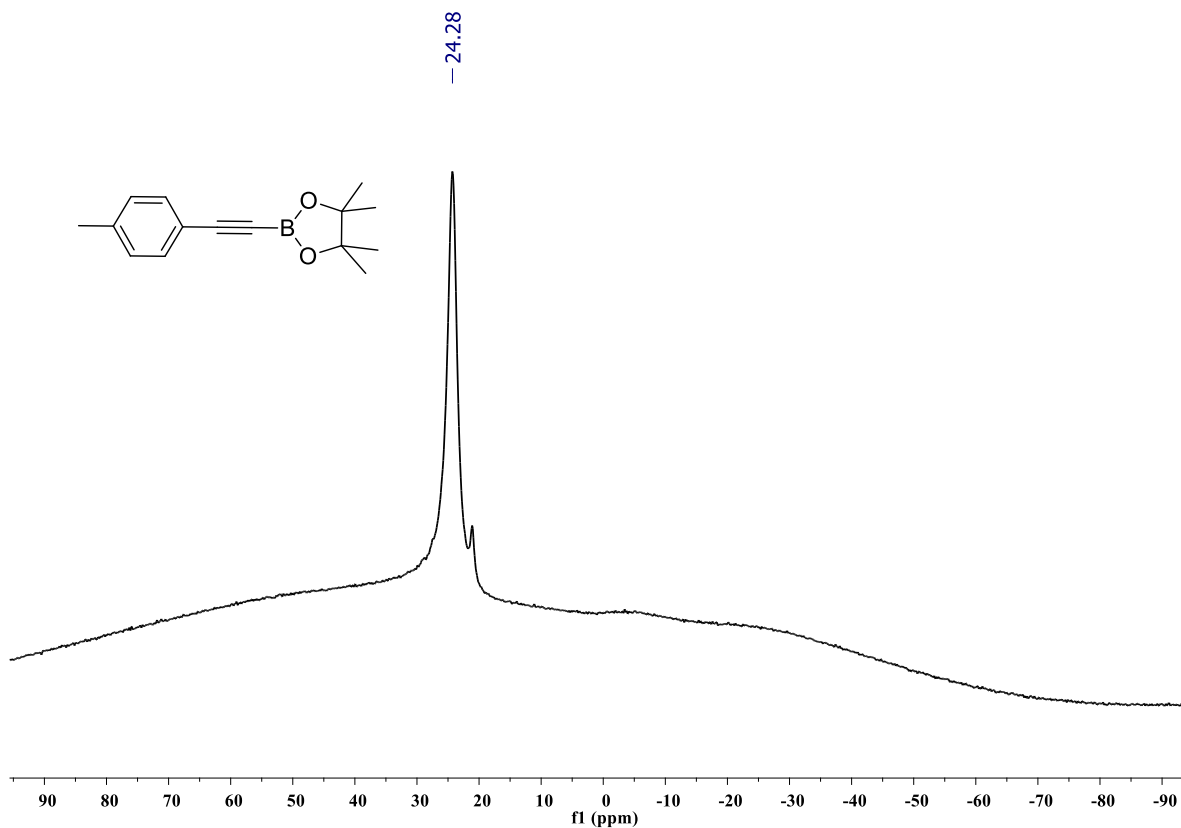


Figure S69: ^{11}B NMR spectrum of compound **2c** (128 MHz, CDCl_3).

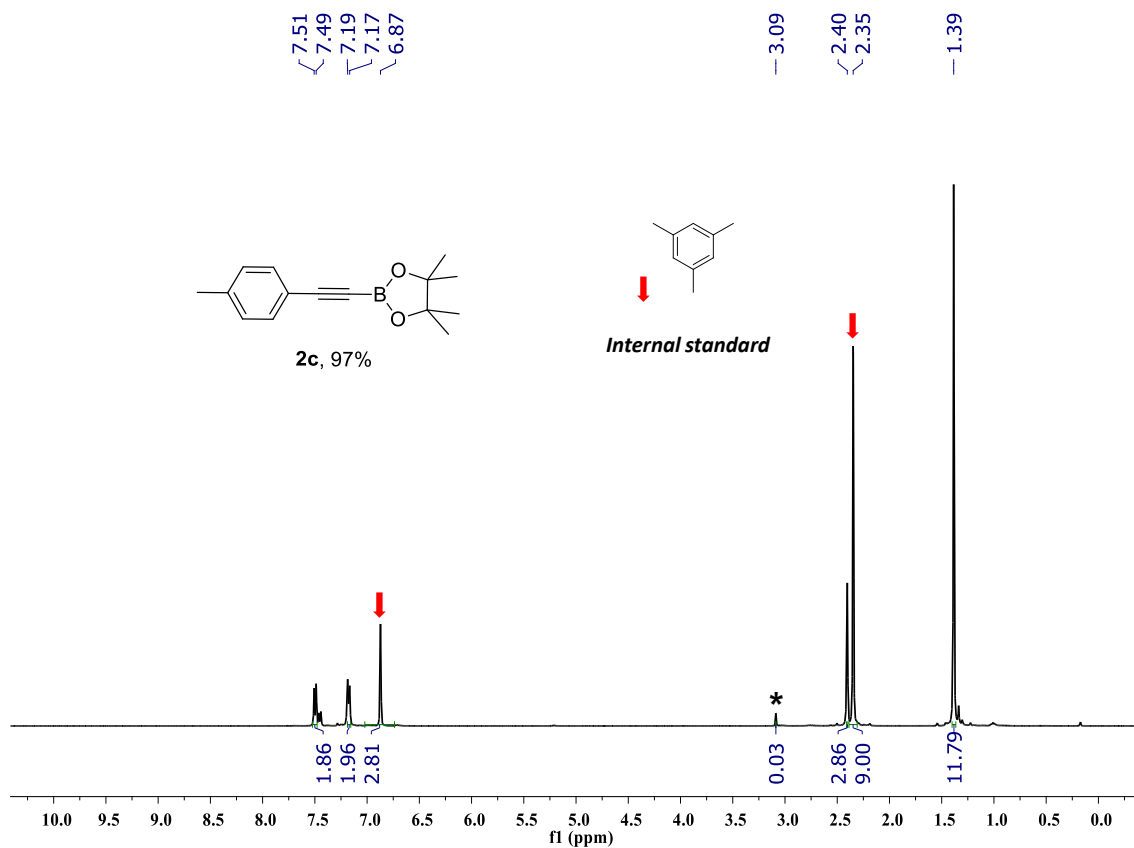


Figure S70: ^1H NMR spectrum of compound **2c** (400 MHz, CDCl_3). Mesitylene was used as an internal standard. * = unreacted compound **1c**.

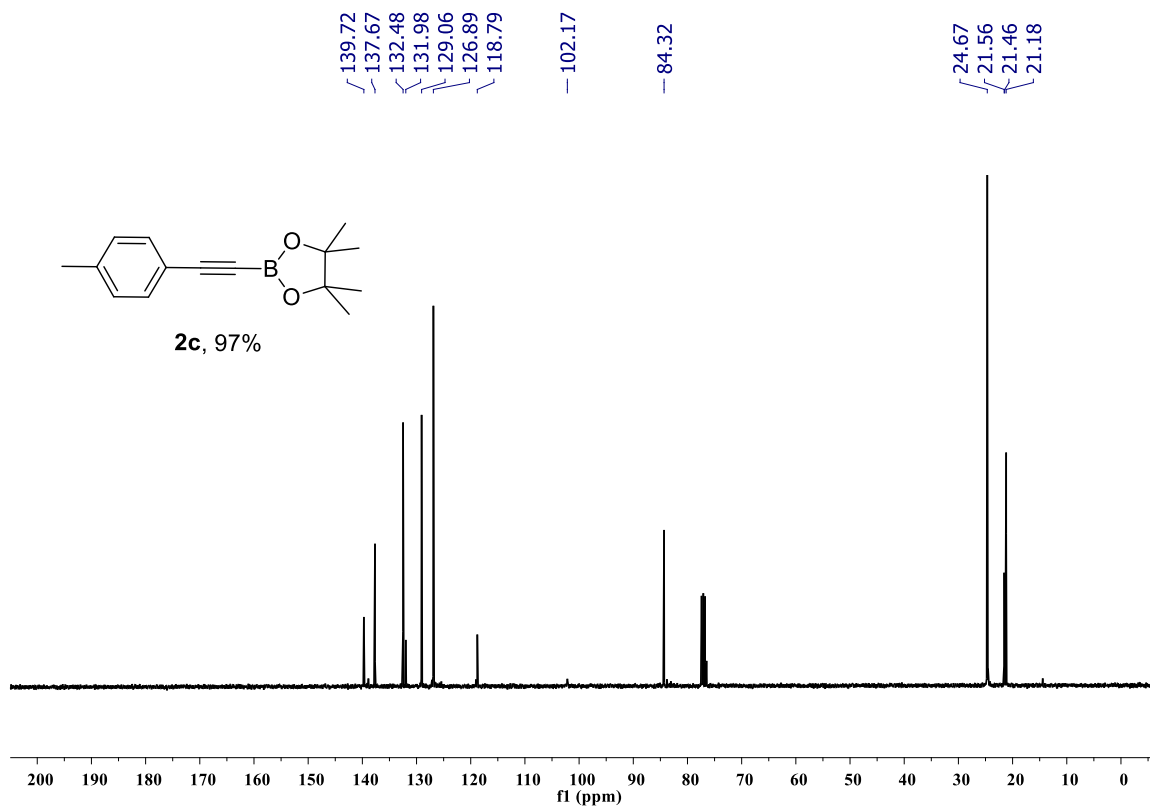


Figure S71: $^{13}\text{C}\{^1\text{H}\}$ NMR spectrum of compound **2c** (100 MHz, CDCl_3). Mesitylene was used as an internal standard.

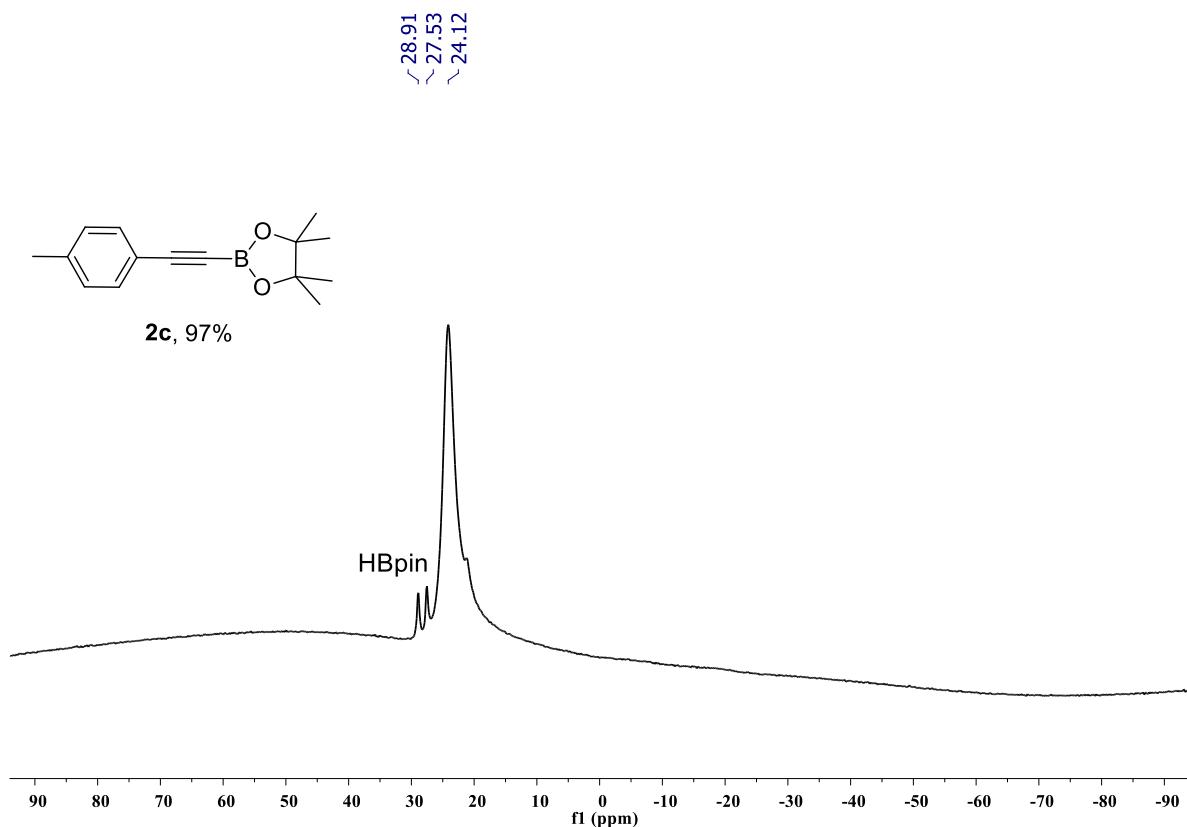


Figure S72: ^{11}B NMR spectrum of compound **2c** (128 MHz, CDCl_3). Mesitylene was used as an internal standard.

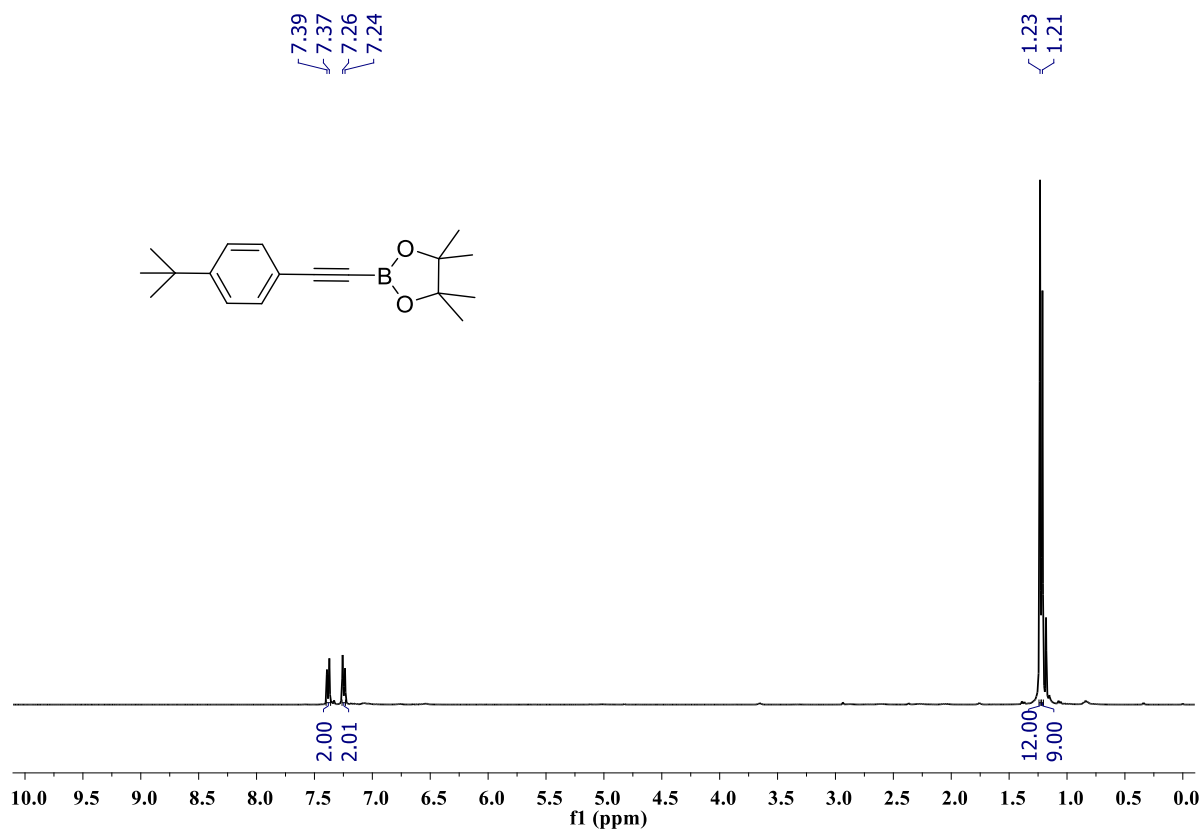


Figure S73: ^1H NMR spectrum of compound **2d** (400 MHz, CDCl_3).

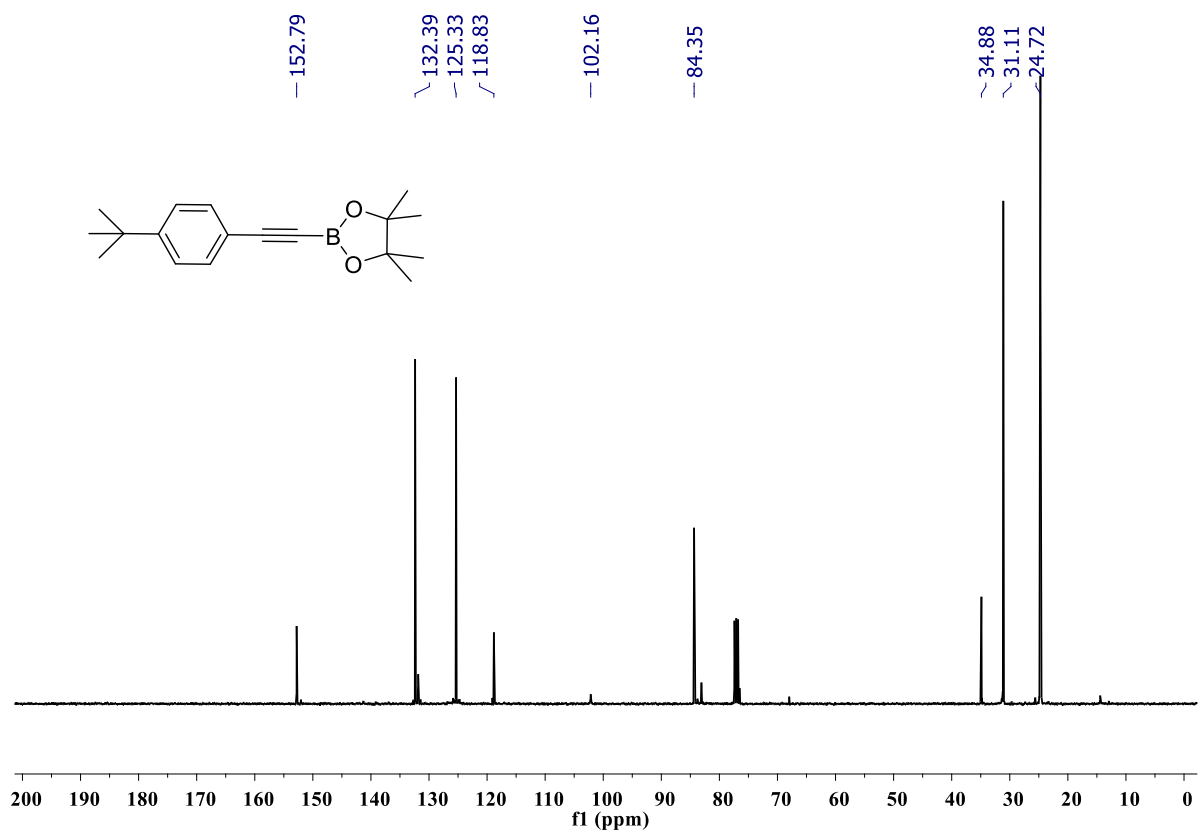


Figure S74: $^{13}\text{C}\{^1\text{H}\}$ NMR spectrum of compound **2d** (100 MHz, CDCl_3).

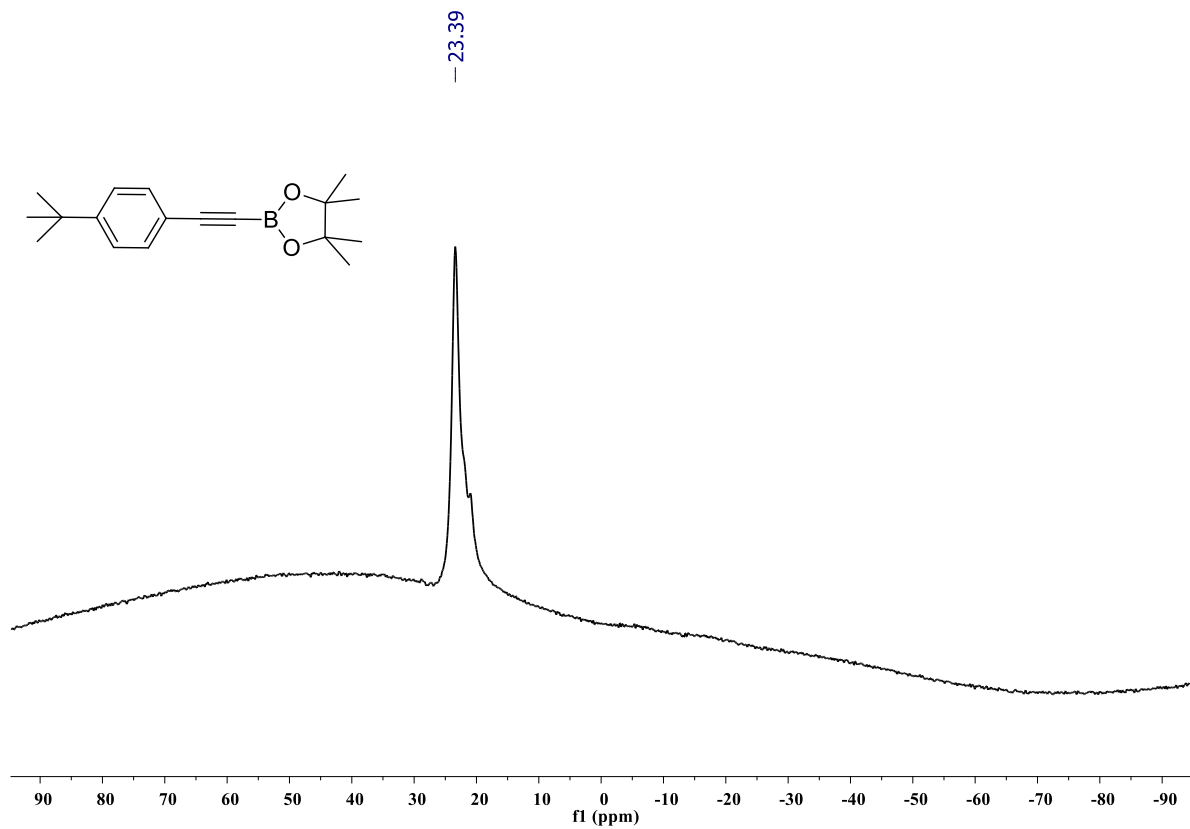


Figure S75: ^{11}B NMR spectrum of compound **2d** (128 MHz, CDCl_3).

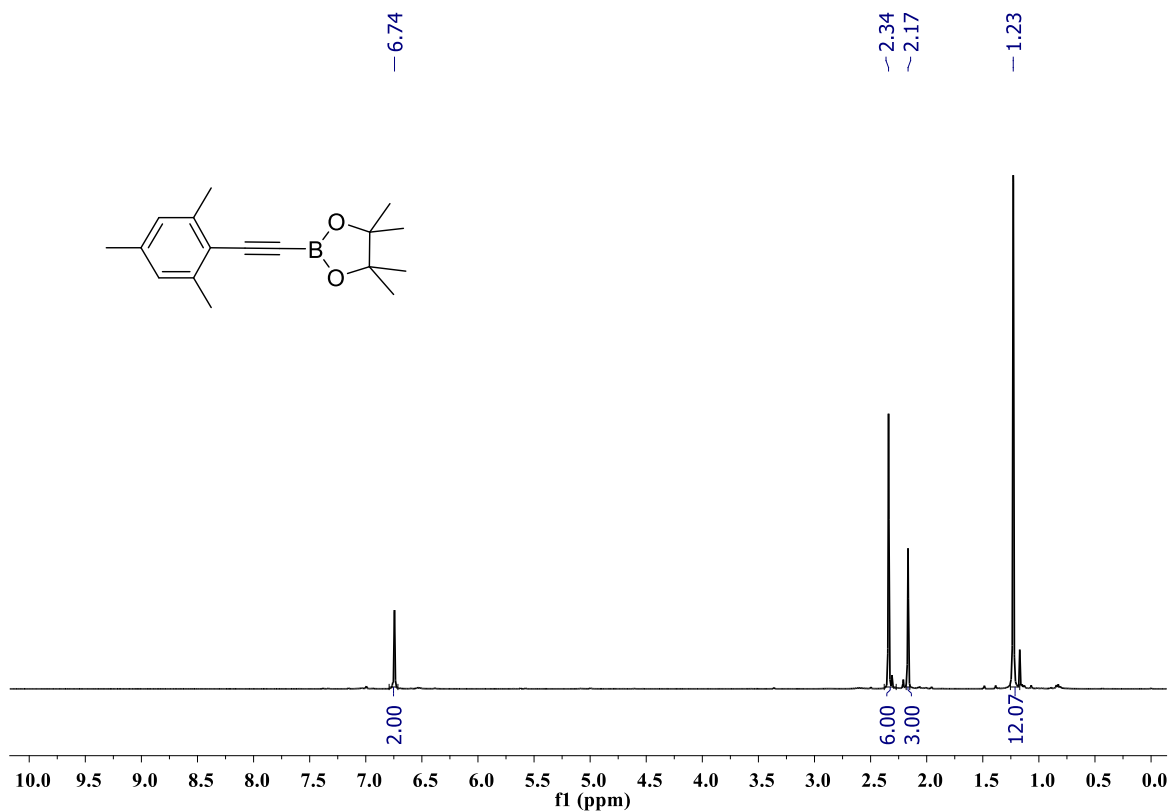


Figure S76: ^1H NMR spectrum of compound **2e** (400 MHz, CDCl_3).

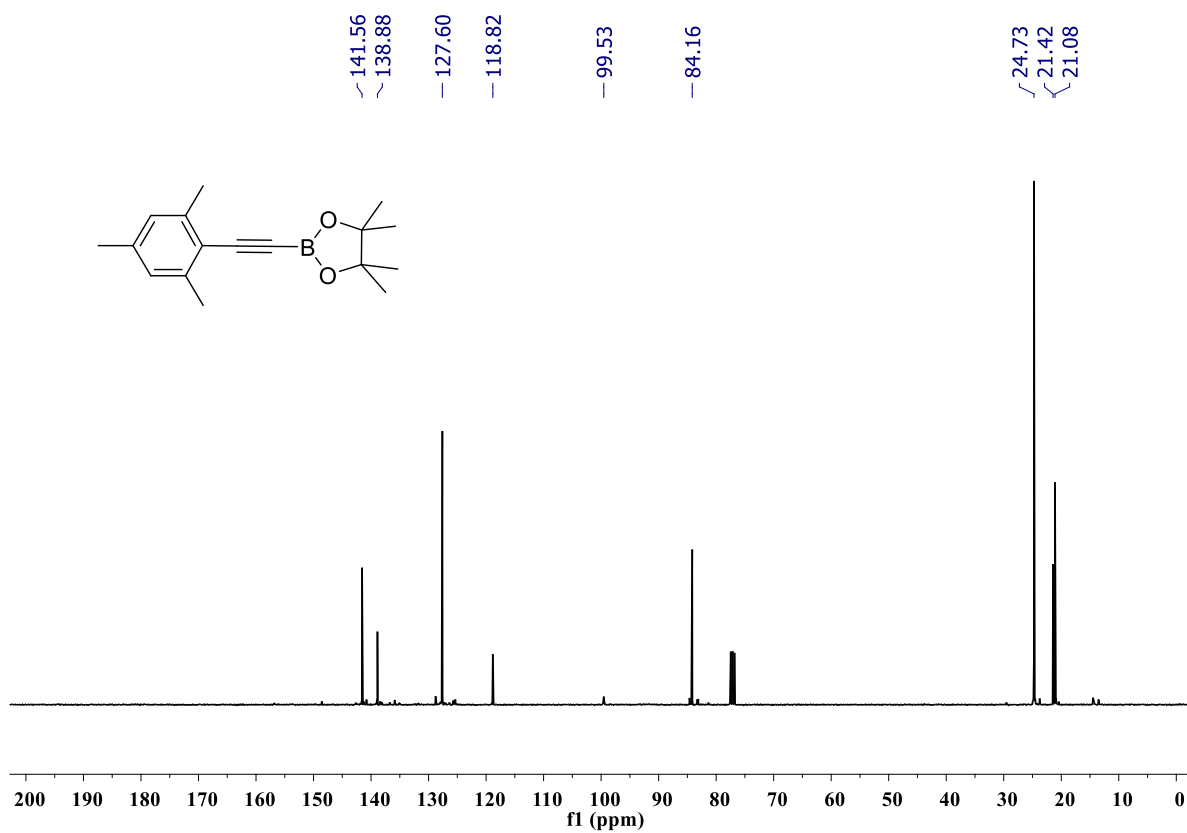


Figure S77: $^{13}\text{C}\{^1\text{H}\}$ NMR spectrum of compound **2e** (100 MHz, CDCl_3).

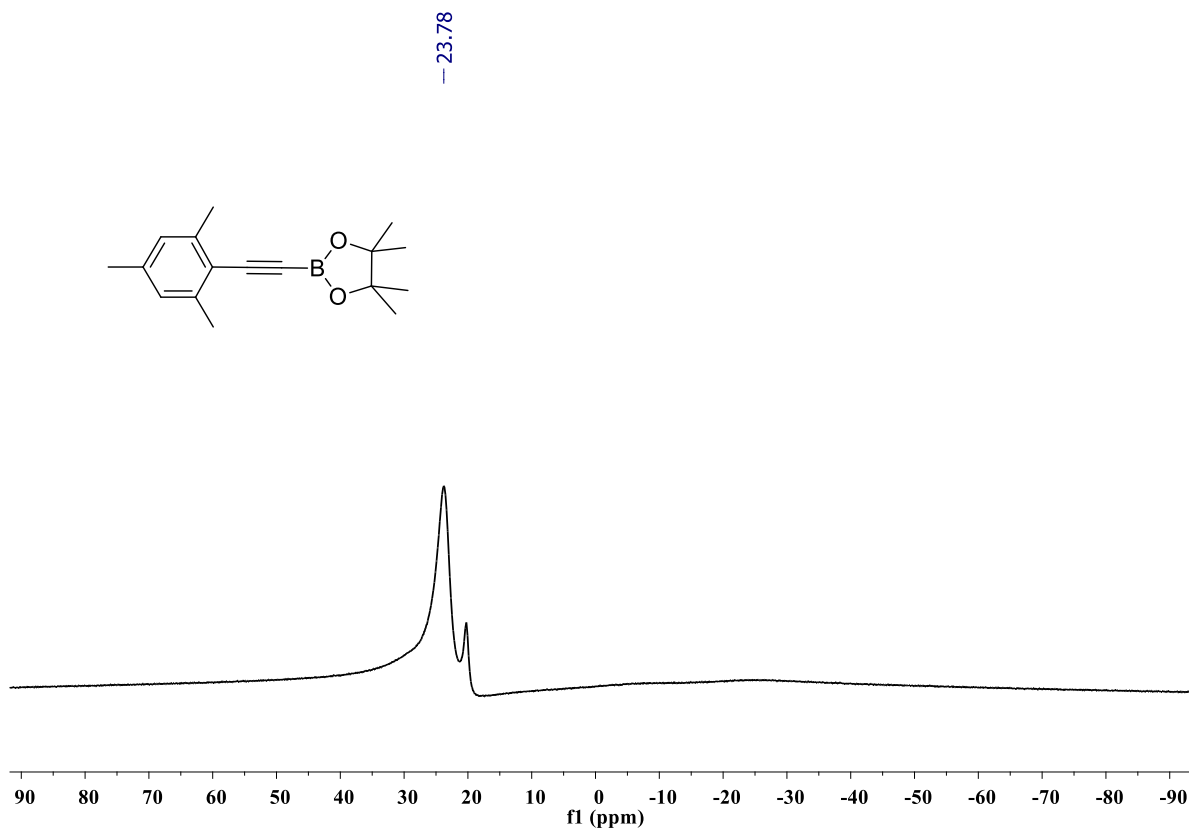


Figure S78: ^{11}B NMR spectrum of compound **2e** (128 MHz, CDCl_3).

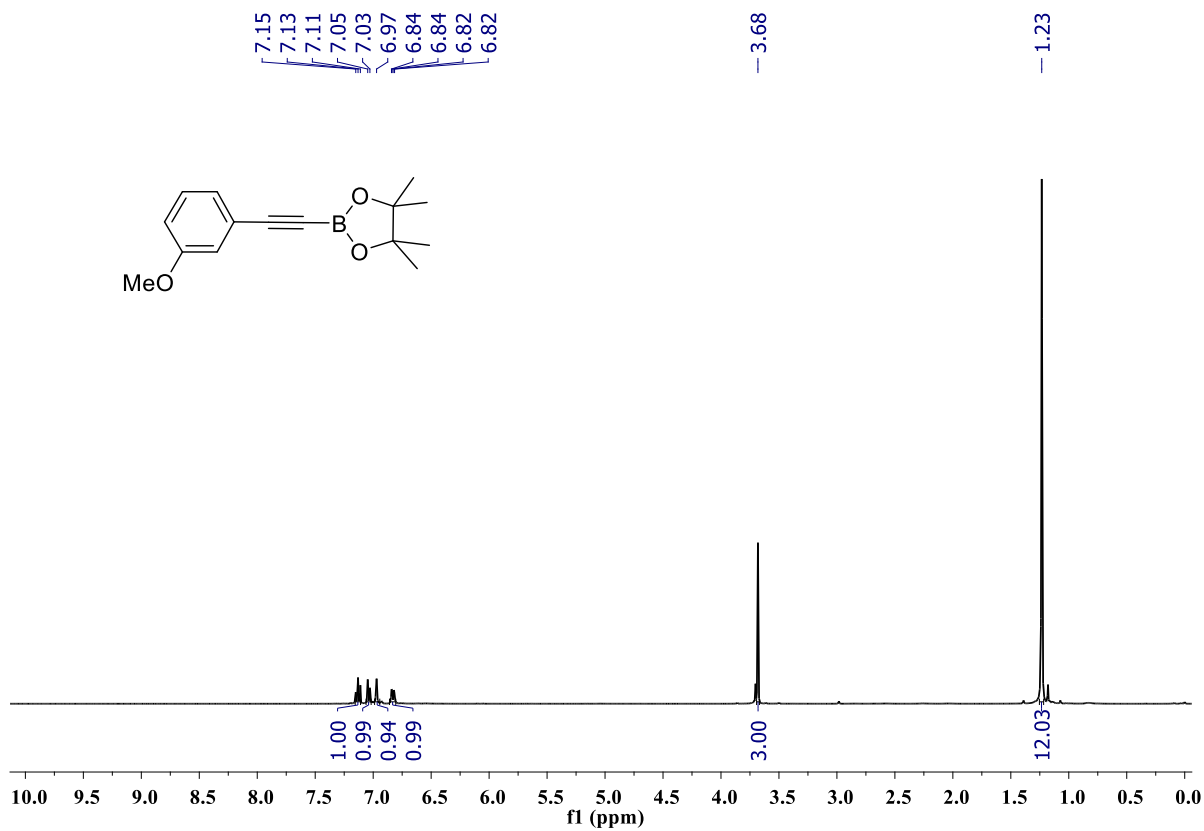


Figure S79: ^1H NMR spectrum of compound **2f** (400 MHz, CDCl_3).

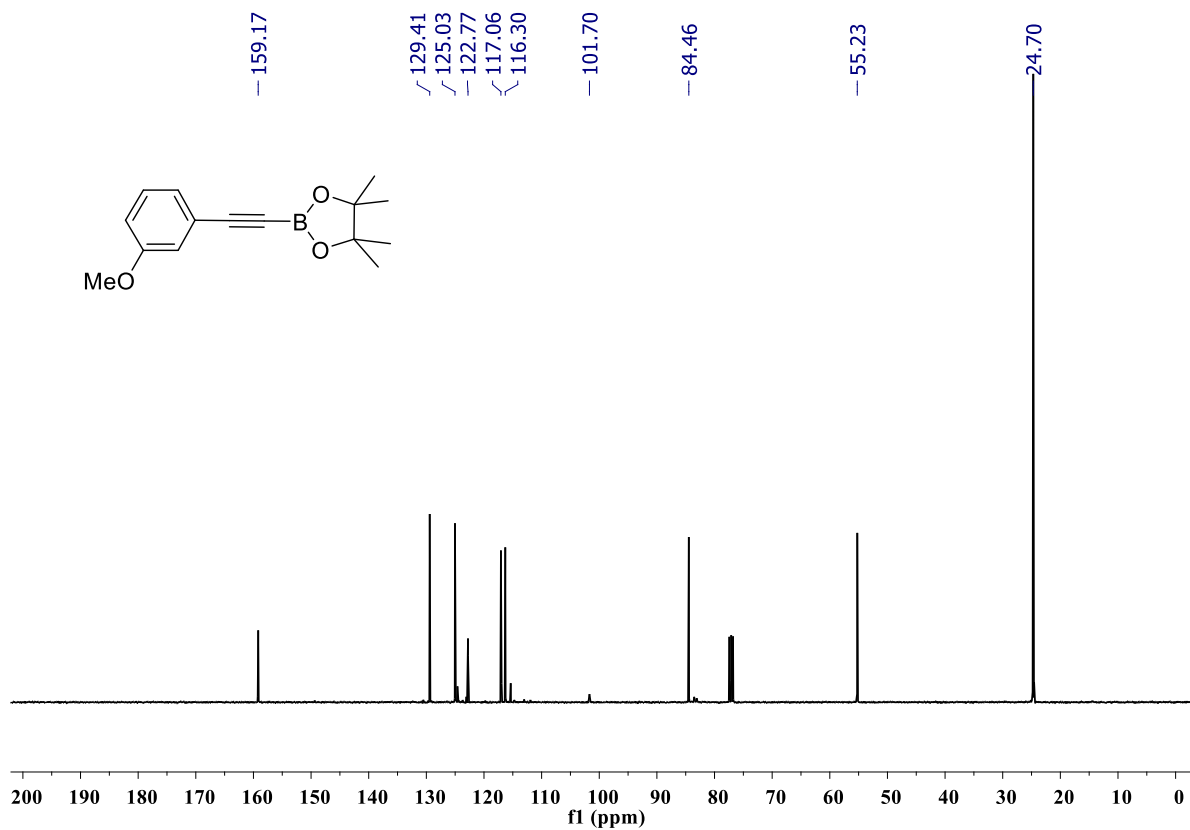


Figure S80: $^{13}\text{C}\{^1\text{H}\}$ NMR spectrum of compound **2f** (100 MHz, CDCl_3).

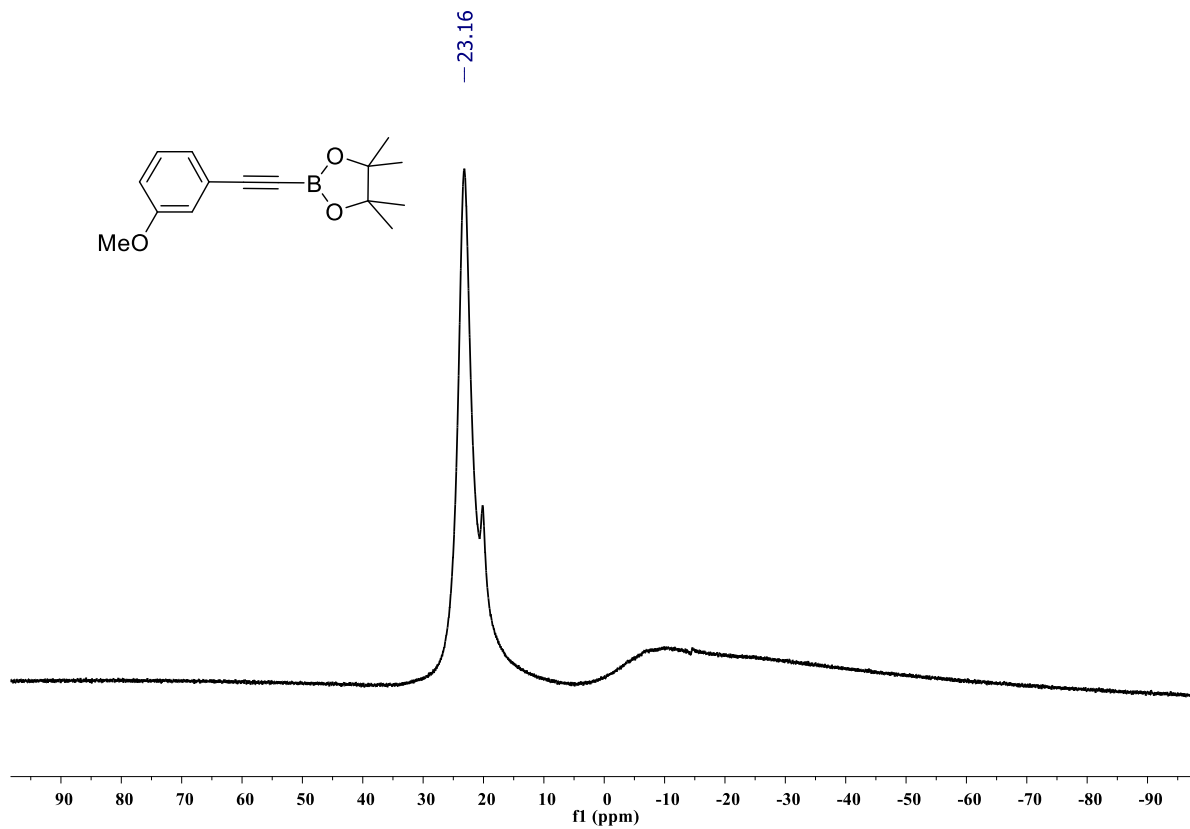


Figure S81: ^{11}B NMR spectrum of compound **2f** (128 MHz, CDCl_3).

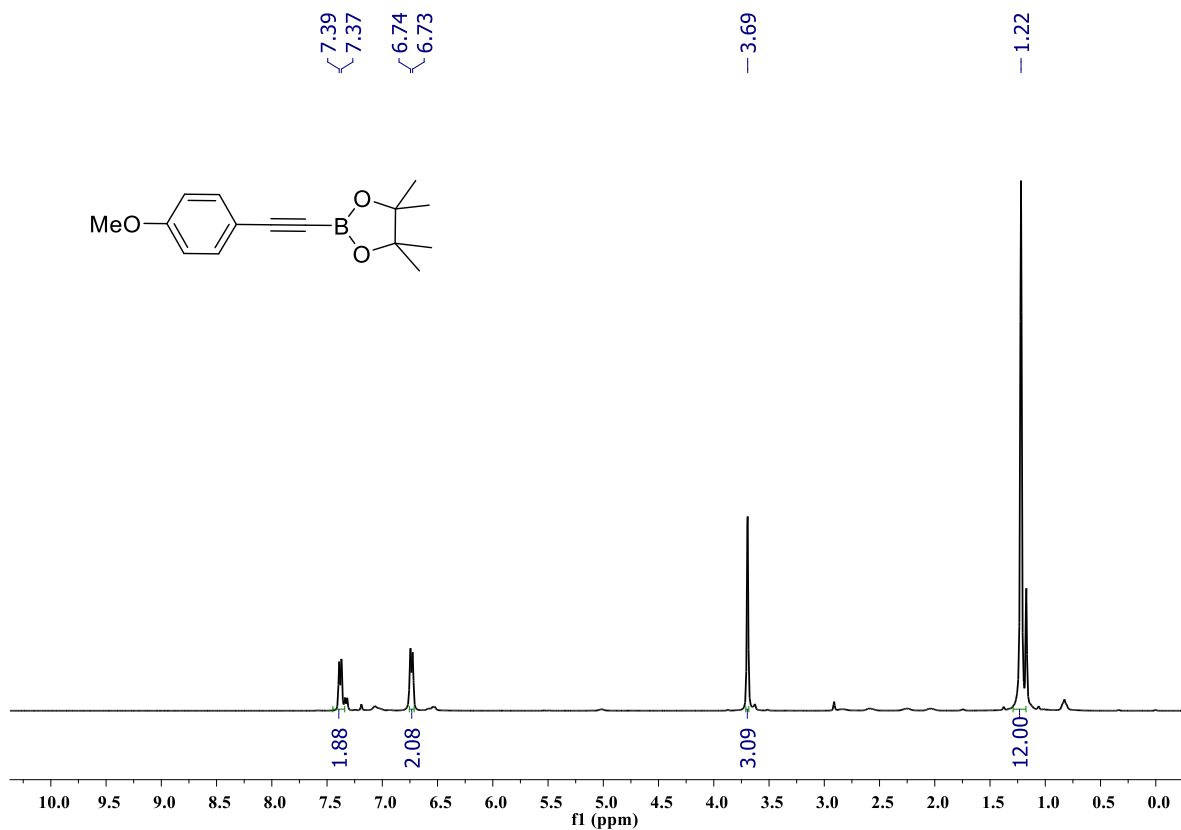


Figure S82: ^1H NMR spectrum of compound **2g** (400 MHz, CDCl_3).

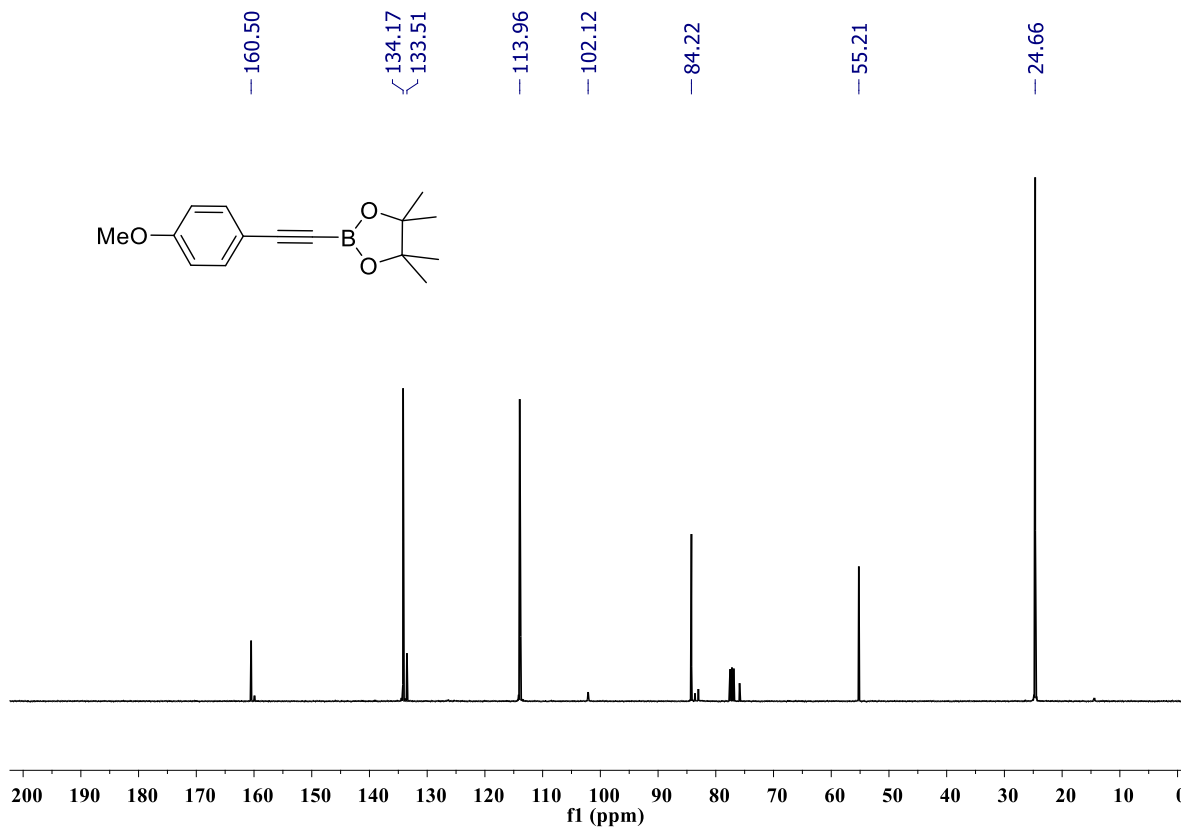


Figure S83: $^{13}\text{C}\{^1\text{H}\}$ NMR spectrum of compound **2g** (100 MHz, CDCl_3).

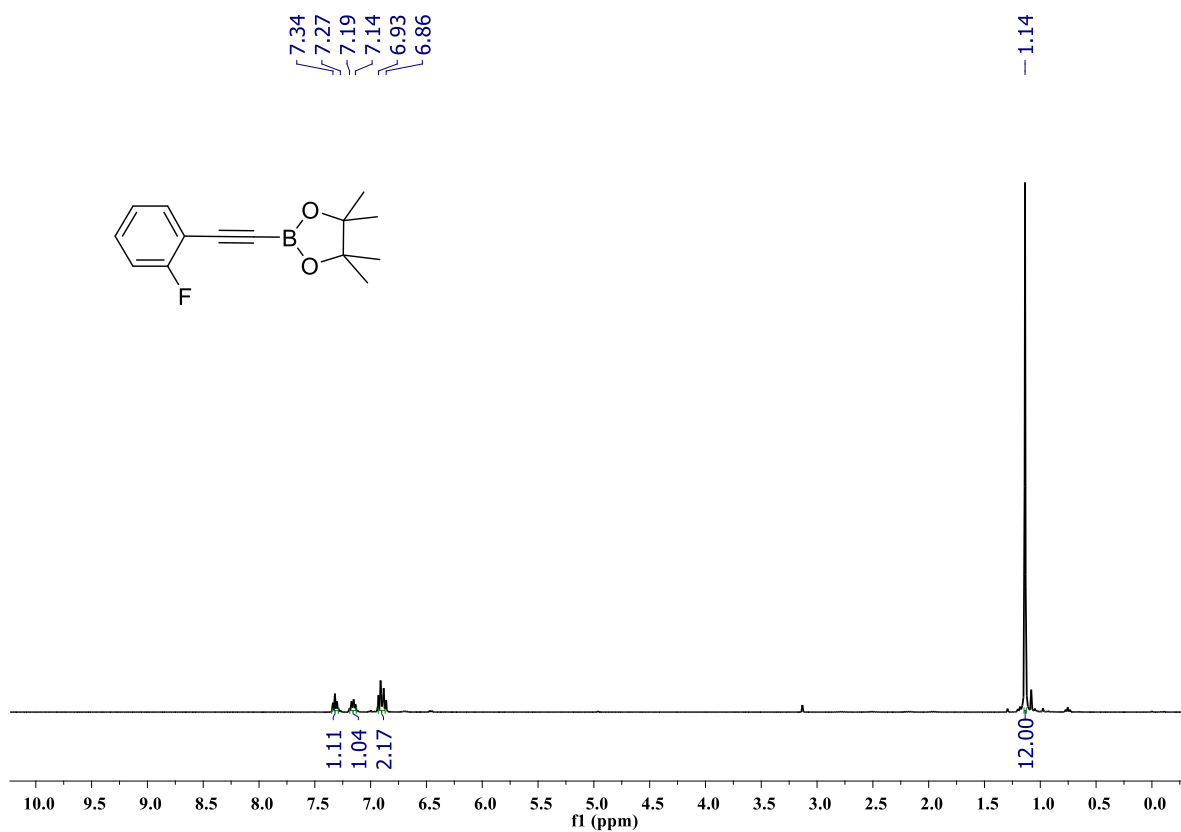


Figure S84: ¹H NMR spectrum of compound **2h** (400 MHz, CDCl₃).

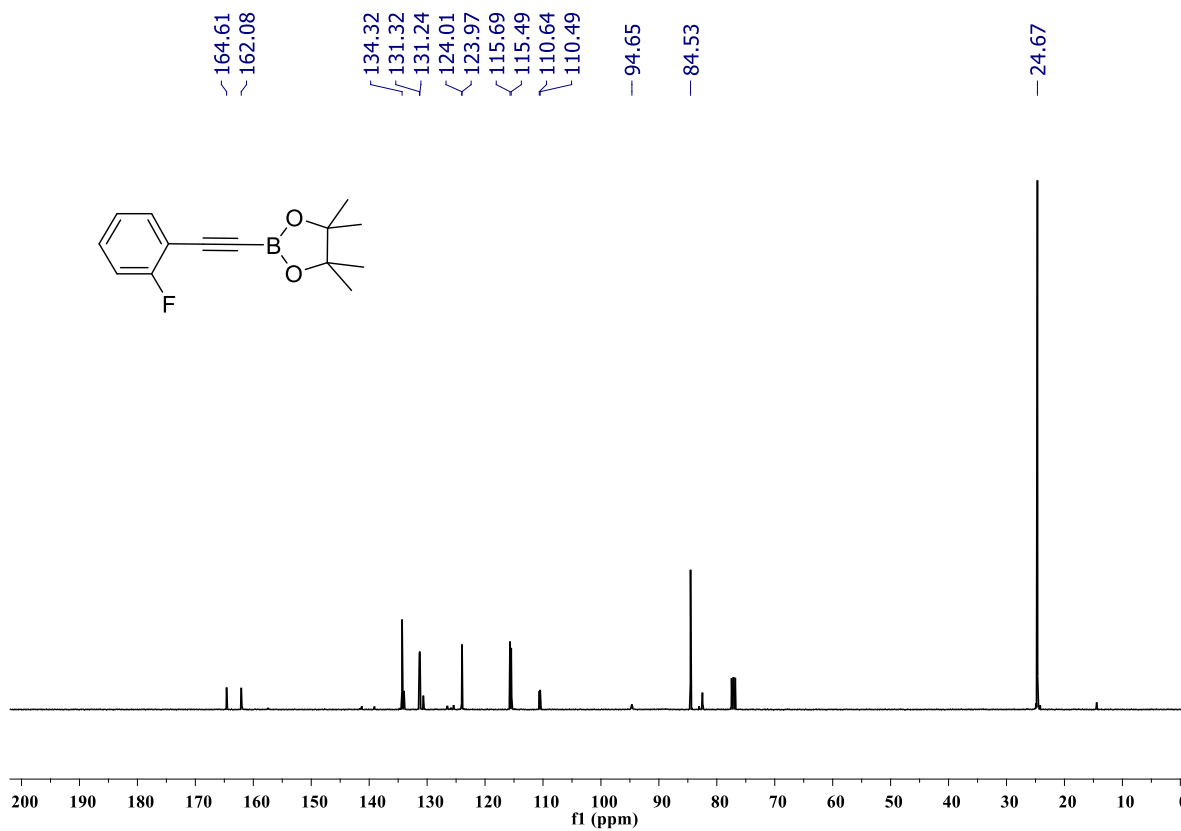


Figure S85: ¹³C{¹H} NMR spectrum of compound **2h** (100 MHz, CDCl₃).

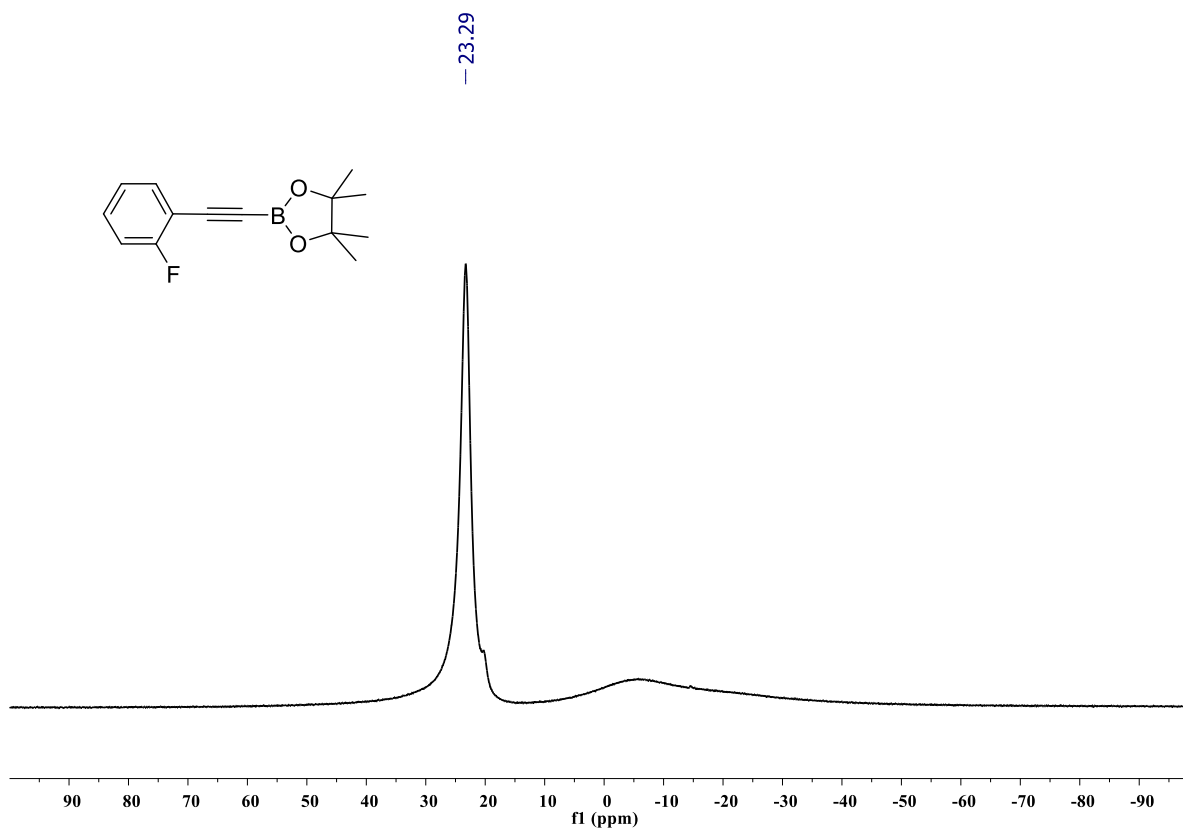


Figure S86: ^{11}B NMR spectrum of compound **2h** (128 MHz, CDCl_3).

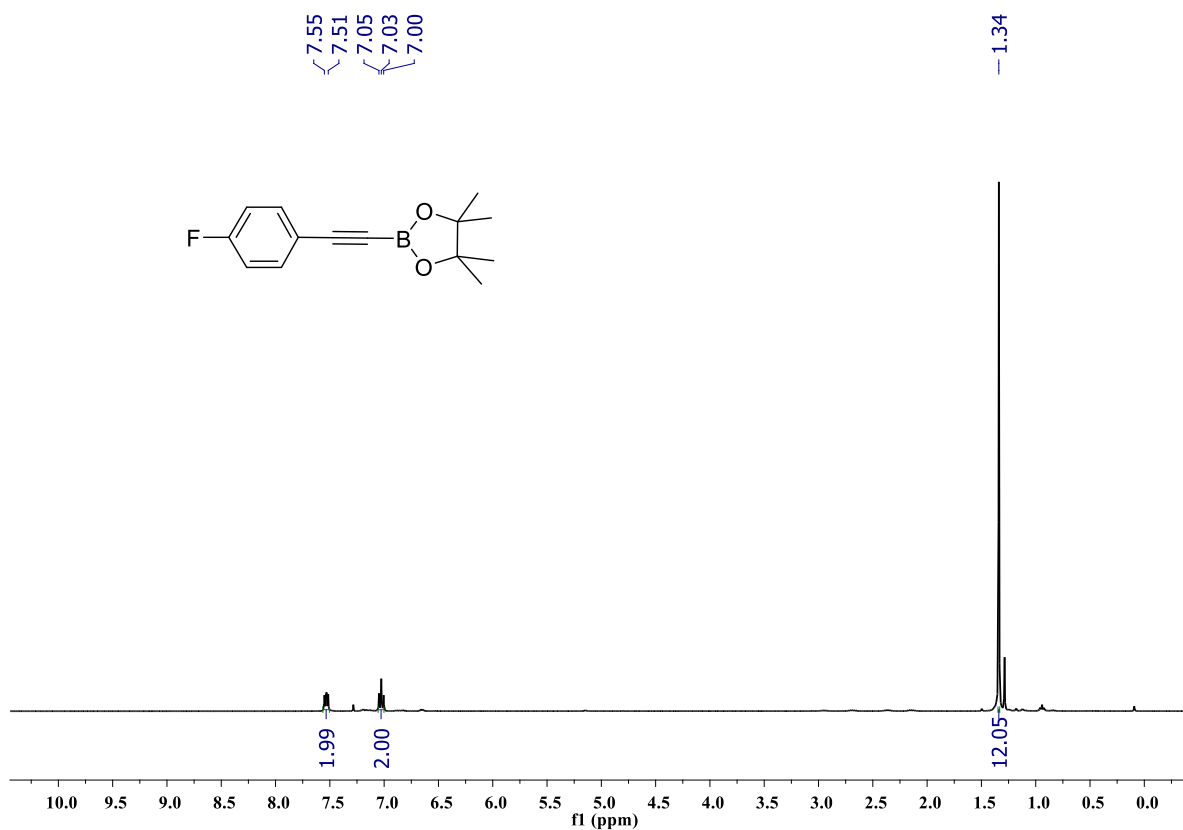


Figure S87: ^1H NMR spectrum of compound **2i** (400 MHz, CDCl_3).

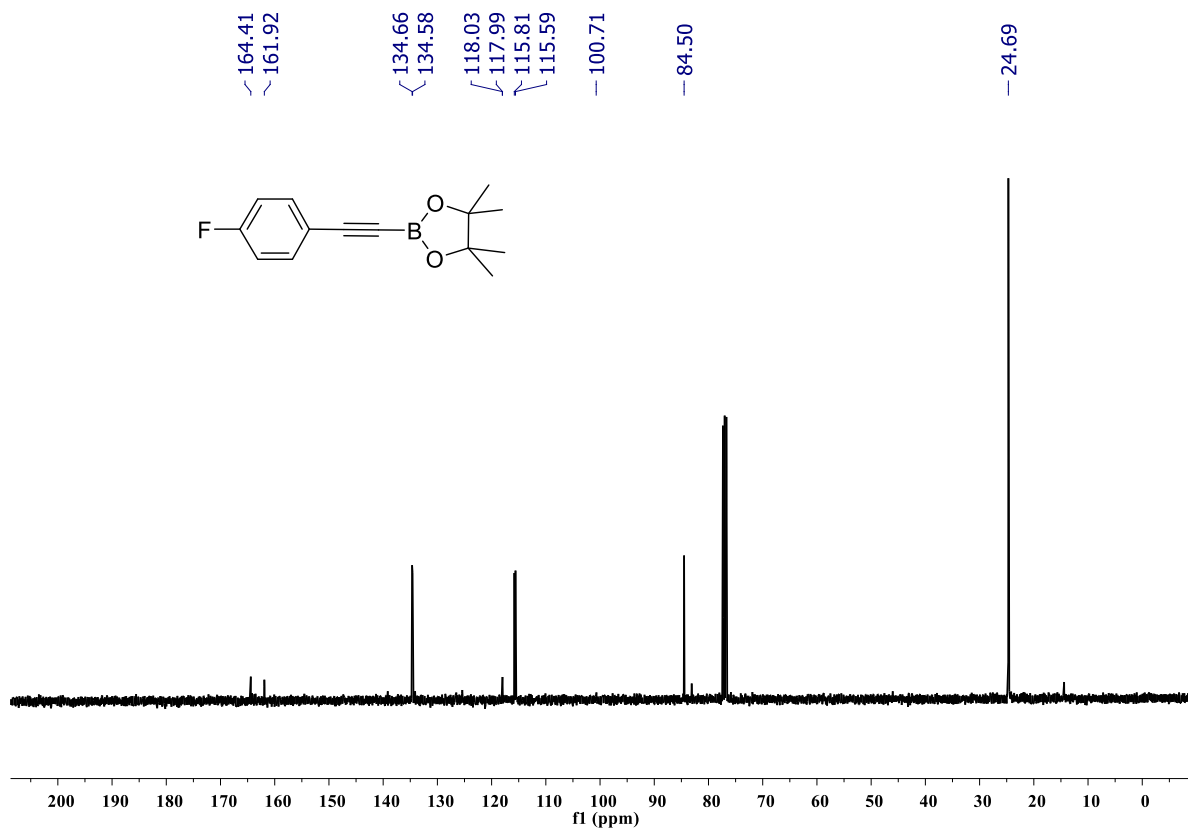


Figure S88: $^{13}\text{C}\{^1\text{H}\}$ NMR spectrum of compound **2i** (100 MHz, CDCl_3).

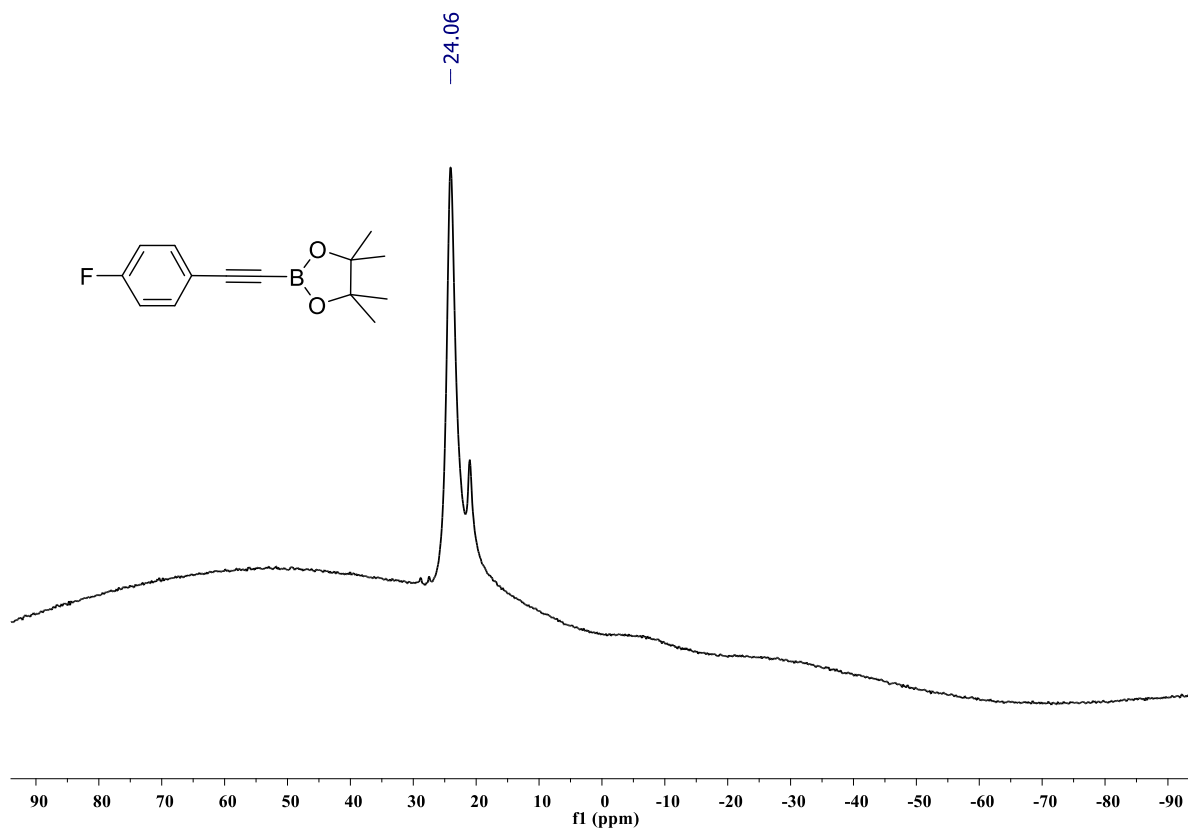


Figure S89: ^{11}B NMR spectrum of compound **2i** (128 MHz, CDCl_3).

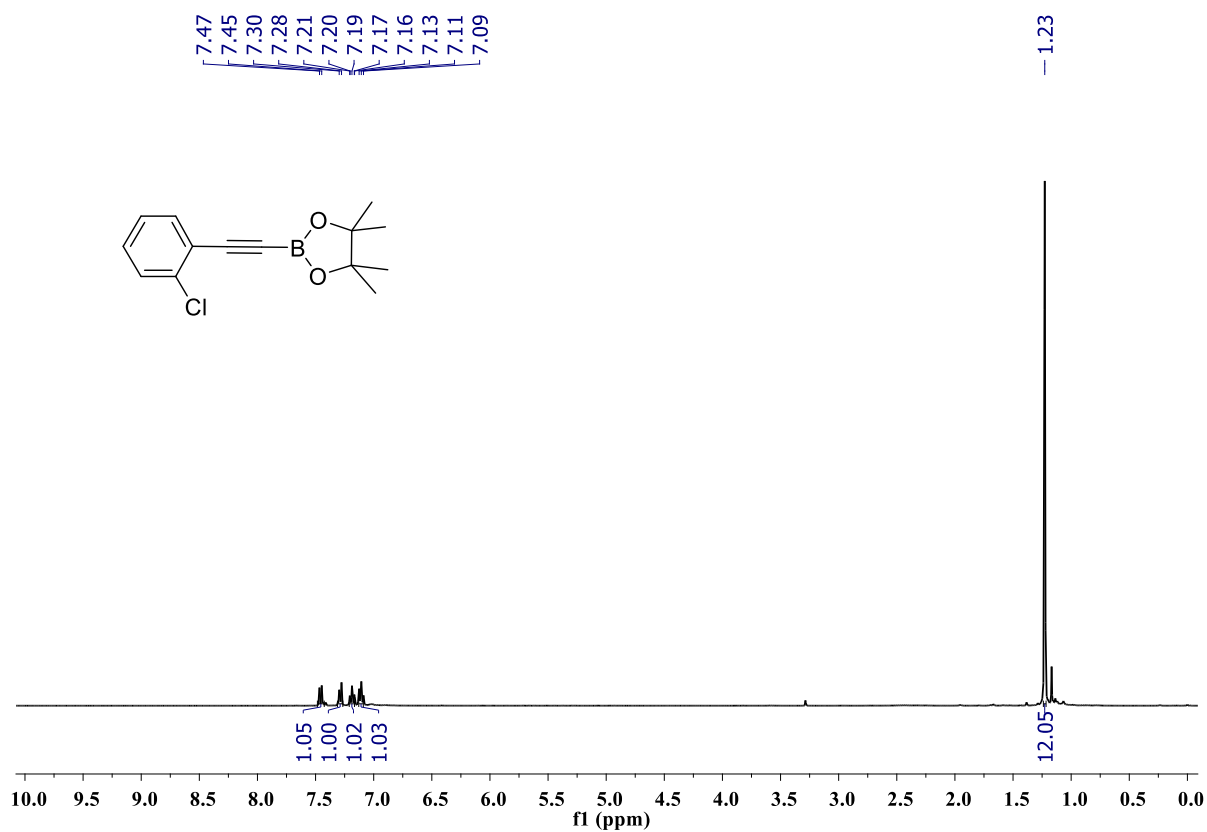


Figure S90: $^1\text{H NMR}$ spectrum of compound **2j** (400 MHz, CDCl_3).

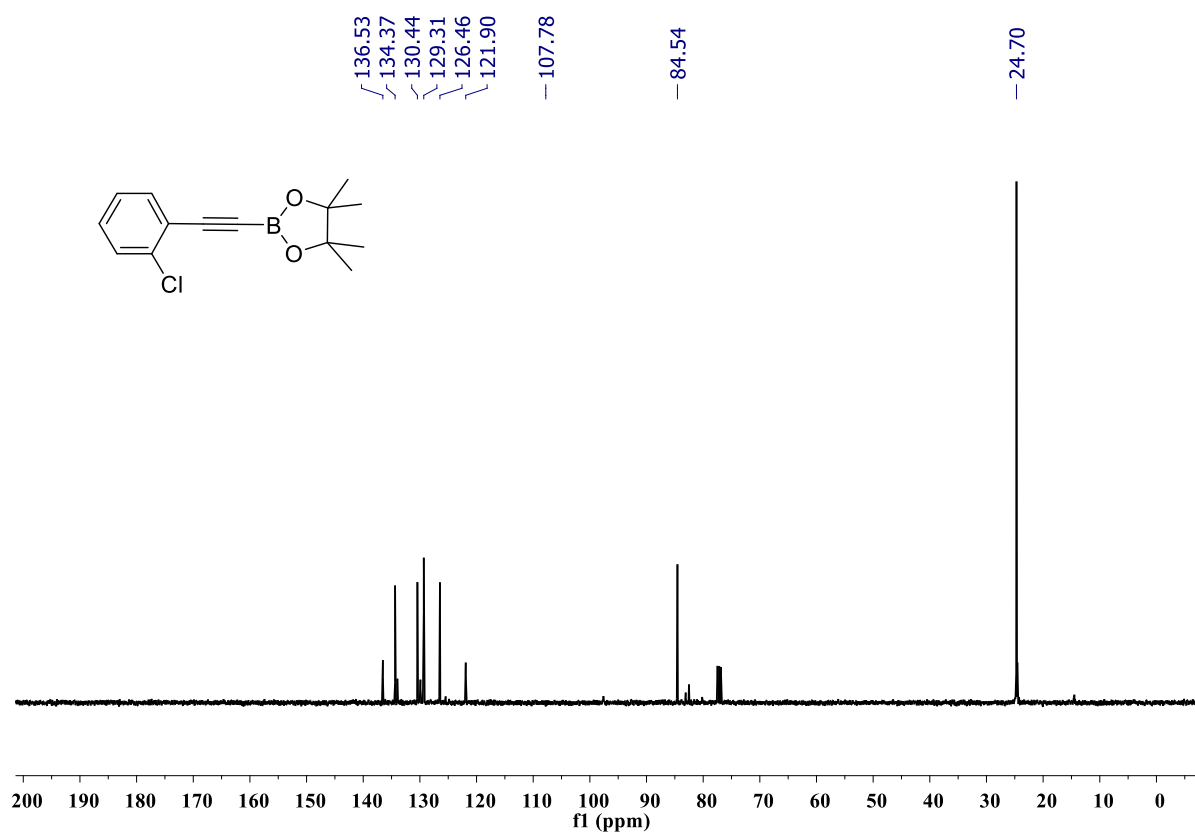


Figure S91: $^{13}\text{C}\{^1\text{H}\}$ NMR spectrum of compound **2j** (100 MHz, CDCl_3).

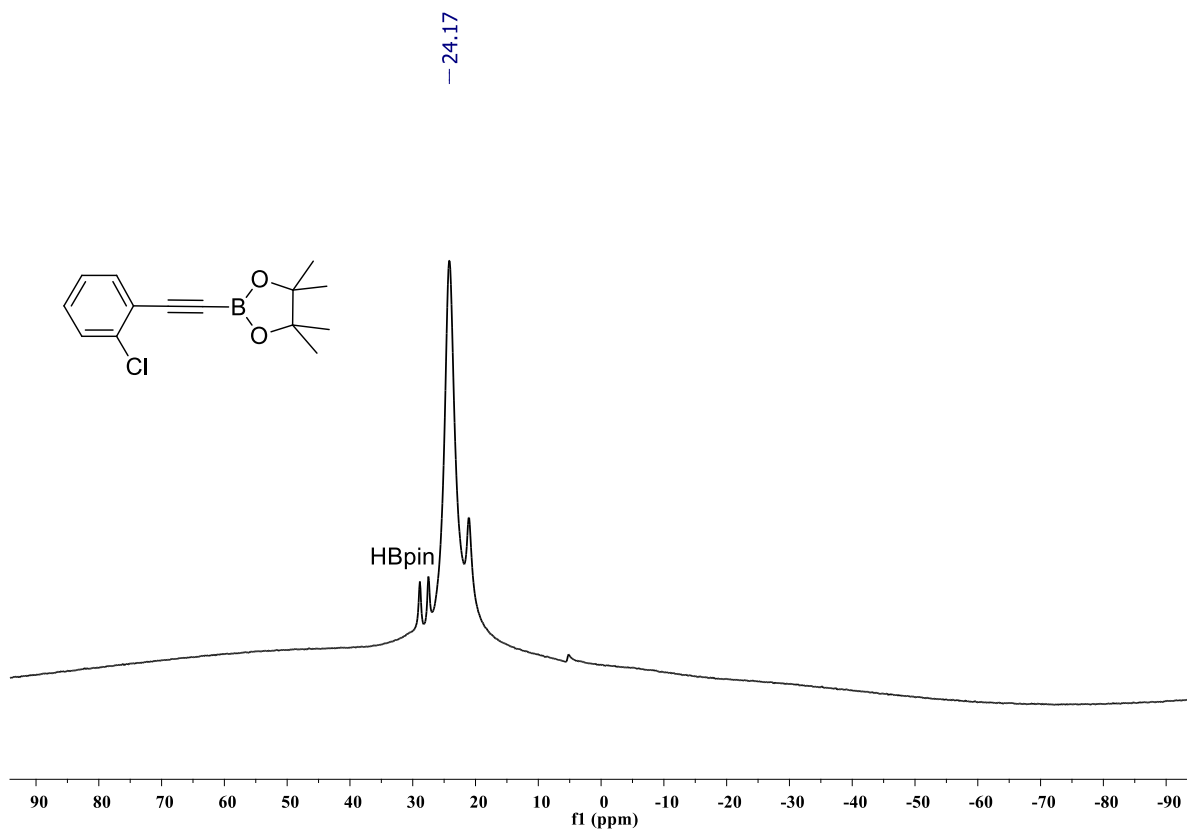


Figure S92: ^{11}B NMR spectrum of compound **2j** (128 MHz, CDCl_3).

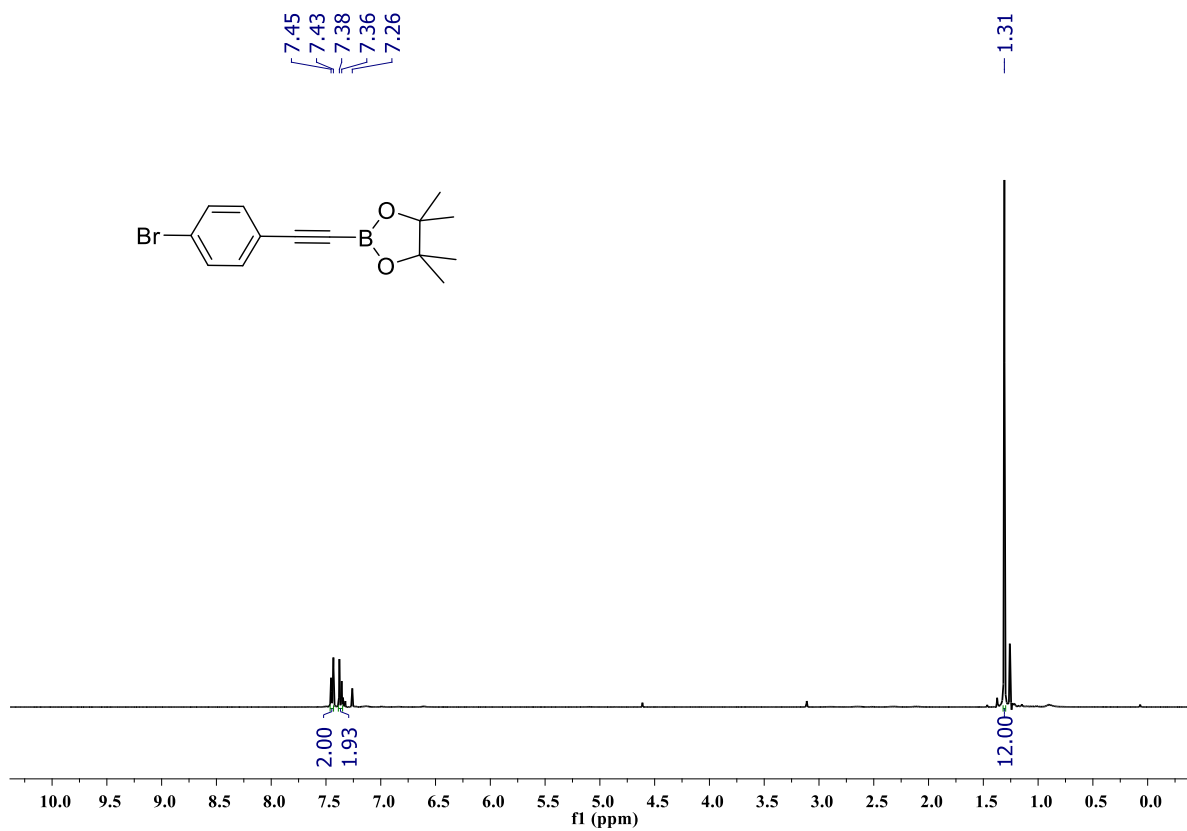


Figure S93: ^1H NMR spectrum of compound **2k** (400 MHz, CDCl_3).

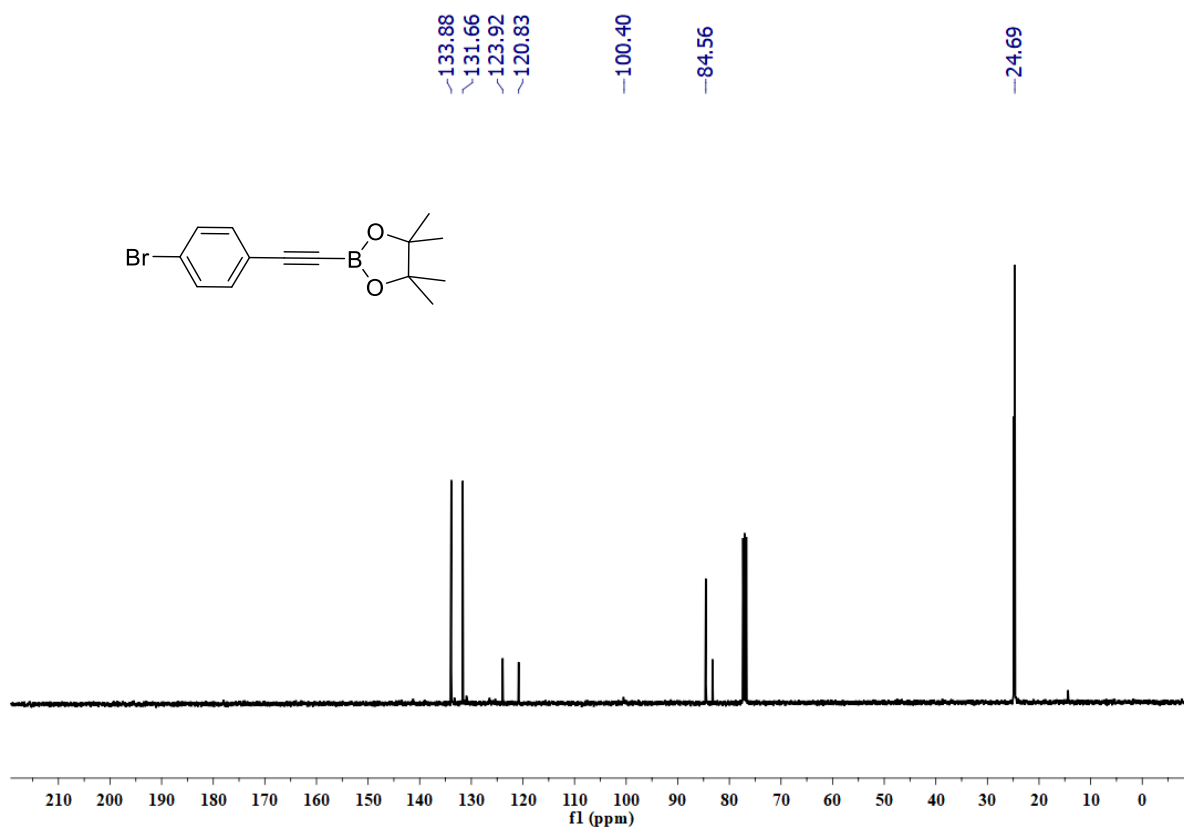


Figure S94: $^{13}\text{C}\{^1\text{H}\}$ NMR spectrum of compound **2k** (100 MHz, CDCl_3).

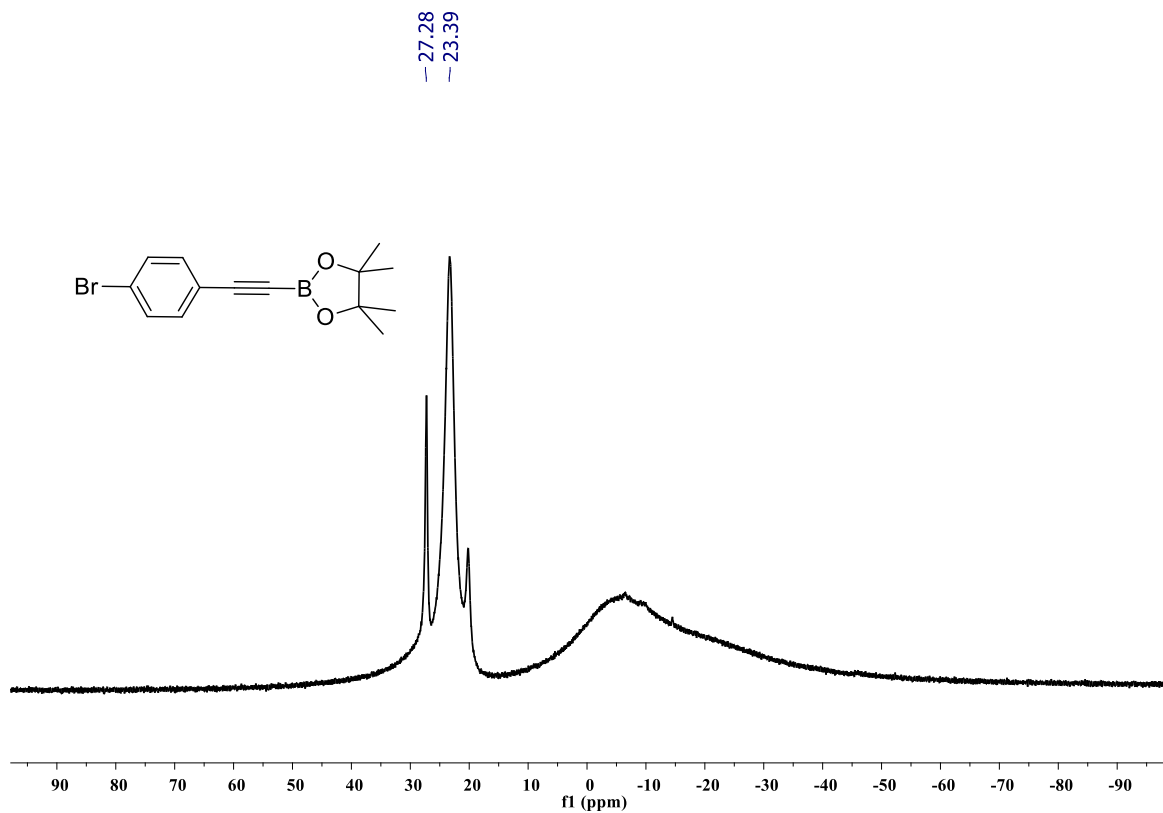


Figure S95: $^{11}\text{B}\{^1\text{H}\}$ NMR spectrum of compound **2k** (128 MHz, CDCl_3). A peak observed at δ 27.28 ppm arises from free HBpin.

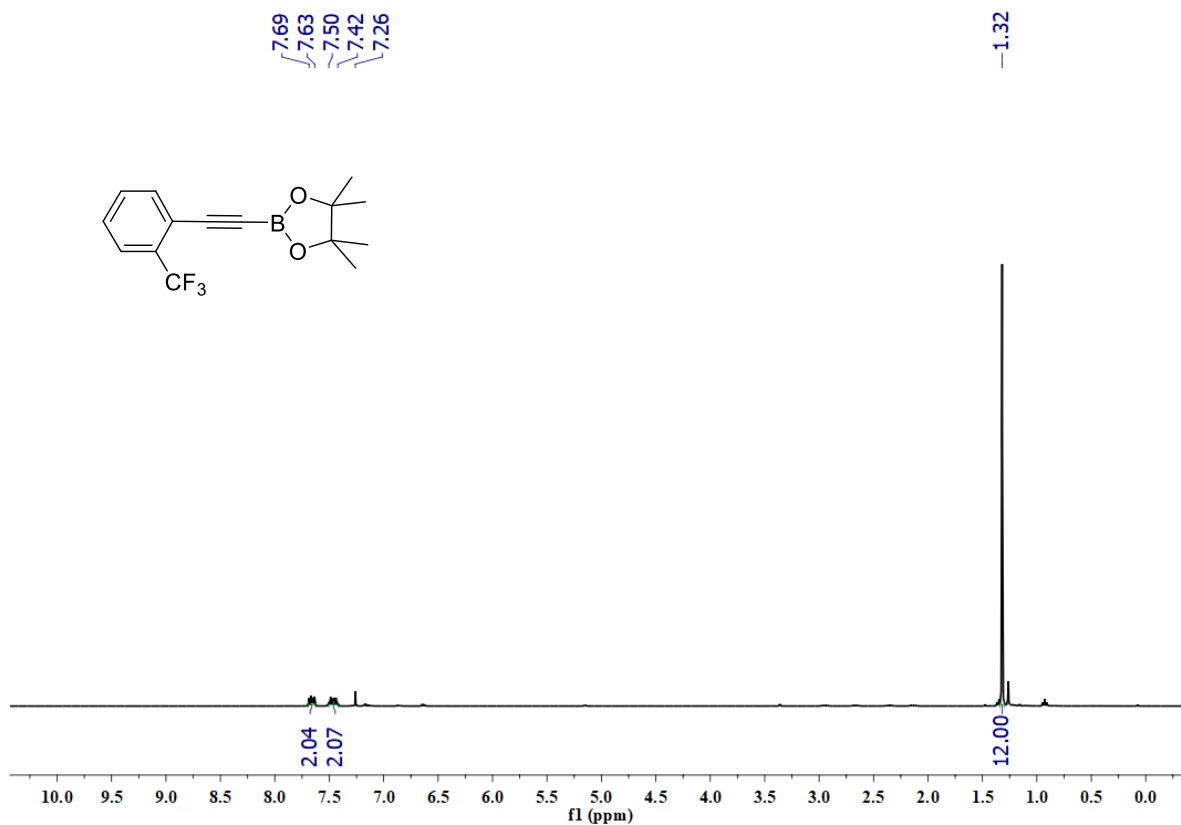


Figure S96: ^1H NMR spectrum of compound **2I** (400 MHz, CDCl_3).

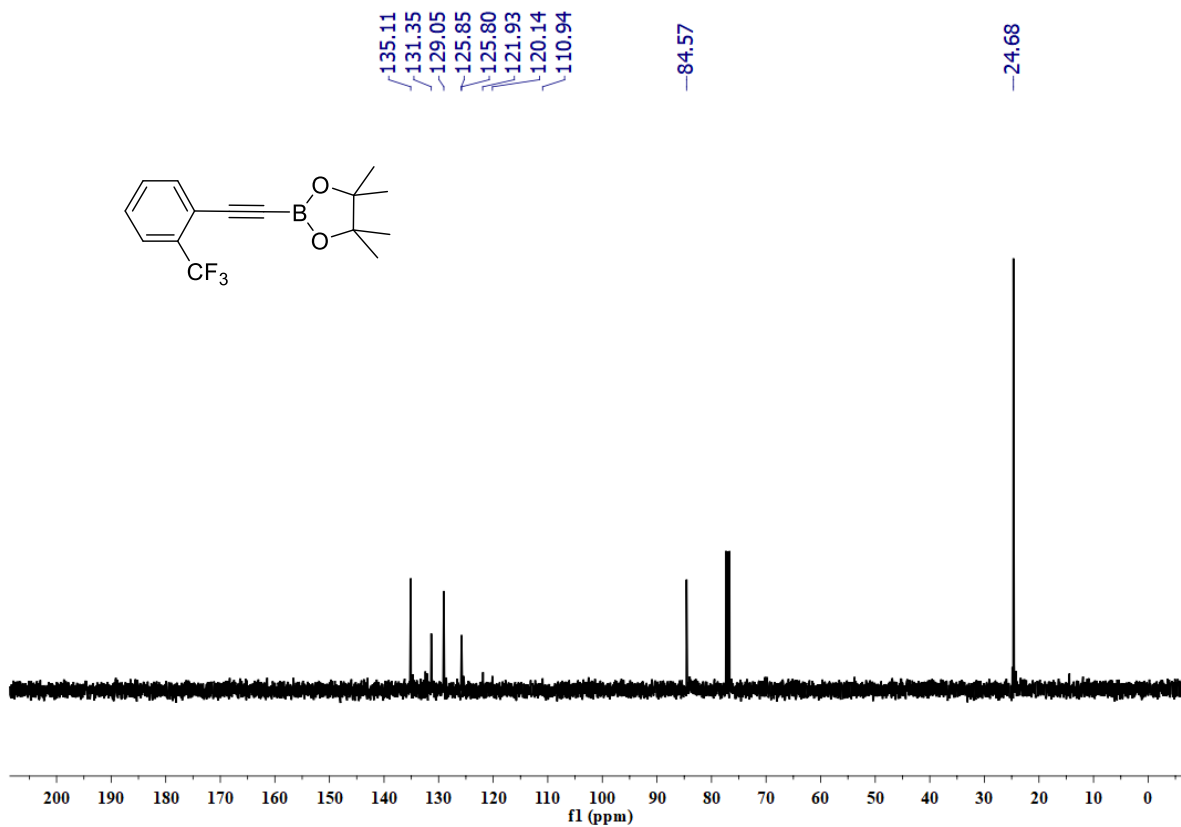


Figure S97: $^{13}\text{C}\{^1\text{H}\}$ NMR spectrum of compound **2I** (100 MHz, CDCl_3).

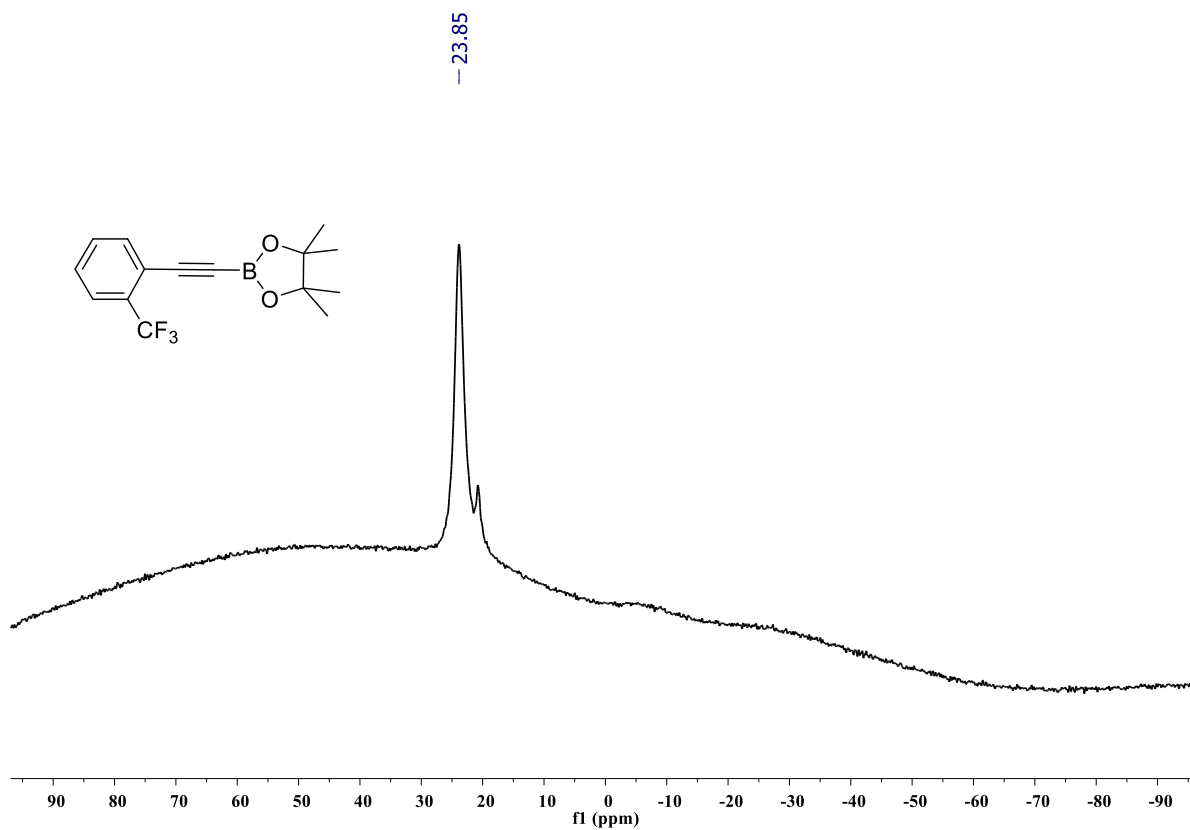


Figure S98: ^{11}B NMR spectrum of compound **2l** (128 MHz, CDCl_3).

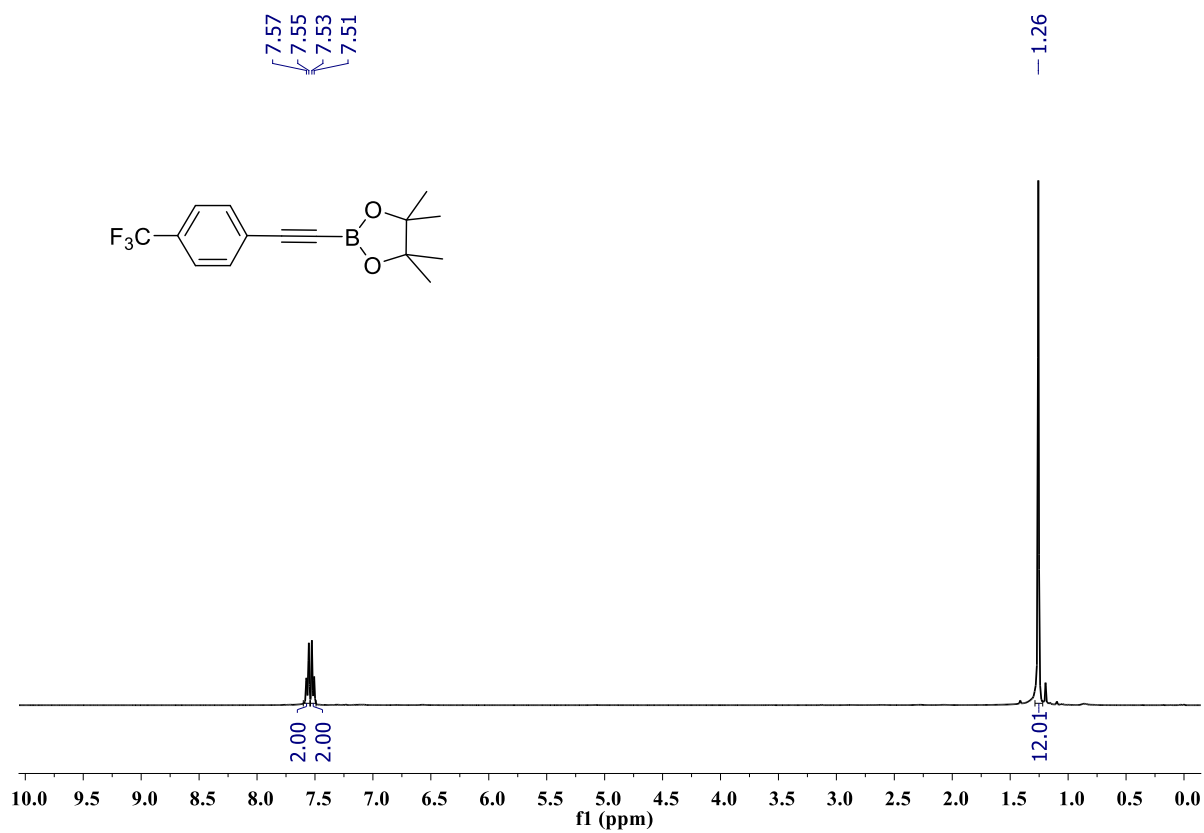


Figure S99: ^1H NMR spectrum of compound **2m** (400 MHz, CDCl_3).

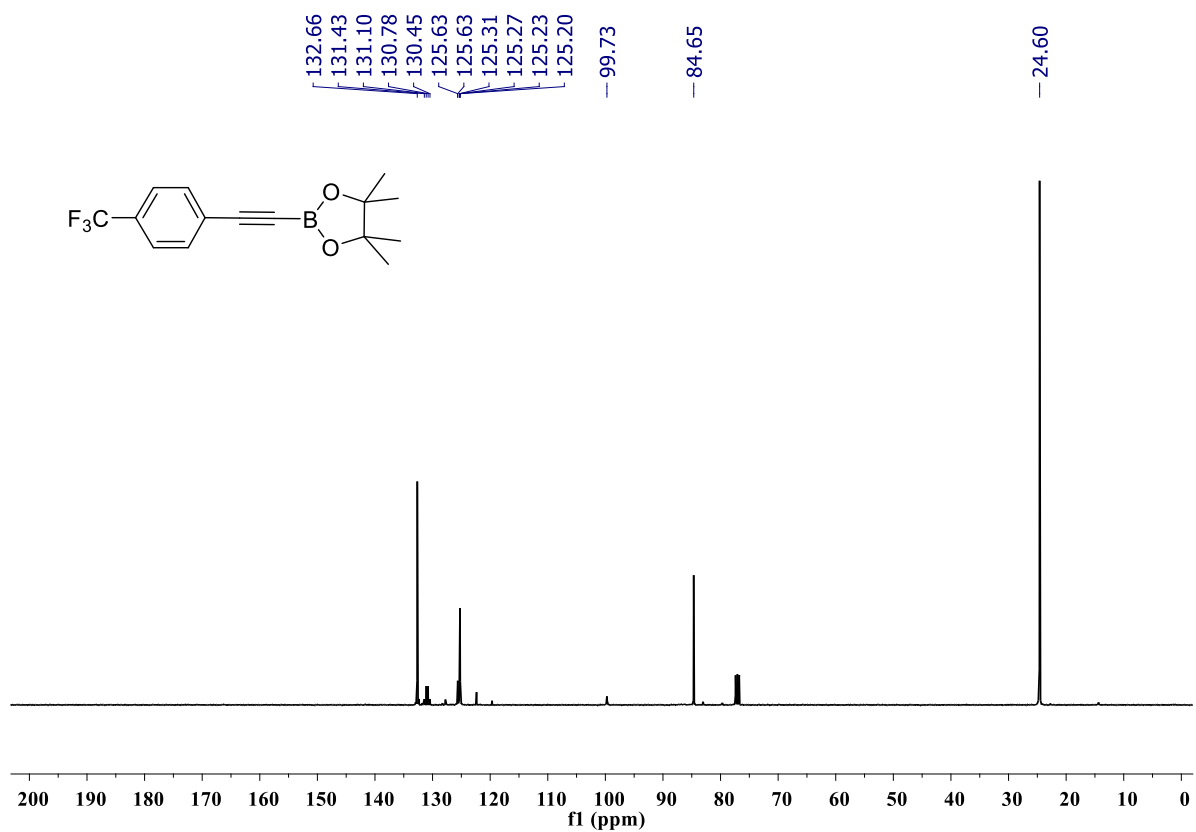


Figure S100: $^{13}\text{C}\{^1\text{H}\}$ NMR spectrum of compound **2m** (100 MHz, CDCl_3).

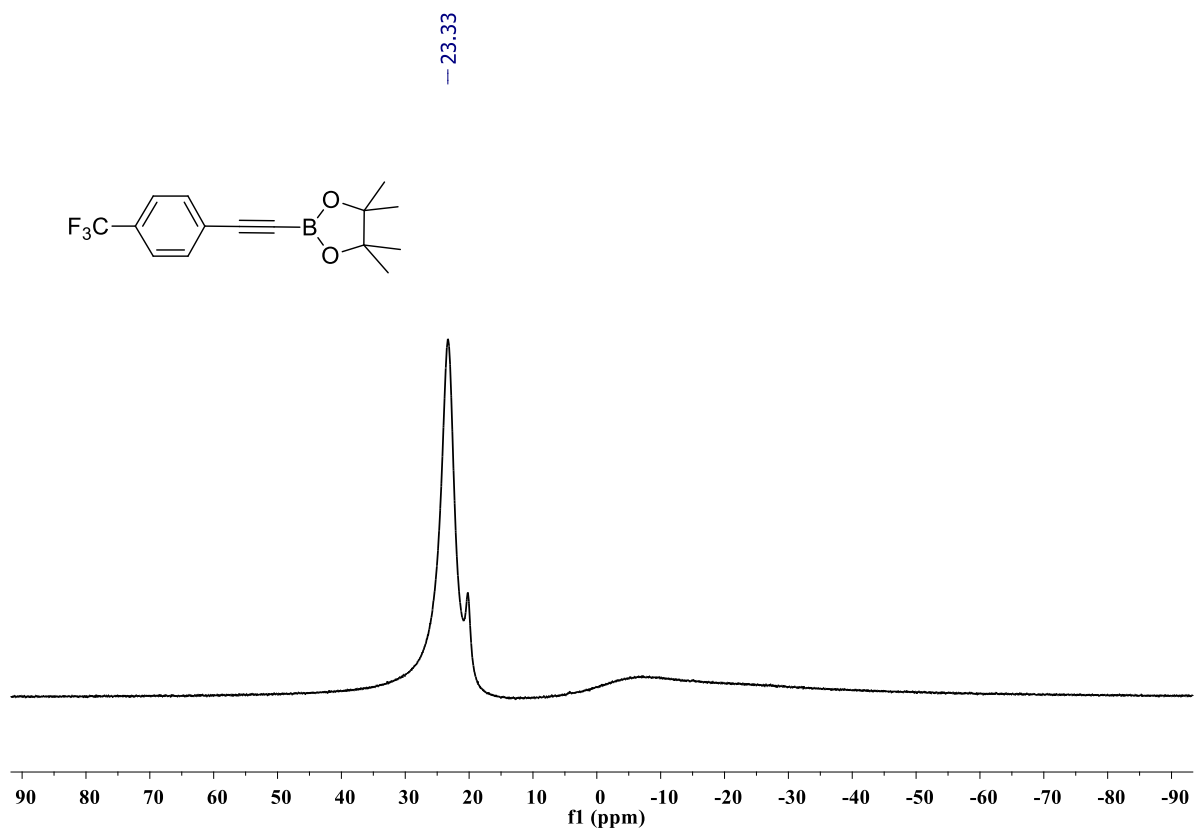
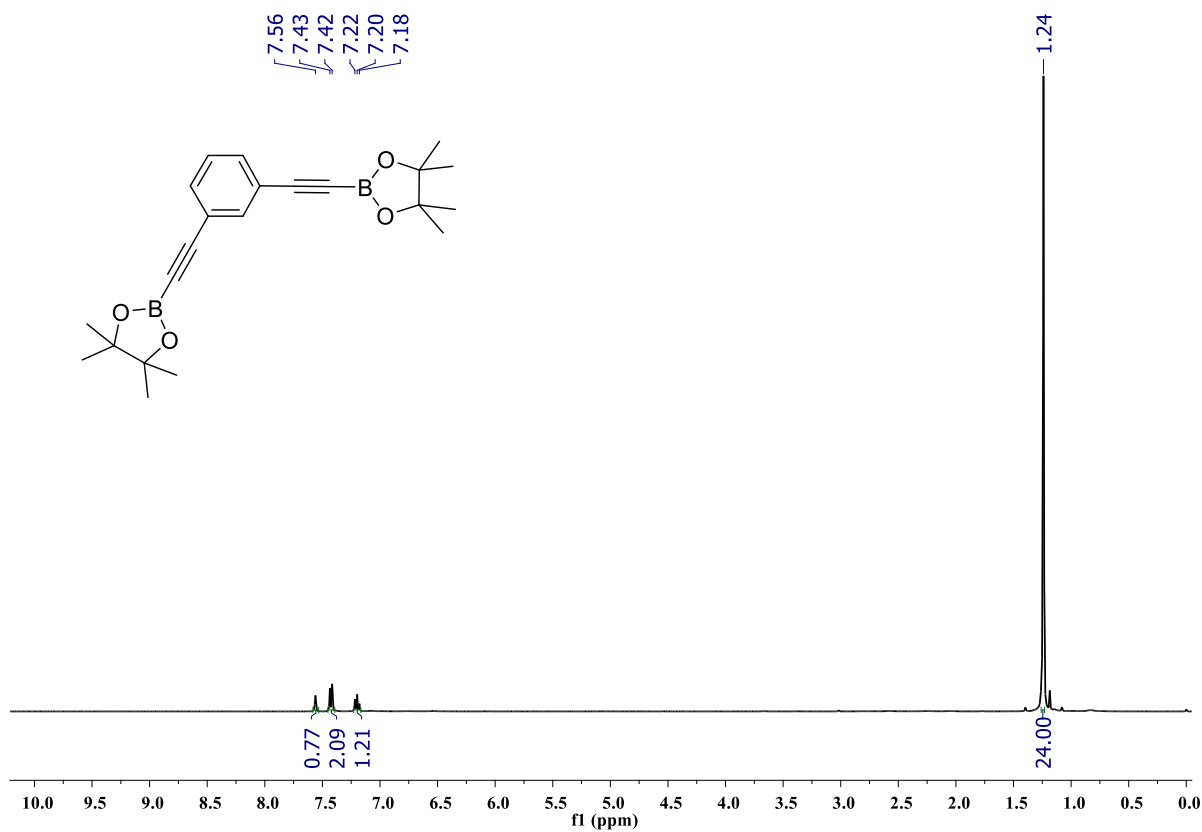
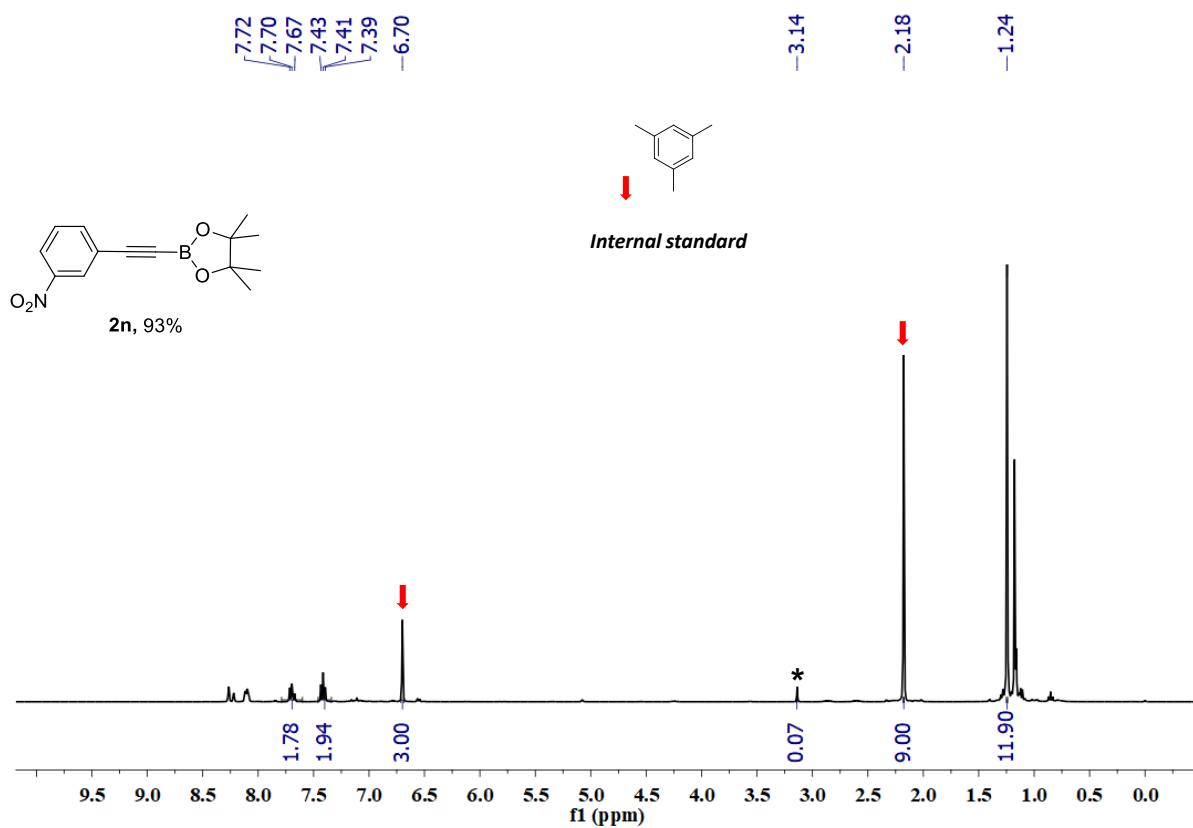


Figure S101: ^{11}B NMR spectrum of compound **2m** (128 MHz, CDCl_3).



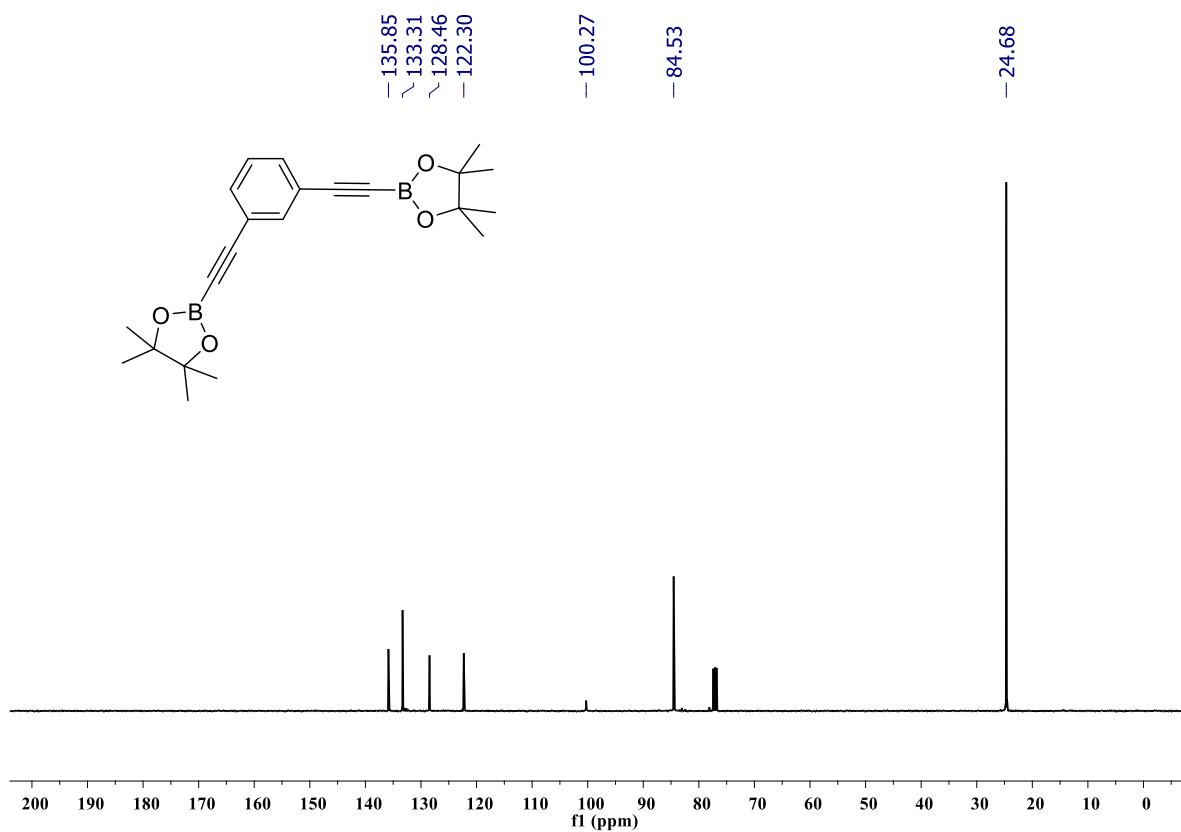


Figure S104: $^{13}\text{C}\{^1\text{H}\}$ NMR spectrum of compound **2o** (100 MHz, CDCl_3).

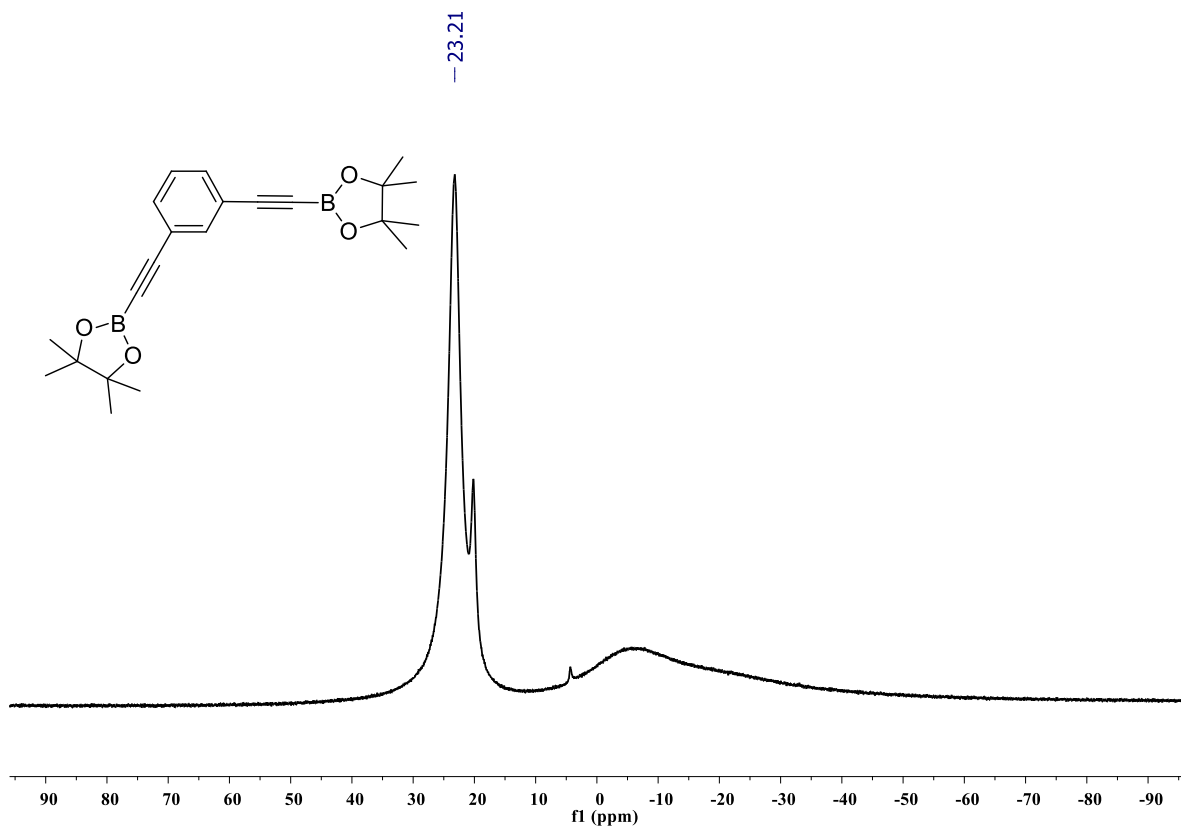


Figure S105: ^{11}B NMR spectrum of compound **2o** (128 MHz, CDCl_3).

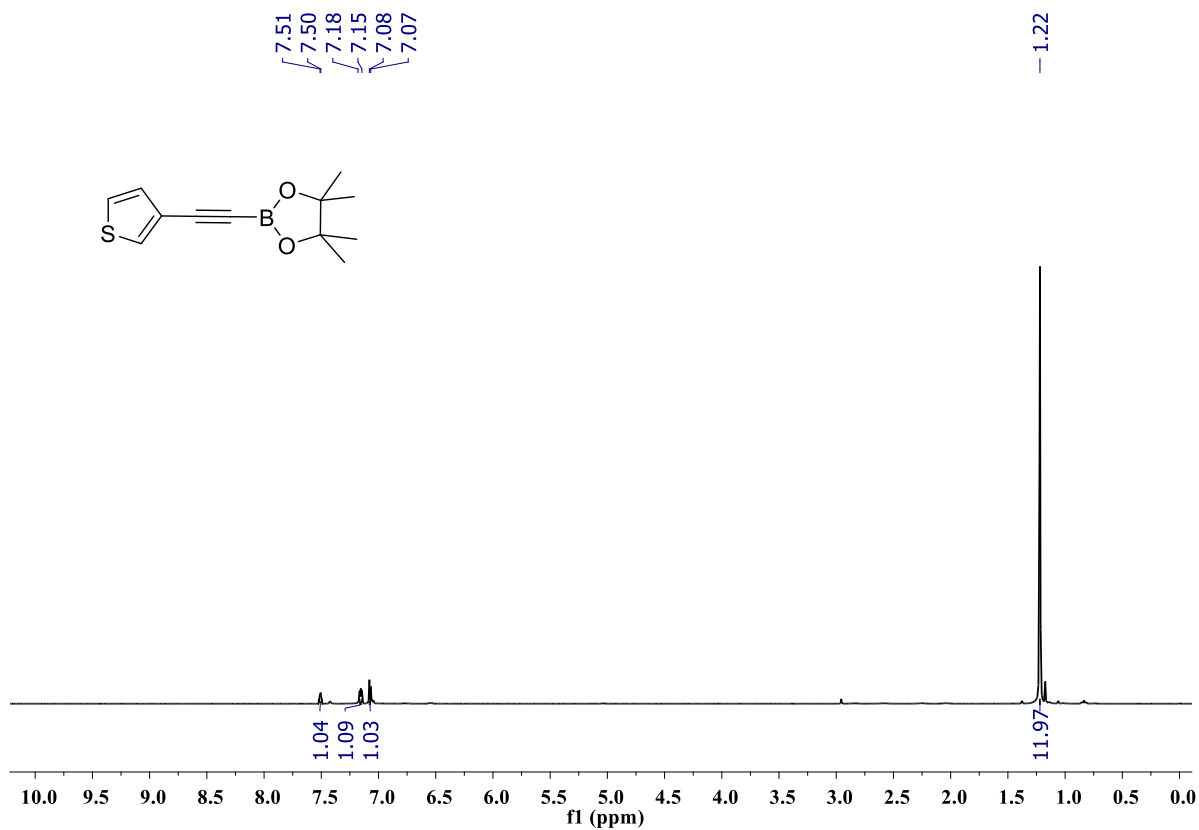


Figure S106: ^1H NMR spectrum of compound **2p** (400 MHz, CDCl_3).

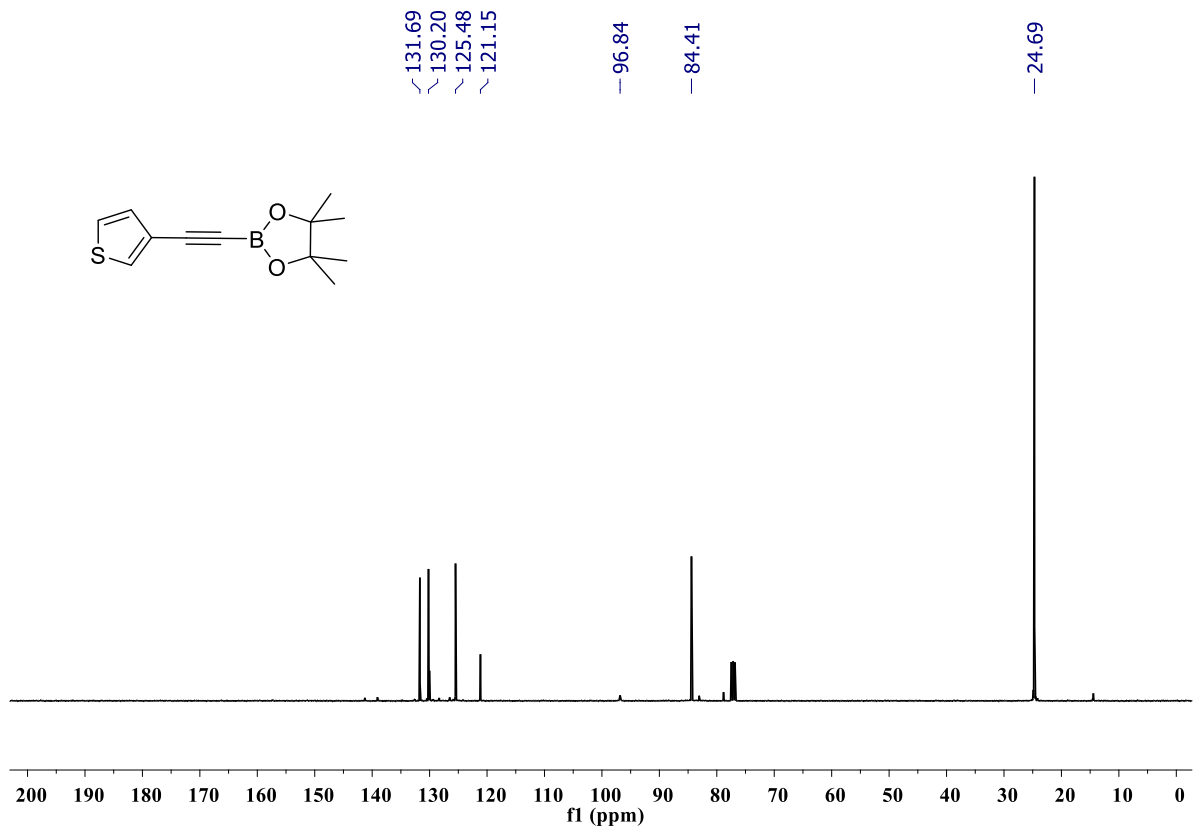


Figure S107: $^{13}\text{C}\{^1\text{H}\}$ NMR spectrum of compound **2p** (100 MHz, CDCl_3).

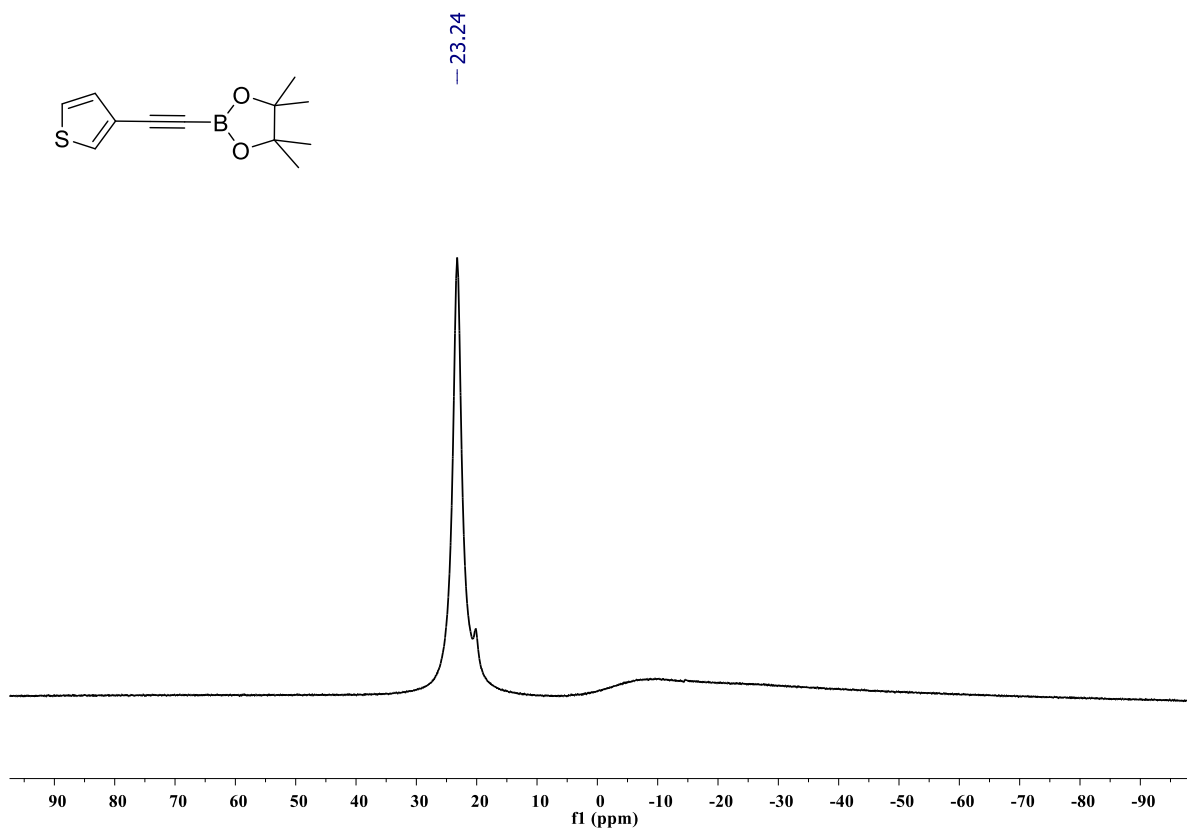


Figure S108: ^{11}B NMR spectrum of compound **2p** (128 MHz, CDCl_3).

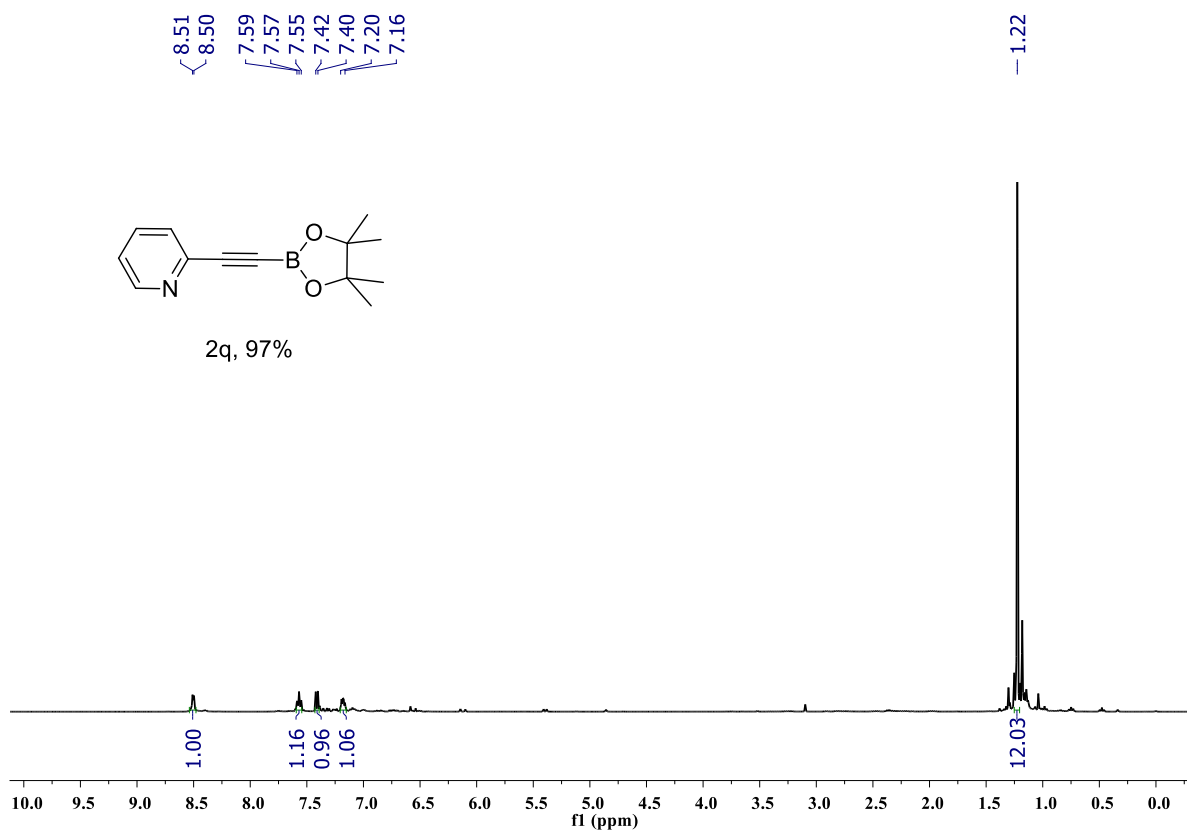


Figure S109: ^1H NMR spectrum of compound **2q** (400 MHz, CDCl_3).

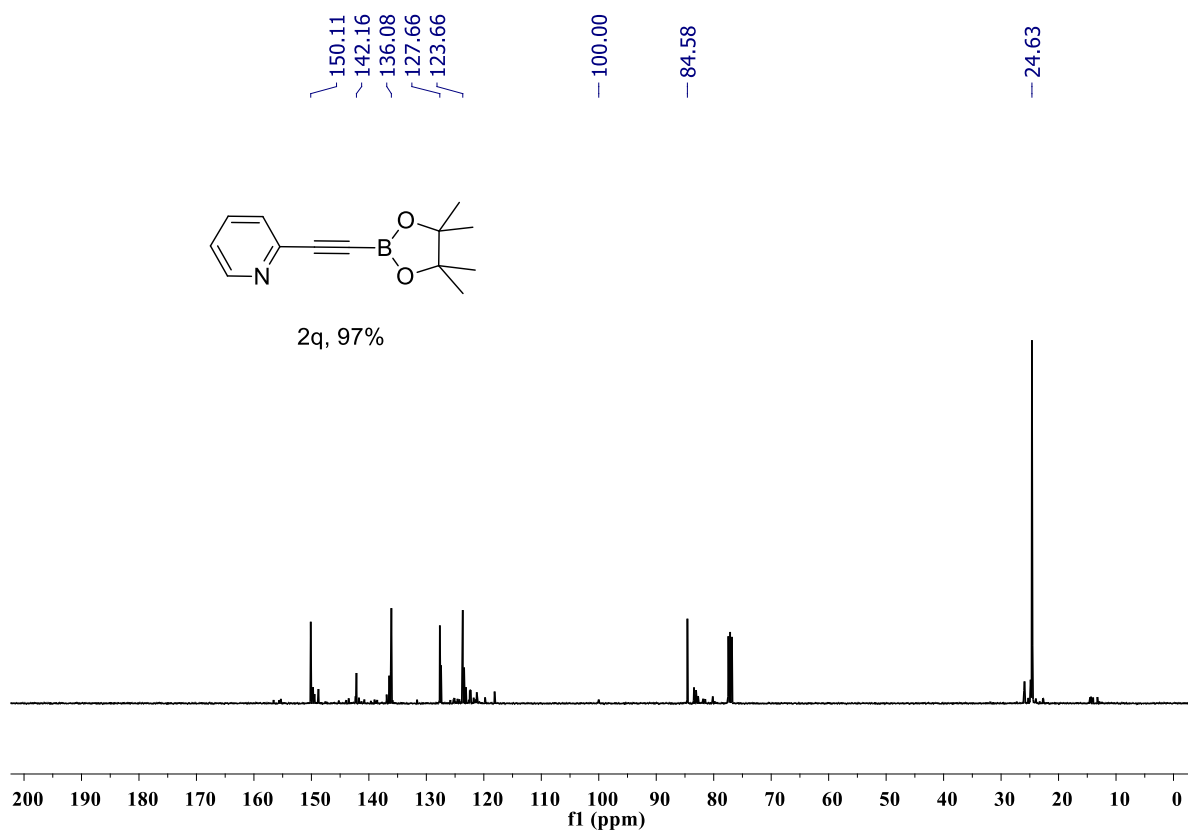


Figure S110: $^{13}\text{C}\{^1\text{H}\}$ NMR spectrum of compound **2q** (100 MHz, CDCl_3).

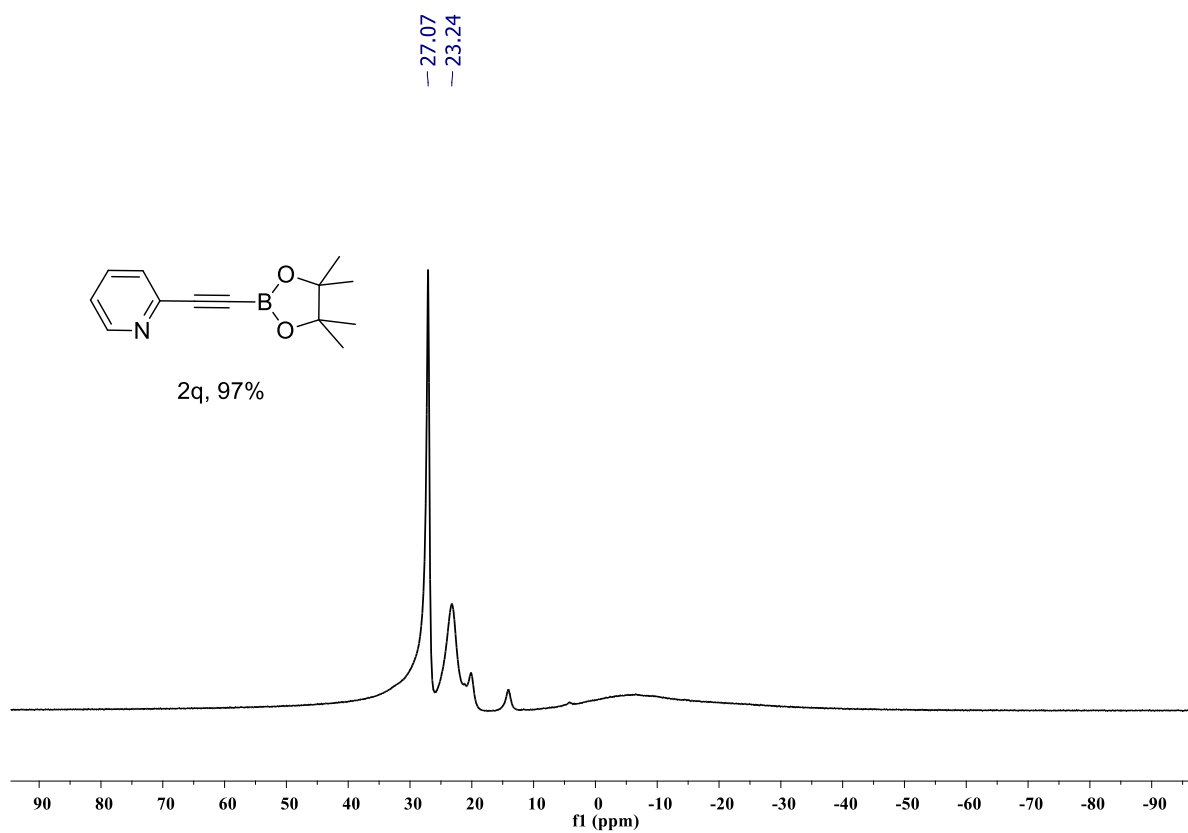


Figure S111: $^{11}\text{B}\{^1\text{H}\}$ NMR spectrum of compound **2q** (128 MHz, CDCl_3). A peak observed at δ 27.07 ppm arises from free HBpin.

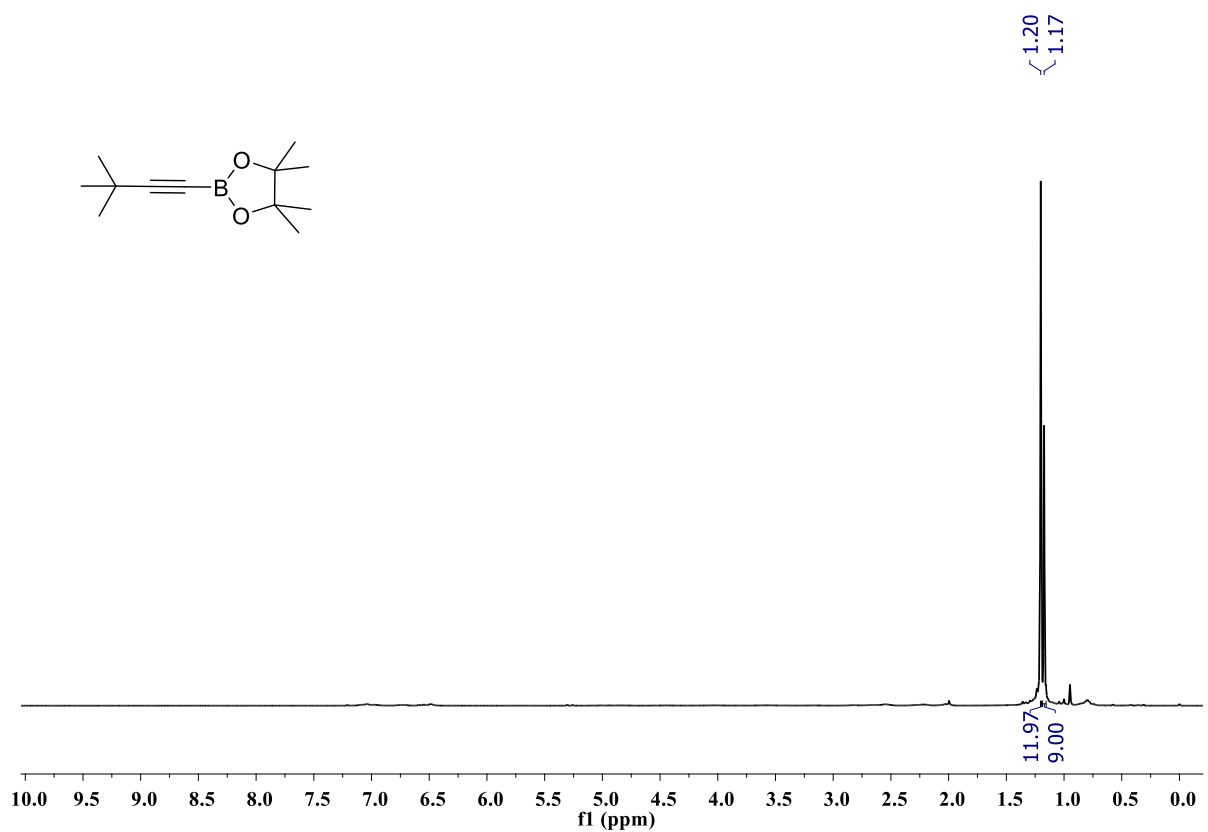


Figure S112: ^1H NMR spectrum of compound **2r** (400 MHz, CDCl_3).

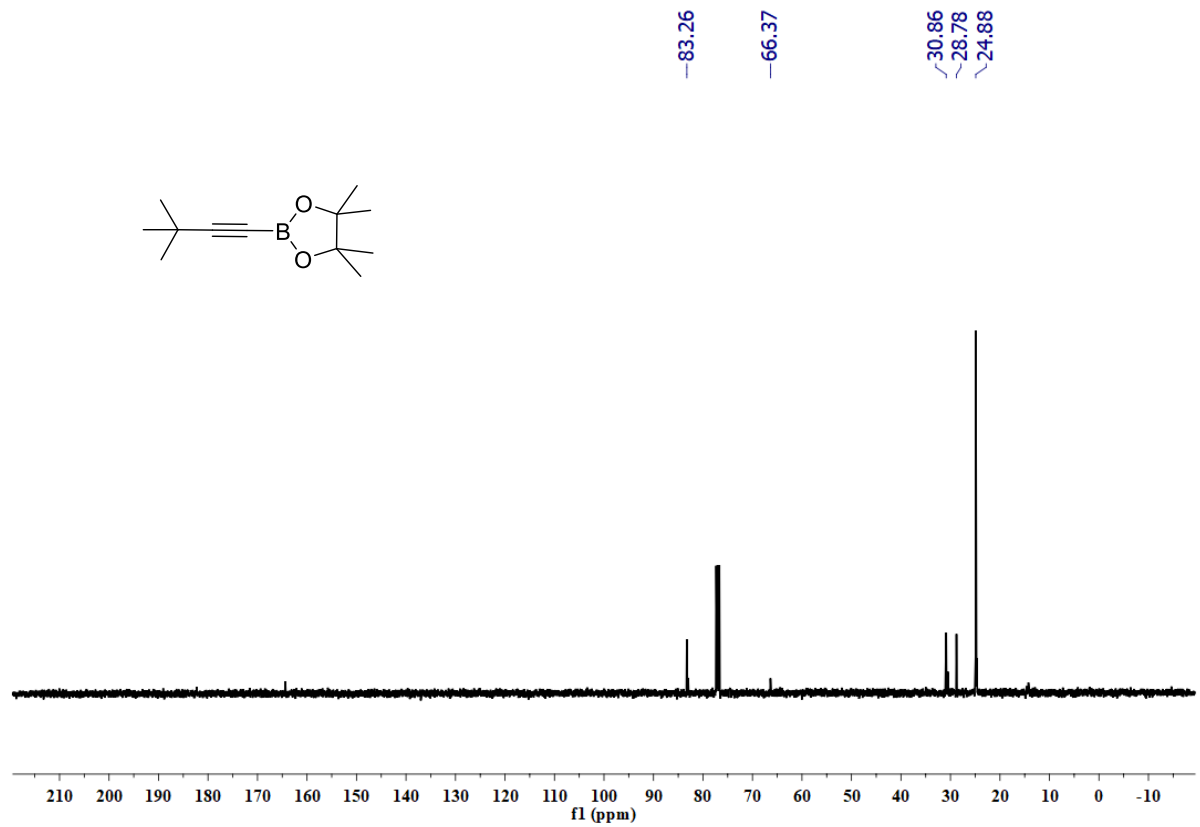


Figure S113: $^{13}\text{C}\{^1\text{H}\}$ NMR spectrum of compound **2r** (100 MHz, CDCl_3).

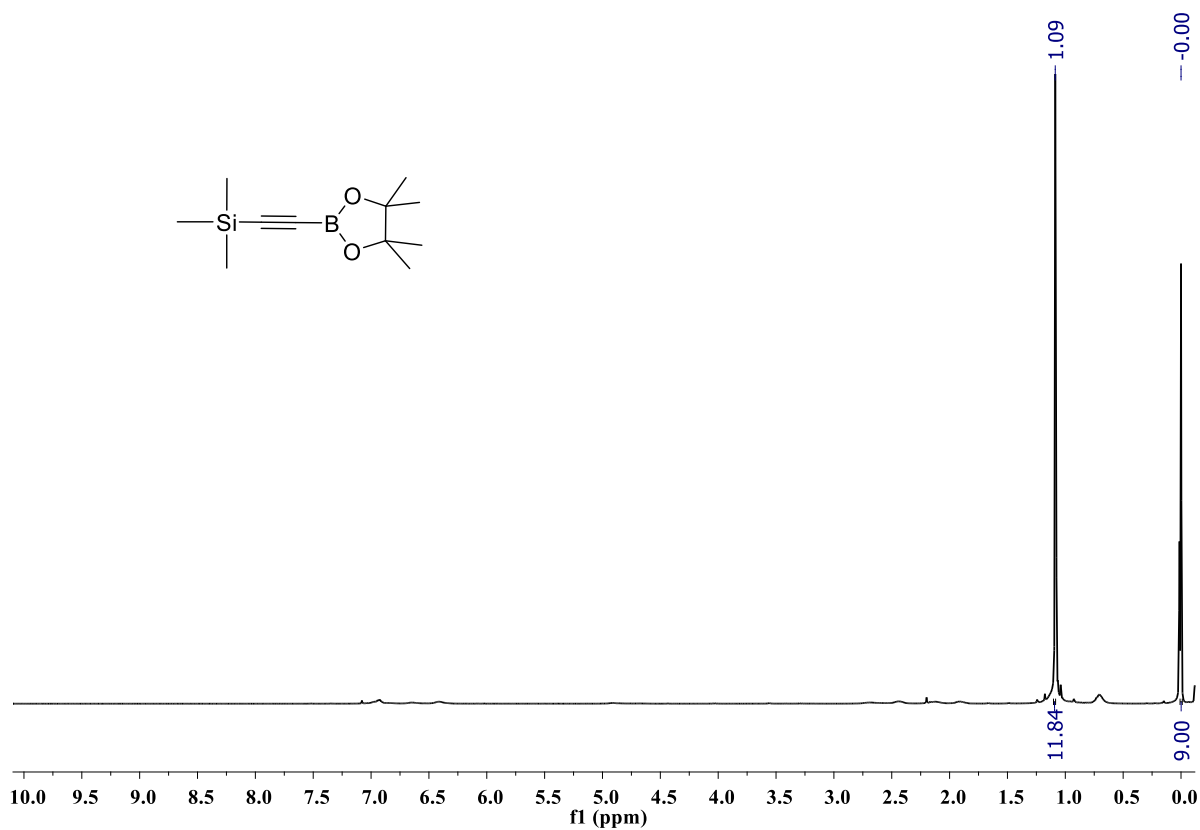


Figure S114: ¹H NMR spectrum of compound 2s (400 MHz, CDCl₃).

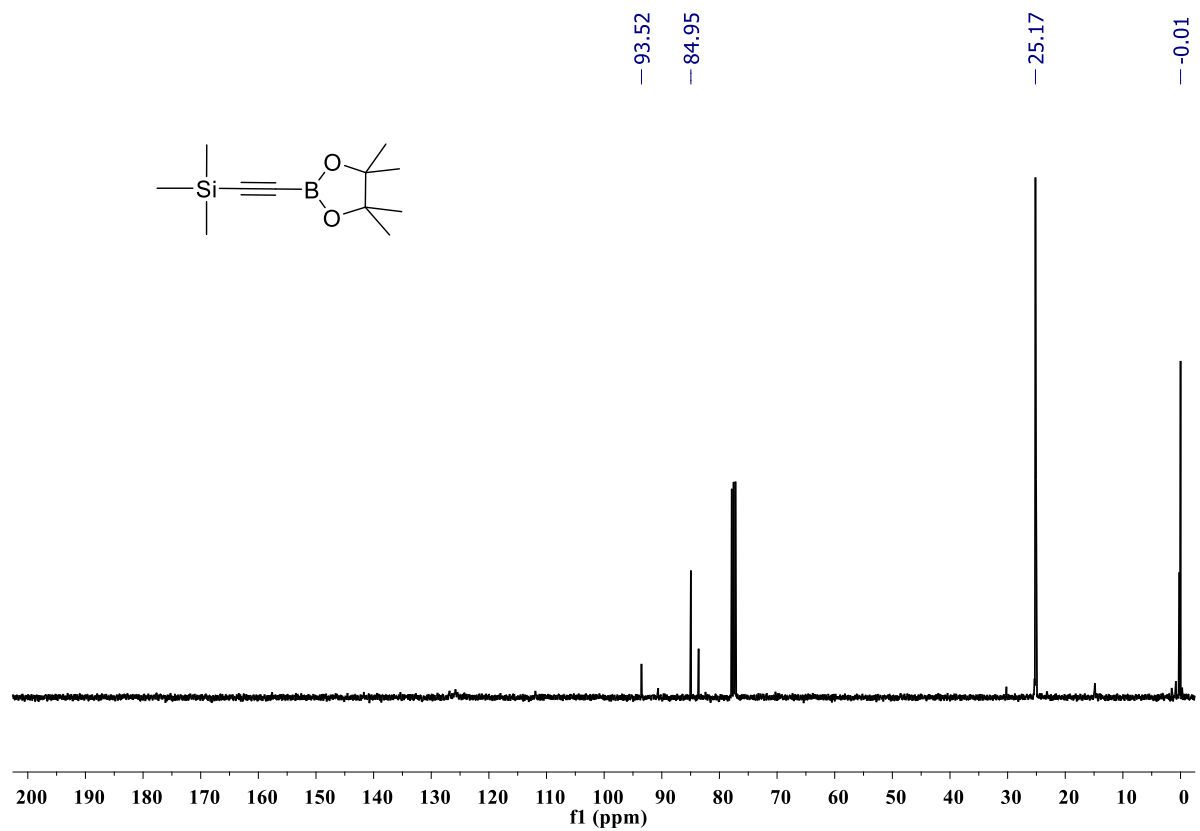


Figure S115: ¹³C{¹H} NMR spectrum of compound 2s (100 MHz, CDCl₃).

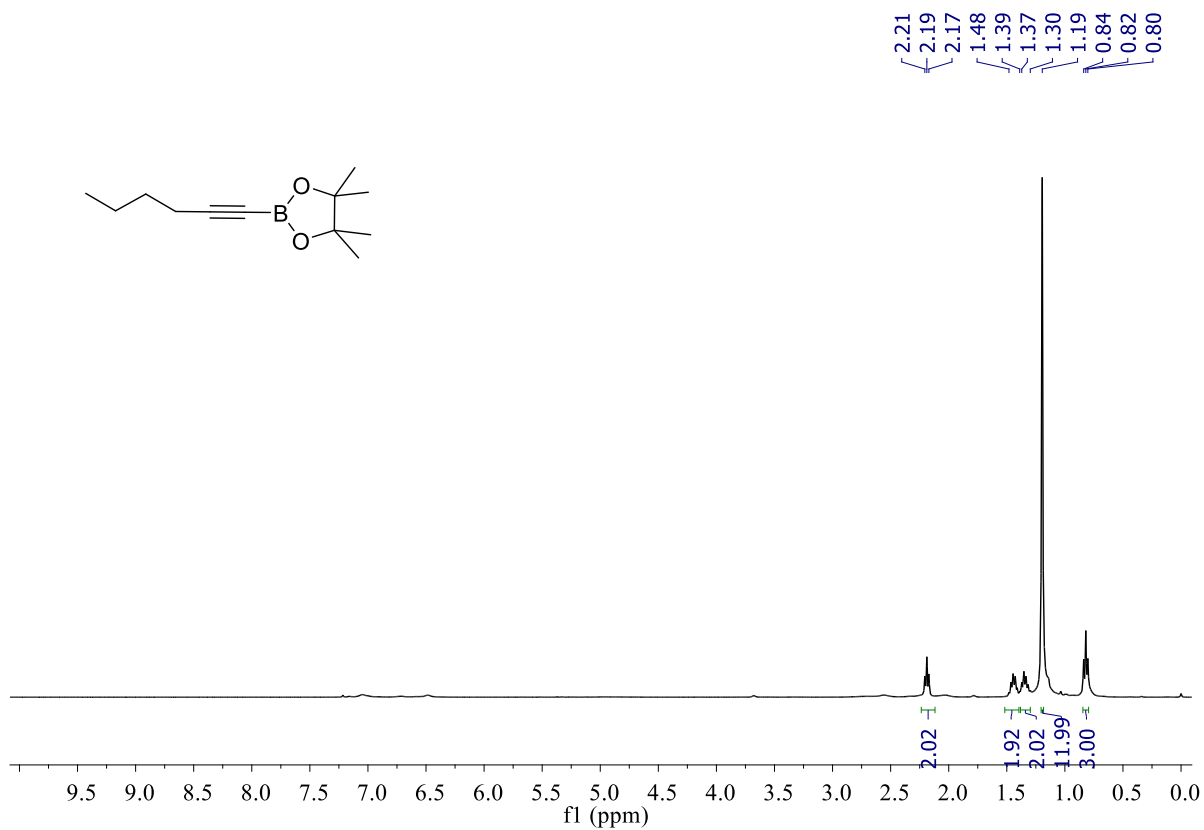


Figure S116: ^1H NMR spectrum of compound **2t** (400 MHz, CDCl_3).

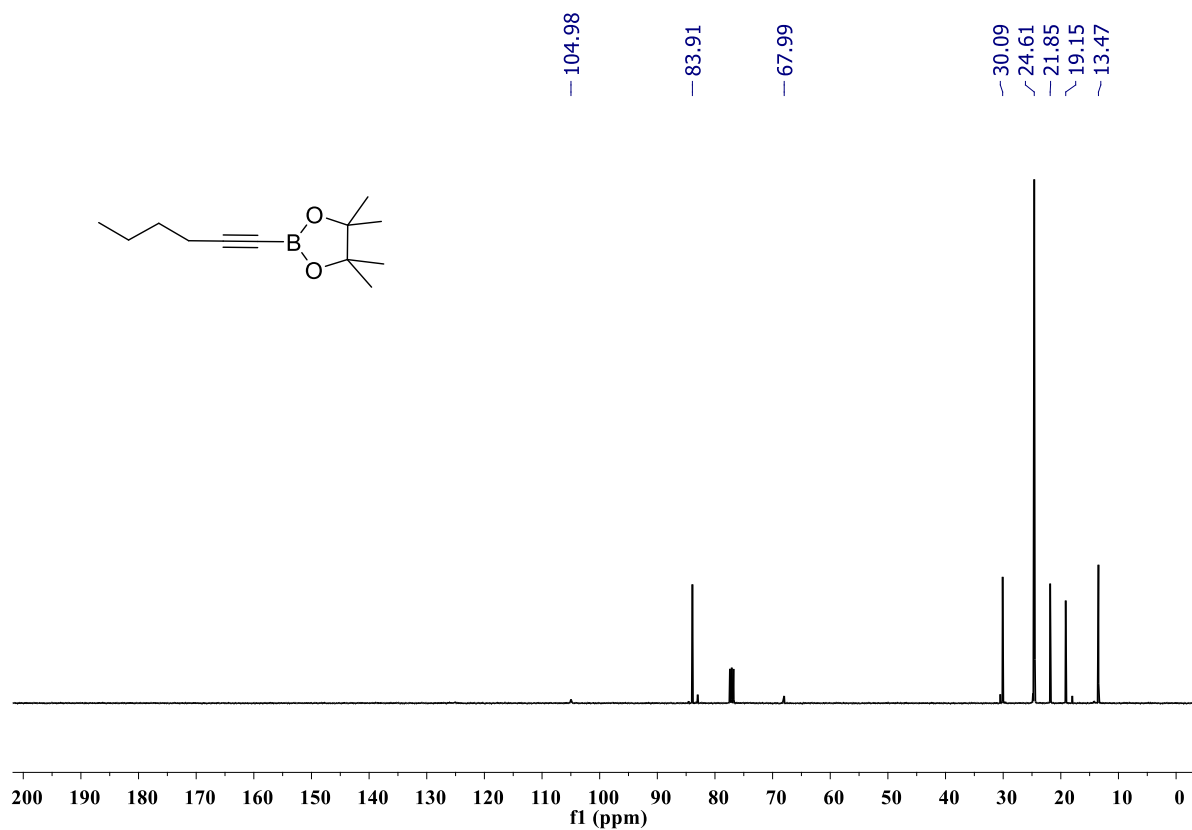


Figure S117: $^{13}\text{C}\{^1\text{H}\}$ NMR spectrum of compound **2t** (100 MHz, CDCl_3).

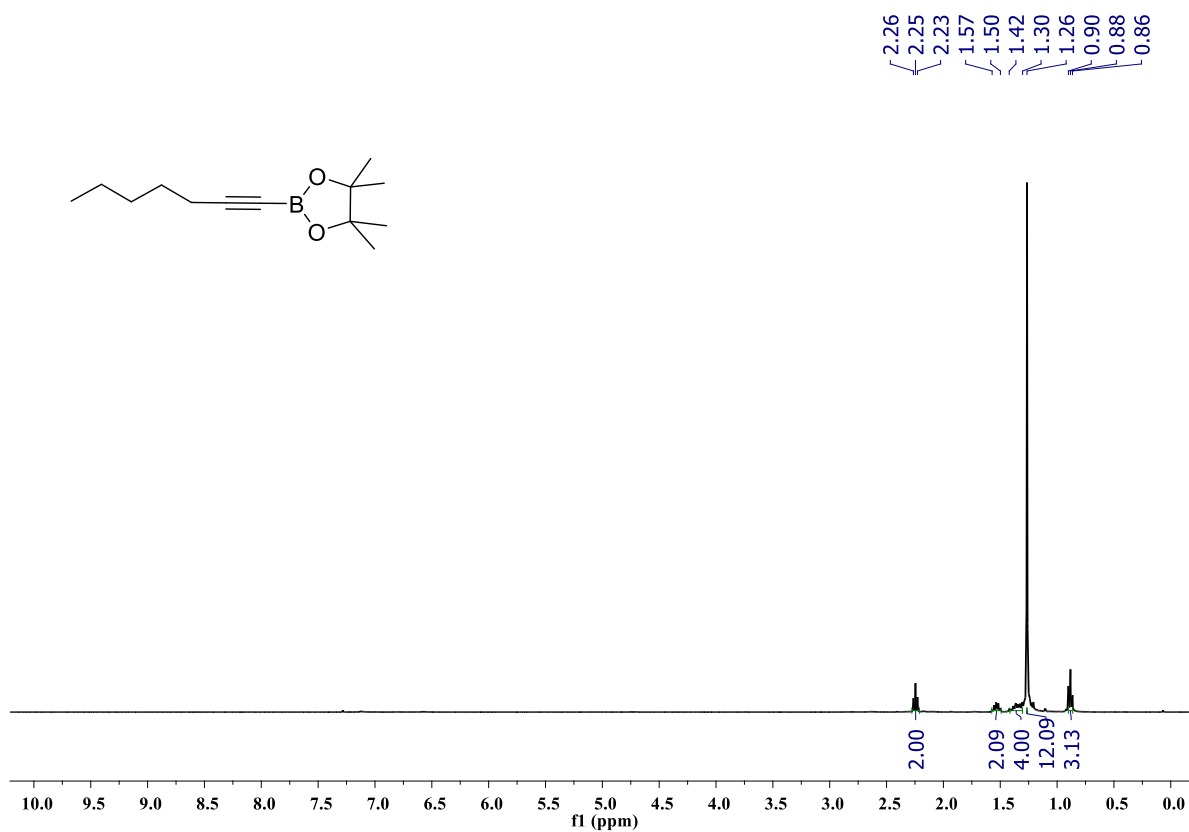


Figure S118: ^1H NMR spectrum of compound **2u** (400 MHz, CDCl_3).

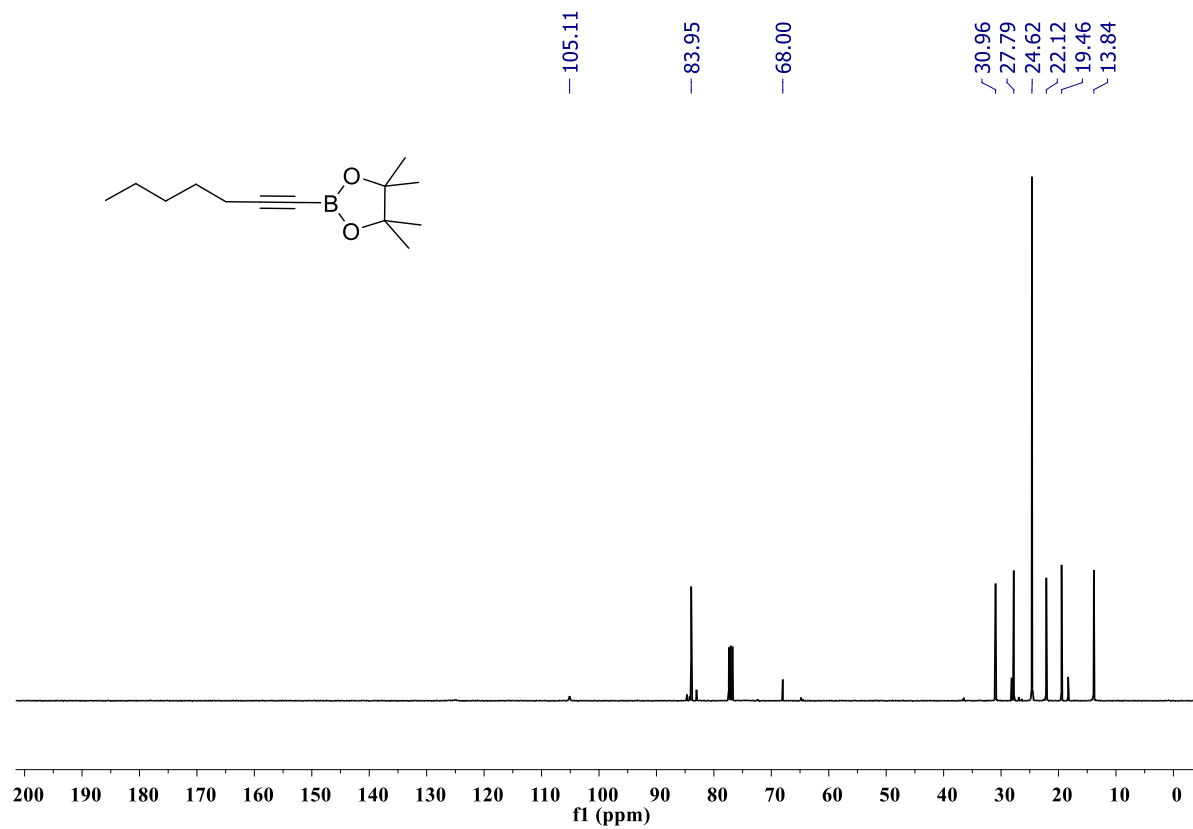


Figure S119: $^{13}\text{C}\{^1\text{H}\}$ NMR spectrum of compound **2u** (100 MHz, CDCl_3).

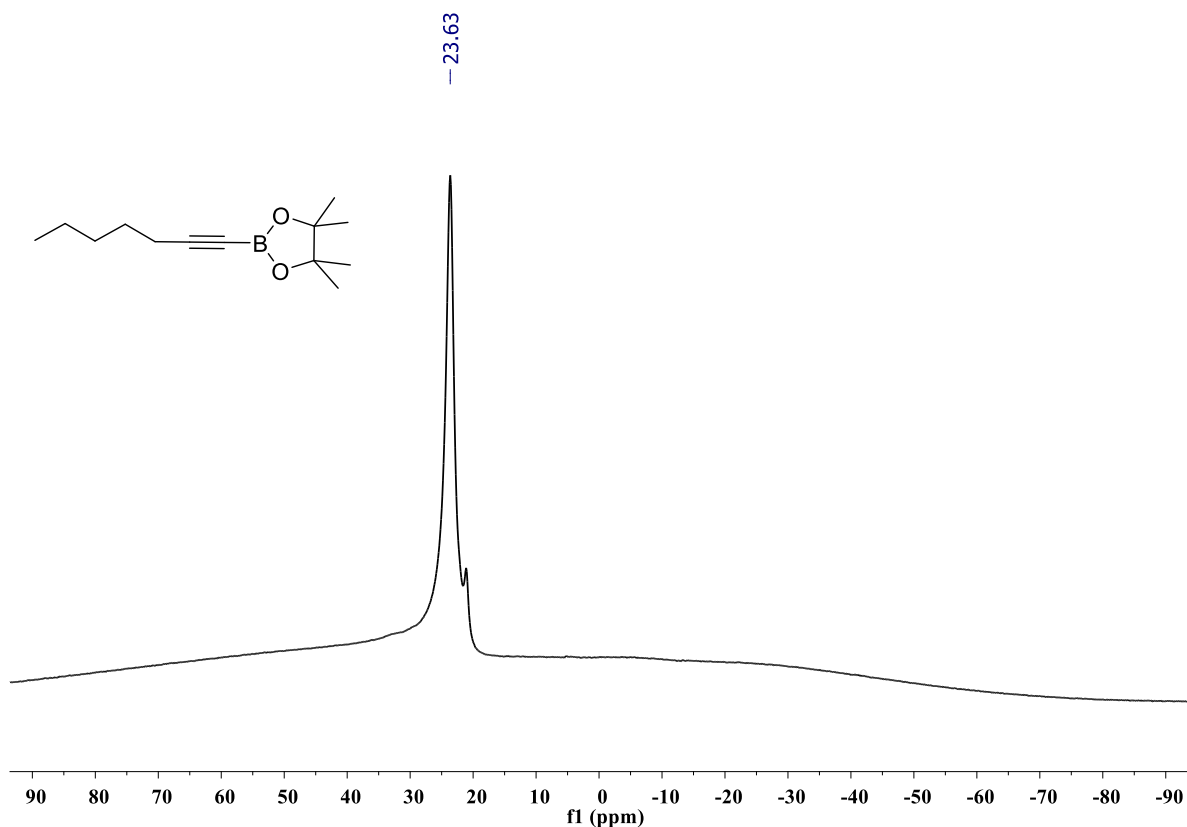


Figure S120: ^{11}B NMR spectrum of compound **2u** (128 MHz, CDCl_3).

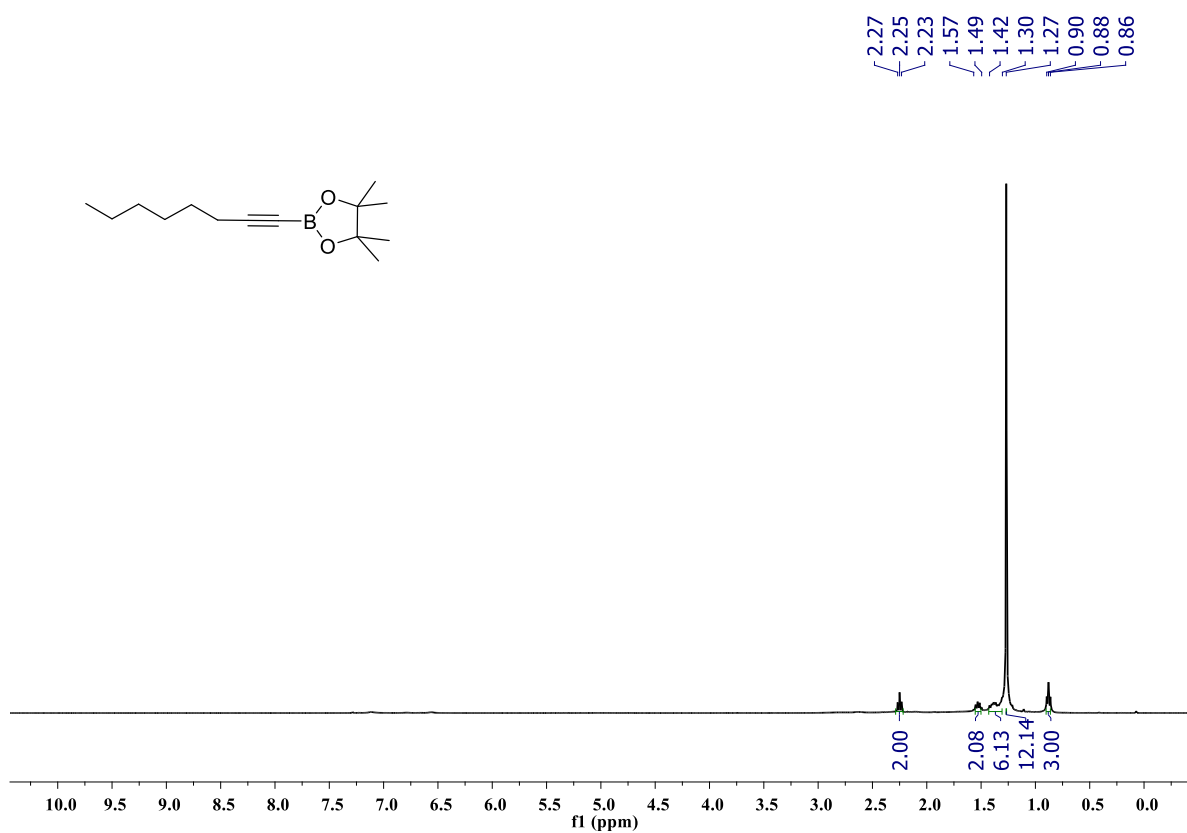


Figure S121: ^1H NMR spectrum of compound **2v** (400 MHz, CDCl_3).

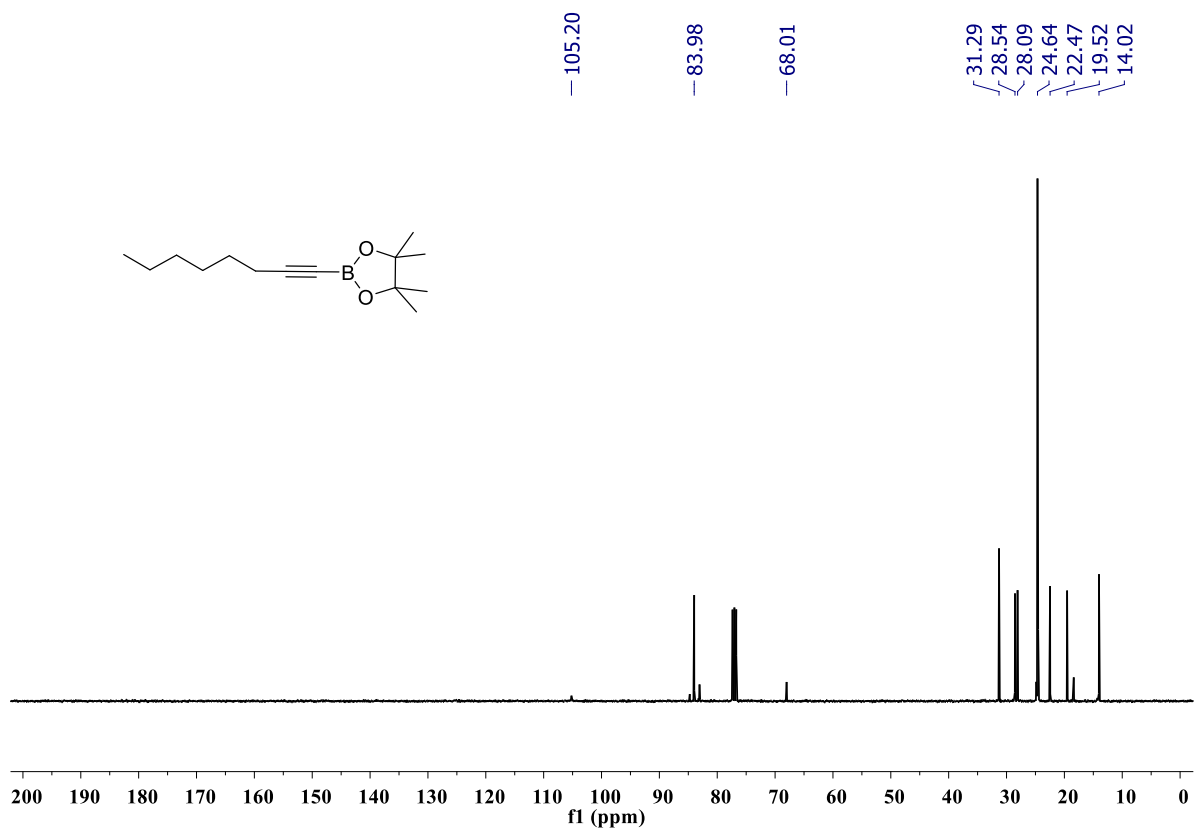


Figure S122: $^{13}\text{C}\{^1\text{H}\}$ NMR spectrum of compound **2v** (100 MHz, CDCl_3).

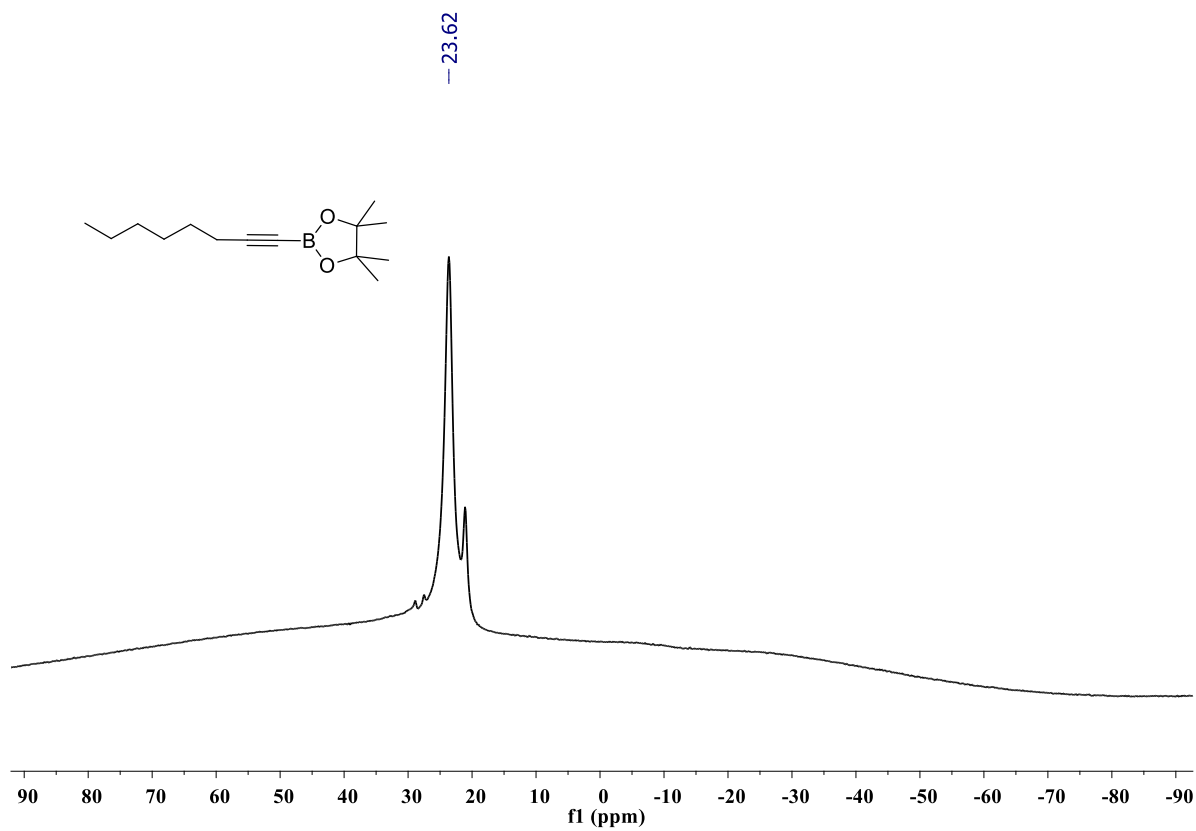


Figure S123: ^{11}B NMR spectrum of compound **2v** (128 MHz, CDCl_3).

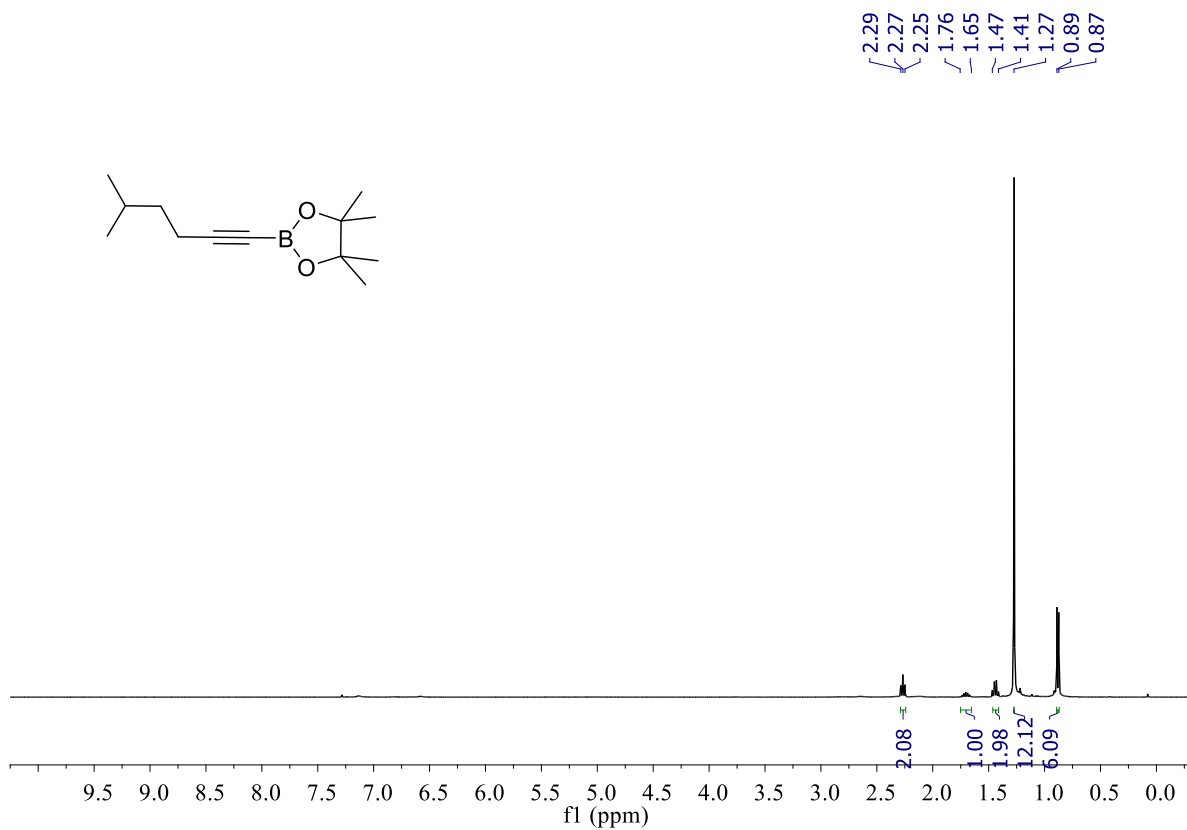


Figure S124: ^1H NMR spectrum of compound **2w** (400 MHz, CDCl_3).

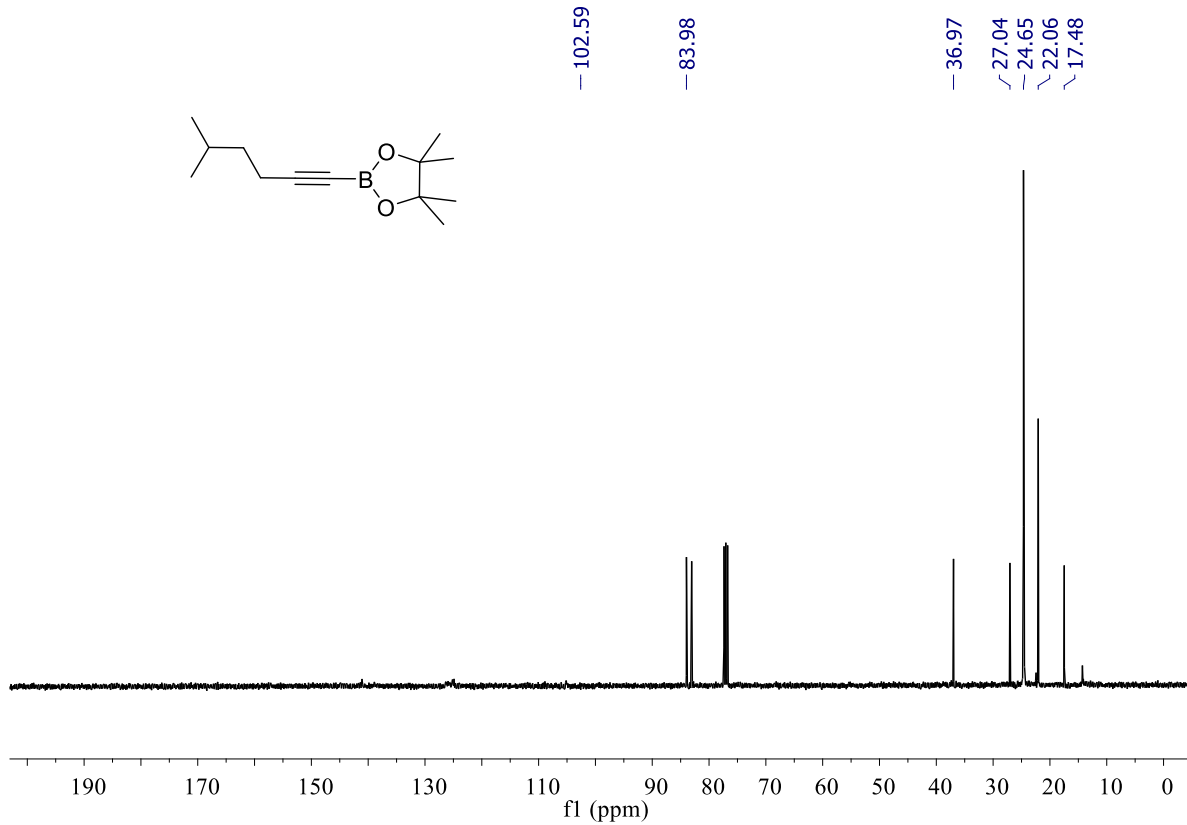


Figure S125: $^{13}\text{C}\{^1\text{H}\}$ NMR spectrum of compound **2w** (100 MHz, CDCl_3).

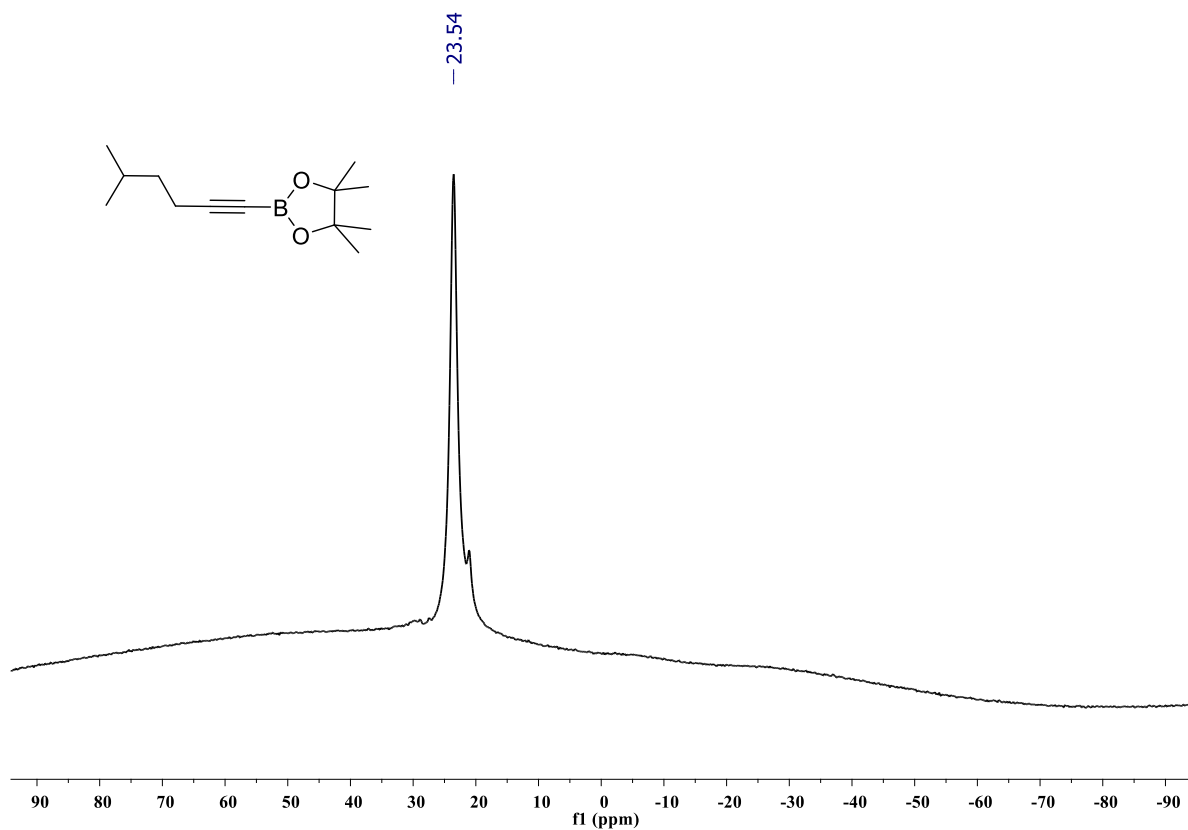


Figure S126: ^{11}B NMR spectrum of compound **2w** (128 MHz, CDCl_3).

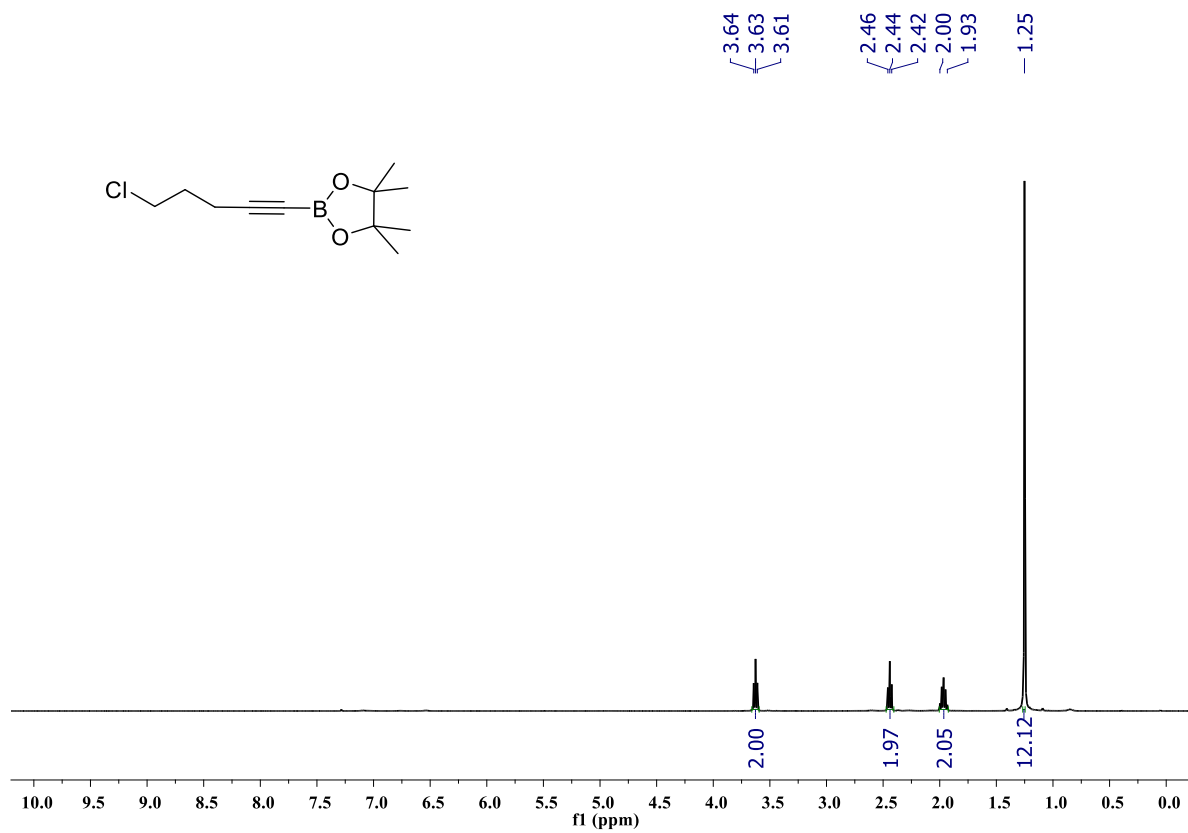


Figure S127: ^1H NMR spectrum of compound **2x** (400 MHz, CDCl_3).

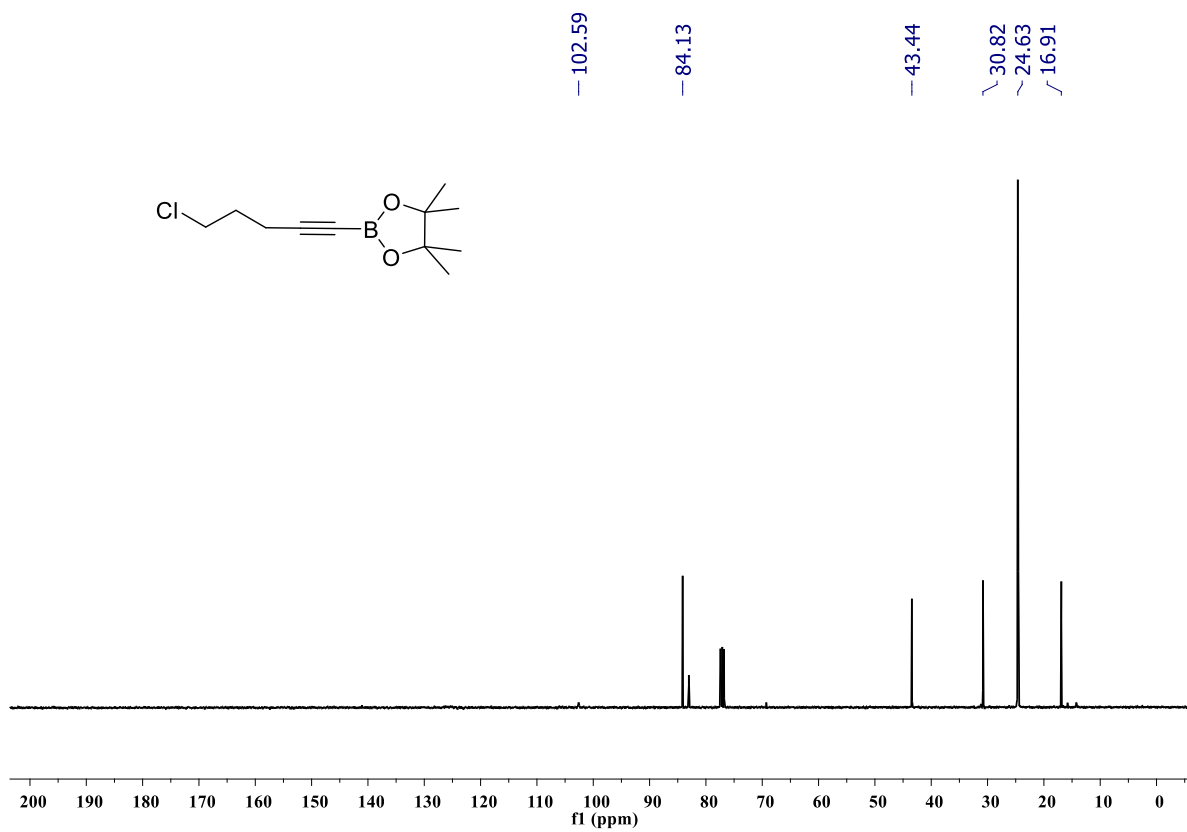


Figure S128: $^{13}\text{C}\{^1\text{H}\}$ NMR spectrum of compound **2x** (100 MHz, CDCl_3).

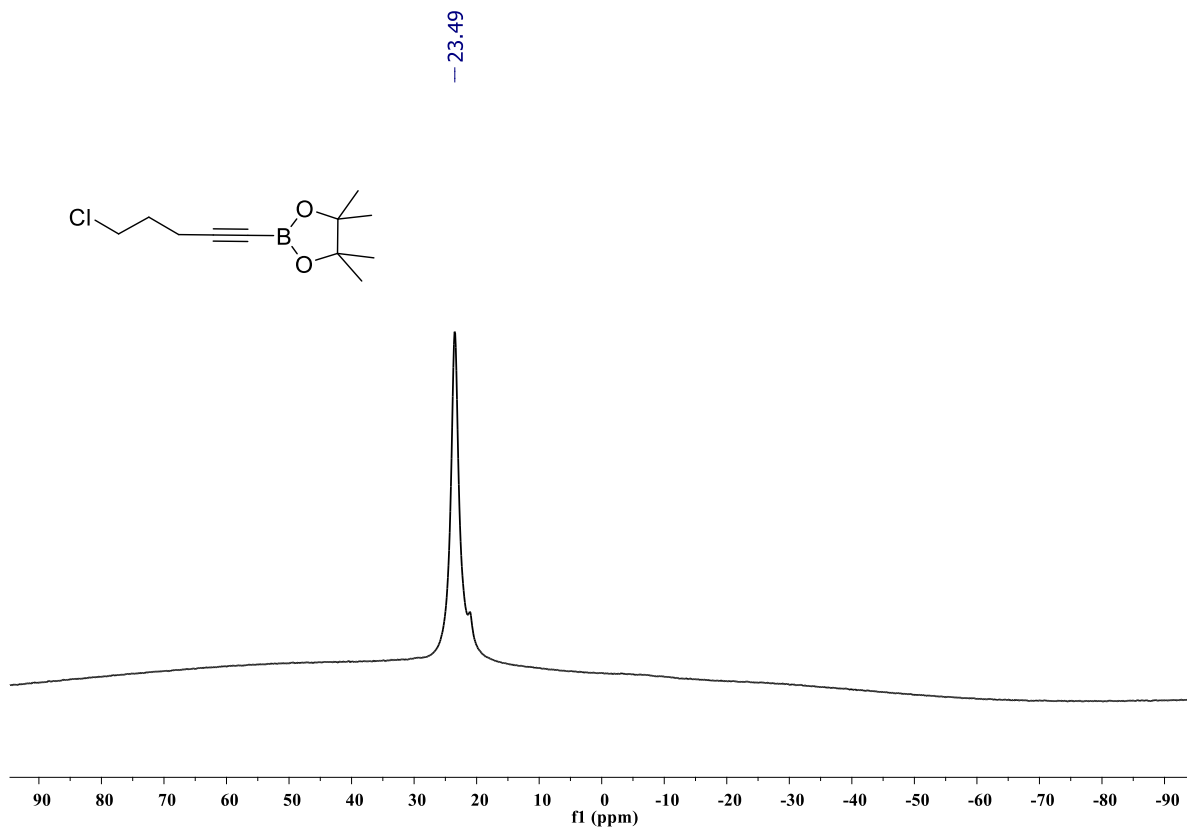


Figure S129: ^{11}B NMR spectrum of compound **2x** (128 MHz, CDCl_3).

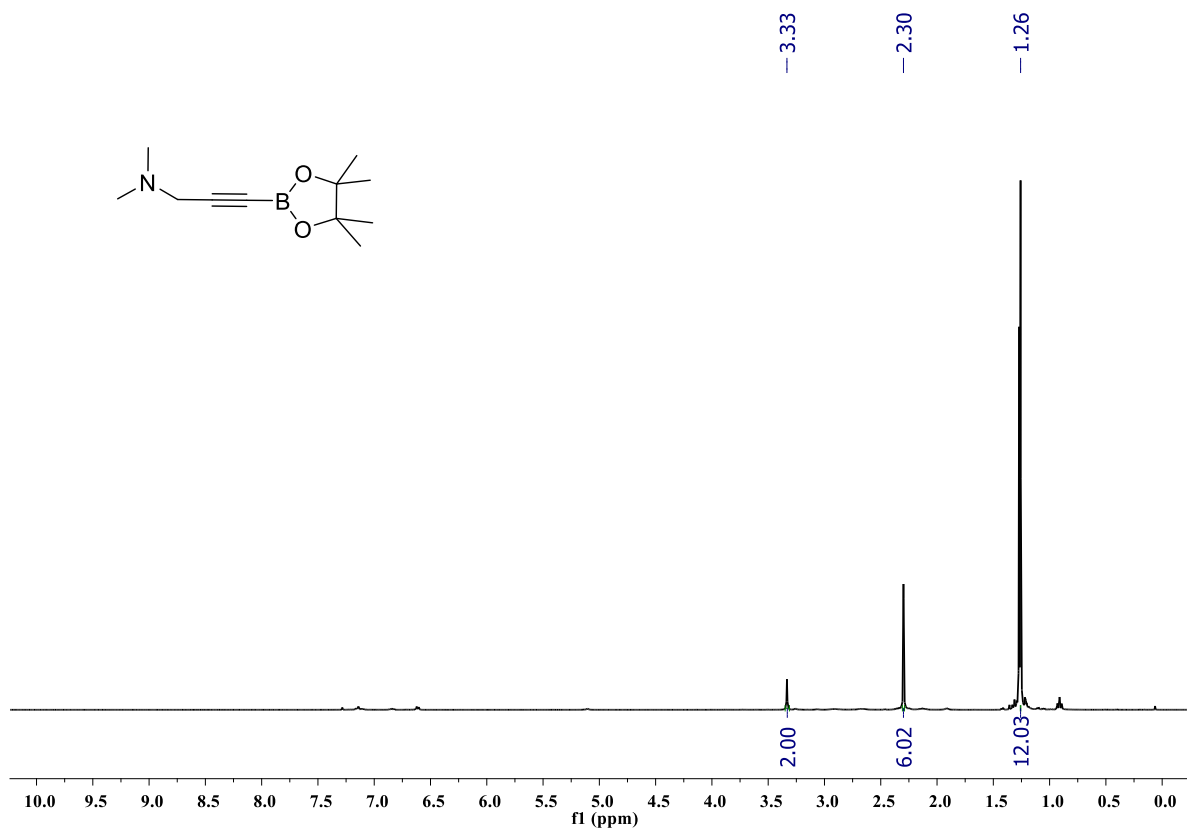


Figure S130: ¹H NMR spectrum of compound **2y** (400 MHz, CDCl₃).

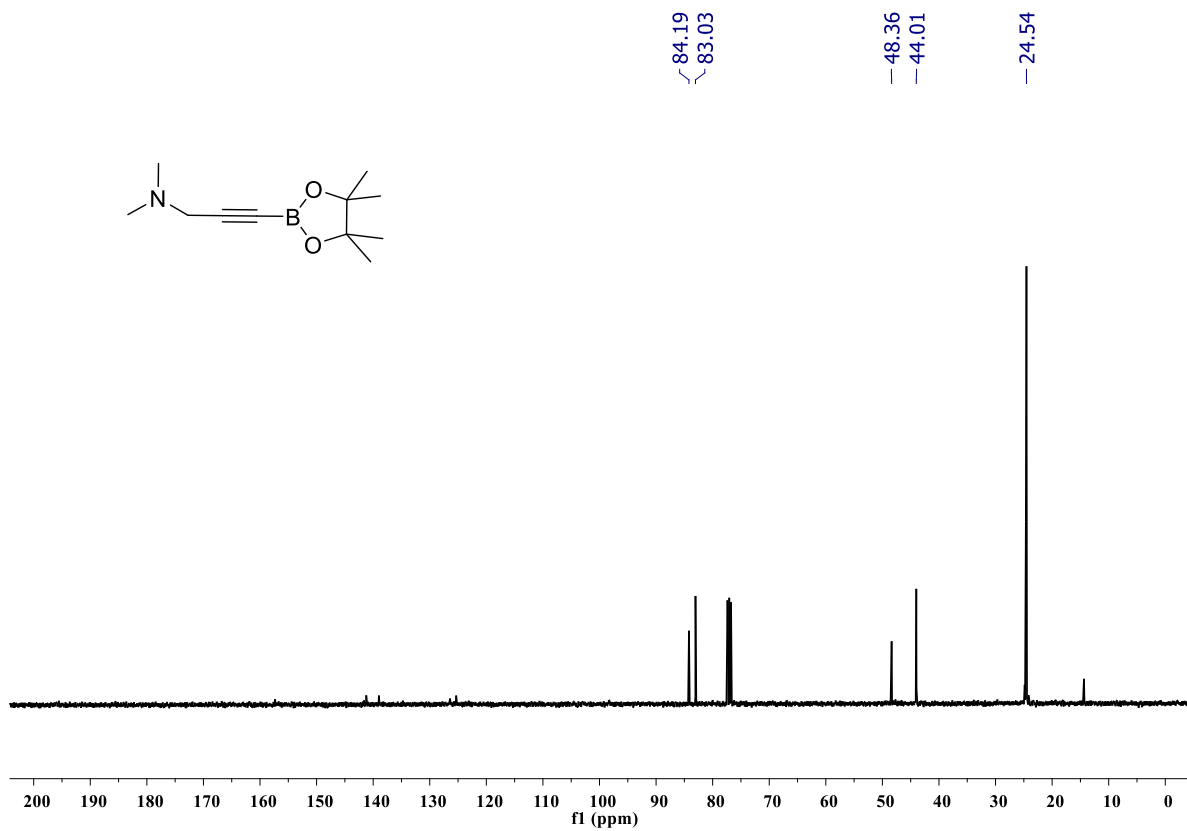


Figure S131: ¹³C{¹H} NMR spectrum of compound **2y** (100 MHz, CDCl₃).

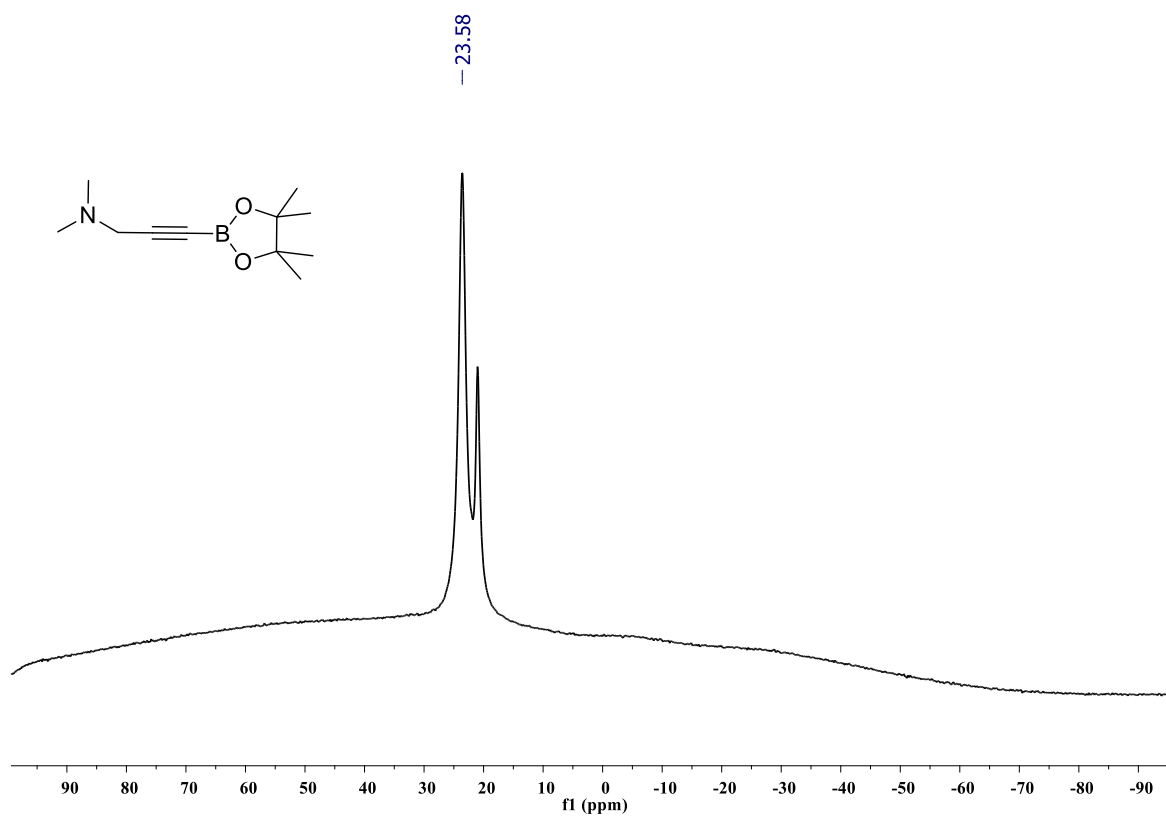


Figure S132: ^{11}B NMR spectrum of compound **2y** (128 MHz, CDCl_3).

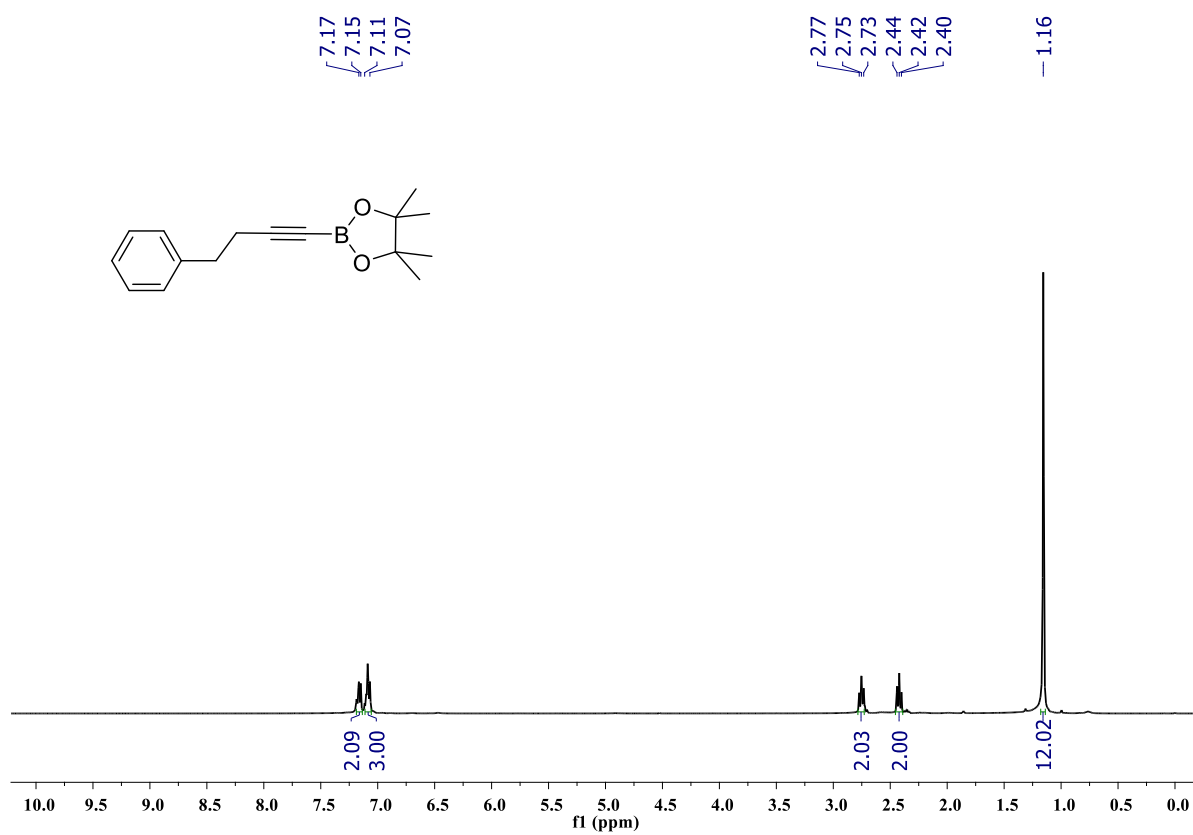


Figure S133: ^1H NMR spectrum of compound **2z** (400 MHz, CDCl_3).

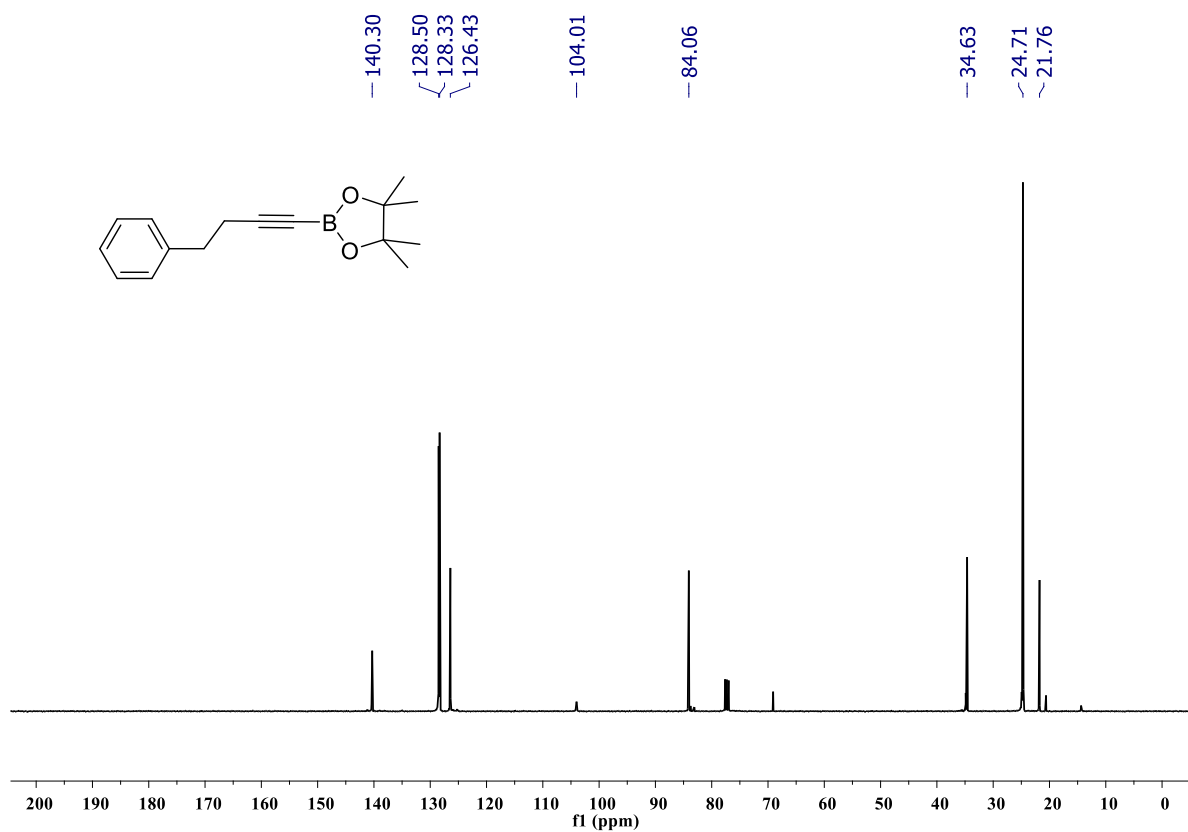


Figure S134: $^{13}\text{C}\{^1\text{H}\}$ NMR spectrum of compound **2z** (100 MHz, CDCl_3).

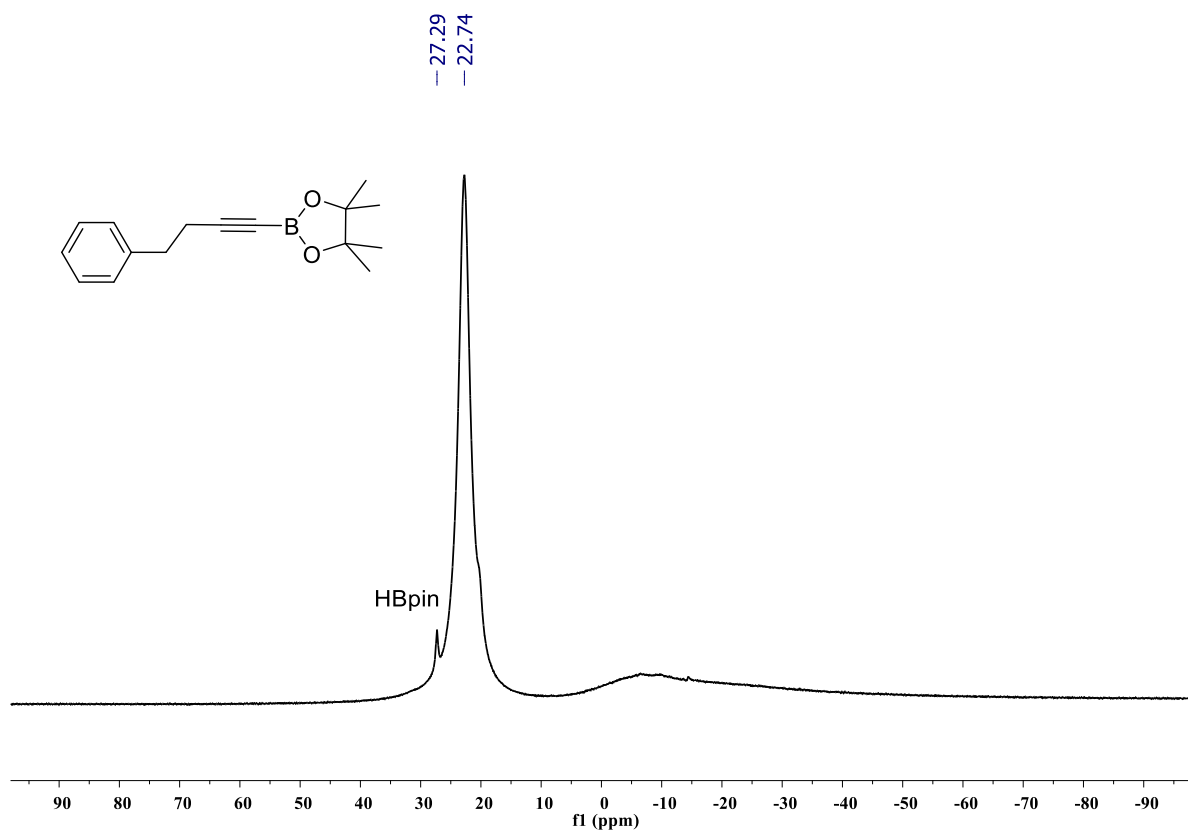


Figure S135: $^{11}\text{B}\{^1\text{H}\}$ NMR spectrum of compound **2z** (128 MHz, CDCl_3).

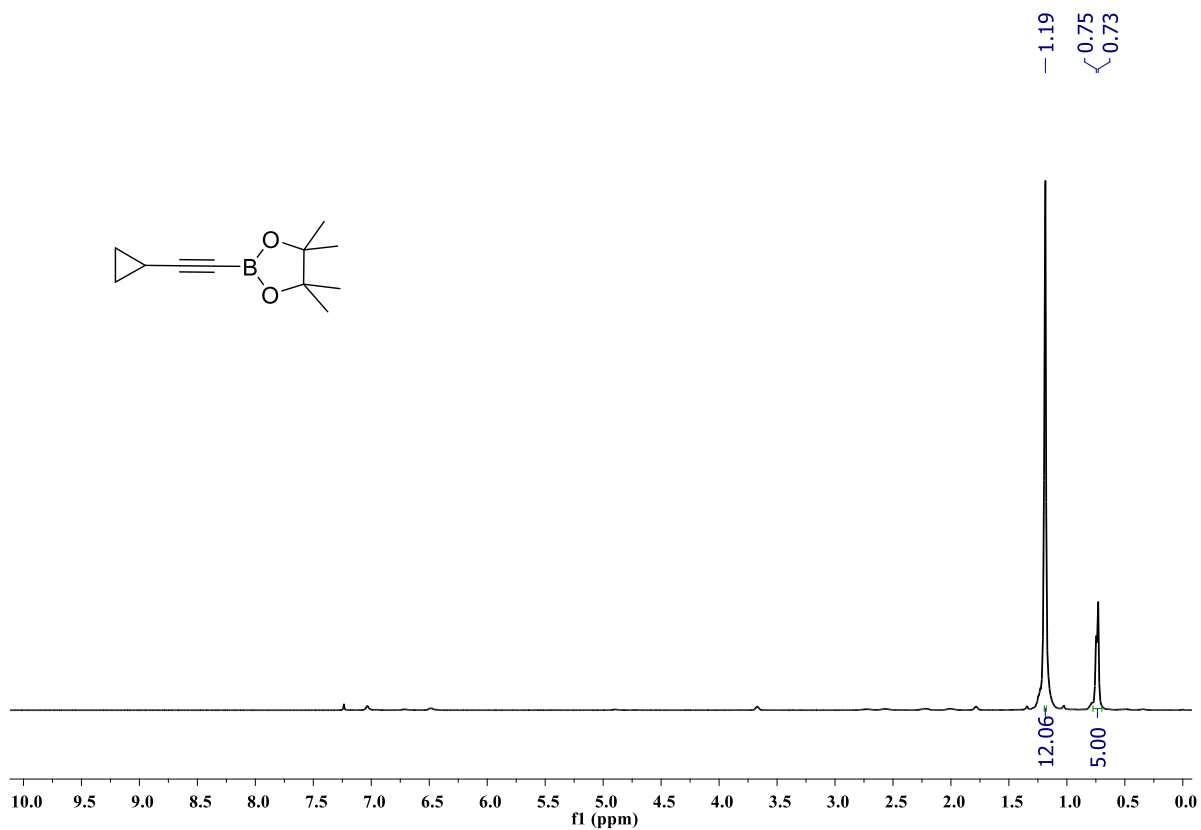


Figure S136: ^1H NMR spectrum of compound **2aa** (400 MHz, CDCl_3).

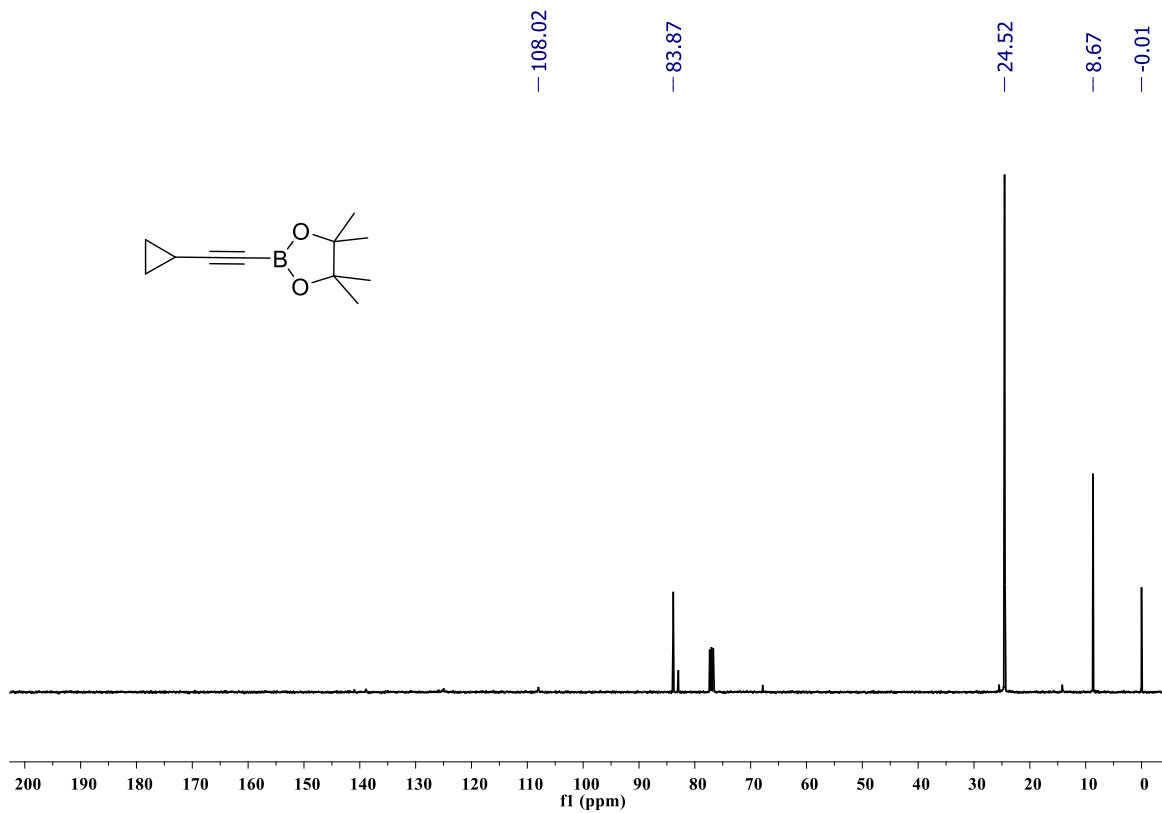


Figure S137: $^{13}\text{C}\{^1\text{H}\}$ NMR spectrum of compound **2aa** (100 MHz, CDCl_3).

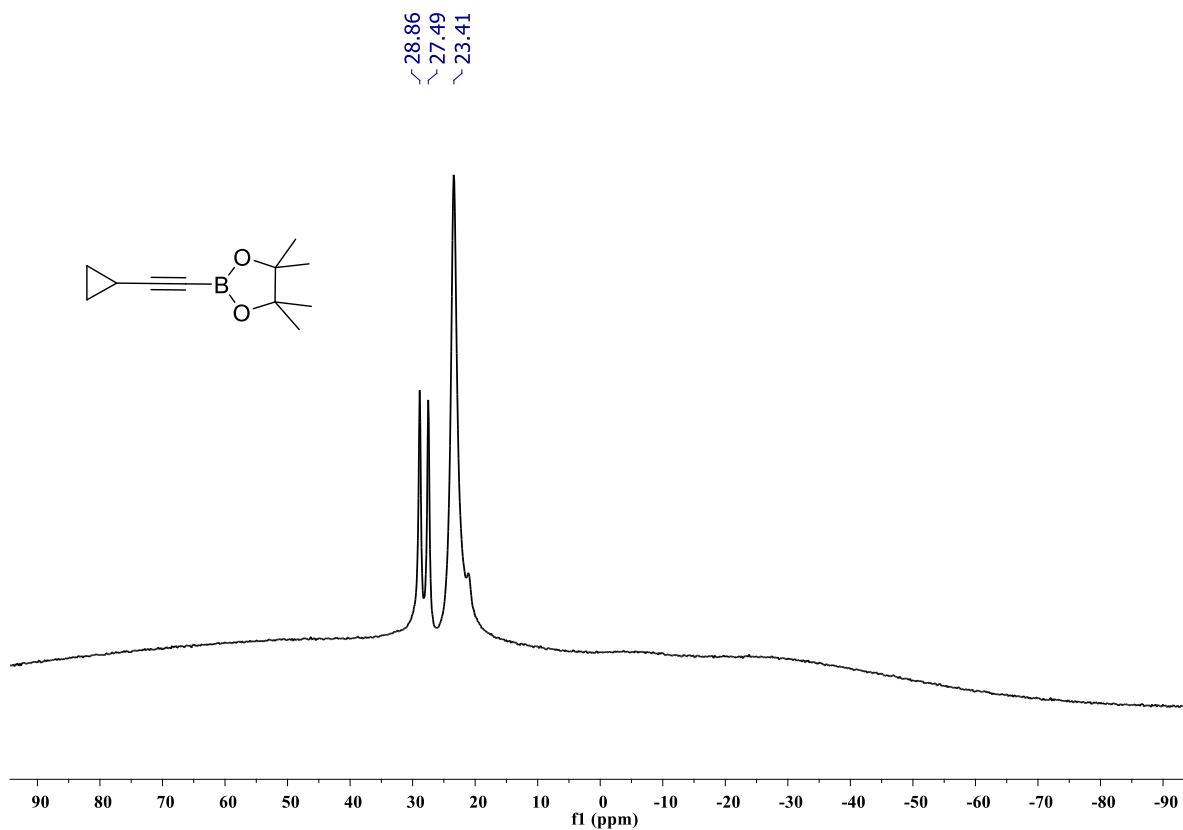


Figure S138: ^{11}B NMR spectrum of compound **2aa** (128 MHz, CDCl_3). A doublet peak at δ 27.49-28.86 ppm arises from free HBpin.

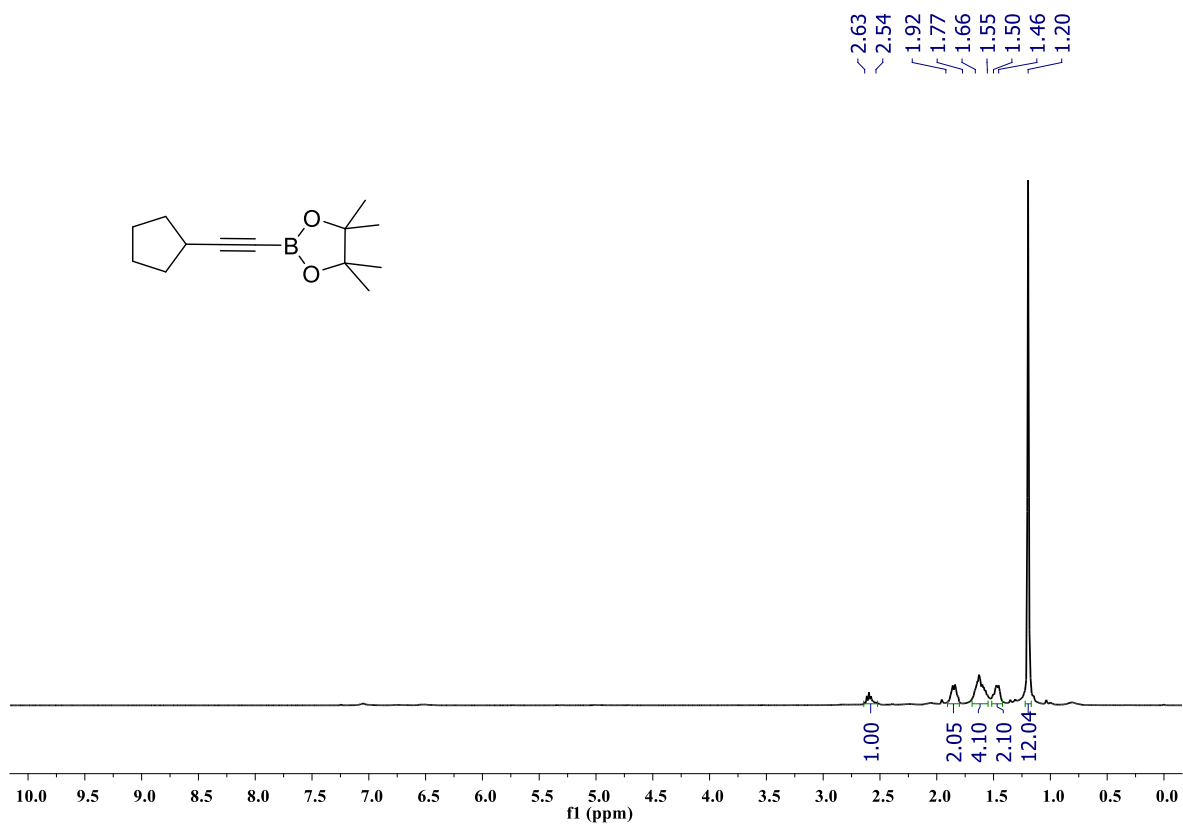


Figure S139: ^1H NMR spectrum of compound **2ab** (400 MHz, CDCl_3).

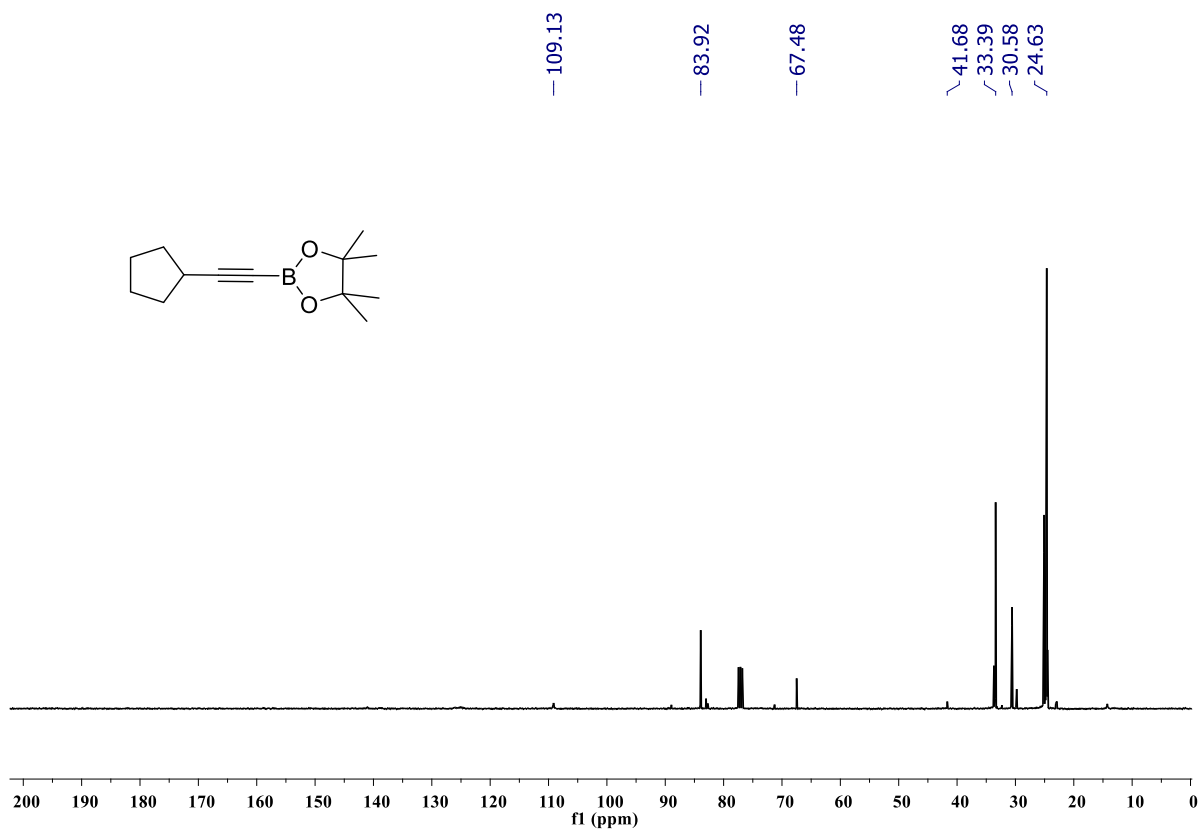


Figure S140: $^{13}\text{C}\{^1\text{H}\}$ NMR spectrum of compound **2ab** (100 MHz, CDCl_3).

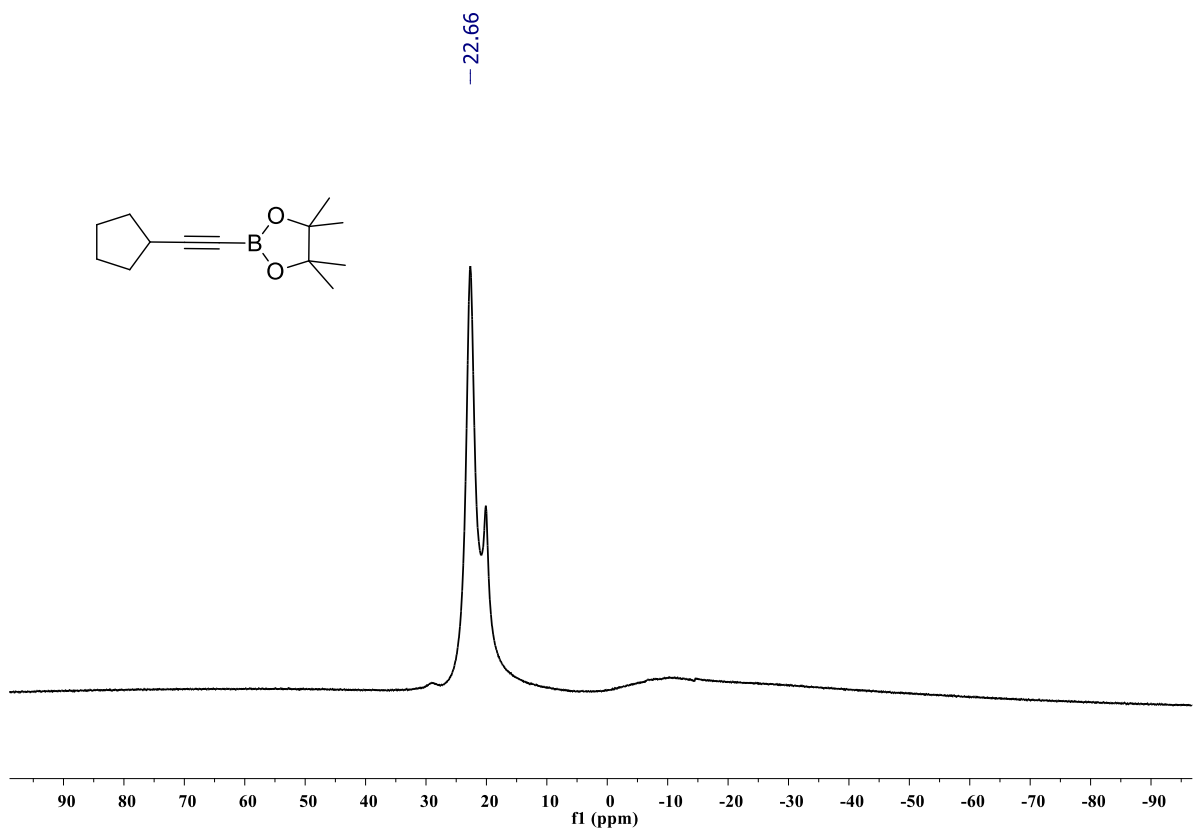


Figure S141: ^{11}B NMR spectrum of compound **2ab** (128 MHz, CDCl_3).

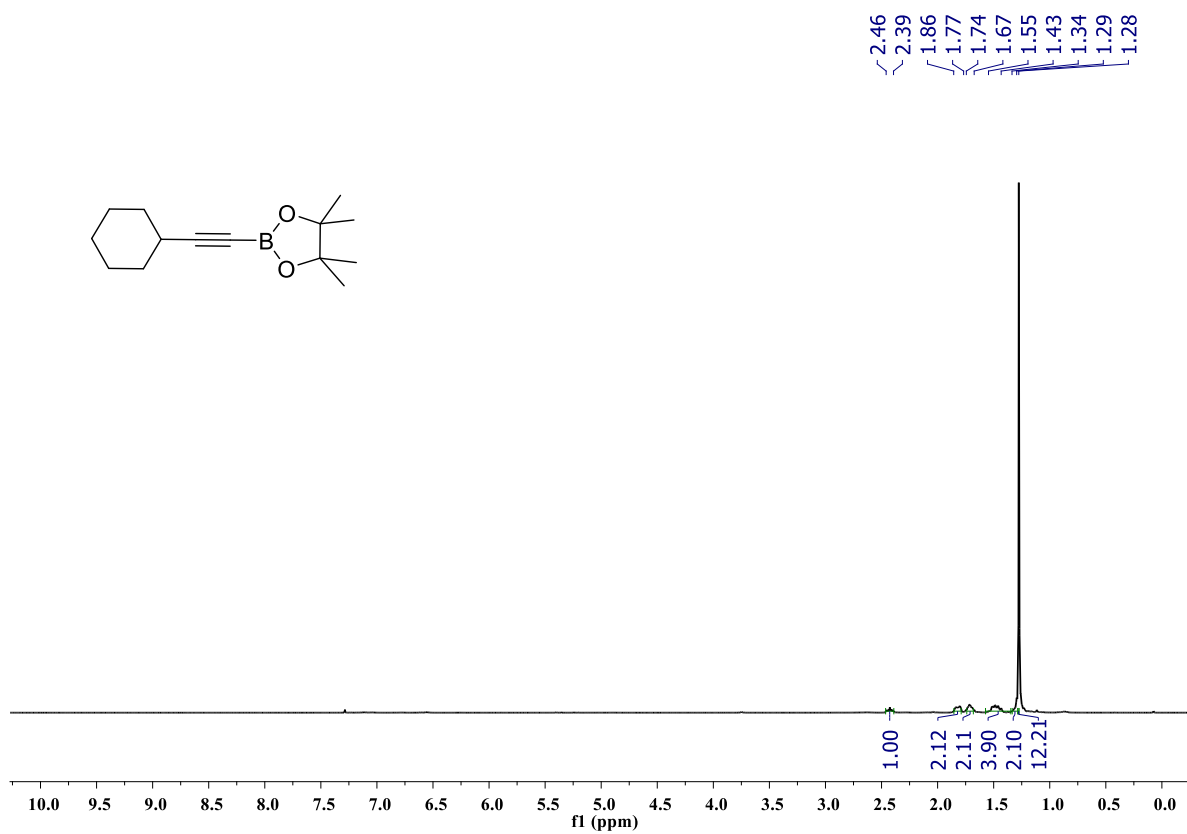


Figure S142: ^1H NMR spectrum of compound **2ac** (400 MHz, CDCl_3).

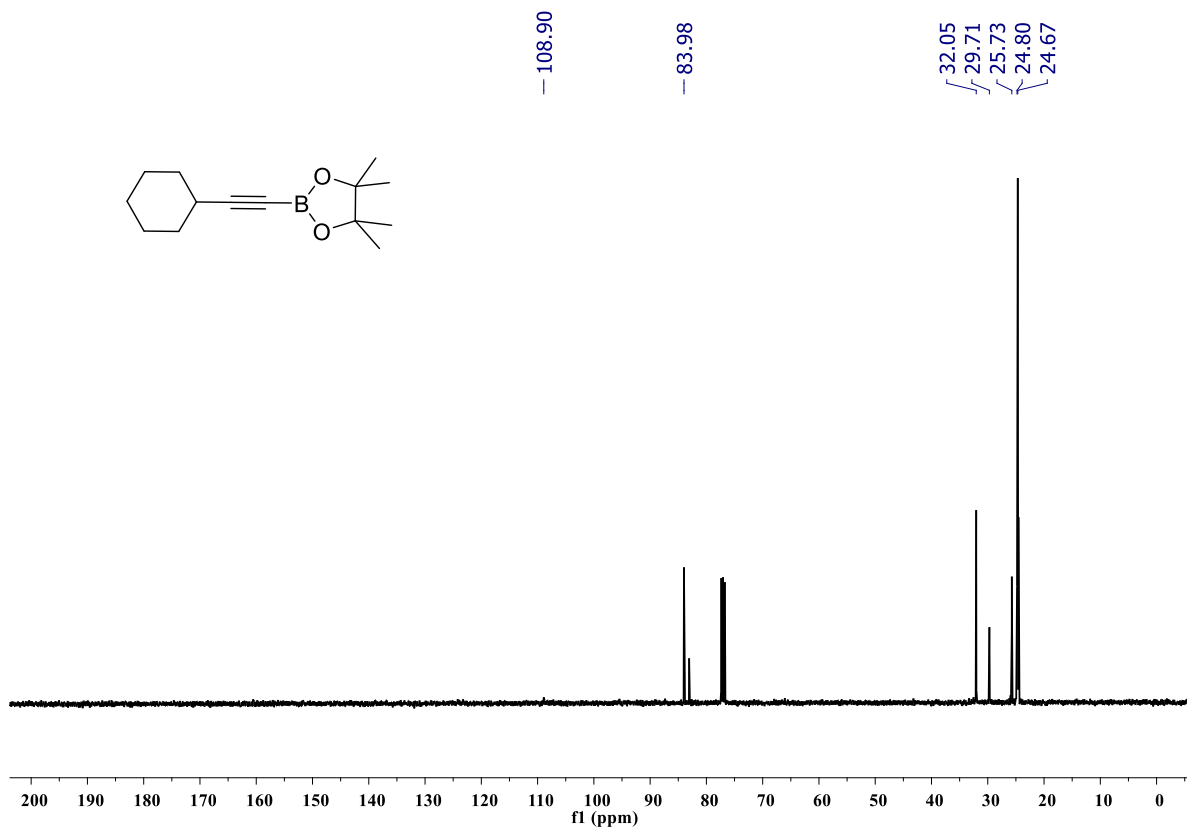


Figure S143: $^{13}\text{C}\{^1\text{H}\}$ NMR spectrum of compound **2ac** (100 MHz, CDCl_3).

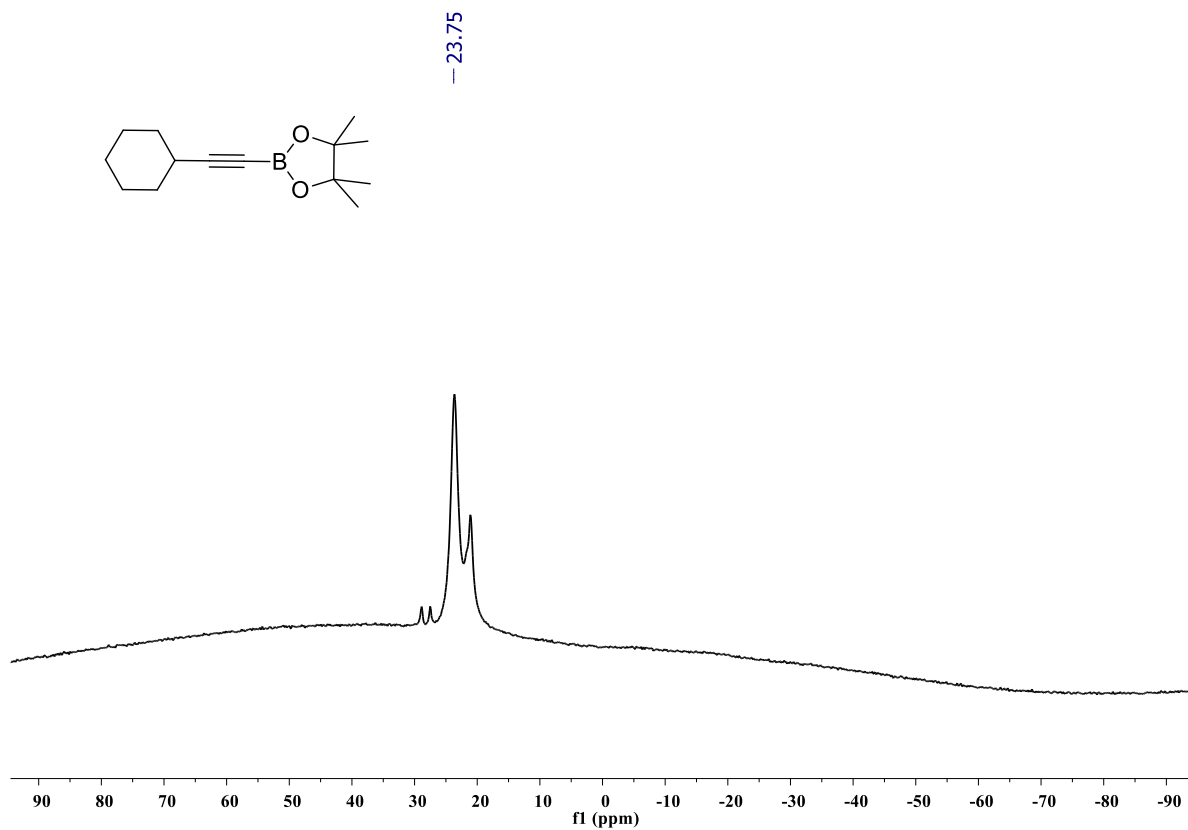


Figure S144: $^{11}\text{B}\{^1\text{H}\}$ NMR spectrum of compound **2ac** (128 MHz, CDCl_3).

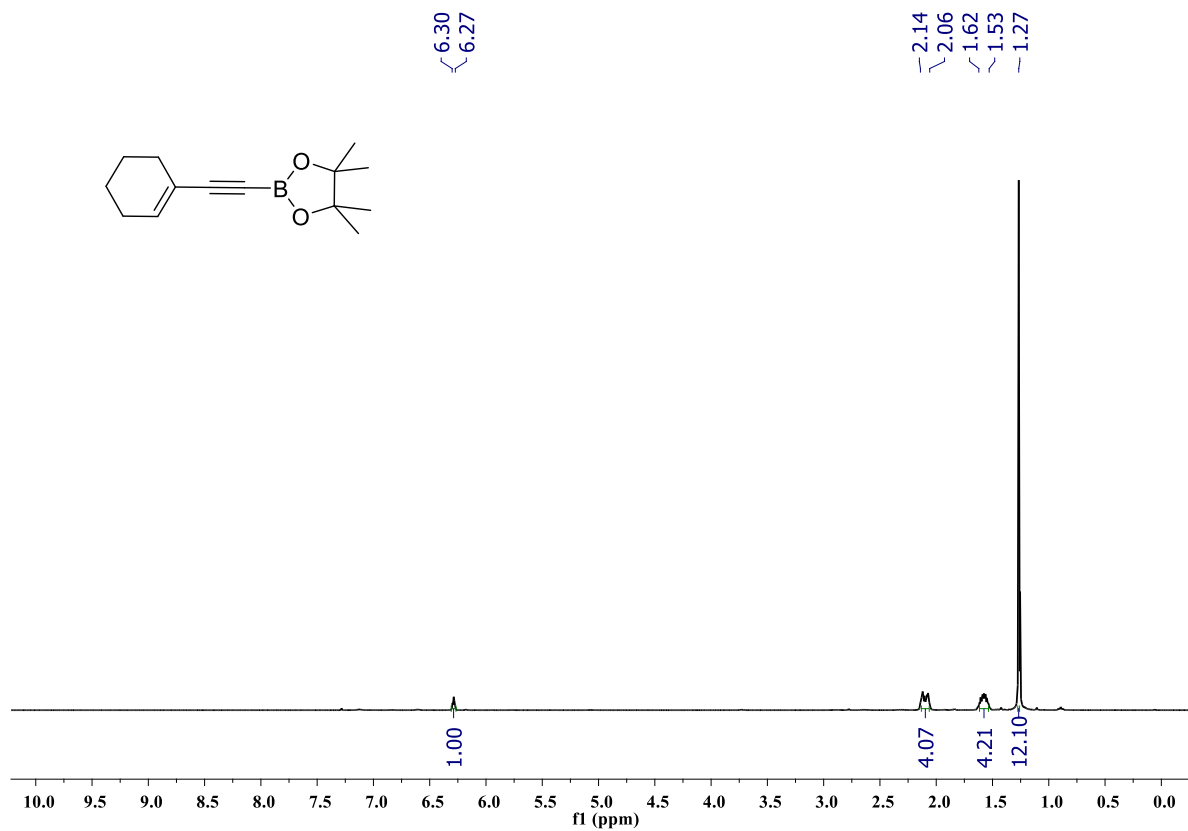


Figure S145: ^1H NMR spectrum of compound **2ad** (400 MHz, CDCl_3).

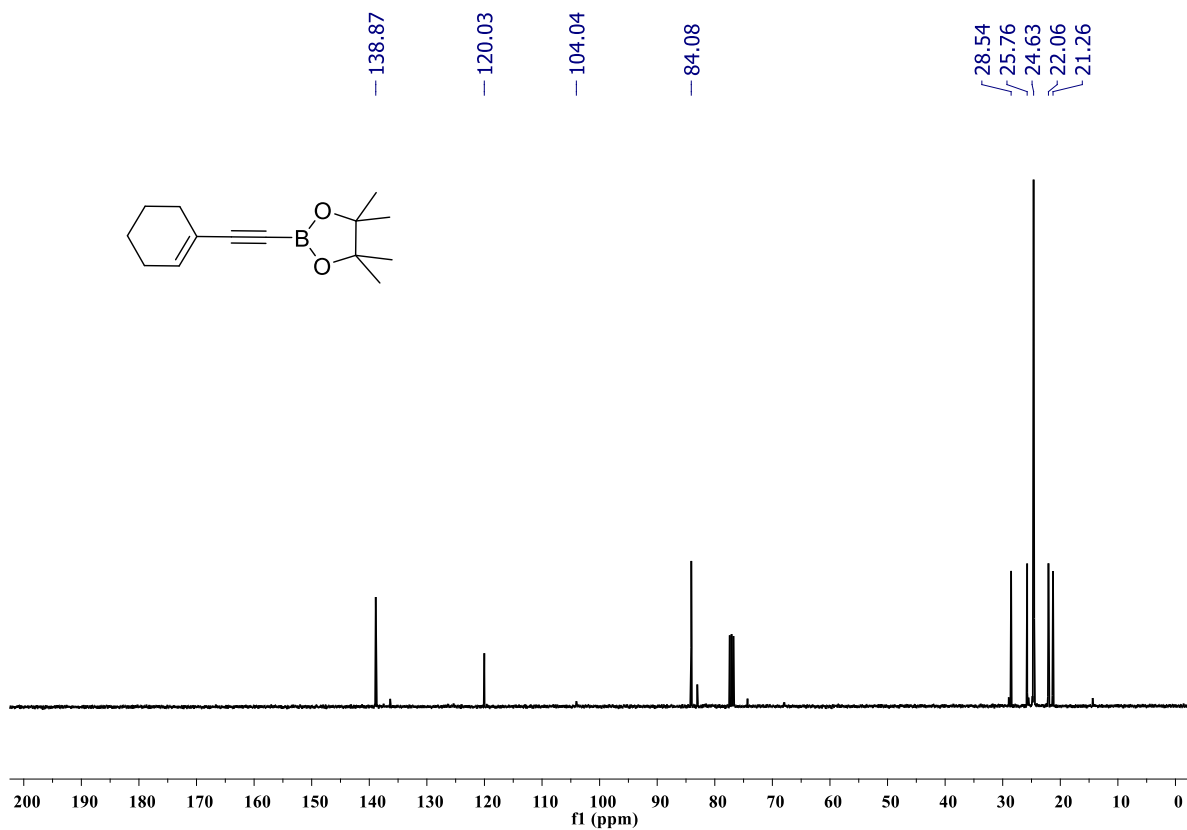


Figure S146: $^{13}\text{C}\{^1\text{H}\}$ NMR spectrum of compound **2ad** (100 MHz, CDCl_3).

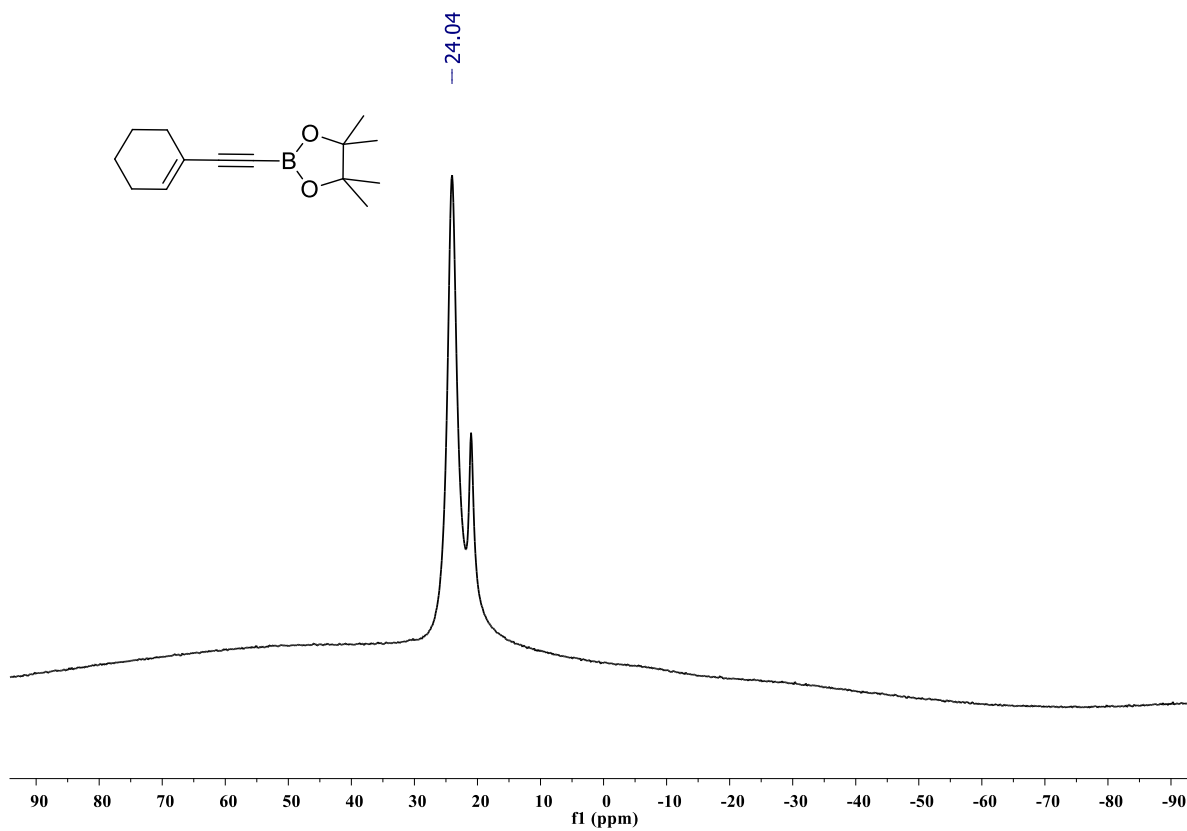


Figure S147: ^{11}B NMR spectrum of compound **2ad** (128 MHz, CDCl_3).

^1H , $^{13}\text{C}\{^1\text{H}\}$ and ^{11}B NMR Spectra of Intermolecular Chemoselective Reactions

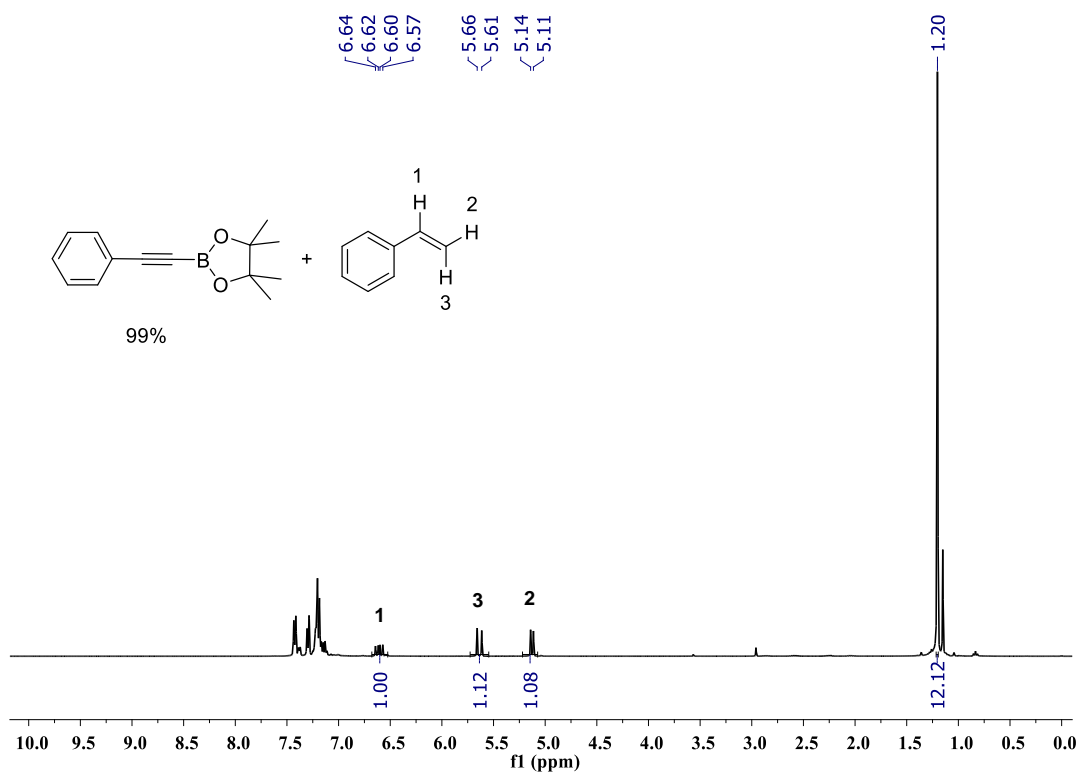


Figure S148: ^1H NMR spectrum of compound **2a** and unreacted styrene (400 MHz, CDCl_3).

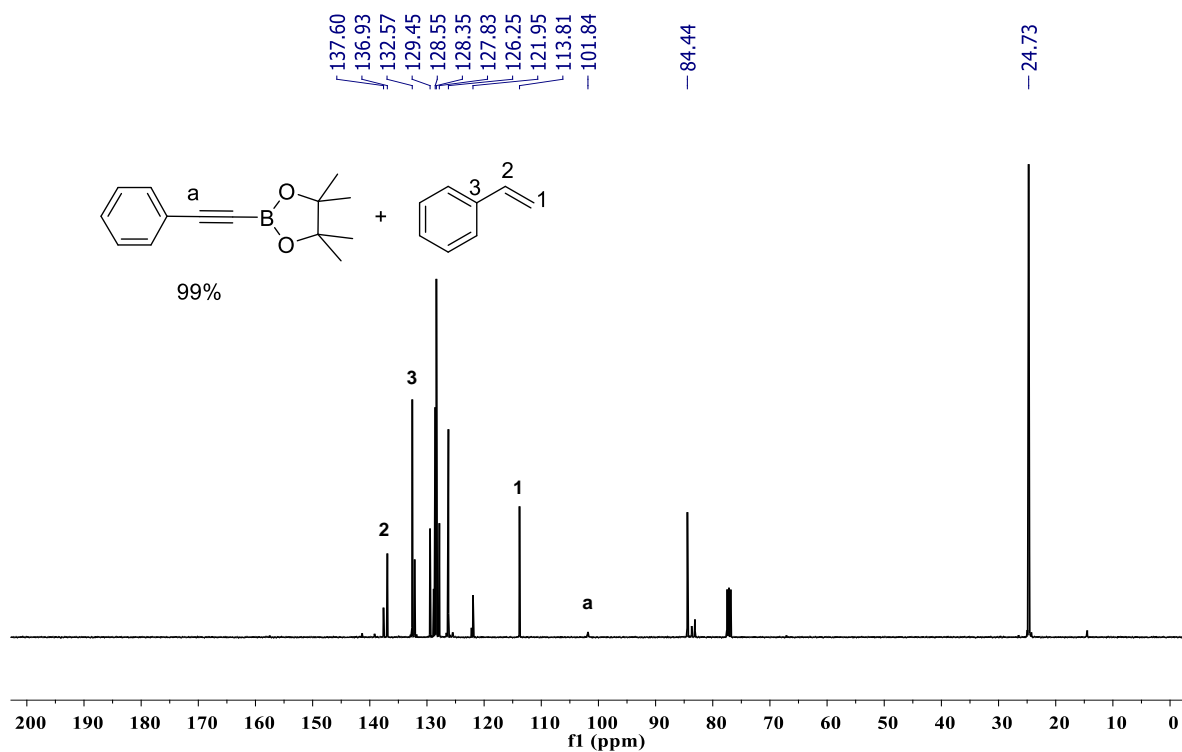


Figure S149: $^{13}\text{C}\{^1\text{H}\}$ NMR spectrum of compound **2a** and unreacted styrene (100 MHz, CDCl_3).

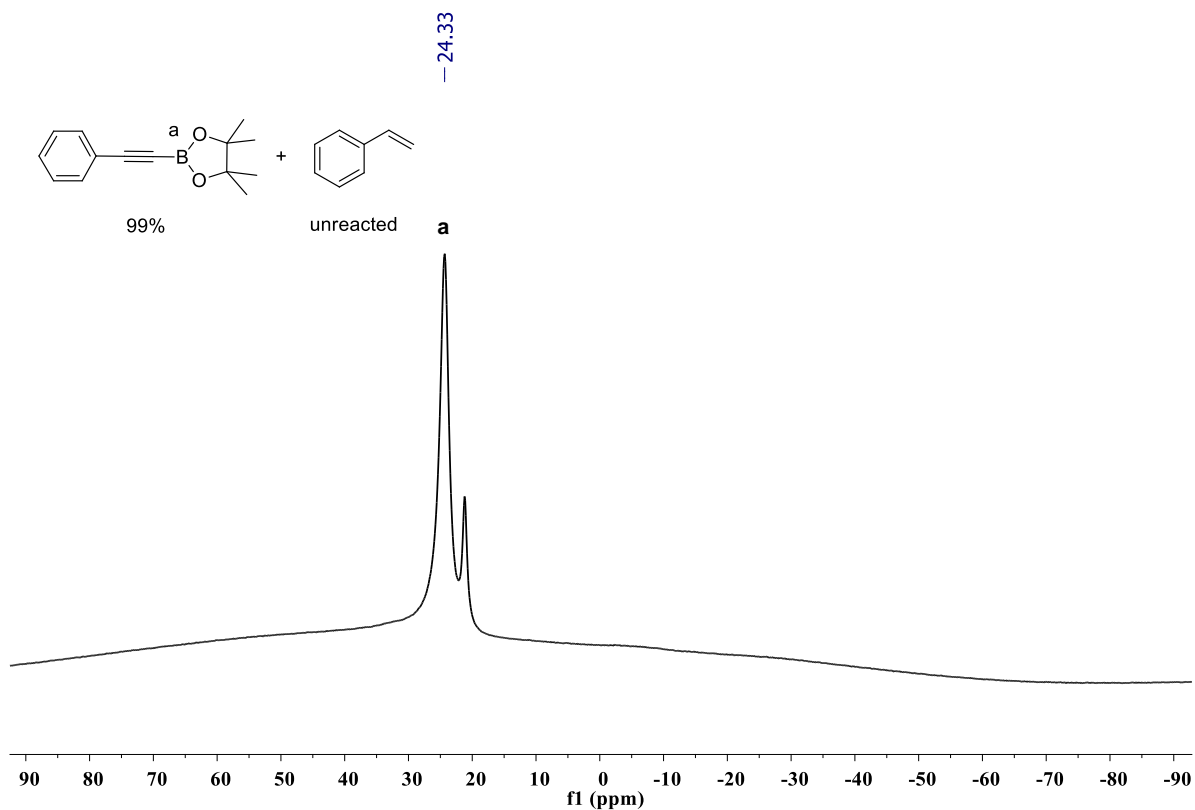


Figure S150: ^{11}B NMR spectrum of compound **2a** and unreacted styrene (128 MHz, CDCl_3).

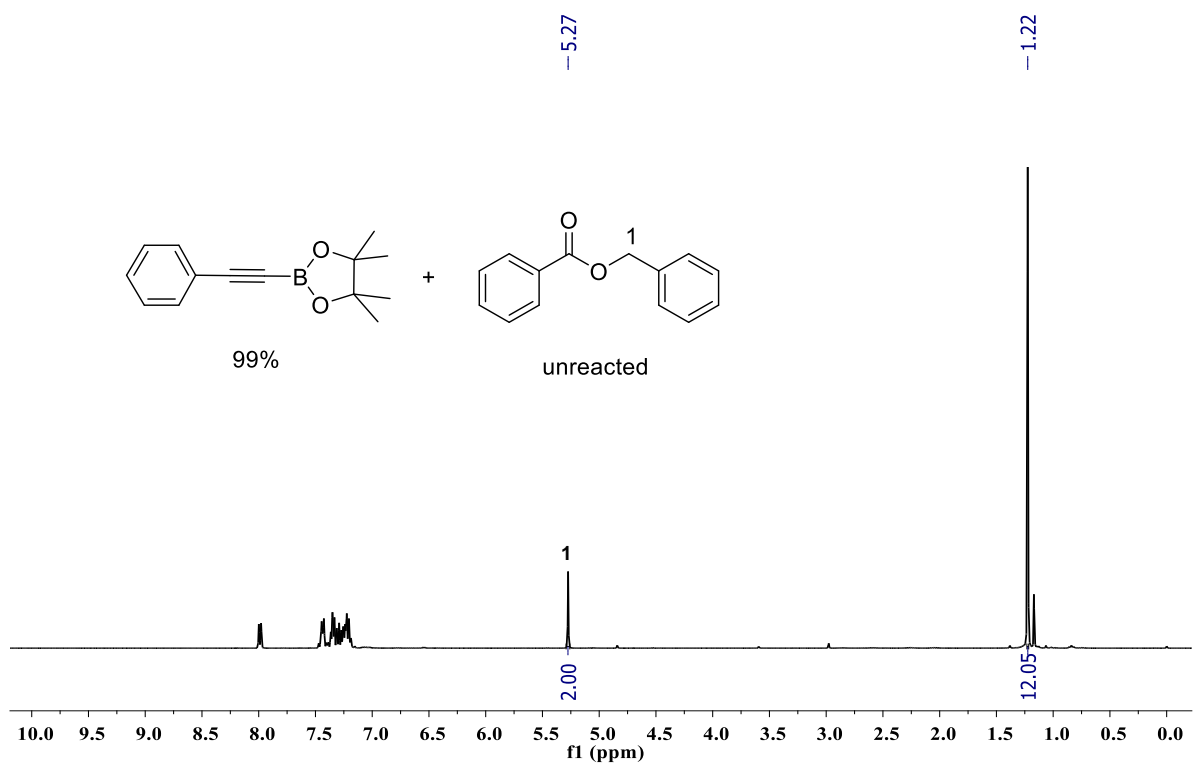


Figure S151: ^1H NMR spectrum of compound **2a** and unreacted benzyl benzoate (400 MHz, CDCl_3).

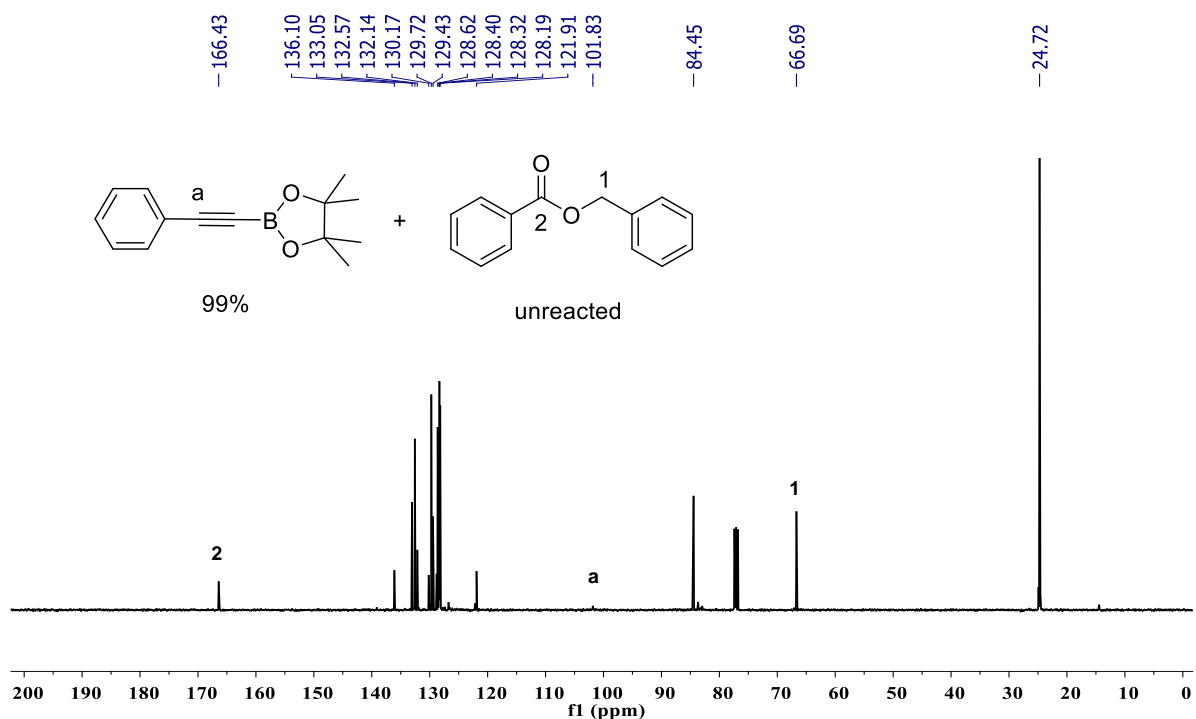


Figure S152: $^{13}\text{C}\{^1\text{H}\}$ NMR spectrum of compound **2a** and unreacted benzyl benzoate (100 MHz, CDCl_3).

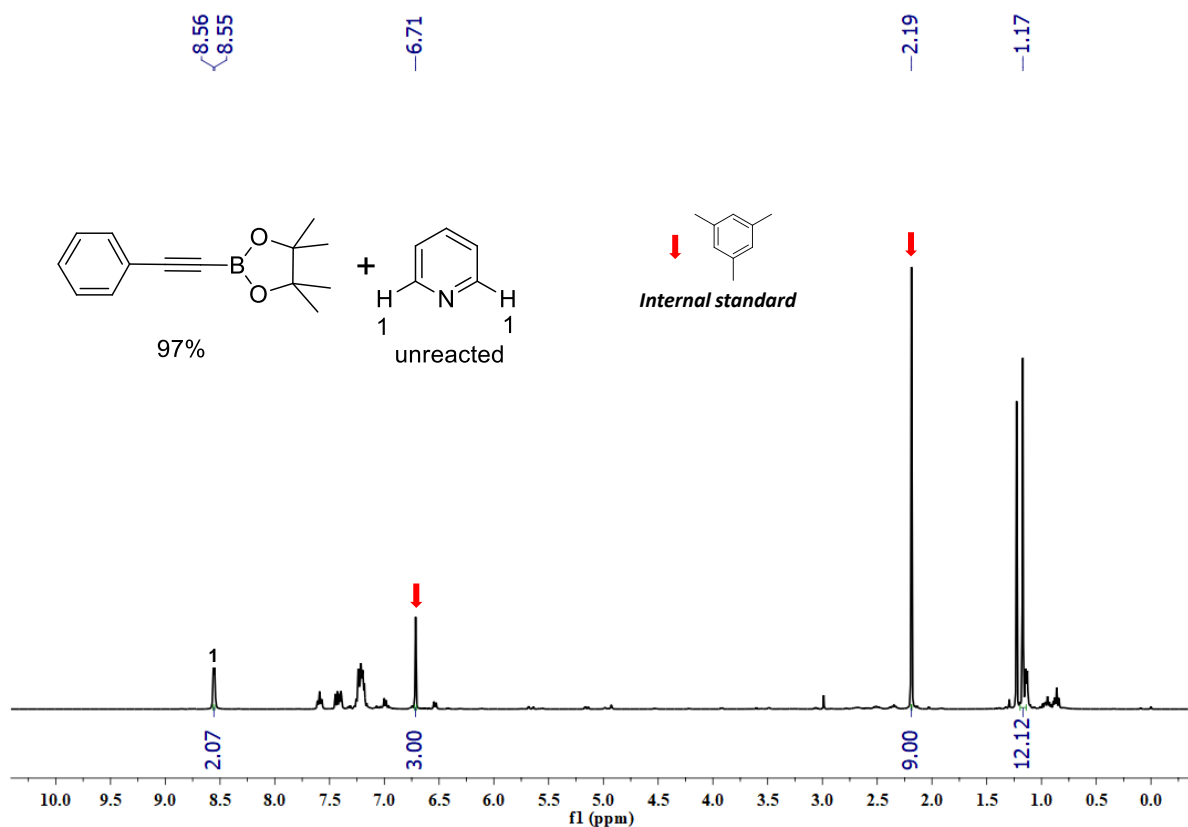


Figure S153: ^1H NMR spectrum of compound **2a** and unreacted pyridine (400 MHz, CDCl_3).

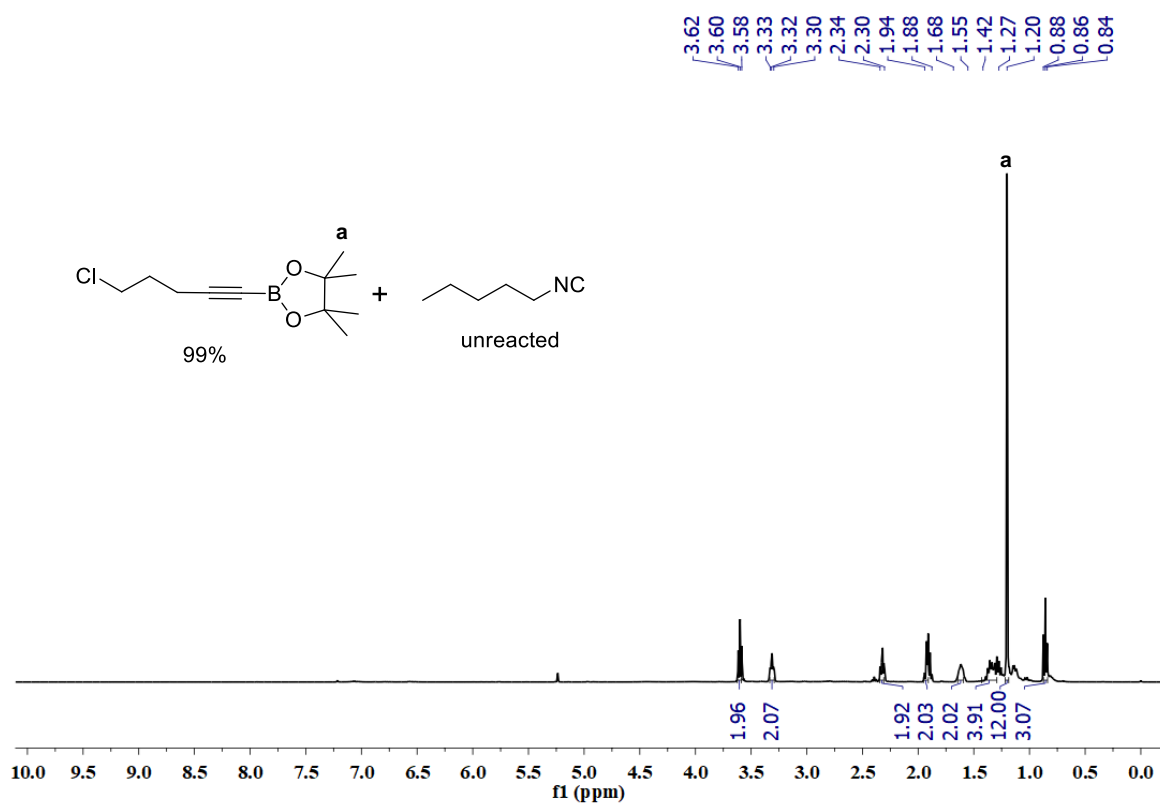


Figure S154: ¹H NMR spectrum of compound **2x** and unreacted 1-pentyl isocyanide (400 MHz, CDCl₃).

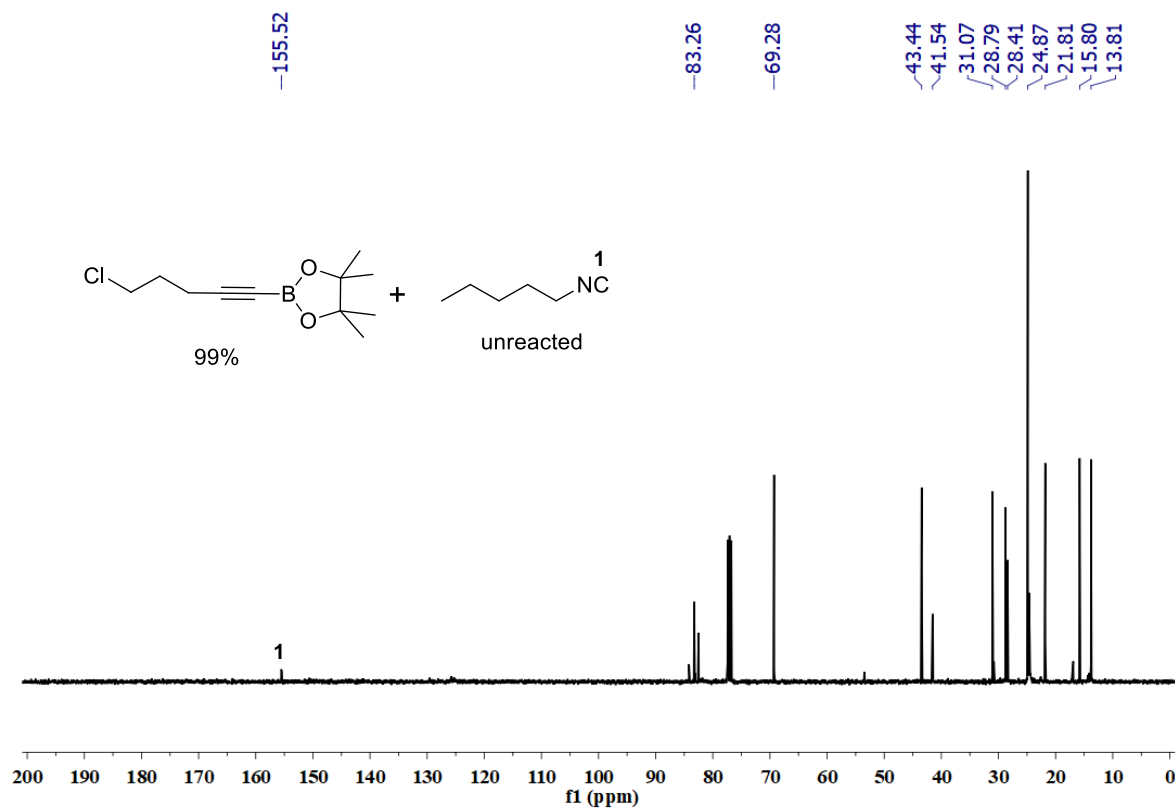


Figure S155: ¹³C{¹H} NMR spectrum of compound **2x** and unreacted 1-pentyl isocyanide (100 MHz, CDCl₃).

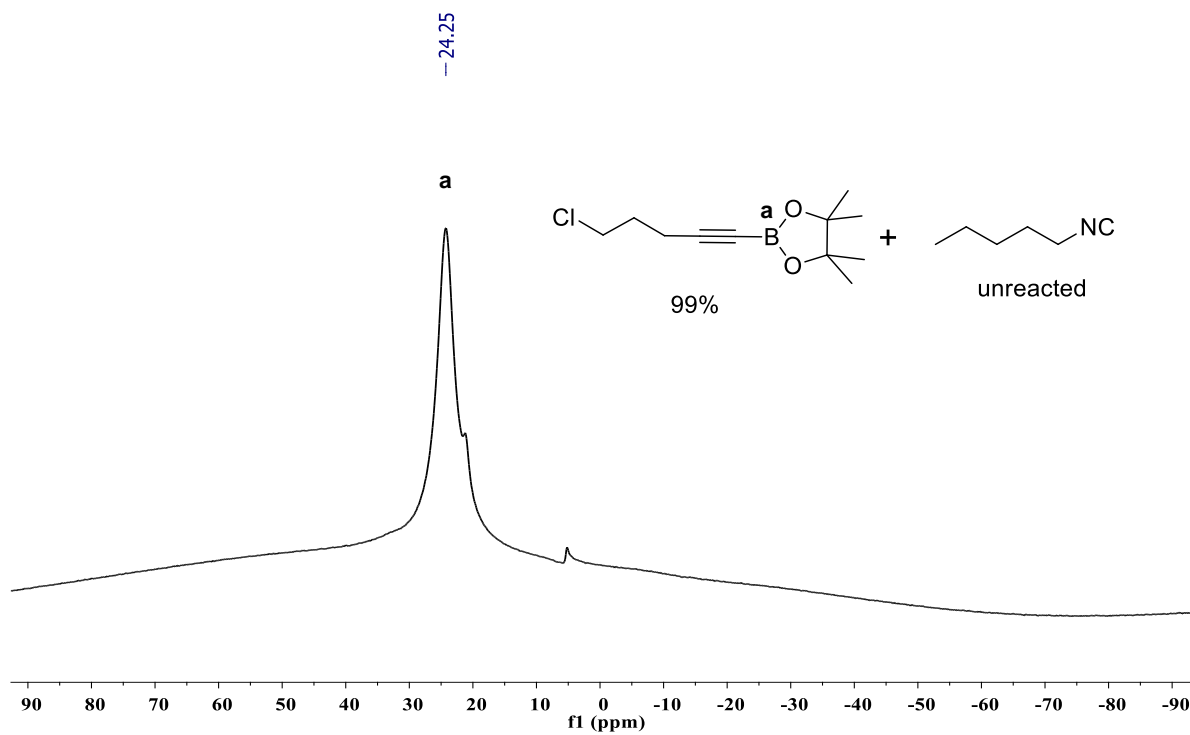


Figure S156: ^{11}B NMR spectrum of compound **2x** and unreacted 1-pentyl isocyanide (128 MHz, CDCl_3).

X-ray Crystallographic Data of **II** and **IV**

X-ray Crystallography

The single crystals of compounds **II** and **IV** were crystallized from Benzene at rt as colorless blocks after 2 d. The crystal data of compounds **II** and **IV** were collected on a Rigaku Oxford diffractometer with graphite-monochromated Cu-K α radiation ($\lambda = 1.54184 \text{ \AA}$) and Mo-K α radiation ($\lambda = 0.71073 \text{ \AA}$) respectively at 100 K. Selected data collection parameters, and other crystallographic results are summarized in Table S2. The structure was determined using direct methods employed in *ShelXT*,¹ *OleX*,² and refinement was carried out using least-square minimization implemented in *ShelXL*.³ All non-hydrogen atoms were refined with anisotropic displacement parameters. Hydrogen atom positions were fixed geometrically in idealized positions and were refined using a riding model.

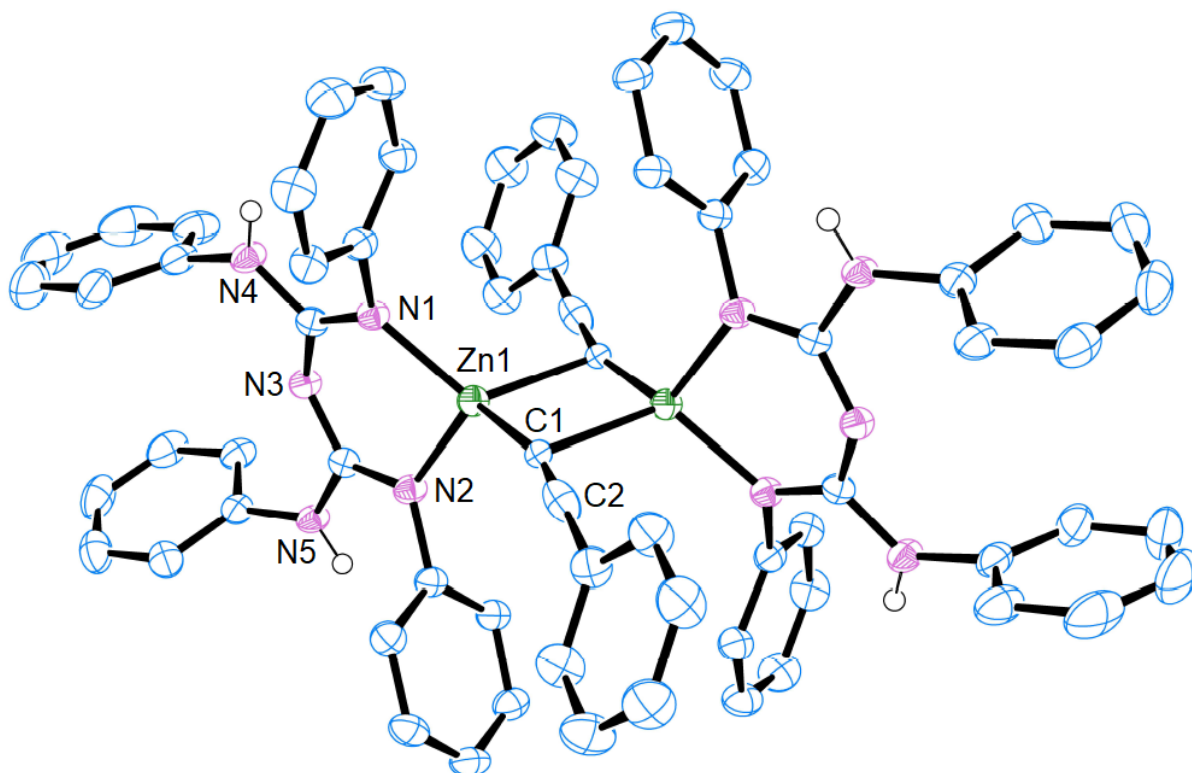


Figure 157. Molecular structure of **II**. The thermal ellipsoids are shown at 50% probability, and all the hydrogen atoms (except for H(4), H(5)) and ethyl groups have been removed for clarity. Selected bond lengths (Å) and angles (deg), For **II**: Zn1-N1 1.9612(17), Zn1-N2 1.9539(16), Zn1-C1 2.026(2), Zn1-C1' 2.316(2), Zn1-Zn1' 2.8705(5), C1-C2 1.167(3); N1-Zn1-N2 94.82(7), N1-Zn1-C1 115.44(7), N2-Zn1-C1 124.65(8), C1-Zn1-C1' 97.52(8), Zn1-C1-Zn1' 82.48(8).

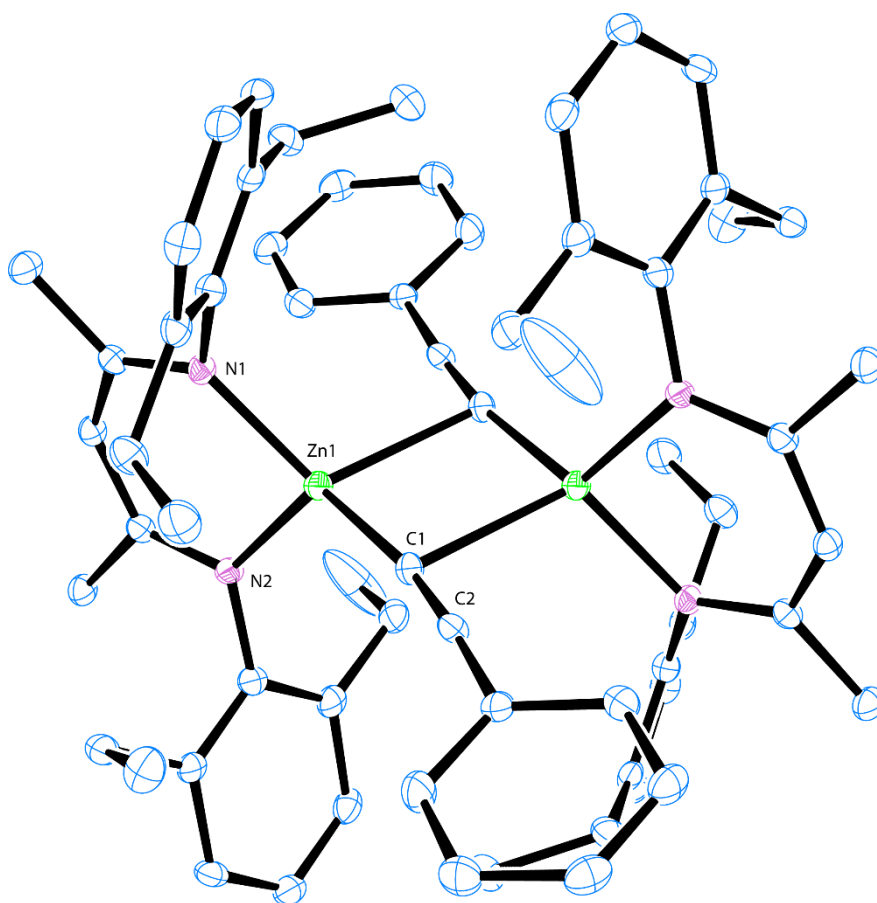


Figure 158. Molecular structure of **IV**. The thermal ellipsoids are shown at 50% probability, and all the hydrogen atoms have been removed for clarity. Selected bond lengths (Å) and angles (deg), For **II**: Zn1-N1 1.984(4), Zn1-N2 1.988(4), Zn1-C1 1.979(5), C1-C2 1.213(7); N1-Zn1-N2 97.20(16), N1-Zn1-C1 119.02(19), N2-Zn1-C1 123.33(18).

Table S2. Crystallographic Data and Refinement Parameters for Compounds **II** and **IV**.

Compound	II	IV
Empirical Formula	C ₁₀₀ H ₁₁₈ N ₁₀ Zn ₂ 2 (C ₆ H ₆)	C ₆₆ H ₇₆ N ₄ Zn ₂
CCDC	2177018	2177019
Molecular mass	1746.99	1056.16
Temperature (K)	100	100
Wavelength (Å)	1.54184	0.71073
Size(mm)	0.2×0.18×0.17	0.2×0.18×0.17
Crystal system	triclinic	monoclinic
Space group	P -1	P2 ₁ /c
a (Å)	12.0811(3)	17.8516(6)
b (Å)	13.0427(3)	18.4478(7)
c (Å)	16.7425(4)	16.8605(5)
α (deg) ^o	83.465(2)	90
β (deg) ^o	86.107(2)	94.032(3)
γ (deg) ^o	63.721(2)	90
Volume (Å ³)	2349.64(10)	5538.8(3)
Z	1	4
Calculated density (g/cm ³)	1.235	1.2664
Absorption coefficient (mm ⁻¹)	1.041	0.911
F(000)	932.0	2243.1
Theta range for data collection (deg) ^o	7.592 to 136.478	6.8 to 50.7
Limiting indices	-14 ≤ h ≤ 14, -15 ≤ k ≤ 15, -20 ≤ l ≤ 19	-25 ≤ h ≤ 23, -25 ≤ k ≤ 23, -23 ≤ l ≤ 23
Reflections collected	34507	47199
Independent reflections	8567 [R _{int} = 0.0358, R _{sigma} = 0.0252]	10002 [R _{int} = 0.0776, R _{sigma} = 0.0828]
Completeness to theta	99 %	99 %
Absorption correction	Empirical	Empirical
Data/restraints/parameters	8567 / 7 / 567	10002 / 0 / 661
Goodness – of–fit on F ²	1.016	1.161
Final R indices [I>2 sigma(I)]	R ₁ = 0.0452, wR ₂ = 0.1218	R ₁ = 0.0600, wR ₂ = 0.1655

REFERENCES

- (1) Sheldrick, G. Crystal structure refinement with SHELXL. *Acta Crystallogr. C.* **2015**, *71*, 3–8.
- (2) Dolomanov, O. V.; Bourhis, L. J.; Gildea, R. J.; Howard, J. A. K.; Puschmann, H. OLEX₂: a complete structure solution, refinement, and analysis program. *J. Appl. Crystallogr.* **2009**, *42*, 339-341.
- (3) (a) Sheldrick, G. M. A short history of SHELX. *Acta Crystallogr., Sect. A: Found. Crystallogr.* **2008**, *64*, 112-122. (b) Sheldrick, G. M. SHELXT - Integrated space-group and crystal-structure determination. *Acta Crystallogr., Sect. A: Found. Adv.* **2015**, *71*, 3-8.